

**Tailoring of whey protein isolate stabilized oil-water interfaces  
for improved emulsification**

A Thesis Submitted to the College of  
Graduate Studies and Research  
in Partial Fulfillment of the Requirements  
for the Doctor of Philosophy  
in the Department of Food and Bioproduct Sciences  
University of Saskatchewan  
Saskatoon, SK

By  
Ricky Sze Ho Lam

© Copyright Ricky Sze Ho Lam, August 2014. All rights reserved.

## **PERMISSION TO USE**

In presenting this thesis in partial fulfillment of the requirements for a postgraduate degree from the University of Saskatchewan, I agree that the Libraries of this University may make it freely available for inspection. I further agree that permission for copying of this thesis in any manner, in whole or in part, for scholarly purposes may be granted by the professor or professors who supervised my thesis, work or, in their absence, by the Head of the Department of the Dean of the College in which my thesis work was done. It is understood that any copying or publication or use of this thesis or parts thereof for financial gain shall not be allowed without my written permission. It is also understood that due recognition shall be given to me and to the University of Saskatchewan in any scholarly use which may be made of any material in my thesis.

Requests for permission to copy or to make other uses of materials in this thesis in whole or part should be addressed to:

Head of the Department of Food and Bioproduct Sciences  
University of Saskatchewan  
Saskatoon, Saskatchewan S7N 5A8  
Canada

## ABSTRACT

In this thesis, mechanisms for enhancing the stability of whey protein emulsions using two approaches were investigated. First, the physicochemical and emulsifying properties of whey protein isolate (WPI), and its two main proteins, alpha-lactalbumin (ALA) and beta-lactoglobulin ( $\beta$ -LG), were investigated in response to changes in pH and temperature pre-treatments. Solvent conditions which inhibit protein aggregation, such as pHs away from the isoelectric point, were found to form stable emulsions. In contrast, thermal treatments were found to negatively affect emulsion stability, where the most stable emulsions for WPI, ALA and  $\beta$ -LG were formed at room temperature (*i.e.* 25°C) at pH 7.0. It was also determined that emulsions formed using WPI, ALA and  $\beta$ -LG were stabilized by electrostatically repulsive forces which prevent flocculation and creaming. Secondly, the use of tailored protein-polysaccharide interactions involving WPI and carrageenan (CG) were explored as a means of enhancing emulsion stability. Carrageenan (CG) partakes in electrostatic attraction with WPI when acidified, leading to the formation of coupled gel networks. CG was selected for its anionic properties and for its well-characterized structure in that  $\kappa$ -,  $\iota$ - and  $\lambda$ -type CG contain 1-, 2- and 3-sulfated groups per disaccharide repeating unit respectively. WPI-CG mixtures formed gel networks once acidified, where WPI- $\kappa$ -CG and WPI- $\iota$ -CG mixtures formed stiff networks, whereas WPI- $\lambda$ -CG formed a weak fluid network. WPI-CG complexes were found to be surface active, causing changes to the interfacial tension and interfacial rheology at pHs corresponding to where electrostatic attraction occurs upon acidification. Electrostatically coupled gel networks were formed in an emulsion, where oil droplets became entrapped within the biopolymer matrix. WPI-CG mixtures were sensitive to WPI-CG mixing ratio as stiffer gels were formed at higher CG content. Furthermore, WPI- $\iota$ -CG gels were stiffer than those made with WPI- $\kappa$ -CG gels presumably due to the higher number of sulfated groups lending greater opportunities for  $\iota$ -CG to form bonds with neighboring polymers compared to  $\kappa$ -CG.

## **ACKNOWLEDGEMENTS**

This thesis is dedicated to my family and especially my parents (Danny Kam Wah Lam and Jennifer Kam Woon Lam) for their love, hard work, support and guidance over me throughout my life. I give thanks to God for his provision and care over my life.

My research would not have been possible without the continual guidance and mentoring from my supervisor Dr. Michael T. Nickerson. I would like to thank him for his mentorship and friendship which began while I was a Master's student. I would like to thank him also for his friendship, constant support and encouragement throughout my thesis and his advice has been invaluable to me. I would also like to thank my committee members Drs. Gordon Zello, Supratim Ghosh, Robert Tyler and Takuji Tanaka, my graduate chairs, Drs. George Khatchatourians and Xiao Qiu, and my external examiner Dr. Eunice C. Y. Li-Chan.

I would like to thank the professors and staff within the Department of Food and Bioproduct Sciences for their friendship, support and guidance throughout my studies.

I am grateful for the financial assistance provided by the Canadian Dairy Commission and NSERC which funded my research.

I would also like to thank my friends both within the department and those I have come to know in Saskatoon for their friendship and support which had made my studies such an enjoyable time.

## TABLE OF CONTENTS

PERMISSION TO USE .....	i
ABSTRACT .....	ii
ACKNOWLEDGEMENTS .....	iii
TABLE OF CONTENTS .....	iv
LIST OF FIGURES .....	ix
LIST OF TABLES .....	xiii
LIST OF ABBREVIATIONS .....	xiv
1. OVERVIEW .....	1
1.1 Summary .....	1
1.2 Hypotheses .....	2
1.3 Objectives .....	2
2. LITERATURE REVIEW .....	4
2.1 Abstract .....	4
2.2 Introduction .....	4
2.3 Protein-stabilized emulsions .....	8
2.4 Destabilizing mechanisms in protein-stabilized emulsions .....	11
2.5 Protein dynamics and affinity to the oil-water interface .....	13
2.6 Effect of polysaccharides on protein-stabilized emulsions .....	17
2.7 Choice of materials .....	21
2.7.1 Whey proteins .....	21
2.7.2 $\beta$ -Lactoglobulin .....	23
2.7.3 $\alpha$ -Lactalbumin .....	23
2.7.4 Carrageenan .....	24

3. THE EFFECT OF PH AND TEMPERATURE PRE-TREATMENTS ON THE PHYSICOCHEMICAL AND EMULSIFYING PROPERTIES OF WHEY PROTEIN ISOLATES .....	26
3.1 Abstract .....	26
3.2 Introduction.....	26
3.3 Materials and methods .....	28
3.3.1 Materials .....	28
3.3.2 Sample preparation .....	28
3.3.3 Circular dichroism .....	28
3.3.4 Surface hydrophobicity .....	29
3.3.5 Electrophoretic mobility .....	30
3.3.6 Aggregate size.....	30
3.3.7 Interfacial tension.....	31
3.3.8 Emulsification stability and activity indices .....	31
3.3.9 Statistics .....	32
3.4 Results and discussion .....	32
3.4.1 Structural characteristics.....	32
3.4.2 Surface characteristics .....	34
3.4.3 WPI aggregation .....	38
3.4.4 Interfacial properties of WPI .....	39
3.4.5 Emulsifying properties.....	41
3.5 Conclusions.....	44
3.6 Connection to the next study.....	44
4. THE EFFECT OF PH AND HEAT PRE-TREATMENTS ON THE PHYSICOCHEMICAL AND EMULSIFYING PROPERTIES OF $\beta$ -LACTOGLOBULIN.....	46
4.1 Abstract .....	46
4.2 Introduction.....	47
4.3 Materials and Methods.....	48
4.3.1 Materials .....	48
4.3.2 Sample preparation .....	48
4.3.3 Surface hydrophobicity .....	49

4.3.4 Electrophoretic mobility .....	50
4.3.5 Dynamic light scattering for determination of the hydrodynamic radius of $\beta$ -LG aggregates.....	50
4.3.6 Interfacial tension.....	51
4.3.7 Emulsification stability and activity indices .....	51
4.3.8 Statistics .....	52
4.4 Results and discussion .....	52
4.4.1 Physicochemical properties .....	52
4.4.2 Emulsifying properties.....	60
4.5 Conclusions.....	64
4.6 Connection to the next study.....	64
 5. THE EFFECT OF PH AND TEMPERATURE PRE-TREATMENTS ON THE STRUCTURE, SURFACE CHARACTERISTICS AND EMULSIFYING PROPERTIES OF ALPHA-LACTALBUMIN .....	66
5.1 Abstract .....	66
5.2 Introduction.....	66
5.3 Materials and methods .....	67
5.3.1 Materials .....	67
5.3.2 Sample preparation .....	68
5.3.3 Circular dichroism .....	68
5.3.4 Surface hydrophobicity .....	68
5.3.5 Surface charge.....	69
5.3.6 Hydrodynamic radius.....	69
5.3.7 Interfacial tension.....	70
5.3.8 Emulsification stability and activity indices .....	70
5.3.9 Statistics .....	71
5.4 Results and discussion .....	71
5.4.1 Protein conformation .....	71
5.4.2 Surface characteristics .....	74
5.4.3 Protein aggregation .....	76
5.4.4 Interfacial properties .....	78

5.4.5 Emulsifying properties.....	79
5.5 Conclusions.....	84
5.6 Connection to the next study.....	85
6. THE RHEOLOGICAL PROPERTIES OF WHEY PROTEIN-CARRAGEENAN MIXTURES DURING THE FORMATION OF ELECTROSTATICALLY COUPLED BIOPOLYMER AND EMULSION GELS .....	86
6.1 Abstract .....	86
6.2 Introduction.....	87
6.3 Materials and methods .....	89
6.3.1 Materials .....	89
6.3.2 Sample preparation .....	90
6.3.3 Turbidimetric pH-titration over time for WPI: carrageenan mixtures.....	90
6.3.4 Interfacial tension.....	91
6.3.5 Small deformation rheology .....	91
6.3.6 Light microscopy .....	92
6.3.6 Statistics .....	92
6.4 Results and discussion .....	92
6.4.1 Turbidimetric pH titrations .....	92
6.4.2 Rheology of WPI and WPI-carrageenan solutions .....	95
6.4.3 Interfacial properties of WPI and WPI-carrageenan complexes.....	100
6.4.4 Rheology of WPI and WPI-carrageenan stabilized emulsions .....	103
6.4.5 Emulsion droplet sizes of WPI and WPI-CG emulsions .....	108
6.5 Conclusions.....	109
6.6 Connection to the next study.....	110
7. THE EFFECT OF BIOPOLYMER MIXING RATIO ON THE FORMATION OF ELECTROSTATICALLY COUPLED WHEY PROTEIN-(KAPPA- AND IOTA- TYPE) CARRAGEENAN NETWORKS IN THE PRESENCE AND ABSENCE OF OIL DROPLETS .....	111
7.1 Abstract .....	111
7.2 Introduction.....	111

7.3 Materials and methods .....	114
7.3.1 Materials .....	114
7.3.2 Sample preparation .....	114
7.3.3 Interfacial tension.....	115
7.3.4 Oscillatory shear deformation of the bulk solution.....	115
7.3.5 Oscillatory shear deformation at the oil-water interface.....	116
7.4 Results and discussion .....	116
7.4.1 Formation of electrostatic coupled biopolymer networks .....	116
7.4.2 Interfacial properties of WPI-CG complexes at the oil-water interface .....	123
7.4.3 Formation of electrostatic coupled biopolymer emulsion gels .....	128
7.5 Conclusions.....	132
 8. GENERAL DISCUSSION .....	134
8.1 Comparisons of the physicochemical and emulsifying properties of WPI, $\beta$ -LG and ALA .....	134
8.2 Comparison of pH-dependent physicochemical properties such as the surface charge and interfacial tension of WPI, $\beta$ -LG and ALA .....	135
8.3 Comparison of pH and temperature dependent changes to the surface hydrophobicity and aggregate size of WPI, $\beta$ -LG and ALA .....	137
8.4 The effect of protein conformation on the functionality of WPI, $\beta$ -LG and ALA .....	138
8.5 Comparison of changes in the emulsifying properties of WPI, $\beta$ -LG and ALA .....	139
8.6 The effect of carrageenan addition on WPI-stabilized emulsions .....	140
8.7 The effect of carrageenan-type and mixing ratio on the rheological properties of WPI-CG coupled networks and emulsion gels.....	140
8.8 Summary .....	141
8.9 Future directions .....	142
 9. GENERAL CONCLUSION .....	143
 10. REFERENCES .....	145

## LIST OF FIGURES

<b>Figure 2.1</b>	A depiction of globular proteins migrating to the water-oil interface (A) followed by reorientation (B) and viscoelastic film formation (C). ....	9
<b>Figure 2.2</b>	Mechanisms for emulsion stability by (A) electrostatic repulsion and (B) steric stabilization.....	10
<b>Figure 2.3</b>	Representations of a (A) homogenous mixed polysaccharide-protein emulsion and (B) emulsion formed using a layer-by-layer deposition technique.....	18
<b>Figure 2.4</b>	Mechanisms for protein-polysaccharide emulsion destabilization as represented by (A) bridging flocculation and (B) depletion flocculation. ....	20
<b>Figure 3.1</b>	Circular dichroism in mean residue molar ellipticity (deg cm <sup>2</sup> dmol <sup>-1</sup> ) for WPI solutions as a function of pH (7.0 (A), 5.0 (B), 3.0 (C)) and pre-treatment temperatures.....	33
<b>Figure 3.2</b>	Intrinsic fluorescence (arbitrary units (a.u.) (A) and surface hydrophobicity (a.u.) as measured using an ANS fluorescent probe (B) for WPI solutions as a function of pH and pre-treatment temperature conditions. ....	35
<b>Figure 3.3</b>	Zeta potential (mV) for WPI solutions as a function of pH and pre-treatment temperature conditions. ....	37
<b>Figure 3.4</b>	Hydrodynamic radius (nm) for WPI solutions as a function of pH and pre-treatment temperature conditions. ....	38
<b>Figure 3.5</b>	The interfacial tension (mN/m) for WPI solutions as a function of pH and pre-treatment temperature conditions. ....	40
<b>Figure 3.6</b>	The emulsion activity (EAI, m <sup>2</sup> /g) (A) and stability (ESI, min) indices for WPI solutions as a function of pH and pre-treatment temperature conditions. ....	42
<b>Figure 4.1</b>	Intrinsic fluorescence (arbitrary units (a.u.) (A) and surface hydrophobicity (a.u.) as measured using an ANS fluorescent probe (B) for $\beta$ -lactoglobulin solutions as a function of pH and pre-treatment temperature conditions.....	55
<b>Figure 4.2</b>	Zeta potential (mV) for $\beta$ -lactoglobulin solutions as a function of pH and pre-treatment temperature conditions. ....	56
<b>Figure 4.3</b>	Hydrodynamic radius (nm) for $\beta$ -lactoglobulin solutions as a function of pH and pre-treatment temperature conditions. ....	57
<b>Figure 4.4</b>	The interfacial tension (mN/m) for $\beta$ -lactoglobulin solutions as a function of pH and pre-treatment temperature conditions. ....	60
<b>Figure 4.5</b>	The emulsion activity (EAI, m <sup>2</sup> /g) (A) and stability (ESI, min) indices for $\beta$ -lactoglobulin solutions as a function of pH and pre-treatment temperature conditions .....	62

<b>Figure 5.1</b>	Mean residue molar ellipticity data for ALA-1 (A-B) and ALA-3 (C-D) at pH 5.00 (A, C) and 7.00 (B, D) as a function of wavelength and temperature pre-treatments.	73
<b>Figure 5.2</b>	Zeta potential of ALA-1 and ALA-3 proteins as a function of pH and temperature pre-treatments.	74
<b>Figure 5.3</b>	Maximum fluorescent intensity of ALA-1 and ALA-3 proteins as a function of pH and temperature pre-treatments.	75
<b>Figure 5.4</b>	Mean hydrodynamic radius (nm) of ALA-1 and ALA-3 proteins as a function of pH and temperature pre-treatments.	77
<b>Figure 5.5</b>	Mean interfacial tension (mN/m) of ALA-1 and ALA-3 proteins as a function of pH and temperature pre-treatments.	79
<b>Figure 5.6</b>	Mean emulsification activity ( $m^2/g$ ) (A) and stability (min) (B) indices for ALA-1 and ALA-3 proteins as a function of pH and temperature pre-treatments.	81
<b>Figure 6.1</b>	Changes to the optical density for an individual WPI (A) solution and mixtures of WPI and $\kappa$ -CG (B), $\iota$ -CG (C) and $\lambda$ -CG (D) solutions as a function of pH (open circles) and time (min).	93
<b>Figure 6.2</b>	Dynamic viscoelastic storage ( $G'$ (solid line)) and loss ( $G''$ (dashed line)) moduli for an individual WPI (A) solution and mixtures of WPI and $\kappa$ -CG (B), $\iota$ -CG (C) and $\lambda$ -CG (D) as a function of pH (open circles) and time (min).	96
<b>Figure 6.3</b>	Dynamic viscoelastic storage ( $G'$ (solid circles)) and loss ( $G''$ (open circles)) moduli for an individual WPI (A) solution and mixtures of WPI and $\kappa$ -CG (B), $\iota$ -CG (C) and $\lambda$ -CG (D) as a function of frequency (Hz) (on double logarithmic axes) after 90 min of acidification with 0.5% (w/w) GDL and, after running the time sweep measurements.	97
<b>Figure 6.4</b>	Dynamic viscoelastic storage ( $G'$ (solid circles)) and loss ( $G''$ (open circles)) moduli for an individual WPI (A) solution and mixtures of WPI and $\kappa$ -CG (B), $\iota$ -CG (C) and $\lambda$ -CG (D) as a function of shear strain (%) (on double logarithmic axes) after 90 min of acidification with 0.5% (w/w) GDL and, after running both the time and frequency sweep measurements.	98
<b>Figure 6.5</b>	Interfacial tension (nM/m) (solid circle) and pH (open circle) for an individual WPI (A) solution and mixtures of WPI and $\kappa$ -CG (B), $\iota$ -CG (C) and $\lambda$ -CG (D) as a function of time (min).	102
<b>Figure 6.6</b>	Dynamic viscoelastic storage ( $G'$ (solid line)) and loss ( $G''$ (dashed line)) moduli for emulsions stabilized by an individual WPI (A) solution and mixtures of WPI and $\kappa$ -CG (B), $\iota$ -CG (C) and $\lambda$ -CG (D) as a function of pH (open circles) and time (min).	104

<b>Figure 6.7</b>	Dynamic viscoelastic storage ( $G'$ (solid circles)) and loss ( $G''$ (open circles)) moduli for emulsions stabilized by an individual WPI (A) solution and mixtures of WPI and $\kappa$ -CG (B), $\iota$ -CG (C) and $\lambda$ -CG (D) as a function of frequency (Hz) (on double logarithmic axes) after 90 min of acidification with 0.5% (w/w) GDL and, after running the time sweep measurements.....	105
<b>Figure 6.8</b>	Dynamic viscoelastic storage ( $G'$ (solid circles)) and loss ( $G''$ (open circles)) moduli for emulsions stabilized by an individual WPI (A) solution and mixtures of WPI and $\kappa$ -CG (B), $\iota$ -CG (C) and $\lambda$ -CG (D) as a function of shear strain (%) (on double logarithmic axes) after 90 min of acidification with 0.5% (w/w) GDL and, after running both the time and frequency sweep measurements.....	106
<b>Figure 6.9</b>	Brightfield microscopy of emulsion gels stabilized with WPI- $\kappa$ -CG (A), WPI- $\iota$ -CG (B) and WPI- $\lambda$ -CG (C) mixtures, and an individual WPI solution (D).....	107
<b>Figure 6.10</b>	Schematic of an emulsion-filled protein gel (A) and a protein stabilized-emulsion gel (B).....	108
<b>Figure 7.1</b>	Dynamic viscoelastic storage ( $G'$ (solid line)) and loss ( $G''$ (dashed line)) moduli for mixtures of WPI- $\kappa$ -CG (A-C) and WPI- $\iota$ -CG (D-F) at various mixing ratios as a function of pH (closed circles) and time (min).....	117
<b>Figure 7.2</b>	Dynamic viscoelastic storage ( $G'$ (closed symbol)) and loss ( $G''$ (open symbol)) moduli for mixtures of WPI- $\kappa$ -CG (A-B) and WPI- $\iota$ -CG (C-D) at various mixing ratios as a function of frequency (A and C) and strain (B and D). WPI- $\kappa$ -CG (A-B) mixtures were mixed at ratios of 8:1 (circle symbol), 12:1 (square symbol) and 16:1 (triangle symbol) while WPI- $\iota$ -CG (C-D) were mixed at 16:1 (circle symbol), 20:1 (square symbol) and 24:1 (triangle symbol).....	120
<b>Figure 7.3</b>	A schematic of a sample WPI- $\iota$ -CG biopolymer gel at the ratio of 20:1 in response to strain (graph: $G'$ (closed symbols) and $G''$ (open symbols)) where the gelled network comprised of WPI (open circle) complexed with CG (lines) are elastic at low strains (A), re-arrange in their molecular bonding at higher strains (B) which leads to the breakdown of the network (C).....	122
<b>Figure 7.4</b>	Interfacial properties of WPI:CG mixtures at the canola oil: water interface measured by interfacial tension (open circles) for mixtures of WPI- $\kappa$ -CG (A-C) and WPI- $\iota$ -CG (D-F) at various mixing ratios as a function of pH (closed circles) and time (min).....	124
<b>Figure 7.5</b>	Interfacial rheological properties of WPI:CG mixtures at the canola oil: water interface measured by interfacial storage moduli (solid line) and interfacial loss moduli (dashed line) for mixtures of WPI- $\kappa$ -CG (A-C) and WPI- $\iota$ -CG (D-F) at various mixing ratios as a function of pH (closed circles) and time (min) .....	125

- Figure 7.6** Dynamic viscoelastic storage ( $G'$  (solid line)) and loss ( $G''$  (dashed line)) moduli for 1:1 water: canola oil emulsions stabilized with WPI- $\kappa$ -CG (A-C) and WPI- $\tau$ -CG (D-F) at various mixing ratios as a function of time (min) and pH (closed circles). ..... 127
- Figure 7.7** Dynamic viscoelastic storage ( $G'$  (closed symbol)) and loss ( $G''$  (open symbol)) moduli for 1:1 water: canola oil emulsions stabilized with WPI- $\kappa$ -CG (A and C) and WPI- $\tau$ -CG (B and D) at various mixing ratios as a function of frequency (A-B) and strain (C-D). WPI- $\kappa$ -CG (A and C) mixtures were mixed at ratios of 8:1 (circle symbol), 12:1 (square symbol) and 16:1 (triangle symbol) while WPI- $\tau$ -CG (B and D) were mixed at 16:1 (circle symbol), 20:1 (square symbol) and 24:1 (triangle symbol). ..... 129
- Figure 7.8** A schematic of a sample WPI- $\tau$ -CG emulsion gel at the biopolymer ratio of 20:1 and an aqueous: oil ratio of 1:1 in response to strain (graph:  $G'$  (closed symbols) and  $G''$  (open symbols)) where the gelled network comprised of WPI (open oval) complexed with CG (lines) stabilizing oil droplets (grey circles) are elastic at low strains (A) and their breakdown at higher strains (B). ..... 131

## LIST OF TABLES

<b>Table 2.1</b>	Mechanistic studies utilizing plant and animal proteins as emulsifiers.....	6
<b>Table 3.1</b>	A summary of the two-way ANOVA tested for the main factors pH and temperature and their interaction on the physicochemical and emulsifying properties of WPI ...	36
<b>Table 4.1</b>	A summary of the two-way ANOVA tested for the main factors pH and temperature and their interaction on the physicochemical and emulsifying properties of $\beta$ -lactoglobulin .....	54
<b>Table 7.1</b>	The dynamic storage ( $G'$ ) and loss ( $G''$ ) moduli for electrostatic coupled networks involving WPI-CG mixtures as a function of mixing ratio and in the absence and presence of oil after a 90 min time sweep. All biopolymer solutions were at 1.0%, and were acidified with 0.5% (w/w) GDL to pH 4.28 and 4.15 for the WPI- $\kappa$ -CG and WPI- $\iota$ -CG mixtures, respectively. ....	118

## LIST OF ABBREVIATIONS

Å	Angstroms
A <sub>0</sub>	Initial absorbance
A <sub>10</sub>	Absorbance after 10 min
ALA	$\alpha$ -lactalbumin
ALA-1	$\alpha$ -lactalbumin with calcium
ALA-3	calcium depleted $\alpha$ -lactalbumin
ANOVA	Analysis of variance
ANS	8-anilino-1-naphthalenesulfonate
AOAC	Association of Official Analytical Chemists
a.u.	Arbitrary units
$\beta$ -LG	$\beta$ -lactoglobulin
°C	Degrees Celcius
Ca <sup>2+</sup>	Calcium ion
CaCl <sub>2</sub>	Calcium chloride
CD	Circular dichroism
CG	Carrageenan
cm	Centimeters
deg	Degree
dmol	Decimoles
$\Delta A$	Change in absorbance over time
$\epsilon$	Permittivity
EAI	Emulsifying activity index
ESI	Emulsion stability index
F	Farad/meter

FI	Florescence intensity
FTIR	Fourier transform infrared spectroscopy
g	Grams
G'	Storage modulus
G' <sub>i</sub>	Interfacial storage modulus
G''	Loss modulus
G'' <sub>i</sub>	Interfacial loss modulus
GDL	glucono-delta-lactone
HCl	hydrochloric acid
Hz	Hertz
J	Joules
$\kappa$	Debye length (nm <sup>-1</sup> )
K <sup>+</sup>	Potassium ion
KCl	Potassium chloride
kDa	Kilodalton
m	Meter
mg	Milligrams
min	Minutes
mL	Milliliter
mM	Millimolar
mm	Millimeter
mN	Millinewton
$\mu$ m	Micrometers
mPa	Millipascals
mV	Millivolt

mW	Milliwatt
$\eta$	Dispersion viscosity
n	Replicates
N	Newton's
$\text{Na}^+$	Sodium
NaCl	Sodium chloride
NaOH	Sodium hydroxide
nm	Nanometers
OD	Optical density
O/W	Oil-in-water
O/W/O	Oil-in-water-in-oil
PAGE	Polyacrylamide gel electrophoresis
Pa	Pascals
pH <sub>c</sub>	pH where 'soluble complexes' form
pH <sub>opt</sub>	pH associated with the maximum optical density
pH <sub>φ1</sub>	pH where 'insoluble complexes' form
pH <sub>φ2</sub>	pH where complexes dissolve
pI	Isoelectric point
$\phi$	Volume fraction
r	Radius
rpm	Revolutions per minute
s	Seconds
SDS	Sodium dodecyl sulfate
t	Time
T	Absolute temperature in Kelvin

TEM	Transmission electron microscopy
$U_E$	Electrophoretic mobility
W	Watt
WPI	Whey protein isolate
W/O	Water-in-oil
W/O/W	Water-in-oil-in-water
w/w	Weight per weight
$\gamma$	Interfacial Tension (mN/m)

## 1. OVERVIEW

### 1.1 Summary

Emulsion-based products are of great economic importance to the food industry. They comprise of two immiscible phases, such as oil and water, in which one phase is dispersed as droplets within the continuous phase of the other upon the addition of mechanical energy (Schultz *et al.*, 2004). Emulsions may be either oil-in-water (O/W) mixtures, in the case of milk, creams, salad dressings, mayonnaise and soups, or water-in-oil (W/O) mixtures, in the case of margarine and butter. Depending on processing and ingredient formulations, emulsions can be tailored to improve the quality (*e.g.*, mouth feel, texture and viscosity), stability and shelf life of foods, or be used to carry bioactive ingredients for enhanced consumer health (McClements *et al.*, 2007).

Since oil and water are immiscible, the emulsion remains thermodynamically unstable and will tend to separate into distinct phases over time, unless an emulsifier is added to help lower the interfacial tension at the oil-water interface to inhibit the separation process (McClements *et al.*, 2007). Proteins are of great interest due to their amphiphilic nature, which allows them to reduce this tension to make more stable systems. During emulsion formation, proteins diffuse through the aqueous continuous phase to the oil-water interface, and then re-align/unfold to position hydrophobic amino groups' inwards to oil droplets and hydrophilic amino groups outwards towards the water phase (Walstra, 2003). Upon further aggregation, a viscoelastic film forms around the oil droplets to help inhibit phase separation. The film can lead to enhanced stability by exerting an electrostatic repulsive charge into solution (depending on emulsion pH) that repels neighboring droplets, offers steric hindrance that physically restricts droplet flocculation and offers resistance to physical damage (*e.g.*, puncture from ice crystal growth in the case of a frozen product such as ice cream) (Tcholakova *et al.*, 2006a).

The systematic study of proteins at interfaces and the factors that affect their stability (*i.e.*, conformation, pH, solvent conditions and thermal treatment) has allowed for a broader use of protein-stabilized emulsions tailored for various applications. The overall goal of this thesis research were to investigate the effects of pH, temperature pre-treatments and the

addition of carrageenan (CG) on the emulsifying properties of whey proteins in order to better understand underlying structure-function mechanisms. Specifically, the emulsifying properties of  $\beta$ -lactoglobulin ( $\beta$ -LG),  $\alpha$ -lactalbumin (ALA) and a commercial whey protein isolate (WPI) were investigated. The use of carrageenan ( $\kappa$ -,  $\iota$ - and  $\lambda$ -types) to complex with proteins were also explored as it relates to gel formation and its ability to enhance emulsion stability.

## **1.2 Hypotheses**

To address the overall goal of this thesis research, the following hypotheses were tested:

- The influence of pH and temperature pre-treatments on the emulsifying properties of whey proteins will be similar for WPI,  $\beta$ -LG and ALA.
- Emulsion stability will be improved at emulsion pH away from the protein's isoelectric point due to increased electrostatic repulsion, and at higher temperatures of pre-treatment, where protein unfolding will lead to greater exposure of hydrophobic sites and integration into the oil-water interface.
- The addition of carrageenan will improve the emulsion stability when complexed with WPI.
- Emulsions formed using whey protein–carrageenan complexes will show greater stability depending on whether the carrageenan used can form gels (*i.e.* gel-forming  $\kappa$ - and  $\iota$ -types and non-gel forming  $\lambda$ -type).
- Emulsion gels formed with whey protein–carrageenan complexes will be stiffer than their corresponding biopolymer gels.
- Emulsion gels formed with whey protein–carrageenan complexes will become stiffer as a function of carrageenan concentration.

## **1.3 Objectives**

To test the thesis hypotheses, the following objectives were examined:

- To examine the effect of pH and temperature pre-treatment on the physicochemical properties (*e.g.*, surface charge, surface hydrophobicity, interfacial tension and aggregate size) of WPI,  $\beta$ -LG and ALA materials.
- To examine the effect of pH and temperature pre-treatment on the emulsifying properties (*e.g.*, emulsification activity and stability indices) of WPI,  $\beta$ -LG and ALA.
- To examine the effect of WPI-carrageenan-type ( $\kappa$ -,  $\iota$ - and  $\lambda$ -types) coacervation on its gel- and emulsion-forming abilities (*i.e.* turbidity profiles and interfacial properties).
- To characterize the gels formed using small deformation rheology (*i.e.* time sweeps, frequency sweeps and strain sweeps) with WPI–carrageenan coacervates as a biopolymer and as an emulsion gel.
- To examine the effect of carrageenan concentration (for  $\kappa$ - and  $\iota$ -types) on the physical properties of biopolymer and emulsion gels formed with WPI–carrageenan coacervates.

## **2. LITERATURE REVIEW<sup>1</sup>**

### **2.1 Abstract**

Proteins are of great interest due to their amphiphilic nature which allows them to reduce the interfacial tension at the oil-and-water interface. The incorporation of proteins at the oil-and-water interface has allowed scientists to utilize them to form emulsions (O/W or W/O) which may be used in food formulations, drug and nutrient delivery. The systematic study of the proteins at the interface and the factors that affect their stability (*i.e.*, conformation, pH, solvent conditions, and thermal treatment) has allowed for a broader use of these emulsions tailored for various applications. In this review, the factors affecting the stability of emulsions using food proteins will be discussed. The use of polysaccharides to complex with proteins will also be explored as it relates to enhancing emulsion stability.

### **2.2 Introduction**

Emulsions are defined as a dispersion of two or more immiscible liquids in which one of the liquids is dispersed in the other as small droplets (0.1-100 µm) (Dickinson & Stainsby, 1982; Dickinson, 1992; Friberg & Larsson, 1997). Typically in the food industry, emulsions are either oil-in-water (O/W) mixtures, in the case of milk, creams, salad dressings, mayonnaise and soups, or water-in-oil (W/O) mixtures, in the case of margarine and butter. In more advanced systems, multiple emulsions (W/O/W or O/W/O) (Garti, 1997; Sajjaid *et al.*, 2002; Muschiolik, 2007; Pal, 2011) or nanoemulsions (Date *et al.*, 2010; Divsalar *et al.*, 2012; Shakeel *et al.*, 2012) can be formed, which are particularly advantageous for targeted drug/nutraceutical delivery applications (Divsalar *et al.*, 2012; Shakeel *et al.*, 2012). Though emulsions typically form droplet sizes in the (0.1-100 µm), nanoemulsions contain dispersed droplet sizes in the ≤100 nm range (Shakeel *et al.*, 2012). Emulsions are formed by inducing mechanical shear to the mixture either using a

---

<sup>1</sup> Published as: Lam, R. and Nickerson, M.T. (2013) Food proteins: a structure-function approach to their emulsifying properties. *Food Chemistry*, 141, 975-984 (Sections 2.1-2.6 only).

homogenizer, a valve (high pressure) homogenizer or through sparging in order to create small droplets of one liquid dispersed in the other (Schultz *et al.*, 2004).

Emulsions are also formed in the presence of an emulsifier, which comprise of both hydrophobic and hydrophilic components that become integrated at the oil-water or water-oil interface to lower the interfacial tension (Bos & van Vliet, 2001). Emulsifiers may also be in the form of low molecular weight synthetic compounds (*e.g.*, monoglycerides (Goldstein & Seetharaman, 2011), sucrose esters (Tual *et al.*, 2006), polyglycerol esters (Su *et al.*, 2006) natural (*e.g.*, soy or egg lecithin (Palacios & Wang, 2005)) molecules, or be comprised of larger macromolecules, such as proteins (Damodaran, 2006). Emulsifiers form viscoelastic films around dispersed droplets to keep the emulsions stable over time.

Commonly used proteins used by the food industry for their emulsifying abilities include: whey protein isolate (Hu *et al.*, 2003; Ye & Singh, 2006; Li *et al.*, 2012), casein (Mulvihill & Murphy, 1991; Dagleish, 1993; Hu *et al.*, 2003), ovalbumin (Mine *et al.*, 1991; Nakamura *et al.*, 1992; Galazka *et al.*, 2000), soy (Hu *et al.*, 2003; Palazolo *et al.*, 2005; Puppo *et al.*, 2011) and bovine serum albumin (Castelain & Genot, 1996; Kim *et al.*, 2003; Derkach *et al.*, 2007). In addition, the emulsifying properties of emerging protein ingredients, such as from legume (faba bean, lentil, pea and chickpea) (Can Karaca *et al.*, 2011a) and oilseed (canola (Aluko & McIntosh, 2001; Uruakpa & Arntfield, 2005; Can Karaca, Low, & Nickerson, 2011b) and flaxseed (Khalloifi *et al.*, 2009; Wang *et al.*, 2010; Can Karaca *et al.*, 2011b)) crops have also been studied. Table 2.1 gives a summary of various mechanistic studies involving both plant and animal proteins as emulsifiers.

**Table 2.1** Mechanistic studies utilizing plant and animal proteins as emulsifiers.

<b>Protein</b>	<b>Factors Investigated</b>	<b>Measuring Parameters</b>	<b>Reference</b>
Soy and Wheat Gluten	Protein-type, pH, temperature, alteration to pH post-emulsification	Rheology, droplet size	Bengoechea <i>et al.</i> , 2010
Wheat (gliadins)	Hydrolysis, pH, ionic strength	Surface hydrophobicity, emulsion activity index, emulsion stability index, foam capacity, foam drainage	Agyare <i>et al.</i> , 2009
Wheat (Gluten), Bovine Serum Albumin, Casein	Hydrolysis, ionic strength, pH	Foam stability, foam capacity, creaming kinetics, droplet size, resistance to coalescence	Popineau <i>et al.</i> , 1999
Soy and corn germ protein flour	Protein type (soy isolate vs. flour vs. concentrate), pH, temperature	Emulsifying capacity, emulsion stability	Wang & Zayas, 1992
Soy	Temperature	Protein aggregate size, droplet size, calorimetry, interfacial composition, emulsion viscosity, TEM	Keerati-u-rai & Corredig, 2009
Egg	Protein-type (egg yolk vs. whole egg), temperature, addition of sugar, protein concentration, addition of salt (ionic strength)	Turbidity, droplet size, aggregate size (Native-PAGE electrophoresis)	Campbell <i>et al.</i> , 2005
Egg	Protein-type (egg yolk vs. egg white), addition of xanthan gum, storage time	Droplet size, creaming test, optical microscopy, emulsion viscosity, SDS-PAGE	Drakos & Kiosseoglou, 2006
Egg	Addition of polysaccharide, pH	Surface charge, protein adsorption, droplet size	Padala <i>et al.</i> , 2009
Milk (Whey)	Oil concentration, protein concentration, emulsion viscosity, addition of salt, heat treatments	Accelerated creaming test, emulsion viscosity, droplet size	Djordjevic <i>et al.</i> , 2004
Milk	Protein-type (casein vs. whey), pH modification post-emulsification, addition of salt, heat treatment	Droplet size	Hunt & Dagleish, 1995
Milk (Caseinate)	Preparation method (single step vs. two-step), addition of surfactant	Creaming stability, emulsion activity index, droplet size	Einhorn-Stoll <i>et al.</i> , 2002
Lentil	Protein concentration, ionic strength	Interfacial tension, surface hydrophobicity, emulsion stability index, emulsion activity index	Joshi <i>et al.</i> , 2012
Pea	Protein type (commercial preparations vs. isolate), pH, protein concentration	Emulsion stability, foam stability, droplet size	Aluko <i>et al.</i> , 2009
Pea, Fava Bean, Cowpea, French Bean, & Soybean	Protein type, protein concentration, ionic strength, comparison of subunits	Thermal stability, SDS-Page, hydrophobicity, protein solubility, emulsion stability	Kimura <i>et al.</i> , 2008

Soy, Pea, Lentil, Chickpea, & Faba bean	Protein-type, extraction (isoelectric vs. salt extraction)	Surface charge, surface hydrophobicity, protein solubility, interfacial tension, emulsion capacity, emulsion activity index, emulsion stability index, droplet size, creaming stability	Can Karaca <i>et al.</i> , 2011a
Chickpea	Protein extraction (ultrafiltration vs. isoelectric), concentration, protein fractionation	SDS-PAGE, interfacial tension, interfacial rheology, aggregate size, droplet size, concentration of protein at interface, emulsion stability, zeta-potential	Papalamprou <i>et al.</i> , 2010
Milk (Whey), Canola & flaxseed	Protein-type, extraction (isoelectric vs. salt extraction)	Emulsion capacity, emulsion stability, creaming stability, emulsion activity index, surface charge, surface hydrophobicity, interfacial tension, protein solubility, droplet size	Can Karaca <i>et al.</i> , 2011b
Canola	Protein concentration, pH, ionic strength, addition of hydrocolloid	Emulsion activity index, emulsion stability index	Uruakpa & Arntfield, 2005
Gelatin	Hydrolysis, oil polarity, addition of surfactant, pH	Surface tension, interfacial tension, surface charge, emulsion stability	Olijve <i>et al.</i> , 2001
Gelatin and Milk (whey)	Protein content (alone and in mixtures), pH, protein concentration	Surface charge, droplet size, surface protein concentration, surface protein content, emulsion stability, emulsion rheology, optical microscopy, oil oxidative stability	Taherian <i>et al.</i> , 2011

### **2.3 Protein-stabilized emulsions**

Proteins are of particular interest in terms of their emulsifying properties due to their amphiphilic nature (*i.e.*, having both hydrophobic and hydrophilic groups) and film forming abilities (Foegeding & Davis, 2011). Unlike small molecular weight emulsifiers that diffuse rapidly to the interface to give excellent emulsion forming abilities, proteins tend to be bulkier and diffuse at a much slower rate (Figure 2.1A) (McClements, 2005). Once at the interface, some level of partial denaturation (or unraveling) is often needed in order to expose buried hydrophobic amino acids to the surface (Figure 2.1B). Proteins then re-align themselves to position their surface hydrophobic amino acids within the oil phase and hydrophilic amino acids within the aqueous phase (Walstra, 2003). Consequently, emulsion capacity (amount of grams oil per grams protein that can be held, prior to a phase inversion from taking place) tends to be lower than with small molecular weight molecules (Surh *et al.*, 2006). However, once at the interface, strong viscoelastic films can be developed (Figure 2.1C) that resists mechanical stresses, and provides electrostatic (Figure 2.2A) (depending on the solvent conditions) and steric (depending on the protein) stabilization (Figure 2.2B) (Tcholakova *et al.*, 2006a).

The physicochemical properties of proteins play an important role in determining their emulsifying abilities (Moure *et al.*, 2006; Bueno *et al.*, 2009; Papalamprou *et al.*, 2010). For instance, surface hydrophobicity influences the ability for the protein to adsorb to the oil side of the interface, where greater integration typically leads to higher emulsion capacities (Kim *et al.*, 2005). In contrast, surface charge of the protein influences the solubility of the proteins within the aqueous phase, where high solubility is desired for having greater diffusion rates to the interface (Can Karaca *et al.*, 2011a). Once the viscoelastic film is formed, droplets can assume a negative or positive charge depending on whether the emulsion pH is above or below the protein's isoelectric point (and low ionic strength), respectively. High electrostatic repulsion between oil droplets tends to lead to greater emulsion stability, whereas under pH conditions close to the protein's isoelectric point (or high ionic strength) droplet flocculation/aggregation dominates leading coalescence and instability (McClements, 2005). Depending on the protein's size, structure and conformational freedom, 'loops' or 'tails' of protein segments may radiate from the interface comprised of mainly hydrophilic amino acids to create steric stabilization,

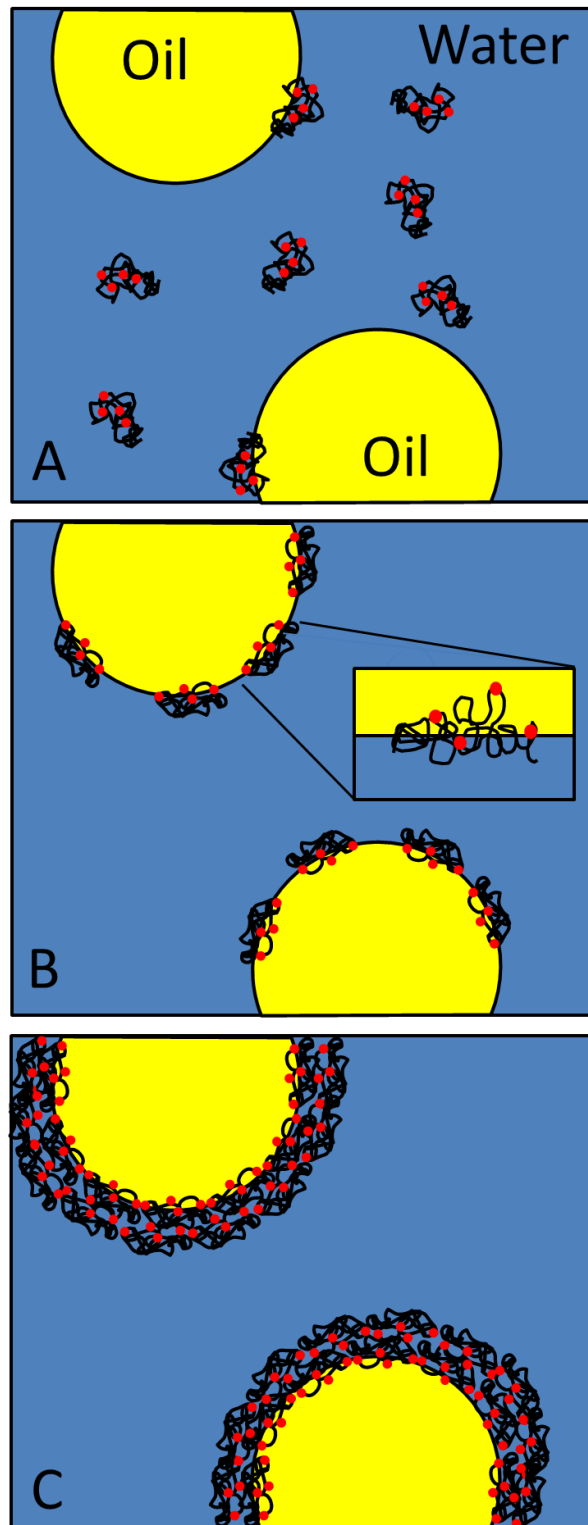


**Figure 2.1** A depiction of globular proteins migrating to the water-oil interface (A) followed by reorientation (B) and viscoelastic film formation (C). The red dots represent hydrophobic moieties found in proteins.

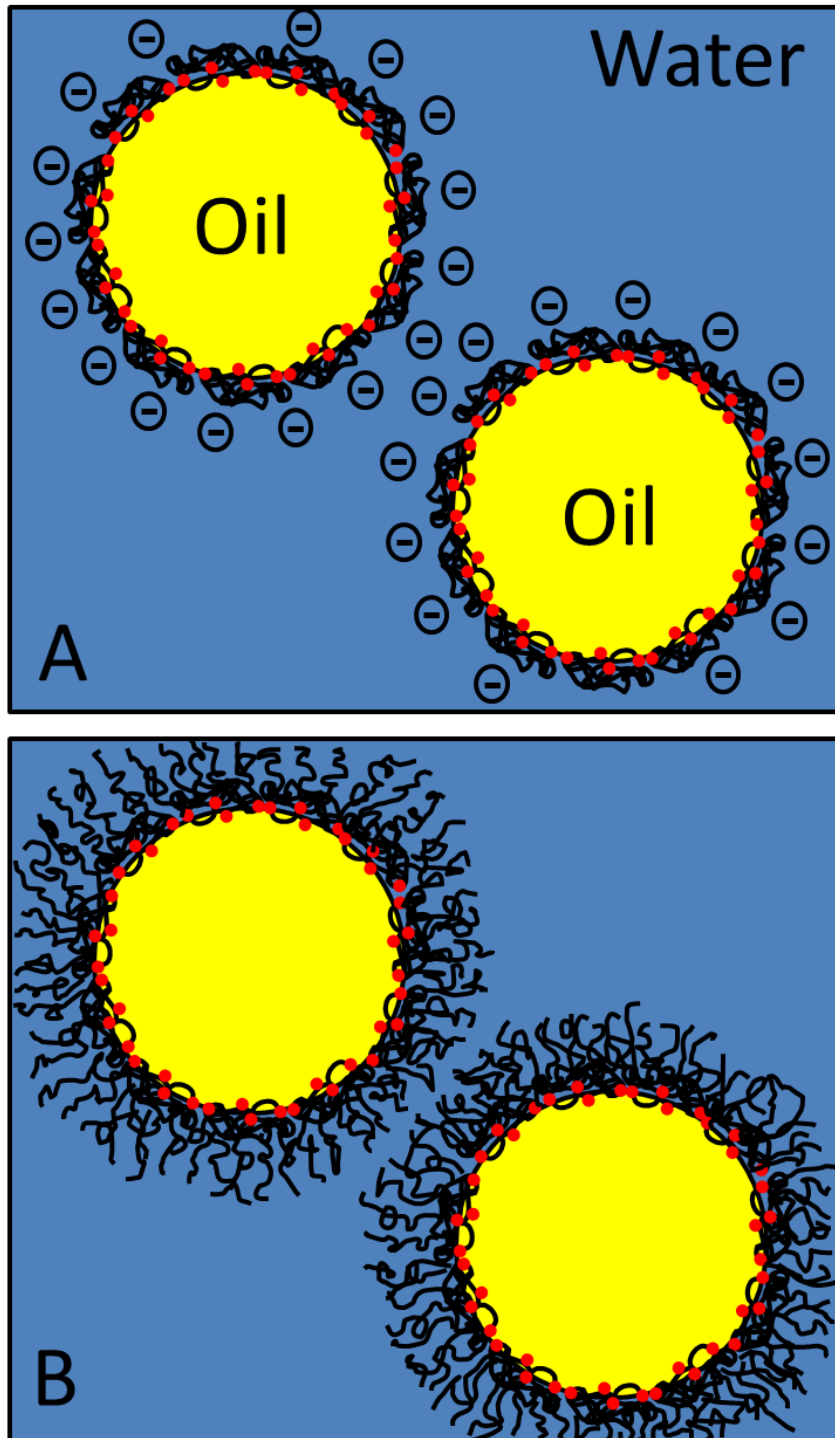


**Figure 2.2** Mechanisms for emulsion stability by (A) electrostatic repulsion and (B) steric stabilization. The red dots represent hydrophobic moieties found in proteins.

physically restricting droplets from coming together (Damodaran, 1996; Tcholakova *et al.*, 2006a). The presence of protein within the continuous phase also acts to increase emulsion viscosity, reducing the mobility and diffusing of oil droplets within the emulsion (Jafari *et al.*, 2012).

Researchers have investigated the use of partial protein hydrolysis to enhance their emulsifying properties. A variety of protein sources (milk (Chobert *et al.*, 1988; Agboola & Dalgleish, 1996; Ramkumar *et al.*, 2000), soy (Jung *et al.*, 2005; Lamsal *et al.*, 2007; Chen *et al.*, 2011), and wheat (Bombara *et al.*, 1997; Popineau *et al.*, 1999; Wang *et al.*, 2006)) have been studied for the effects of hydrolysis on emulsion characteristics. Partial hydrolysis has been used to improve the emulsifying properties of the protein by increasing solubility, revealing hidden hydrophobic groups, increasing its surface hydrophobicity and reducing its molecular weight which allows for better adherence to the oil-water interface (Govindaraju & Srinivas, 2006; Radha & Prakash, 2009; Tsumura, 2009). Protein hydrolysis and the associated improvement to functionality are dependent on the degree of hydrolysis where factors such as the time, temperature and enzyme selected control the resulting product characteristics and functionality (Chobert *et al.*, 1988; Jung *et al.*, 2005; Lamsal *et al.*, 2007). When proteins are highly hydrolyzed, the high concentration of hydrolyzed protein tends to saturate the continuous phase rather than adhere to the water-oil interface (Conde & Patino, 2007). This indicates that the use of protein hydrolysis for increased functionality is limited to low degrees of hydrolysis (Conde & Patino, 2007). In a comparative study of an air-in-water emulsion, partially hydrolyzed proteins were found to decrease both the interfacial viscosity and elasticity while increasing the adherence of the proteins to the interface and improve foam stability (Ipsen *et al.*, 2001).

## 2.4 Destabilizing mechanisms in protein-stabilized emulsions

Over the past decade, mechanisms driving instability within protein-stabilized emulsions have been well documented (Reiffers-Magnani *et al.*, 2000; Ercelebi & İbanoğlu, 2007; van Aken *et al.*, 2011), along with a number of comprehensive reviews (van Aken *et al.*, 2003; Capek, 2004; Tcholakova *et al.*, 2006a; McClements, 2012). Emulsions are inherently thermodynamically unstable systems, where over time the two phases move towards a more stable state that minimizes free energy (*i.e.*, complete phase separation into a denser aqueous layer on the bottom and a less dense upper layer) (Capek, 2004). Under conditions where electrostatic repulsion is reduced (*i.e.*, near the isoelectric point of the protein film or in the presence of high ionic strength), flocculation

and aggregation of oil droplets can lead to partial or complete coalescence (Tcholakova *et al.*, 2006a). The latter refers to the process where films of neighboring droplets fuse and exchange their material, ultimately leading to the formation of a larger droplet. Due to density differences, the larger droplets gravitationally separate and migrate upwards, a process known as creaming (Robins, 2000). Although not dominant, Ostwald ripening also can occur in protein-stabilized emulsions, whereby small oil droplets diffuse through the continuous phase to merge with larger ones (Taylor, 1998).

In addition to thermodynamic instability, emulsions destabilize in the presence of competing biopolymers or changes in protein conformation during aging. Commercial protein preparations (isolates, concentrates) are often mixtures of proteins. The presence of other proteins and/or surfactants influences the interfacial properties by competitive adsorption which is often a factor of the environmental conditions (*i.e.*, pH, ionic strength, *etc.*) in the continuous phase of an emulsion (Tcholakova *et al.*, 2006b). In a study on milk proteins, the dominant protein at an interface is dependent on the concentration of proteins (Sharma & Singh, 1998). Furthermore, the authors demonstrated that there were preferences to adherence on the interface even between proteins among different casein or whey types. Changes in environmental conditions affect the surface hydrophobicity of the protein and its affinity towards the interface (Ramon *et al.*, 2004). Therefore the protein with the highest affinity towards an interface may displace another protein at the interface. Surfactants molecules (*i.e.*, tweens, spans, *etc.*) often displace proteins at the interface as their small molecular weight, maneuverability and strong affinity towards the interface allows them to displace proteins (Diftis & Kiosseoglou, 2004; van Aken, 2003). It was found that though a surfactant may lead to the displacement of proteins from the interface, only certain surfactants, such as Span 80, would lead to coalescence by spontaneous rupture of the thin film formed between droplets (van Aken, 2003). It was noted by van Aken (2003) that though Span 80 is not capable of forming an emulsion itself, its displacement of the proteins at the interface led to a rapid destabilization of the emulsion. Finally, the stability of an emulsion decreases over time due to changes in the protein conformation in addition to the thermodynamic drive for phase separation (Tcholakova *et al.*, 2006a). During aging, proteins form non-covalent bonds, such as hydrogen and hydrophobic bonds, with neighboring proteins at the interface due to conformational changes of the protein over time (Fang & Dingleish, 1997; Kim *et al.*, 2005; Tcholakova *et al.*, 2006a). This change in conformational change and the new non-covalent bonds formed led to a

decrease in emulsion stability (Fang & Dalgleish, 1997; Kim *et al.*, 2005; Tcholakova *et al.*, 2006a).

## 2.5 Protein dynamics and affinity to the oil-water interface

The oil-water interface can be considered as a planar surface with infinitesimal thickness however the interfacial region/film is quite dynamic in nature (McClements, 2005). For instance, within this region there are water-water (*via* hydrogen bonding), oil-oil (*via* van der Waals forces) and water-oil (*via* a hydrophobic effect, whereby water molecules orient away from the non-polar triglycerides to minimize contact) interactions taking place (Mishchuk *et al.*, 2004). With the addition of a protein to the oil-water interface, and depending on its structure/conformation, polar and non-polar amino groups may become dissolved in each phase, despite in some cases being unfavorable. Proteins will then re-orient and re-align to minimize the number of thermodynamically unfavorably interactions, resulting in a decrease in interfacial tension (Bos & van Vliet, 2001). The latter is defined as the free energy required to increase the area of an interface by a unit amount (J/m<sup>2</sup> or N/m) (Bos & van Vliet, 2001). By adhering to the interface, proteins form a viscoelastic film that helps stabilize the dispersed droplets (Tcholakova *et al.*, 2006a).  $\beta$ -lactoglobulin has been reported to be capable of forming a viscoelastic film at the oil-water interface where the interfacial protein film was found to be strengthened following high pressure treatment (Dickinson & James, 1999). However, the types of bonds formed (*i.e.*, hydrophobic, van der Waals, *etc.*) within the protein film will also influence whether or not it will remain at the interface (Tcholakova *et al.*, 2006a). It has been reported that when soy proteins were heat treated at 90°C, proteins exhibited great surface hydrophobicity and formed disulfide bonds with neighboring proteins which enhanced their emulsion stability (Wang *et al.*, 2012). Conversely, excessive hydrophobic bonding among soy proteins treated at 120°C caused aggregates to form which reduced their emulsifying capabilities (Wang *et al.*, 2012). The concentration of proteins occupying the interface tends to be at equilibrium with those in the continuous phase; therefore altering levels present may destabilize/stabilize the equilibrium balance and the concentration of proteins at the interface (McClements, 2005). For example, increases in protein concentration in the continuous phase often correlates to an increase in protein concentration at the interface (Conde & Patino, 2007). Furthermore, changes in concentration have been found to cause changes in the interfacial tension at the oil-water interface (Romero *et al.*, 2011a).

Proteins contain many ionizable groups which alters the electrical characteristics of an interface of oil droplets once adsorbed (Charlambous & Doxstakis, 1989; Damadaran, 1996; Magdassi, 1996; Linfield, 1976; Myers, 1988; Richmond, 1990; Jönsson *et al.*, 1998). These ionisable groups may contain acidic ( $\text{COOH}$ ,  $\text{COO}^-$ , or  $\text{H}^+$ ) or basic ( $\text{NH}_2$  or  $\text{NH}_3^+$ ) moieties which are positively or negatively charged depending on the pH and ionic strength of the aqueous solvent (Charlambous & Doxstakis, 1989; Damadaran, 1996; Magdassi, 1996; Linfield, 1976; Myers, 1988; Richmond, 1990; Jönsson *et al.*, 1998). In a recent study of emulsions stabilized with potato proteins, a change in pH from 2 to 8 improved emulsion stability by changes in the protein surface charge and improved the viscoelastic properties of the interface (Romero *et al.*, 2011a). The improved emulsion stability was attributed to enhanced electrostatic repulsion of potato proteins at pH 8 and the increased elasticity of the proteins at the oil-water interface which resisted mechanical deformation of the droplets (Romero *et al.*, 2011a). At the isoelectric pH, the net charge is neutral which causes a tendency for the protein to aggregate (Foegeding & Davis, 2011). It is the charge and magnitude of these ionisable groups which affect the stability and physical-chemical properties of protein coated oil droplets (Guzey & McClements, 2007). When the interface is highly charged, the stability is enhanced due to electrostatic repulsion between droplets (Guzey & McClements, 2007). Charged surfaces may also attract various molecules such as ions, antioxidants, and flavours which may screen the charge on the interface (McClements, 2005). If the charge at the interface is neutral due to charge screening by ionisable molecules, the stability of the emulsion will be reduced due to the tendency for flocculation (Foegeding & Davis, 2011). Charged interfaces may also bind to divalent ions which may destabilize the emulsion by crosslinking proteins on different droplets causing aggregation to occur (McClements, 2005).

The composition of the continuous phase also dictates how well the protein adsorbs to the interface with respect to quantity and time (Tcholakova *et al.*, 2006a). When proteins adsorb, they often undergo conformational changes to reduce the interfacial tension between the two immiscible liquids (Bos & van Vliet, 2001). Conformational changes are dependent on the structure of the protein and solvent conditions, such that open random-coil structures (*e.g.*,  $\beta$ -casein and gelatins A, B, and F (Bohin *et al.*, 2012)) may rapidly undergo changes while globular structures (*e.g.*,  $\beta$ -lactoglobulin, bovine serum albumin (Baier & McClements, 2005), & ovalbumin (Najbar *et al.*, 2003)) undergo slower changes due to physical restraints (Malmsten, 2003; Norde, 2003; Dickinson, 1992). Proteins that adsorb at high rates may undergo little to no

changes in conformation prior to the saturation of the interface to produce a thick interfacial layer under high concentrations (Bouyer *et al.*, 2012). Yet the thickness of the interfacial layer is not arbitrary such that a study on caseins revealed that the minimum surface coverage was 1 mg/m<sup>2</sup> with a thickness of 5 nm and the maximum surface coverage was reported as 3 mg/m<sup>2</sup> with an interfacial layer of 10 nm (Fang & Dalgliesh, 1993). It has been reported that the four types of caseins have been found to obtain varying thickness at the water and oil interface (Dalgliesh, 1993). Caseins occupy a thickness from 5.4 nm for  $\alpha_{\text{SI}}$ -casein to 11.1 nm for  $\beta$ -casein (Dalgliesh, 1993). Due to changes in conformation, proteins at the interface may display differing proteolytic rates and profiles at the water-oil interface compared to in solution (Agboola & Dalgleish, 1996; Dufour *et al.*, 1998). The degree of proteolysis was reported to be affected by the polarity of the oil-phase due to the conformation of the protein at the water-oil interface (Maldonado-Valderrama *et al.*, 2012). It was previously reported that for  $\beta$ -lactoglobulins, hydrolysis at the interface was much greater than in the bulk solution which was attributed to change in conformation at the interface which enable better access to proteolytic sites (Agboola & Dalgleish, 1996).

Solvent composition (*i.e.*, pH and ionic strength) also affects the ability for proteins to have an affinity for and adhere to the interface (Chen & Dickinson, 1993). Proteins which interact strongly with the interface will adsorb and undergo little to no change in conformation whereas those with weak interactions will adsorb and undergo conformational changes to minimize unfavourable interactions (McClements, 2005). At extreme pHs, proteins tend to unravel or disassociate which exposes more of its hydrophobic core allowing it to better adhere to the interface (Tcholakova *et al.*, 2006b). When a protein unravels, previously hidden sulphydryl groups may form disulfide bonds with itself or other proteins (Wu *et al.*, 2011). This is beneficial if disulfide bonds formed between proteins on the same interface (Dickinson & Matsumura, 1991; Dickinson, 1992) and detrimental for proteins on different droplets (McClements *et al.*, 1993; Kim, Decker, & McClements, 2002a,b). When disulfide bonds are formed at the oil-water interface, enhanced emulsion stability is achieved (Wu *et al.*, 2011). In a study where the sulphydryl group on proteins were successively chemically blocked, emulsions formed yielded less stable emulsions where the interfacial protein layer was found to be ruptured and the oil content ‘leaked’ into the continuous phase (Wu *et al.*, 2011). In contrast, a study using lentil protein isolates indicated that emulsion stability improved when the disulfide bonds were reduced (Joshi *et al.*, 2012). The reduction in disulfide bonds reduced the amount of inter-interface bonding which leads to

coalescence (Joshi *et al.*, 2012). This indicates that though bonding at the interface is important to improve on the viscoelastic properties of the interface which increases emulsion stability, the bonds formed may also occur between two droplet interfaces which are detrimental to emulsion stability.

Changes in the interfacial layer with regards to composition, thickness and the bonds formed between them can also influence the interfacial rheology and tension at the oil-water interface, which dictates how well the interface deforms under stress (McClements, 2005). The interfacial tension measures how effective the protein is at reducing unfavourable interactions, whereas interfacial rheology determines how well proteins are arranged and interacting at the interface which takes into account any bonds (*i.e.*, hydrophobic, disulfide, *etc.*) formed between proteins at the interface (McClements, 2005). Interfacial rheological properties consist of both elastic and fluid-like properties determined by applying a shear stress to the interface to give an interfacial elastic constant and an interfacial viscosity (McClements, 2005). It has been reported from research done on crayfish protein isolates that though changes in pH may have a minor effect on the interfacial tension and the thickness of the interfacial layer, the changes to protein conformation may drastically affect the viscoelasticity of the interfacial layer (Romero *et al.*, 2011b). It was found by Romero and co-workers (2011b) that crayfish protein isolates exhibited much more elasticity at pH 8 than at pH 2 allowing for greater emulsion stability which demonstrates how the bonds formed and conformational changes of the protein affect the viscoelasticity of the interfacial layer. This indicates that interfacial dynamics are an important factor contributing to emulsion stability. The rheological properties of the interface have been found to affect the bulk viscoelasticity of the creams formed (Mackie *et al.*, 2007). Furthermore, protein-based emulsions have been found to have improved emulsion stability in comparison to surfactant-based emulsion which was attributed to differences in the interfacial organization of the protein or emulsifier (Mackie *et al.*, 2007). Proteins formed an elastic interfacial layer due to the bonds formed between adjacent proteins which increased the elasticity of the emulsion (Mackie *et al.*, 2007). Protein's superior emulsifying properties is attributed to their slower changes in conformation at the interface which leads to a lower density network in comparison to surfactant-based emulsions (Mackie *et al.*, 2007). In contrast, surfactant-based emulsions undergo faster conformational changes at the interface due to its small molecular weight which gave a well-packed, concentrated cream layer (Mackie *et al.*, 2007).

## **2.6 Effect of polysaccharides on protein-stabilized emulsions**

The addition of anionic polysaccharides to protein-stabilized emulsions may result in either a positive or negative effect on emulsion stability. The level of protein-polysaccharide interactions can depend on a large number of factors, including biopolymer characteristics (*i.e.*, size, conformation, mixing ratio, biopolymer-type, and type and distribution of reactive sites), solvent conditions (*i.e.*, pH, salts and temperature), total biopolymer concentration and emulsion preparation method (Neirynck *et al.*, 2004; Padala *et al.*, 2009; Liu *et al.*, 2010; Stone & Nickerson, 2012; Tippetts & Martini, 2012; Yin *et al.*, 2012). A comprehensive review on complex coacervation involving biopolymer interactions has been given by Schmitt and co-workers (Schmitt *et al.*, 1998), and as such is not within the scope of this review. Emulsion preparation in mixed systems, can greatly influence the composition, structure and dynamic behaviour of biopolymers at the interface. For instance, homogenization involving a mixed protein-polysaccharide aqueous solution (under specific solvent conditions) and an oil phase leads to the formation of a homogenous biopolymer film at the interface (Figure 2.3A) (Weinbreck *et al.*, 2004a). In contrast, using a multi-step process in which a primary emulsion involving an aqueous protein and oil mixture is first formed and then followed by the addition of a polysaccharide solution (under specific solvent conditions) to a pre-formed emulsion (Figure 2.3B). The latter process can result in a multi-layer biopolymer interface based on the principle of layer-by-layer deposition (Klinkesorn *et al.*, 2005; Guzey & McClements, 2006).

The addition of a polysaccharide to protein-based emulsions has been reported to enhance emulsion stability. Polysaccharides have been found to electrostatically associate with proteins forming a coacervate (Liu *et al.*, 2009). Researchers have reported that emulsions made with mixtures of protein and polysaccharide were less susceptible to destabilization by flocculation compared to those formed by multi-layer deposition (Jourdain *et al.*, 2008). The choice of polysaccharide (*i.e.*, type and size) has also been found to greatly affect the stability of the

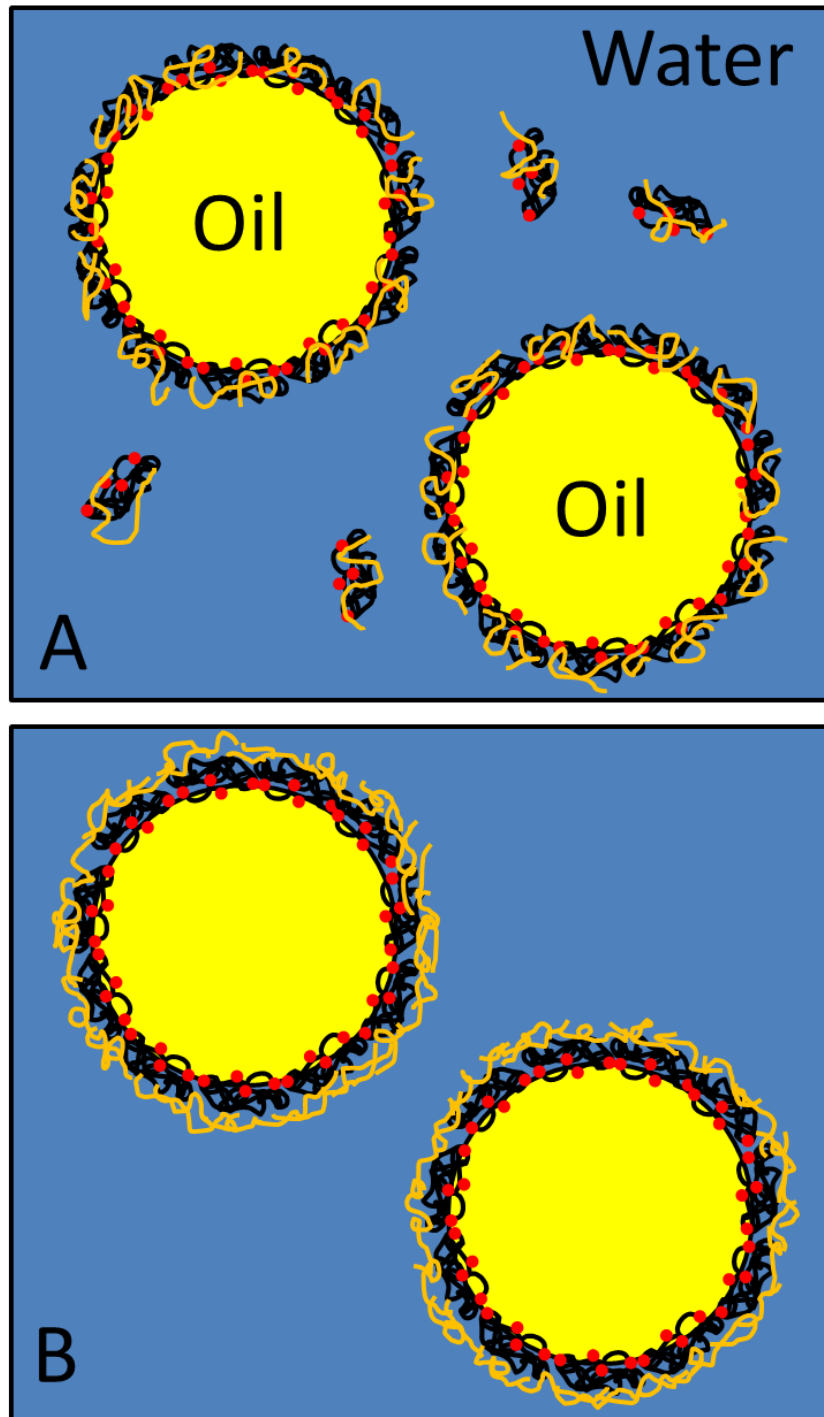


**Figure 2.3** Representations of a (A) homogenous mixed polysaccharide-protein emulsion and (B) emulsion formed using a layer-by-layer deposition technique. The red dots represent hydrophobic moieties found in proteins whereas orange strands represent polysaccharides.

emulsion dependent on solvent conditions (*i.e.*, pH and ionic strength) (Hayati *et al.*, 2009). Other factors such as the biopolymer characteristics (*e.g.*, protein surface charged groups), concentration, ratio, and solvent conditions (*e.g.*, pH, temperature and ionic strength) all play a significant role as to the formation of a coacervate (Turgeon *et al.*, 2003; Weinbreck *et al.*, 2003; Chourpa *et al.*, 2006). In a study where soy soluble polysaccharides were mixed with soy protein isolate, greater emulsion stability using this protein-polysaccharide mixture was attributed to the capacity for polysaccharides to coat the proteins to prevent protein-protein interactions between two droplets (Tran & Rousseau, 2013). When polysaccharides bind to proteins at the interface, they change the rheology of the emulsion depending on the polysaccharide used (Hayati *et al.*, 2009). For instance, the addition of gum Arabic to an egg protein-stabilized emulsion turned the rheology of the emulsion from a Newtonian fluid to a Bingham plastic while the use of the other polysaccharides (*i.e.*, locust bean gum, guar gum, carboxymethyl cellulose and xanthan gum) resulted in shear thinning behavior (Hayati *et al.*, 2009). Stone and Nickerson (2012) investigated the nature of the protein-polysaccharide interaction and have reported for three forms of carrageenan (kappa-, iota-, and lambda-) that the adsorption of carrageenan onto the whey protein isolate depended on their linear charge densities and conformation. Harnsilawat and co-workers (2006) found that protein-polysaccharide complexes increase emulsion stability when the polysaccharide was able to coat the protein's surface. Mixed protein-polysaccharide emulsions have also been reported to have better freeze-thaw stability in freeze-dried emulsions (Mun *et al.*, 2008) and have been utilized to improve the stability of double emulsions used for drug delivery (O'Regan & Mulvihill, 2010; Perrechil & Cunha, 2012).

In contrast, mixed biopolymer systems have also led to emulsion instability. Due to the electrostatic nature of this complexation, emulsions stabilized by protein-polysaccharide coacervates are sensitive to changes in pH and ionic strength (Tran & Rousseau, 2013; Jourdain *et al.*, 2008). For instance, bridging flocculation whereby a polysaccharide molecule electrostatically complexes to a protein-film surround more than one oil droplet leading to aggregation (Figure 2.4A) (Blijdenstein *et al.*, 2004). This process has been reported for bovine serum albumin-dextran sulfate (Dickinson & Pawlowsky, 1996), pea protein-high methoxyl pectin (Gharsallaoui *et al.*, 2010), faba bean protein-dextran (Dickinson & Semenova, 1992) and  $\beta$ -lactoglobulin-sodium alginate (Pongsawatmanit *et al.*, 2006) stabilized emulsions. Depletion flocculation may also occur where a non-adsorbing polysaccharide in solution causes

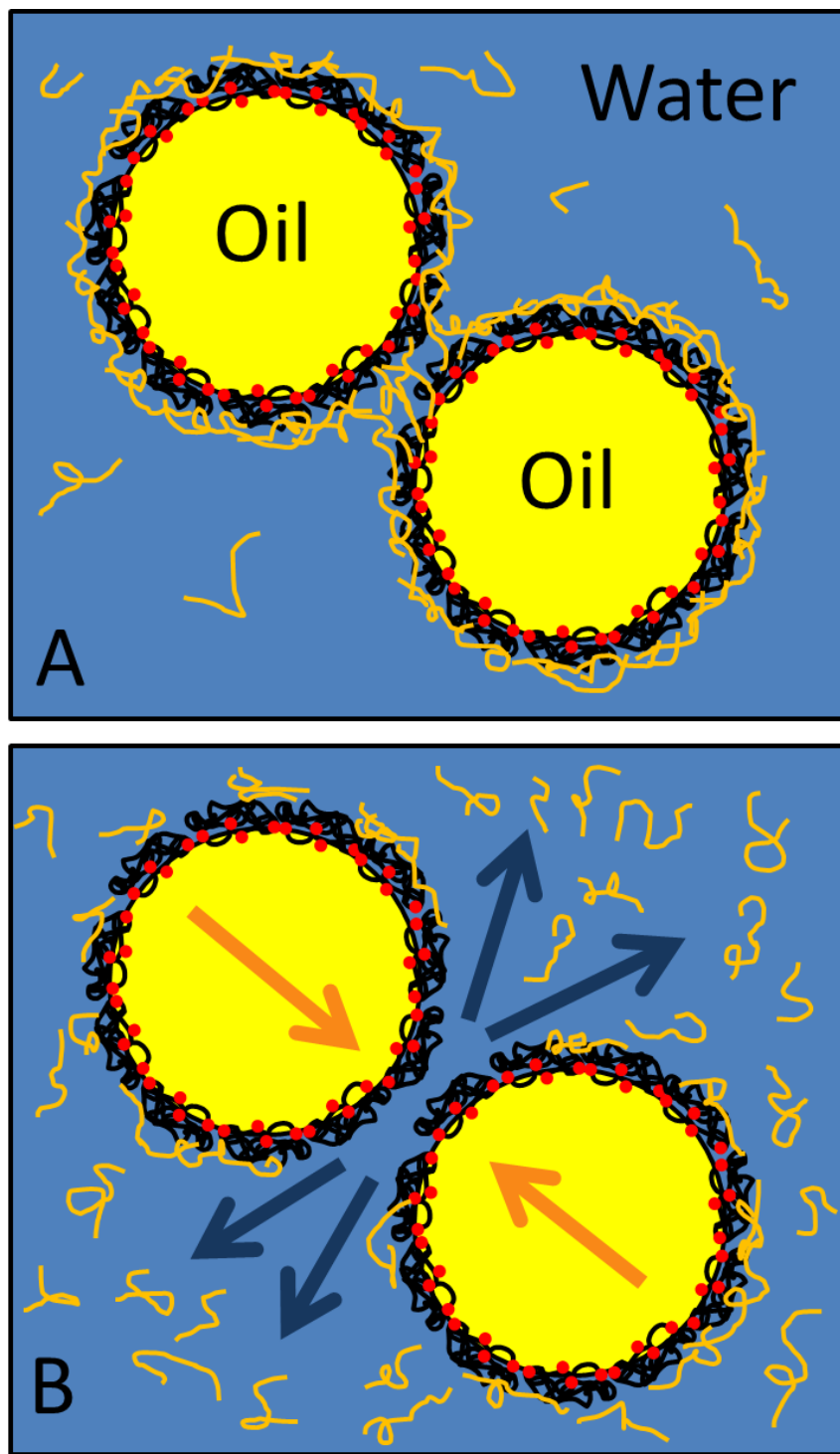


**Figure 2.4** Mechanisms for protein-polysaccharide emulsion destabilization as represented by (A) bridging flocculation and (B) depletion flocculation. The red dots represent hydrophobic moieties found in proteins whereas orange strands represent polysaccharides.

flocculation when the non-adsorbing polysaccharide is above a specific concentration (Figure 2.4B) (Jenkins & Snowden, 1996; Chanamai & McClements, 2006). At the depletion flocculation concentration, when two adjacent droplets approach each other, the space between the two droplets is devoid of polysaccharide which drives an osmotic gradient to remove the solvent between the two droplets causing flocculation (Jenkins & Snowden, 1996; Chanamai & McClements, 2006). Depletion flocculation occurs when both the protein and polysaccharide are both similarly charged (*i.e.*, cationic or anionic) and is characterized by an increased stability below and decreased stability above the respective critical concentration (Jenkins & Snowden, 1996; Chanamai & McClements, 2006). This process has been reported for faba bean protein-dextran (Dickinson & Semenova, 1992), ovalbumin-carrageenan (Galazka *et al.*, 2000), soy protein isolate-high methoxyl pectin (Roudsari *et al.*, 2006) and sodium caseinate-kappa-carrageenan (Vega *et al.*, 2005) stabilized emulsions. Both mechanisms of instability have also been reviewed by Dickinson (2003) and Syrbe and co-workers (1998).

## 2.7 Choice of materials

### 2.7.1 Whey proteins

Whey is a fluid by-product from the manufacture of cheese after either acid (known as acid whey) or enzymatic (with rennet, known as sweet whey) precipitation of casein proteins (Kilara, 2008). Whey is comprised of 94% water, 4.5% lactose, 0.8% protein and 0.7% minerals (Kilara, 2008). The protein content represents ~20% of the total proteins found in bovine milk, whereas caseins ( $\alpha_{s1}$ ,  $\alpha_{s2}$ ,  $\beta$ - and  $\gamma$ -types) represent the remaining 80% (Swaisgood, 2008). Whey proteins are considered highly nutritious due to their high levels of sulfur-containing amino acids, and are of functional importance due to their high solubility, and good foaming, emulsifying and gelling properties (El-Salam *et al.*, 2009). Whey proteins have been utilized in a variety of food applications such as baked products, beverages, desserts, confectionery and meat products (Mulvihill, 1992). Whey proteins are typically extracted from whey using various membrane technologies, such as ultrafiltration and reverse osmosis in order to concentrate the proteins, and to remove other milk constituents. Depending on the process, different compositions may arise in the final product, associated with the different pore sizes of the membrane used for extraction. For instance, when reverse osmosis is used, only water passes through leaving proteins, minerals and sugars in the retentate. In contrast, extraction by ultrafiltration enables water, minerals and sugars

to pass, leaving mainly proteins in the retentate (Goff, 2011). The protein-rich retentate is typically then spray dried to yield a whey protein concentrate (>80% protein, on a dry weight basis) or isolate (>90% protein, on a dry weight basis) product.

In the present research, the emulsifying properties of whey protein isolate (WPI),  $\beta$ -lactoglobulin ( $\beta$ -LG) and  $\alpha$ -lactalbumin (ALA) will be investigated, as it relates to their role in stabilizing the oil-water interface. The latter two were selected since they represent the dominant sub-class of whey proteins. Whey proteins were also selected over casein for this study due to the increasing frequency of allergenicity towards bovine caseins in humans (Spuergin *et al.*, 1997; Bernard *et al.*, 1998; Sharma *et al.*, 2001). Although the emulsifying properties of WPI,  $\beta$ -LG and ALA have been widely been studied, there is a continual need for information on how changes in protein conformation in response to different solvent conditions (*i.e.*, ionic strength, pH, temperature) and interactions with other biopolymers (*i.e.*, polysaccharides) influence their interfacial and emulsifying properties.

Whey proteins are dominated by  $\beta$ -LG (~9.8% of total protein in bovine milk) and ALA (3.7%) proteins, along with blood proteins such as proteose-peptones (2.4%), serum albumin (1.2%) and immunoglobulins (2.1%) (Walstra & Jenness, 1984). These proteins can be separated by further processing the isolate product by electrodialysis or ion exchange chromatography to separate out the specific proteins based on charge (Goff, 2011). Lee and co-workers (2008) reported the isoelectric point of WPI to be pH 4.6 and, Bernal and Jelen (1985) found the denaturation temperature to be 88°C, however the exact temperature depends on the materials preparation method, heating conditions and protein composition within the isolate. The emulsifying properties of WPI have been widely studied in literature. For instance, Hunt and Dalgleish (1995) studied the stability of WPI emulsions where they were able to form stable emulsions at pH 3.0 and 7.0 at high temperatures (*i.e.*, 90°C) while the addition of salt (KCl) or adjusting the pH (*i.e.*, to 3.5-4.0) led to the destabilization of these emulsions. Sliwinski and co-workers (2003) found that at temperatures above 70°C, there is a heat-induced thickening behavior of the formed emulsions. Furthermore Dickinson and Parkinson (2004) reported that emulsion stability also depended on the method of WPI extraction.

## 2.7.2 $\beta$ -Lactoglobulin

$\beta$ -LG (18.2 kDa; pI = 5.2) is a globular  $\beta$ -barrel shaped protein with a short  $\alpha$ -helix on its surface (de Wit & Kessel, 1996; Shin *et al.*, 2007; Swaisgood, 2008). The barrel cavity is ~20 Å in diameter, and comprised primarily of hydrophobic amino groups (Abduragimov *et al.*, 2000). As a result,  $\beta$ -LG only interacts weakly with other proteins, but is capable of carrying hydrophobic compounds (*e.g.*, fatty acids (Abduragimov *et al.*, 2000), vitamin D and cholesterol (Wang *et al.*, 1997)) within its cavity (Swaisgood, 2008). The presence of sulfhydryl groups also enables it to participate in inter- and intra-molecular disulphide bridging. Its structure is sensitive to both pH and temperature changes, where depending on the solvent pH,  $\beta$ -LG is known to form monomers, dimers and octamers (Swaisgood, 2008). At solvent pH below 3.5 and above 7.5,  $\beta$ -LG exists as a monomer, whereas between pH 5.2 and 7.5,  $\beta$ -LG forms dimers which then tetramerizes into an octamer between pH 3.5 and 5.2 (Swaisgood, 2008). Haug and co-workers (2009) determined that the denaturation temperature of  $\beta$ -LG using differential scanning calorimetry is dependent on both pH and salt conditions where the denaturation temperature may raise as much as 18°C from pH 9 to 2 and increase approximately 7°C at pH 9 by increasing the salt content from 100 mM to 500 mM.

The emulsifying properties of  $\beta$ -LG have also widely been studied in the literature (Dickinson & Hong, 1994; Fang & Dalgleish, 1997; Kim *et al.*, 2004; Tcholakova *et al.* (2006b)). Dickinson and Hong (1994) reported that the application of a temperature pre-treatment to the proteins prior to emulsification lead to better surface coverage. Tcholakova *et al.* (2006b) reported similar findings, and also found that at higher pre-treatment temperatures, proteins absorbed irreversibly to the interface leading to greater steric repulsion and enhanced emulsion stability. Kim and co-workers (2004) reported the formation of stable  $\beta$ -LG emulsions at pH 3 and 7, but found emulsions pH 7 became unstable in the presence of salt and isothermally heat treated for 20 minutes at >70°C. And, Fang and Dalgleish (1997) studied conformational changes of  $\beta$ -LG at the water-oil interface to find the resistance to heat denaturation was greater at pH 6 than 7 using FTIR, caused by the formation of intermolecular beta-sheets.

## 2.7.3 $\alpha$ -Lactalbumin

In contrast, ALA is a globular protein (14-16 kDa; pI = 4.2) that consists of two domains: the  $\alpha$ -domain, is comprised of four  $\alpha$ -helices, whereas the  $\beta$ -domain is comprised of  $\beta$ -sheets and

looped regions (Bramaud *et al.*, 1995; Wu *et al.*, 1996; Wang & Lucey, 2003). ALA, which contain four disulphide bonds, whose tertiary structure folds or unfolds in the presence and absence of calcium, respectively (Swaisgood, 2008). Calcium binds to ALA to cause it to fold into a compact structure where more of its hydrophobic groups are buried in the interior. In contrast, in the absence of this calcium, ALA exists in an open, unfolded conformation (Owusu, 1992; Swaisgood, 2008). Boye and Alli (2000), and Relkin and co-workers (1993) reported that there are two denaturation temperatures associated with ALA at ~35°C and ~64°C, corresponding to the denaturation of the calcium-free and calcium-bound ALA, respectively. ALA is also capable of refolding, and unlike other milk proteins, is not irreversibly denatured under milk processing (Swaisgood, 2008).

The emulsifying properties of  $\alpha$ -LA have also been widely studied in literature (Hunt & Dalgleish, 1994a; Matsumura *et al.*, 1994; Fang & Dalgleish; 1998; Tossavainen *et al.*, 1998). Tossavainen and co-workers (1998) reported that heat aggregated ALA showed reduced emulsion stability compared to those obtained using an anion exchange process. Hunt and Dalgleish (1994) reported that both ALA and  $\beta$ -LG formed stable emulsions at pH 7, however ALA was preferentially adsorbed, by analyzing the proteins found in the cream layer, to the interface at lower pH. Matsumura *et al.* (1994) investigated the conformation of ALA at the oil-water interface and reported that in the absence of calcium and at low pH, ALA assumes an unfolded conformation enabling greater absorption to the interface. Fang and Dalgleish (1998) reported using FTIR that heating  $\geq 90^\circ\text{C}$  irreversibly alters the structure of ALA and changes in pH had less of an effect on the absorption characteristics whereas conformational changes of ALA at the water-oil interface greatly depended on the protein concentration.

## 2.7.4 Carrageenan

Carrageenan (CG) is a family of linear, sulphated polysaccharides which has been extracted from red seaweeds (*Rhodophyta* species) (van der Velde *et al.*, 2002). They have been extensively used in the food industry to enhance the rheology of a product as thickeners, stabilizers and gelling agents (Campo *et al.*, 2009). They have also been incorporated in meat products to replace fat (Trius *et al.*, 1996) and to help stabilize drinks such as chocolate milk. CG polysaccharides consist of disaccharide repeating units comprised of D-galactose and 3,6-anhydro-D-galactose residues, with one, two or three sulphate groups associated with the disaccharide repeating unit of  $\kappa$ -,  $\iota$ - and  $\lambda$ -type CG, respectively (Weinbreck *et al.*, 2004b; Campo *et al.*, 2009). However, three other forms

have been identified ( $\mu$ -,  $\nu$ - and  $\theta$ -type) by Knutsen *et al.* (1994). The  $\mu$ - and  $\nu$ -type CGs are thought to be biological precursors to the more abundant  $\kappa$ - and  $\iota$ -types (van de Velde *et al.*, 2001; Campo *et al.*, 2009). Commercial CG typically has an average molecular mass between 100 and 1000 kDa (Campo *et al.*, 2009).

Recently, the electrostatic complexation between WPI and CG ( $\kappa$ -,  $\iota$ - and  $\lambda$ -type) was studied as a function of pH, biopolymer mixing ratio and NaCl addition by Stone and Nickerson (2012). The authors reported complex formation followed by two pH-dependent events associated with the formation of soluble and insoluble complexes. Maximum complexation was found to occur at a 12:1 ratio for both the WPI- $\kappa$ -CG and WPI- $\lambda$ -CG mixtures, and a 20:1 ratio for the WPI- $\iota$ -CG mixture near pH 4.5. The addition of NaCl disrupted complexation within WPI- $\kappa$ -CG mixtures as levels were raised, whereas when  $\iota$ -CG or  $\lambda$ -CG was present, complexation was enhanced up to a critical NaCl concentration before declining. Emulsion stability in the mixed systems (12:1 mixing ratio), irrespective of the CG type ( $\kappa$ ,  $\iota$  or  $\lambda$ ), was significantly higher than in WPI solutions, indicating enhanced ability to stabilize the oil-in-water interface.

### **3. THE EFFECT OF PH AND TEMPERATURE PRE-TREATMENTS ON THE PHYSICOCHEMICAL AND EMULSIFYING PROPERTIES OF WHEY PROTEIN ISOLATES<sup>2</sup>**

#### **3.1 Abstract**

The overall goal of this research was to investigate the structure-function mechanisms associated with the emulsifying properties of whey protein isolate (WPI) as a function of pH (3.0, 5.0 and 7.0) and temperature pre-treatments (at 25, 55 and 85°C). Specifically, the physicochemical (*i.e.*, surface charge and hydrophobicity, size and interfacial tension) and emulsifying (*i.e.*, emulsification activity (EAI) and stability indices (ESI)) properties of WPI were assessed. Overall, surface hydrophobicity was greatest at pH 5.0/85°C, whereas at all the other sample treatments it was significantly lower. Surface charge was found to decrease linearly from ~ +40 mV at pH 3.0 to ~ -40 mV at pH 7.0, where net neutrality was obtained between pH 5.1 and 5.4 depending on the pH and temperature conditions. Aggregate size was the highest at pH 5.0 relative to the other pHs, however it declined in size (hydrodynamic radii) at pH 5.0 from 1589 nm to 1450 nm and then to 832 nm as temperature pre-treatments increased from 25°C to 55°C and then to 85°C, respectively. Interfacial tension was reduced from ~28 mN/m to ~14-18 mN/m for systems in the absence and presence of WPI, respectively. Little differences were seen among the various sample treatments for lowering interfacial tension. Emulsion formation (EAI) was found to increase under conditions where WPI aggregation was reduced, whereas stability (ESI) increased under conditions away from its isoelectric point where electrostatic repulsive forces were strongest and under conditions where surface hydrophobicity was reduced.

#### **3.2 Introduction**

Whey protein isolate (WPI) is an economically important by-product of the cheese manufacturing process, used as an ingredient by the food industry because of its high nutritional

---

<sup>2</sup> Accepted as: Lam, R. and Nickerson, M.T. (2014). The effect of pH and Temperature Pre-Treatments on the Physicochemical and Emulsifying Properties of Whey Protein Isolates. *LWT – Food Science and Technology*.

value and functional attributes. Whey proteins comprise of a mixture of proteins, dominated by  $\beta$ -lactoglobulin and  $\alpha$ -lactalbumin with minor amounts of proteose-peptones, serum albumin and immunoglobulins (Walstra & Jenness, 1984; Ju *et al.*, 1999; Schokker *et al.*, 2000a). Functionally, WPI has high solubility, and has good foaming, gelling and emulsifying properties (Swaisgood, 2008). The structure-function relationship of whey proteins has been widely studied in literature, especially as it relates to their aggregative properties and nature of interactions (*e.g.*, hydrophobic interactions, hydrogen bonding, electrostatic interactions and thiol-disulfide exchange reactions) (Altinga *et al.*, 2000; Fessas *et al.*, 2001; Mounsey & O'Kennedy, 2007; Zúñiga *et al.*, 2010; Ryan *et al.* 2012). These interactions can be tailored by altering the physicochemical properties of the WPI molecules by pre-treating the proteins with temperature to partial or completely unravel the protein structure to expose buried hydrophobic moieties (Krebs *et al.*, 2007; Hussain *et al.*, 2012), or by adjusting the pH near or away from its isoelectric point to alter the surface chemistry of the proteins (Bryant & McClements, 1999; Kazmierski & Corredig, 2003). As a consequence, the aggregative nature of the WPI can be altered. For instance, Bryant and McClements (1999) and, Kazmierski and Corredig (2003) reported larger aggregates of whey proteins are formed under conditions where the protein charge is neutral and at higher temperatures. A greater understanding of the effect of pH and pre-treatment conditions on WPI could lead to greater control over functional attributes, such as their ability to align at an oil-water interface to form and stabilize an emulsion.

An emulsion is a mixture of two immiscible liquids where one is finely dispersed as droplets within another (Robins *et al.*, 2002). WPI, like other proteins are amphiphilic in nature allowing them to act as emulsifiers to stabilize the oil-water interface (Laleye *et al.*, 2008). During emulsion formation, mechanical shear is induced to create oil droplets within a continuous aqueous phase. Proteins within this phase act to migrate through the aqueous phase to the interface, and then re-align to position its hydrophilic amino acids towards the water and hydrophobic amino acids towards the oil phase (Dickinson, 2001). Proteins at the interface then accumulate and aggregate to form a viscoelastic film around the oil droplet to keep the emulsion stable (Dickinson, 2001). In the present study, the effect of pH and temperature pre-treatments was studied as a means of modifying the physicochemical properties of WPI so that its emulsion forming properties and stabilizing abilities could be tailored.

### **3.3 Materials and methods**

#### **3.3.1 Materials**

Whey protein isolate (WPI) used in this study was generously donated by Davisco Foods International, Inc. (Le Sueur, MN, USA). The chemical composition of the commercial WPI powder was determined according to AOAC (2003) methods; 925.10 (moisture), 923.03 (ash), 920.87 (crude protein), and 920.85 (lipid). Carbohydrate content was denoted as the difference of the other components (*i.e.* protein, moisture, lipid and ash) from 100%. The WPI powder comprised of 89.78% protein (%N × 6.38), 0.10% lipid, 4.92% moisture, 2.06% ash (including 0.08% Ca<sup>2+</sup>, 0.01% Mg<sup>2+</sup>, 0.02% K<sup>+</sup>, and 0.66% Na<sup>+</sup>), and 3.13% carbohydrate (wet basis). Canola oil used in this study was purchased from a local supermarket. All other chemicals used in this study were of reagent grade and purchased through Sigma-Aldrich (Oakville, ON, Canada). The water used in this research was filtered using a Millipore Milli-Q™ water purification system (Millipore Corp., Milford, MA, USA). The WPI protein solutions were used without further purification.

#### **3.3.2 Sample preparation**

WPI solutions (0.1%, protein w/w) were prepared by dispersing the WPI powder in water adjusted to 3.0, 5.0 or 7.0 pH using either 0.5 M HCl or 0.5 M NaOH, followed by mechanically stirring (500 rpm) at room temperature (21-23°C) for 60 min. Protein solutions were then poured into screw capped test tubes to prevent moisture losses, and held in a water bath for 30 min at 25°C, 55°C and 85°C. Tubes were then cooled down to room temperature prior to analysis. All samples were prepared in triplicate.

#### **3.3.3 Circular dichroism**

Circular dichroism (CD) was performed on 0.02% w/w WPI solutions using the PiSTar-180 spectrometer (Applied Photophysics, Surrey, UK) equipped with a 75W Mercury Xenon Lamp. CD was performed on samples contained in quartz curvettes with a pathlength of 0.5 mm. CD spectra was taken from 190 to 240 nm at intervals of 0.5 nm with slits set at 6.0 nm. This technique was used to measure relative changes in the protein's secondary structure among the various pH and temperature treatments. A flattening of the spectra was taken as a loss in secondary

structure. The average of 4 spectra was reported as a replicate for each sample which was prepared in triplicate.

### 3.3.4 Surface hydrophobicity

Hydrophobicity for each protein solution was determined by extrinsic fluorescence using a fluorescent probe method and, by intrinsic fluorescence as a function of emission wavelength.

(a) *Fluorescent probe method:* Surface hydrophobicity for each protein solution was measured based a modified method of Kato and Nakai (1980), which uses a 8-anilino-1-naphthalenesulfonate (ANS) probe to interact with hydrophobic moieties on the protein's surface to give a fluorescent signal. Stock solutions (0.07% w/w) of each protein solution were prepared, and then diluted to concentrations of 0.03%, 0.04%, 0.05% and 0.06% (w/w). Twenty microliters of a 8 mM ANS solution (in water, adjusted to the specific pH of the protein solution) was then added to 1.6 mL of each protein solution, vortexed for 15 s, and then kept in the dark for 5 min. A similar concentration series was prepared and measured for each protein sample, but without the ANS probe as a control, and a water-ANS probe mixture as a blank. Fluorescence intensity was measured for each sample using a FluoroMax-4 spectrofluorometer (Horiba Jobin Yvon Inc., Edison, N.J., USA) at excitation and emission wavelengths of 390 and 490 nm, respectively, and using a slit width of 1 nm. Net fluorescence intensity was determined by subtracting the intensity of the control (without ANS) and the blank, from the intensity of the protein solution with ANS, at each protein concentration. The slope of the net fluorescence as a function of protein concentration, as determined by linear regression served as an index of sample relative hydrophobicity. All measurements were made in triplicate protein solutions.

(b) *Intrinsic fluorescence:* FluoroMax-4 spectrofluorometer (Horiba Jobin Yvon Inc., Edison, N.J., USA) was used to determine the intrinsic fluorescence for 0.05% (w/w) protein solutions at a constant excitation wavelength of 295 nm using a slit width of 2.5 nm as a function of emission wavelength between 285 to 450 nm using a 5.0 nm slit width at increments of 0.5 nm. Intrinsic hydrophobicity measures the fluorescence the aromatic amino acids of tyrosine, tryptophan and phenylalanine. The maximum fluorescence intensity (in arbitrary units) was determined for each spectra captured. All measurements were made in triplicate.

### 3.3.5 Electrophoretic mobility

The electrophoretic mobility ( $U_E$ ) was determined using the Zetasizer Nano-ZS90 (Malvern Instruments, Westborough, MA) for all protein samples. The zeta-potential ( $\zeta$ ; units: mV) was determined from the electrophoretic mobility ( $U_E$ ) using Henry's equation (eq. 3.1):

$$U_E = \frac{2\epsilon\zeta f(\kappa\alpha)}{3\eta} \quad (\text{eq. 3.1})$$

where  $\epsilon$  is the permittivity (units: F (Farad)/m),  $f(\kappa\alpha)$  is the function related to the ratio of particle radius ( $\alpha$ ; units: nm) and Debye length ( $\kappa$ ; units: nm<sup>-1</sup>), and  $\eta$  is the dispersion viscosity (units: mPa·s) (McClements, 2005). The Smoluchowski approximation  $f(\kappa\alpha)$  was set as 1.5, as is accustom for folded capillary cells and, with particles larger than 0.2 μm dispersed in moderate electrolyte concentration (>1 mM). The Smoluchowski approximation assumes that a) concentration of particles (proteins) is sufficiently high such that such thickness of the electric double layer (Debye length) is small relative to the particle size ( $\kappa\alpha >> I$ ); and b)  $\zeta$  is linearly related to  $U_E$ . All measurements are reported as the mean ± one standard deviation (n = 3).

### 3.3.6 Aggregate size

The hydrodynamic radius for WPI aggregates formed under the different pH and heat pre-treatment conditions were measured using the Zetasizer Nano-ZS90 (Malvern Instruments, Westborough, MA, USA). Approximately 1 mL of each protein solution was placed in a plastic curvette (1 cm path length) within the Zetasizer's sample holder. The scattering intensity was measured at a 90° angle at 633 nm using a 4 mW He/Ne laser at 25.0°C. The hydrodynamic radius was estimated based on the Stokes-Einstein equation (Eq. 3.2 and 3.3):

$$D = \frac{k_B T}{6\pi\eta r} \quad (\text{eq. 3.2})$$

which may be re-written as:

$$r = \frac{k_B T}{6\pi\eta D} \quad (\text{eq. 3.3})$$

Where,  $k_B$  is the Boltzmann constant ( $1.38062 \times 10^{-23}$  J K<sup>-1</sup>),  $D$  is the self-diffusion constant (m<sup>2</sup> s<sup>-1</sup>),  $T$  is the absolute temperature (K),  $\eta$  is viscosity of the medium (kg m<sup>-1</sup> s<sup>-1</sup>) and  $r$  is the radius of the diffusing particle (m) (Hoffman *et al.*, 1998). All measurements were made on triplicate protein solutions.

### 3.3.7 Interfacial tension

The interfacial tension for each protein solution was measured using a Lauda TD 2 Tensiometer (Lauda-Königshofen, Germany) equipped with a Du Nüoy ring (20 mm diameter). Within a 40 mm diameter glass sample cup, a 20 mL protein solution was added, followed by the immersion of the Du Nüoy ring and then the addition of upper canola oil layer (20 mL). The ring was then pulled upwards to stretch the interface to measure the maximum force without breaking into the oil phase. Three consecutive measurements were made on each sample at 3 min intervals (reported as a mean  $\pm$  <0.1 mN/m). Interfacial tension was calculated from the maximum force ( $F_{\max}$ ; units: mN; instrument measures mg  $\times$  gravity) using the following equation (eq. 3.4):

$$\gamma = \frac{F_{\max}}{4\pi R\beta} \quad (\text{eq. 3.4})$$

where,  $\gamma$  is the interfacial tension (mN/m),  $R$  is the radius of the ring (20 mm),  $\beta$  is a correction factor that depends on the dimensions of the ring and the density of the liquid involved (McClements, 2005). All measurements are reported as the mean  $\pm$  one standard deviation ( $n = 3$ ).

### 3.3.8 Emulsification stability and activity indices

Emulsions were prepared by mixing 5 g of the 0.1% (w/w) protein solution with 2 g of canola oil within a 50 mL plastic centrifuge tube, followed by homogenization at 7,200 rpm for 5 min using an Omni Macro Homogenizer (Omni International Inc., Marietta, GA) equipped with a 20 mm saw tooth generating probe. Emulsion stability (ESI) and activity (EAI) indices were determined according to Pearce and Kinsella (1978). The EAI provides an estimate of the relative surface coverage of a protein on an oil droplet within a dilute emulsion, whereas the ESI gives an estimate of its relative stability after a pre-determined time. Immediately after emulsion formation, a 50  $\mu$ L aliquot is transferred into 7.5 mL of pH-adjusted water containing 0.1% sodium dodecyl sulphate (SDS), vortexed for 10 s, and then absorbance read at 500 nm using a ultraviolet-visible spectrophotometer (Genesys 20, Thermo Scientific, Madison, WI) and plastic cuvettes (1 cm path length). A second aliquot of the emulsion was then taken after 10 min, following the same procedure. The EAI and ESI were determined using eq. 3.5 and 3.6, respectively:

$$EAI(m^2/g) = \frac{2 \cdot 2.303 \cdot A_0 \cdot N}{c \cdot \varphi \cdot 10000} \quad (\text{eq. 3.5})$$

$$ESI(\text{min}) = \frac{A_0}{\Delta A} \cdot t \quad (\text{eq. 3.6})$$

where  $A_0$  is the absorbance of the diluted emulsion immediately after homogenization, N is the dilution factor ( $150\times$ ), c is the weight of protein per volume (g/mL),  $\phi$  is the oil volume fraction of the emulsion,  $\Delta A$  is the change in absorbance between 0 and 10 min ( $A_0 - A_{10}$ ) and t is the time interval, 10 min. All measurements are reported as the mean  $\pm$  one standard deviation ( $n = 3$ ).

### 3.3.9 Statistics

All experiments were performed in triplicate and reported as the mean  $\pm$  one standard deviation. A two-way analysis of variance (ANOVA) was performed to test for significance in the main effects of pH (3.0, 5.0, 7.0) and heat pre-treatment conditions (25, 55, 85°C), along with their associated interactions on the physicochemical and emulsifying properties of WPI. A simple Pearson correlation was also performed to relate the physicochemical and emulsifying properties. Statistical analyses were performed with Systat (SPSS Inc., Ver. 10, 2000, Chicago, IL).

## 3.4 Results and discussion

### 3.4.1 Structural characteristics

Circular dichroism was used to determine whether the various temperature pre-treatment and pH combinations affected the secondary structure of WPI (Figure 3.1). Temperature pre-treatments at pH 7.0 had little effect on the mean molar ellipticity (Figure 3.1A) indicating little change in secondary structure. In contrast, at pH 5.0 (near the pI), a loss in secondary structure was evident at 85°C but not at 25°C and 55°C presumed to be associated with protein denaturation as hydrogen bonds become disrupted at elevated temperatures resulting in unfolding (Figure 3.1B). At pH 3.0 less unfolding occurred at 85°C, but more than what was observed at pH 7.0 (Figure 3.1C). The similarities in secondary structure at temperature pre-treatments of 25 and 55°C regardless of the pH is hypothesized to be attributed to the refolding of the protein after partial denaturation when WPI is pre-treated at 55°C. It was hypothesized that WPI molecules at 85°C were completely denatured at pH 5.0 and partially denatured at pH 3.0 and 7.0. Complete

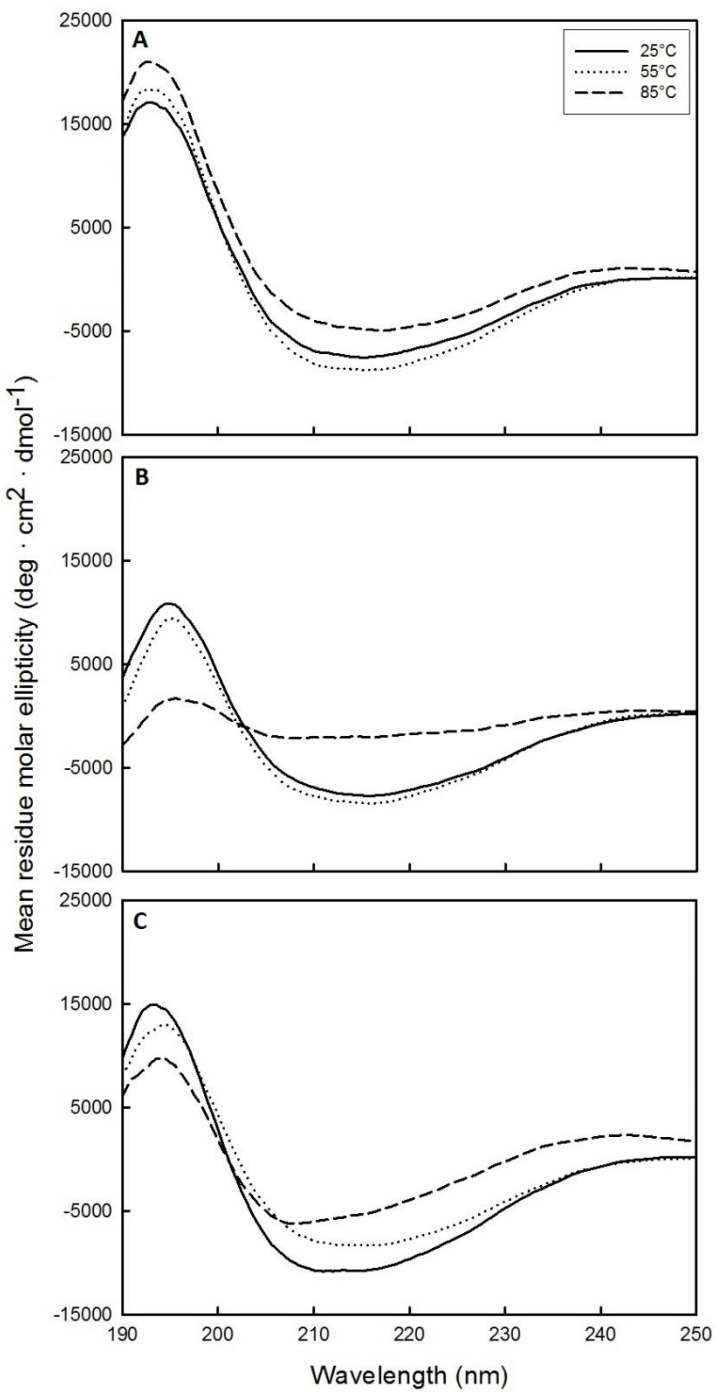


**Figure 3.1** Circular dichroism in mean residue molar ellipticity ( $\text{deg} \cdot \text{cm}^2 \cdot \text{dmol}^{-1}$ ) for WPI solutions as a function of pH (7.0 (A), 5.0 (B), 3.0 (C)) and pre-treatment temperatures. Each spectra is representative for each sample treatment which comprised of the average of 5 scans.

denaturation at pH 5.0 and 85°C is attributed to the neutrally charged WPI (Figure 3.3) which had reduced electrostatic repulsion between varying moieties within WPI; allowing for greater changes in the conformation in response to temperature pre-treatments. The surface charge of WPI at pH 3.0 and 7.0 may confer resistance towards denaturation by temperature pre-treatments as the surface charge might prevent changes to the tertiary structure of WPI which allows for the ability for the unfolded portion of WPI to refold when brought back to room temperature. As there were little changes to the structure of WPI at pH 3.0 and 7.0, it would be expected that physical-chemical properties of WPI would be similar at these two pHs despite the temperature pre-treatments exposed to the proteins.

### 3.4.2 Surface characteristics

Hydrophobicity for WPI solutions as measured by the intrinsic fluorescence (max. intensity) and using the fluorescent probe method, as a function of pH and heat pre-treatment conditions is shown in Figure 3.2A and 3.2B, respectively. An analysis of variance found that for both techniques the two main effects of pH ( $p<0.001$ ) and temperature ( $p<0.001$ ), and their associated interaction ( $p<0.001$ ) were significant (Table 3.1). Similar pH-dependent trends in maximum fluorescent intensity (FI) data were seen at both 25 and 55°C temperature pre-treatments, where FI declined from ~689.9 arbitrary units (a.u.) at pH 3.0, to ~577.8 a.u. at pH 5.0, and then again to ~548.6 a.u. at pH 7.0 (Figure 3.1A). However, at 85°C temperature pre-treatment, FI increased from ~673.6 at pH 3.0, to ~796.2 a.u. at pH 5.0, before declining to ~587.9 a.u. at pH 7.0 (Figure 3.1A).

Surface hydrophobicity as measured using the extrinsic ANS-probe method revealed similar pH and temperature trends (Figure 3.2B). Surface hydrophobicity was the greatest at pH 5.0/85°C based on a combined effect of reduced net charge (~ +6.1 mV, Figure 3.3) and protein denaturation. At 85°C, the tertiary structures of WPI are thought to unfold leading to the exposure of previously buried hydrophobic moieties to the surface, which then fluoresces themselves or interacts with a fluorescent ANS probe (Kato and Nakai, 1980). It was previously reported that the two dominant proteins within WPI:  $\alpha$ -lactalbumin (ALA) and  $\beta$ -lactoglobulin ( $\beta$ -LG) had denaturation temperatures of 64.3°C (Relkin *et al.*, 1993; Boye & Alli, 2000) and 79.8°C (Haug *et al.*, 2009) respectively as measured by differential scanning calorimetry. Reduced fluorescence at pH 3.0 and 7.0 at 85°C may reflect the greater contribution of surface

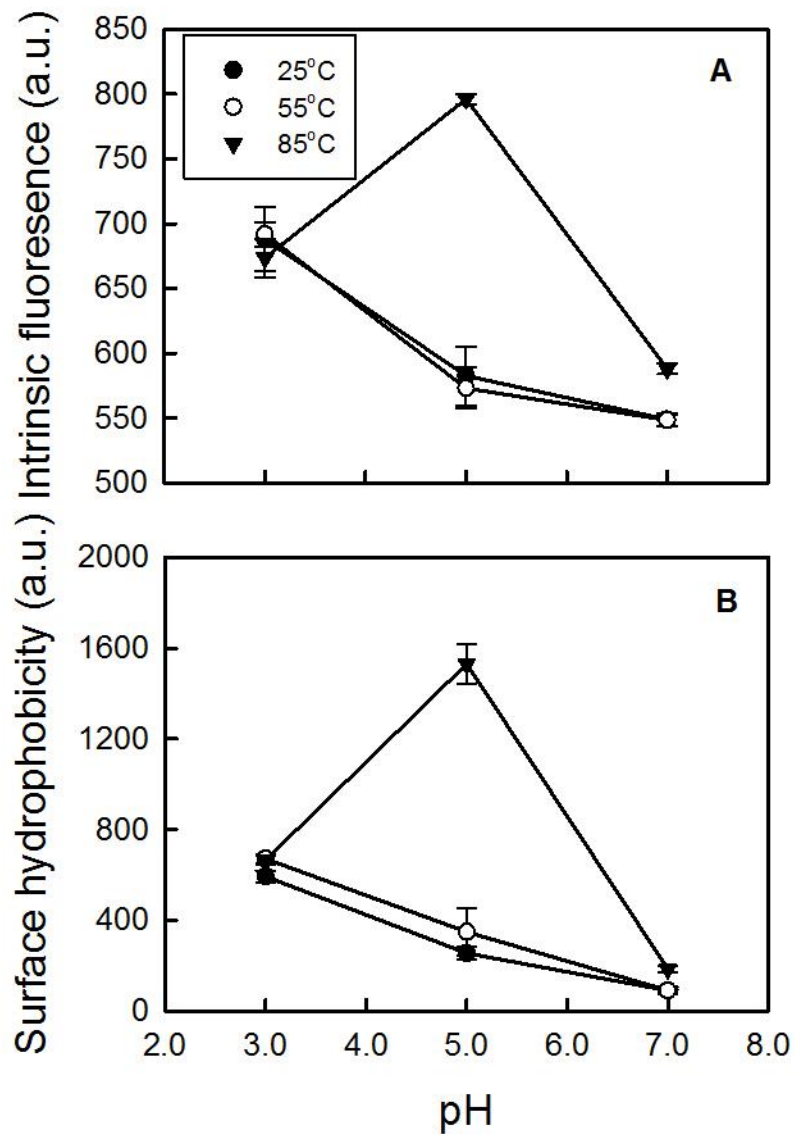


**Figure 3.2** Intrinsic fluorescence (arbitrary units (a.u.) (A) and surface hydrophobicity (a.u.) as measured using an ANS fluorescent probe (B) for WPI solutions as a function of pH and pre-treatment temperature conditions. Data represent the mean  $\pm$  one standard deviation ( $n=3$ ).

**Table 3.1** A summary of the two-way ANOVA tested for the main factors pH and temperature and their interaction on the physicochemical and emulsifying properties of WPI.

Property	pH	Temp.	pH x Temp.
<b>a) Physicochemical properties</b>			
Max. fluorescence intensity	p<0.001	p<0.001	p<0.001
Hydrophobicity (by ANS)	p<0.001	p<0.001	p<0.001
Zeta potential	p<0.001	NS	NS
Hydrodynamic radius	p<0.001	p<0.001	p<0.001
Interfacial tension	p<0.001	p<0.05	NS
<b>b) Emulsifying properties</b>			
Emulsification activity index	p<0.001	p<0.001	p<0.001
Emulsification stability index	p<0.001	p<0.01	p<0.001

charge which could inhibit or restrict complete protein unfolding as seen by circular dichroism (Figure 3.1).

In contrast, for temperatures below the denaturation temperature (25 and 55°C), hydrophobicity was found to decline as pH increased from pH 3.0 to pH 7.0. The change in hydrophobicity is believed to be related to its structural conformation due to level of protonation of charged sites on the protein surface, the aggregation between proteins and its affinity towards the fluorescent probe. Generally, an increase in surface hydrophobicity will cause an increase in the amount of aggregation between proteins. When proteins aggregate, the hydrophobic moieties may be buried within the interior of the aggregate structure, reducing its thermodynamic unfavorable interactions between the hydrophobic with the hydrophilic moieties. Therefore, the size of these aggregates (Figure 3.4) at pH 3.0 and 7.0 are indicators of whether there were changes in the surface hydrophobicity of WPI. The sizes of these aggregates were similarly small at both pHs which suggest that the differences in surface hydrophobicity are due to the conformation of the protein at these pHs and their affinity towards the fluorescent probe. The ANS fluorescent probe is an anionic molecule (Alizadeh-Pasdar & Li-Chan, 2000) which could potentially bind more readily with WPI at pH 3.0 where it is strongly positively charged (Figure 3.3). At pH 7.0, WPI is strongly negatively charged which may electrostatically repel ANS from binding to the protein. Although this may partially explain for the observed differences between the two pHs, changes to protein conformation induced by pH changes are also believed to be a contributing factor. Differences in protein conformation at pH 3.0 and 7.0 may expose or hide hydrophobic

residues such that there were more hydrophobic residues at the surface at pH 3.0 compared to pH 7.0. Alizadeh-Pasdar and Li-Chan (2000) reported a similar decline in hydrophobicity for WPI solutions held at room temperature.

Surface charge (or zeta potential) for WPI as a function of pH and temperature pre-treatments were also measured and given in Figure 3.3. An analysis of variance found that only the main effect of pH was significant ( $p<0.001$ ), whereas the temperature pre-treatment effect and the  $\text{pH} \times$  interaction term were not ( $p>0.05$ ) (Table 3.1). Overall, the zeta potential declined relatively linearly with increasing pH from a positive surface charge (+34.3 mV) at pH 3.0 to a negative charge at pH 7.0 (-36.4 mV). Net neutrality (or isoelectric point, pI) of the WPI was found to occur at near pH 5.1-5.4 (zeta potential = 0 mV (Figure 3.3). Parris and Baginski (1991) reported the pI for WPI to be pH 4.6 by isoelectric precipitation. Slight differences in reported pI values may reflect the slight differences in material and/or the measuring technique. Changes to solution pH acts to alter the electrostatic attractive and repulsive forces of WPI molecules in solution, resulting in good dispersion or protein-protein aggregation. The lack of temperature

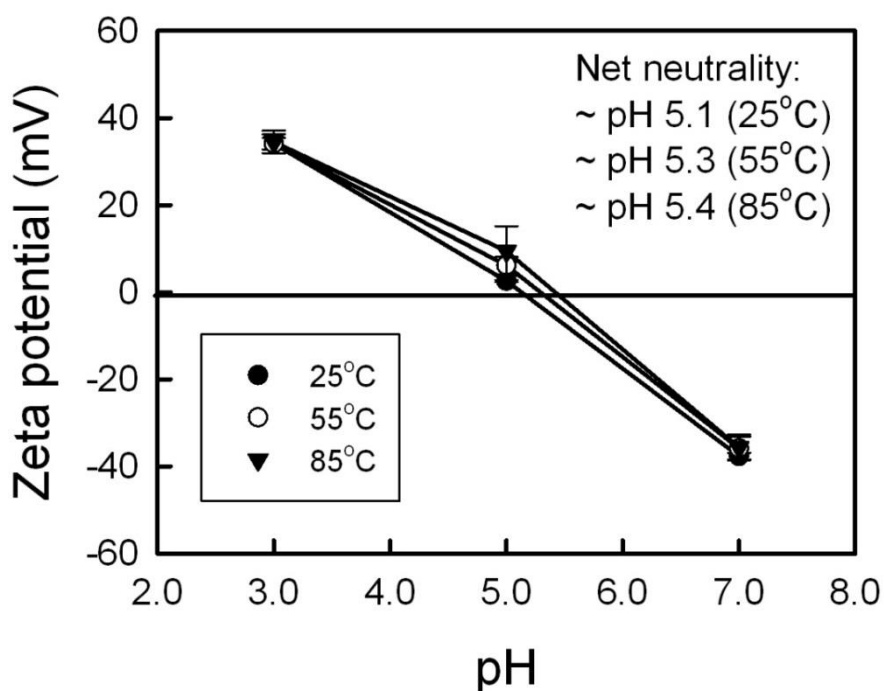


**Figure 3.3** Zeta potential (mV) for WPI solutions as a function of pH and pre-treatment temperature conditions. Data represent the mean  $\pm$  one standard deviation ( $n=3$ ).

dependence of surface charge on the WPI solutions suggests that nature of the protein is very hydrophilic, even when the protein is unraveled (*i.e.*, at 85°C).

### 3.4.3 WPI aggregation

The hydrodynamic radius as measured by dynamic light scattering for WPI solutions as a function of pH and temperature pre-treatments is given in Figure 3.4. An analysis of variance found that for both techniques the two main effects of pH ( $p<0.001$ ) and temperature ( $p<0.001$ ), and their associated interaction ( $p<0.001$ ) were significant (Table 3.1). WPI aggregates at both pH 3.0 and 7.0 were relatively similar regardless of the temperature pre-treatments. For instance at pH 3.0, hydrodynamic radii were reported to be 69.1, 66.5 and 70.2 nm for temperature pre-treatments of 25, 55 and 85°C, respectively, whereas at pH 7.0, radii of WPI aggregates were 95.1, 87.1 and 59.2 nm, respectively (Figure 3.4). In contrast, greater temperature dependence in size data was evident at pH 5.0, where hydrodynamic radii were 1589.0, 1449.7 and 831.8 nm at 25, 55 and 85°C, respectively (Figure 3.4).

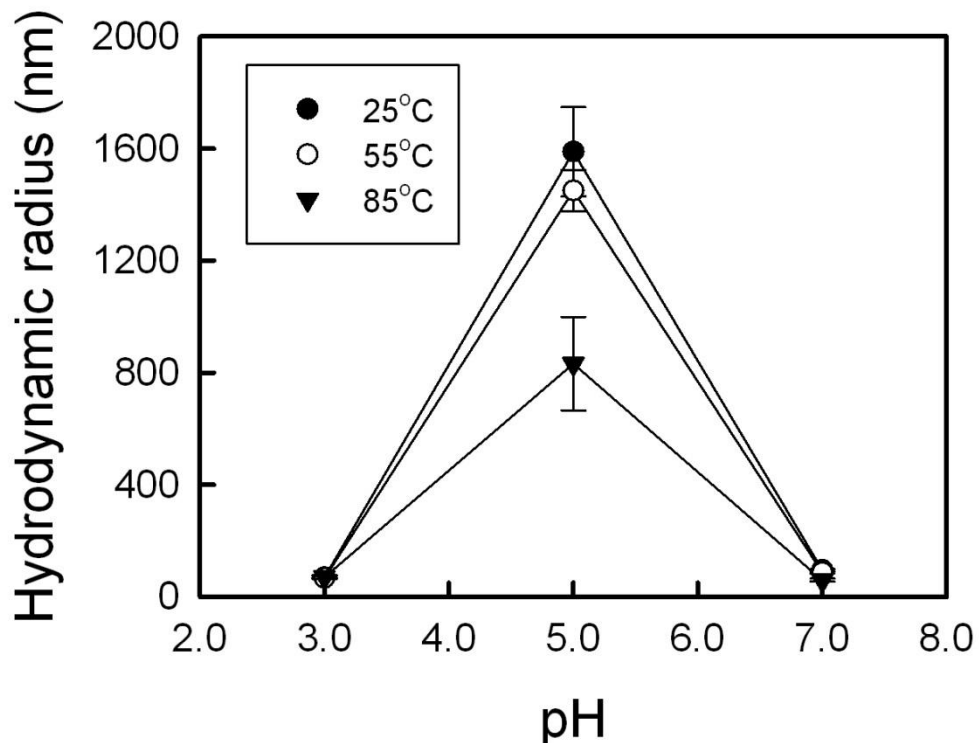


**Figure 3.4** Hydrodynamic radius (nm) for WPI solutions as a function of pH and pre-treatment temperature conditions. Data represent the mean  $\pm$  one standard deviation ( $n=3$ ).

The size of WPI aggregates was greatest at pH 5.0 associated with reduced electrostatic repulsion between neighbouring molecules allowing them to aggregate *via* hydrophobic and non-covalent (*e.g.*, hydrogen bonding and van der Waals attractive forces) interactions (Laligant *et al.*, 1991; Mao *et al.*, 2012). The larger structures most likely involved the co-aggregation of ALA and  $\beta$ -LG proteins. Gezimati, Creamer and Singh (1997) and, Hong and Creamer (2002) suggested that these proteins interact mainly through disulfide bridging and through hydrophobic interactions. WPI aggregates were largest at temperatures below the denaturation temperatures where WPI is more in its native conformation. Although less hydrophobic than WPI at 85°C, it is believed that the higher temperatures resulted in the dissociation of ALA and  $\beta$ -LG structures leading to reduced hydrodynamic radii. Schokker and co-workers (2000a) reported  $\beta$ -LG to be reduced from dimers to monomers at temperatures near 70°C. In addition, although ALA is reported to denature at relatively low temperatures (64.3°C (Relkin *et al.*, 1993; Boye & Alli, 2000)), at  $\geq 85^\circ\text{C}$ , free thiol groups are formed (Schnack & Klostermeyer, 1980; Doi *et al.*, 1983) which makes it highly reactive (Bertrand-Harb *et al.*, 2002; Chaplin & Lyster, 1986; Hong & Creamer, 2002) and prone to aggregation (Livney *et al.*, 2003). This combined effect of the reactivity of ALA and dissociation of  $\beta$ -LG dimers at 85°C and pH 5.0 is suggested to allow for the formation of smaller aggregates. Reduced aggregate size at pH 3.0 and pH 7.0 is believed to be associated with the high electrostatic repulsion between WPI molecules due to the high surface charge.

### 3.4.4 Interfacial properties of WPI

Interfacial tension values between WPI solutions as a function of pH and temperature pre-treatments and canola oil at the oil-water interface are shown in Figure 3.5. An analysis of variance found that only the main effects of pH ( $p<0.001$ ) and temperature pre-treatment ( $p<0.05$ ) were significant, whereas their associated interaction was not ( $p>0.05$ ) (Table 3.1). Overall, WPI ability to reduce interfacial tension increased from pH 3.0 (17.5 mN/m) to pH 5.0 (14.0 mN/m), then declined as pH was raised to pH 7.0 (16.0 mN/m). The effect of temperature pre-treatment was found only be weakly significant, where interfacial tension was similar at 25 and 55°C at  $\sim 15.9$  mN/m, before declining slightly at 85°C (15.7 mN/m) (Figure 3.5). In the

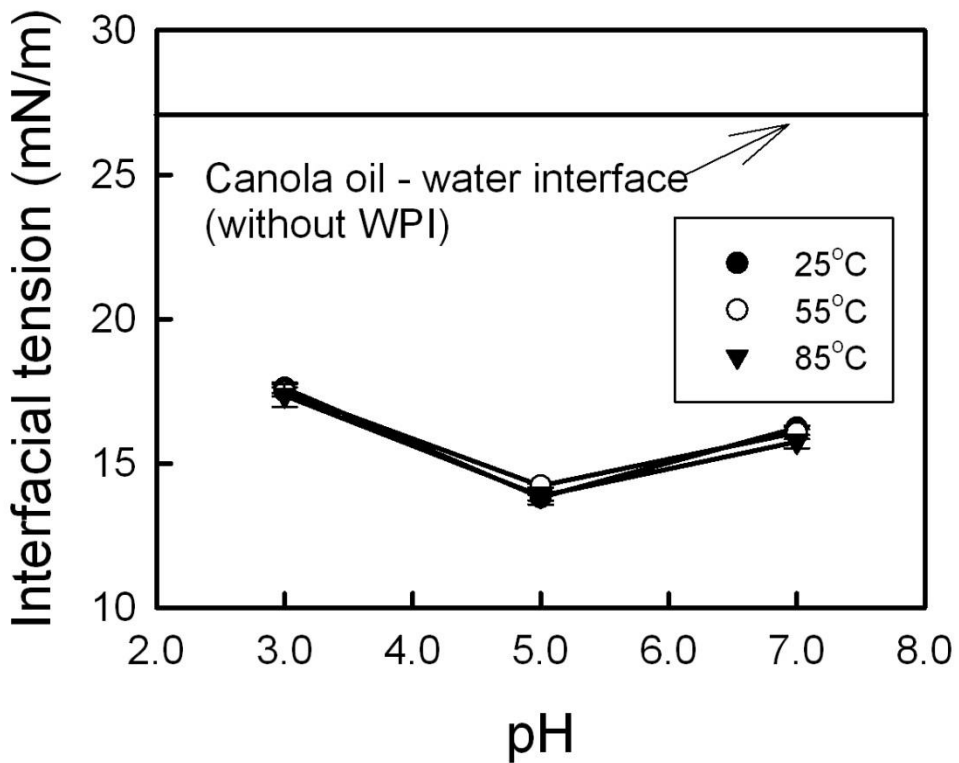


**Figure 3.5** The interfacial tension (mN/m) for WPI solutions as a function of pH and pre-treatment temperature conditions. Data represent the mean  $\pm$  one standard deviation ( $n=3$ ).

present study, surface charge was presumed to have the greatest effect on the ability for WPI to reduce interfacial tension. At pH 3.0 and 7.0, electrostatic repulsion between WPI molecules at the interface was presumed stronger than seen for pH 5.0 (*i.e.*, higher surface charge), resulting in greater difficulties in aligning to form a viscoelastic film. Furthermore at pH 5.0, WPI-WPI aggregation was the highest, possibly leading to the formation of a more ordered or packed viscoelastic film at the interface. A Pearson Correlation analysis found aggregate size and interfacial tension to be inversely related ( $r = -0.885$ ;  $p < 0.001$ ), where larger WPI aggregates were more effective at lowering interfacial tension. Although slight differences were observed among the various pH and temperature treatments, the presence of WPI was effective at reducing the interfacial tension down from  $\sim 28.0$  mN/m for solutions in the absence of protein (Figure 3.5).

### **3.4.5 Emulsifying properties**

#### **3.4.5.1 Emulsion formation**

The emulsifying activity index (EAI) for WPI solutions as a function of pH and temperature pre-treatment conditions is shown in Figure 3.6A. An analysis of variance found both main effects of pH and temperature were significant ( $p<0.001$ ), along with their associated interaction ( $p<0.001$ ) (Table 3.1). Overall, EAI values declined from  $102.5 \text{ m}^2/\text{g}$  at pH 3.0, to  $41.5 \text{ m}^2/\text{g}$  at pH 5.0, before increasing to  $83.8 \text{ m}^2/\text{g}$  at pH 7.0. However the effect of temperature pre-treatments was different at each pH. For instance at pH 3.0, EAI values were relatively similar in magnitude, ranging between  $98.7$  and  $104.6 \text{ m}^2/\text{g}$  (Figure 3.6A). However at pH 5.0, EAI values declined from  $43.7 \text{ m}^2/\text{g}$  at  $25^\circ\text{C}$ , to  $32.2 \text{ m}^2/\text{g}$  at  $55^\circ\text{C}$ , before increasing to  $48.6 \text{ m}^2/\text{g}$  at  $85^\circ\text{C}$  (Figure 3.6A). At pH 7.0, EAI declined from  $94.7 \text{ m}^2/\text{g}$  at  $25^\circ\text{C}$ , to  $87.4 \text{ m}^2/\text{g}$  at  $55^\circ\text{C}$ , and then to  $69.2 \text{ m}^2/\text{g}$  at pH  $85^\circ\text{C}$  (Figure 3.6A). Emulsion activity indices give an indication of the surface area stabilized by a unit weight of protein (Pearce & Kinsella, 1978). A Pearson correlation analysis found that size was negatively correlated with EAI ( $r = -0.885$ ;  $p<0.001$ ). It was proposed EAI was reduced at pH 5.0, since this pH corresponded to conditions where the hydrodynamic radii of the WPI aggregates were the greatest. Aggregation was highest at this pH due to a reduction in electrostatic repulsion between proteins close to their isoelectric point. It was presumed that the larger aggregates would require greater time to migrate, and less capable to re-configure and align with the oil-water interface which would reduce EAI. In contrast, EAI was greater at both pH 3.0 and 7.0 since WPI aggregates were smaller (lower hydrodynamic radii) to allow faster migration and integration into the interface. At pH 7.0, EAI was slightly lower when WPI was treated to  $85^\circ\text{C}$ , relative to the  $25$  and  $55^\circ\text{C}$  treatments presumed to be the result of greater surface hydrophobicity caused by protein unravelling. The effect of heat treatments on the EAI of whey proteins have been previously studied with reportedly opposing results (Voutsinas *et al.*, 1983; Dissanayaki & Vasiljevic, 2009). Voutsinas *et al.* (1983) reported that the emulsifying properties (*i.e.* EAI and ESI) changes as a function of protein type where whey proteins were found to not change much with increasing heat treatments. In contrast, Dissanayaki and Vasiljevic (2009) reported that the EAI of whey proteins increased with thermal treatment and denaturation. The contrasting results is most probably

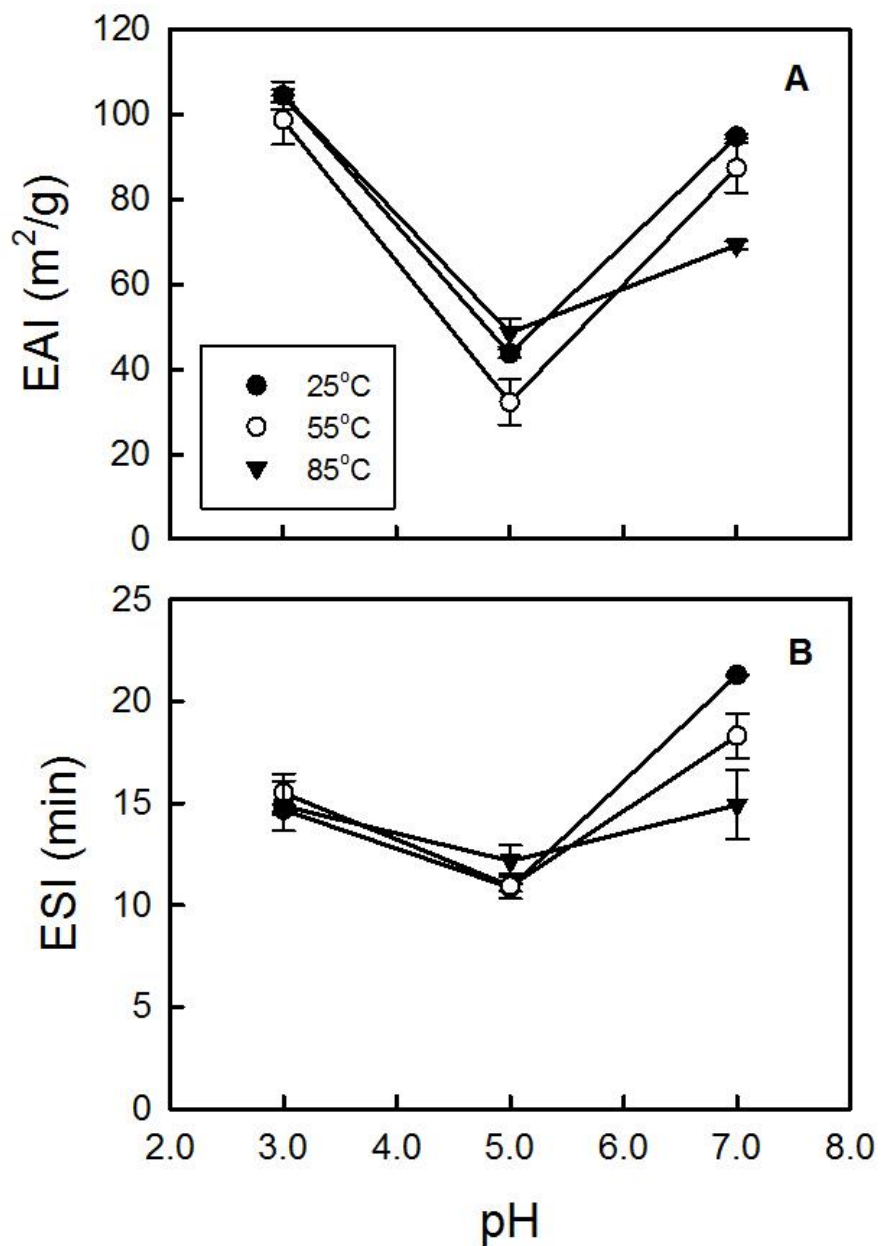


**Figure 3.6** The emulsion activity (EAI,  $\text{m}^2/\text{g}$ ) (A) and stability (ESI, min) indices for WPI solutions as a function of pH and pre-treatment temperature conditions. Data represent the mean  $\pm$  one standard deviation ( $n=3$ ).

due to the differences in the concentration of protein used, pH (pH 6 in Voutsinas *et al.*, (1983) and pH 7 in Dissanayaki and Vasiljevic (2009)), method of thermal treatment and oil used. Dissanayaki and Vasiljevic (2009) postulated that the partial unravelling of whey proteins allowed a thermodynamically favourable conformation for adhering to the water-oil interface.

### 3.4.5.2 Emulsion stability

The emulsion stability index for WPI solutions as a function of pH and temperature pre-treatment conditions is shown in Figure 3.6B. An analysis of variance found both main effects of pH ( $p<0.001$ ) and temperature ( $p<0.01$ ) were significant, along with their associated interaction ( $p<0.001$ ) (Table 3.1). Overall, ESI values declined from 15.0 min at pH 3.0, to 11.3 min at pH 5.0, before increasing to 18.2 min at pH 7.0. However the effect of temperature pre-treatments was different at each pH. For instance, ESI data at pH 3.0 were relatively similar regardless of the temperature pre-treatment conditions, ranging between 14.7 and 15.5 min (Figure 3.6B). At pH 5.0, ESI data were similar at 25 and 55°C (10.9 min), and then increased to 12.2 min at 85°C (Figure 3.6B). In contrast at pH 7.0, ESI values declined from 21.3 min at 25°C, to 18.3 min at 55°C, and then again to 14.9 min at 85°C (Figure 3.6B). The stability of emulsions has been described by many to be associated with 1) electrostatic static repulsion between droplets; 2) steric focus arising from protein tails or loops resonating from the oil droplets surface; and 3) increased continuous phase viscosity (Klemaszewski & Kinsella, 1991; Damodaran, 1996; Tcholakova *et al.*, 2006b). A Pearson correlation analysis found that ESI was negatively correlated with size ( $r = -0.741$ ;  $p<0.001$ ), surface hydrophobicity ( $r = -0.480$ ;  $p<0.05$ ) and charge ( $r = -0.480$ ;  $p<0.05$ ), and positively correlated with interfacial tension ( $r = 0.559$ ;  $p<0.01$ ). In the present study, overall stability was greatest at pH 7.0 most likely to the high net negative charge (~ -40 mV) associated with WPI molecules, which resulted in significant electrostatic repulsion between neighbouring droplets. Stability was slightly lower at pH 7.0 when WPI was treated to 85°C, possibly due to higher surface hydrophobicity which would promote droplet flocculation. In addition, despite WPI carrying a high net positive charge (~ +40 mV) at pH 3.0, surface hydrophobicity was much greater than seen at pH 7.0, possibly leading to the reduction in EAI. Stability was further reduced at pH 5.0 since repulsive forces were significantly reduced enabling for greater associations between droplets. Similarly to EAI, opposing results for the effect of heat treatments on ESI was reported for whey proteins (Voutsinas *et al.*, 1983; Dissanayaki & Vasiljevic, 2009). While Voutsinas *et al.*

(1983) reported an increase in ESI with heat treatment, Dissanayaki and Vasiljevic (2009) reported that no change in ESI was observed with increasing heat treatment. In part, these contrasting results may be due to differences between the two experimental setups as mentioned in the EAI section. Furthermore, Klemaszewski and Kinsella (1991) reported that the stability of proteins is dependent on the charge of the proteins where enhanced stability is observed under conditions where electrostatic repulsion occurs. From the current study, the highly charged pH 3.0 and 7.0 provides such conditions where electrostatic repulsion may increase the ESI of the emulsion.

### **3.5 Conclusions**

In conclusion, both pH and temperature pre-treatment conditioning of the WPI molecules acts to alter their physicochemical properties to enable tailoring of their emulsion forming and stabilizing properties. Overall emulsion formation seems to be strongly associated with the size of WPI aggregates being formed, along with the charge and hydrophobicity on the surface of these structures. Emulsion formation seemed to be improved with reduced WPI aggregation, believed to be associated with greater rates of migration to the oil-water interface, and easier re-alignment once there than larger aggregates. Emulsion stability under the current experimental conditions was strongly influenced by both the electric charge and hydrophobicity on the WPI molecule. Stability seemed greatest at pH conditions away from its isoelectric point where repulsive forces were strongest, and under conditions where surface hydrophobicity was reduced.

### **3.6 Connection to the next study**

In this current study, the physicochemical and emulsifying properties of whey protein isolates were investigated. Changes in their physicochemical properties due to pH modification and temperature pre-treatments and their effects on the emulsifying properties of whey proteins were considered. Although WPI performance is attributed to its main components:  $\beta$ -lactoglobulin and  $\alpha$ -lactalbumin, studies on the functional properties of these two proteins are required to validate this claim. Therefore in the next study, the physicochemical and emulsifying properties of  $\beta$ -lactoglobulins were investigated under the same conditions as this first study. Physicochemical and emulsifying properties such as surface hydrophobicity, surface charge, aggregate size, interfacial tension, emulsifying activity index and stability were studied to

determine the role  $\beta$ -lactoglobulins play towards explaining the functionality of whey protein isolates.

## **4. THE EFFECT OF PH AND HEAT PRE-TREATMENTS ON THE PHYSICOCHEMICAL AND EMULSIFYING PROPERTIES OF $\beta$ -LACTOGLOBULIN<sup>3</sup>**

### **4.1 Abstract**

The overall goal of this research was to investigate structure-function mechanisms associated the emulsifying properties of  $\beta$ -lactoglobulin ( $\beta$ -LG). Specifically the physicochemical (*i.e.*, surface charge and hydrophobicity, size and interfacial tension) and emulsifying (*i.e.*, emulsification activity (EAI) and stability indices (ESI)) properties of  $\beta$ -LG were investigated in response to changes in pH (3.0, 5.0 and 7.0) and heat pre-treatment conditions (25, 55 and 85°C). Hydrophobicity was found to be greatest at pH 5.0/85°C, whereas at all conditions it was significantly lower. Surface charge on  $\beta$ -LG was found to be neutral at ~pH 3.9, regardless of conditions. Aggregate size was also found to be highest at pH 5.0/85°C (avg. hydrodynamic radii of ~714 nm), corresponding to a reduced net surface charge and high hydrophobicity. Little size dependence of aggregates was observed at pH 3.0 regardless to the temperature pre-treatments (radii ~120 nm). In contrast, at pH 7.0 slight temperature dependence was apparent, where treatments at 25, 55 and 85°C lead to radii of 412.8, 307.2 and 232.3 nm, respectively. Overall, the addition of  $\beta$ -LG to a canola oil-water system resulted in a decline in interfacial tension from ~28 mN/m to ~18 mN/m, however the effect of pH/temperature conditions was minimal. EAI was found to be highest when  $\beta$ -LG solutions displayed high surface charge combined with moderate hydrophobicity. In contrast, ESI was higher under conditions where  $\beta$ -LG solutions remained in a native (25°C) or fully denatured state (85°C) versus one in where partially unravelling may be occurring (55°C).

---

<sup>3</sup> Published as: Lam, R. & Nickerson, M.T. (2013). The effect of pH and heat pre-treatments on the physicochemical and emulsifying properties of  $\beta$ -lactoglobulin. *Food Biophysics*, DOI 10.1007/s11483-013-9313-4.

## 4.2 Introduction

Proteins are widely been used in food applications for their emulsifying properties due to their amphiphilic nature, ability to stabilize oil-in-water emulsions and film forming abilities (Augustin & Hemar, 2009). Emulsions are defined as a dispersion of two (or more) immiscible liquids in which one of the liquids is dispersed in the other as small droplets (0.1-100 µm) through the application of mechanical shear (McClements, 2005). Proteins, such as sodium caseinate, whey protein and soy protein act to stabilize the oil-water interface by re-orienting hydrophobic amino groups inwards towards the oil phase, and hydrophilic amino groups outwards towards the aqueous phase (Wong *et al.*, 2012). Proteins, then aggregate at the interface to form a viscoelastic film which resists or inhibits coalescence through electrostatic charge repulsion between neighbouring droplets or steric hindrance (Tocholakova *et al.* 2006b). Due to the charged surface on the interfacial protein film, changes in solution pH can drastically alter emulsion stability, where repulsive (*i.e.*, low ionic strength and a pH away from the protein's isoelectric point) and attractive (*i.e.*, high ionic strength or a pH near the protein's isoelectric point) forces could lead to stability and instability, respectively. Temperature also plays a significant role in determining a protein's emulsifying properties, where heat pre-treatments can cause partial or complete unfolding of the protein's tertiary conformation to expose buried hydrophobic amino groups to the surface, and in the case of globular proteins, open up its conformation to increase its excluded volume and flexibility (Tocholakova *et al.* 2006b).

Whey proteins constitute ~20% of the total proteins found in bovine milk, with caseins ( $\alpha_{s1}$ ,  $\alpha_{s2}$ ,  $\beta$ - and  $\gamma$ -types) representing the remaining 80% (Swaisgood, 2008). Whey proteins are considered highly nutritious due to their high levels of sulphur-containing amino acids, and are of functional importance due to their high solubility, and good foaming, emulsifying and gelling properties (Dagleish, 2006). Whey proteins are a class of proteins comprised of  $\beta$ -lactoglobulin (9.8% of total protein) and  $\alpha$ -lactalbumin (3.7%) proteins, along with smaller amounts of blood proteins such as proteose-peptones (2.4%), serum albumin (1.2%) and immunoglobulins (2.1%) (Walstra & Jenness, 1984). The emulsifying properties of whey protein isolates (Hunt & Dalglish, 1994b; Demetriades *et al.*, 1997; Kulmyrzaev *et al.*, 2000),  $\beta$ -lactoglobulin (Tocholakova *et al.*, 2006a; Dickinson *et al.*, 1993; Kim *et al.*, 2002a) and  $\alpha$ -lactalbumin (Dickinson *et al.*, 1993; Wiacek & Chibowski, 2005; Zhai *et al.*, 2012) have widely been studied in literature due to their economic importance. For instance, Kim and co-workers (2005) and, Kundsen and co-workers

(2008) reported heat pre-treatments to  $\beta$ -lactoglobulin-solutions led to increases in hydrophobicity, enabling a greater amount of protein to adsorb to the oil-interface. Modifications such as temperature pre-treatments have allowed tailoring of their physicochemical properties of proteins for better adsorption to the water-oil interface. Though modifications may enhance the adsorption of proteins, this does not necessarily translate to an increase in emulsion stability. Therefore, this research will investigate the effect of pH and temperature pre-treatments on the physicochemical and emulsifying properties of  $\beta$ -lactoglobulin, in order to elucidate potential relationships between interfacial protein adsorption and emulsion stability. It was hypothesized that changes in pH and temperature (heat pre-treatments) would alter the surface active properties of  $\beta$ -lactoglobulin leading to improved emulsion stability.

### **4.3 Materials and Methods**

#### **4.3.1 Materials**

$\beta$ -Lactoglobulin ( $\beta$ -LG) was purchased from Sigma-Aldrich (Oakville, ON, Canada) with a protein content determined to be 87.0% (%N  $\times$  6.38) as measured using a micro-Kjeldahl digester (Micro Digestor, Labconco, Kansas City, MO, USA) and distillation unit (RapidStill I, Labconco, Kansas City, MO, USA) according to AOAC Official Method 920.87 (AOAC, 2003). Canola oil used in this study was purchased from a local supermarket. All other chemicals used in this study were of reagent grade and purchased through Sigma-Aldrich (Oakville, ON, Canada). The water used in this research was filtered using a Millipore Milli-Q<sup>TM</sup> water purification system (Millipore Corp., Milford, MA, USA).

#### **4.3.2 Sample preparation**

$\beta$ -LG solutions (0.1%, w/w) were prepared by dispersing the weight of the protein into water, pH adjusted to 3.0, 5.0 or 7.0 using either 0.5 M HCl or 0.5 M NaOH, and mechanically stirred (500 rpm) at room temperature (21-23°C) for 60 min. Protein solutions (at their specific pHs) were held in a water bath for an additional 30 min at 25°C, 55°C and 85°C then cooled down to room temperature prior to analysis. Screw capped containers were used to hold the protein solutions to prevent moisture loss. All samples were prepared in triplicate.

### 4.3.3 Surface hydrophobicity

Hydrophobicity for each protein solution was determined by extrinsic fluorescence using a fluorescent probe method and, by intrinsic fluorescence as a function of emission wavelength.

(a) *Fluorescent probe method:* Surface hydrophobicity for each protein solution was measured based a modified method of Kato and Nakai (1980), which uses a 8-anilino-1-naphthalenesulfonate (ANS) probe to interact with hydrophobic moieties on the protein's surface to give a fluorescent signal. Stock solutions (0.07%, w/w) of each protein solution were prepared, and then diluted to concentrations of 0.03%, 0.04%, 0.05%, 0.06% and 0.07% (w/w). Twenty microliters of a 8 mM ANS solution (in water, adjusted to the specific pH of the protein solution) was then added to 1.6 mL of each protein solution, vortexed for 15 s, and then kept in the dark for 5 min. A similar concentration series was prepared for each protein sample, but without the ANS probe as a control, and a water-ANS probe mixture as a blank. Fluorescence intensity was measured for each sample using a FluoroMax-4 spectrofluorometer (Horiba Jobin Yvon Inc., Edison, N.J., USA) at excitation and emission wavelengths of 390 and 490 nm, respectively, and using a slit width of 1 nm. Net fluorescence intensity was determined by subtracting the intensity of the control (without ANS) and the blank (protein solution only), from the intensity of the protein solution with ANS, at each protein concentration. The slope of the net fluorescence as a function of protein concentration, as determined by linear regression served as an index of sample relative hydrophobicity. All measurements were made on triplicate protein solutions.

(b) *Intrinsic fluorescence:* A FluoroMax-4 spectrofluorometer (Horiba Jobin Yvon Inc., Edison, N.J., USA) was used to determine the intrinsic fluorescence for 0.05% (w/w) protein solutions at a constant excitation wavelength of 295 nm using a 2.5 nm slit width as a function of emission wavelength between 285 to 450 nm using a 5.0 nm slit width at 0.5 nm increments. Each spectra captured is corrected by subtracting the spectra of the control (*i.e.* water adjusted to the respective pH) from the spectra of the protein solution. The maximum fluorescence intensity (in arbitrary units) was determined for each spectra corrected. All measurements were made on triplicate protein solutions.

#### 4.3.4 Electrophoretic mobility

The electrophoretic mobility ( $U_E$ ) was determined using the Zetasizer Nano-ZS90 (Malvern Instruments, Westborough, MA) for all protein samples. The zeta-potential ( $\zeta$ ; units: mV) was determined from the electrophoretic mobility ( $U_E$ ) using Henry's equation (eq. 4.1):

$$U_E = \frac{2 \varepsilon \zeta f(\kappa\alpha)}{3\eta} \quad (\text{eq. 4.1})$$

where  $\varepsilon$  is the permittivity (units: F (Farad)/m),  $f(\kappa\alpha)$  is the function related to the ratio of particle radius ( $\alpha$ ; units: nm) and Debye length ( $\kappa$ ; units: nm<sup>-1</sup>), and  $\eta$  is the dispersion viscosity (units: mPa·s) [2]. The Smoluchowski approximation  $f(\kappa\alpha)$  was set as 1.5, as is accustom for folded capillary cells and, with particles larger than 0.2 μm dispersed in moderate electrolyte concentration (>1 mM). The Smoluchowski approximation assumes that a) concentration of particles (proteins) is sufficiently high such that such thickness of the electric double layer (Debye length) is small relative to the particle size ( $\kappa\alpha >> 1$ ); and b)  $\zeta$  is linearly related to  $U_E$ . All measurements are reported as the mean ± one standard deviation (n = 3).

#### 4.3.5 Dynamic light scattering for determination of the hydrodynamic radius of β-LG aggregates

The hydrodynamic radius for β-LG aggregates formed under the different pH and heat pre-treatment conditions were measured using the Zetasizer Nano-ZS90 (Malvern Instruments, Westborough, MA, USA). Approximately, 1 mL of each protein solution was placed in a plastic curvette (1 cm path length) within the Zetasizer's sample holder. The scattering intensity was measured at a 90° angle at 633 nm using a 4 mW He/Ne laser at room temperature (21–23°C). The hydrodynamic radius was estimated based on the Stokes-Einstein equation (Eq. 4.2 and 4.3):

$$D = \frac{\kappa_B T}{6\pi\eta r} \quad (\text{eq. 4.2})$$

which may be re-written as:

$$r = \frac{\kappa_B T}{6\pi\eta D} \quad (\text{eq. 4.3})$$

Where,  $k_B$  is the Boltzmann constant ( $1.38062 \times 10^{-23}$  J K<sup>-1</sup>),  $D$  is the self-diffusion constant (m<sup>2</sup> s<sup>-1</sup>),  $T$  is the absolute temperature (°K),  $\eta$  is viscosity of the medium (Kg m<sup>-1</sup> s<sup>-1</sup>) and  $r$  is the radius

of the diffusing particle (m) (Hoffman *et al.*, 1998). All measurements were made on triplicate protein solutions.

#### 4.3.6 Interfacial tension

The interfacial tension for each protein solution was measured using a Lauda TD 2 Tensiometer (Lauda-Königshofen, Germany) equipped with a Du Nüoy ring (20 mm diameter). Within a 40 mm diameter glass sample cup, a 20 mL protein solution was added, followed by the immersion of the Du Nüoy ring and then the addition of upper canola oil layer (20 mL). The ring was then pulled upwards to stretch the interface to measure the maximum force without breaking into the oil phase. Three consecutive measurements were made on each sample at 3 min intervals (reported as a mean  $\pm$  <0.1 mN/m). Interfacial tension was calculated from the maximum force ( $F_{\max}$ ; units: milli-Newton; instrument measures mg  $\times$  gravity) using the following equation (eq. 4.4):

$$\gamma = \frac{F_{\max}}{4\pi R\beta} \quad (\text{eq. 4.4})$$

where,  $\gamma$  is the interfacial tension (mN/m),  $R$  is the radius of the ring (20 mm),  $\beta$  is a correction factor that depends on the dimensions of the ring and the density of the liquid involved (McClements, 2005). All measurements are reported as the mean  $\pm$  one standard deviation ( $n = 3$ ).

#### 4.3.7 Emulsification stability and activity indices

Emulsions were prepared by mixing 5 g of the 0.1% (w/w) protein solution with 2 g of canola oil within a 50 mL plastic centrifuge tube, followed by homogenization at 7,200 rpm for 5 min using an Omni Macro Homogenizer (Omni International Inc., Marietta, GA) equipped with a 20 mm saw tooth generating probe. Emulsion stability (ESI) and activity (EAI) indices were determined according to Pearce and Kinsella (1978). The EAI provides an estimate of the relative surface coverage of a protein on an oil droplet within a dilute emulsion, whereas the ESI gives an estimate of its relative stability after a pre-determined time. Immediately after emulsion formation, a 50  $\mu$ L aliquot is transferred into 7.5 mL of pH-adjusted water containing 0.1% sodium dodecyl sulphate (SDS), vortexed for 10 s, and then absorbance read at 500 nm using a ultraviolet-visible spectrophotometer (Genesys 20, Thermo Scientific, Madison, WI) and plastic cuvettes (1 cm path

length). A second aliquot of the emulsion was then taken after 10 min, following the same procedure. The EAI and ESI were determined using eq. 4.5 and 4.6, respectively:

$$EAI(m^2/g) = \frac{2 \cdot 2.303 \cdot A_0 \cdot N}{c \cdot \varphi \cdot 10000} \quad (\text{eq. 4.5})$$

$$ESI(\text{min}) = \frac{A_0}{\Delta A} \cdot t \quad (\text{eq. 4.6})$$

where  $A_0$  is the absorbance of the diluted emulsion immediately after homogenization,  $N$  is the dilution factor ( $150\times$ ),  $c$  is the weight of protein per volume (g/mL),  $\varphi$  is the oil volume fraction of the emulsion,  $\Delta A$  is the change in absorbance between 0 and 10 min ( $A_0 - A_{10}$ ) and  $t$  is the time interval, 10 min. All measurements are reported as the mean  $\pm$  one standard deviation ( $n = 3$ ).

### 4.3.8 Statistics

All experiments were performed in triplicate and reported as the mean  $\pm$  one standard deviation. A two-way analysis of variance (ANOVA) was performed to test for significance in the main effects of pH (3.0, 5.0, 7.0) and heat pre-treatment conditions (25, 55, 85°C), along with their associated interactions on the physicochemical and emulsifying properties of  $\beta$ -LG. A simple Pearson correlation was also performed to relate the physicochemical and emulsifying properties. Statistical analyses were performed with Systat (SPSS Inc., Ver. 10, 2000, Chicago, IL).

## 4.4 Results and discussion

### 4.4.1 Physicochemical properties

#### 4.4.1.1 Surface characteristics

Hydrophobicity for  $\beta$ -LG solutions as measured by the intrinsic fluorescence (max. intensity) and using the fluorescent probe method, as a function of pH and heat pre-treatment conditions is shown in Figure 4.1A and 4.1B, respectively. An analysis of variance of maximum intrinsic fluorescence intensity and surface hydrophobicity data, found that for both the main effects, pH ( $p < 0.001$ ) and temperature ( $p < 0.001$ ) and their associated interaction ( $p < 0.001$ ) were significant (Table 4.1). In each case, intrinsic fluorescence of the protein solutions decreased approximately in a linear fashion as pH increased from pH 3.0 to 7.0, for both the 25 and 55°C pre-treatment conditions. In contrast, at the 85°C pre-treatment condition, maximum fluorescent intensity increased from  $\sim 721.8$  arbitrary units (a.u.) at pH 3.0 to 1063.6 a.u. at pH 5.0, and then

declined to 633.3 a.u. at pH 7.0 (Figure 4.1A). A similar pH trend was evident in surface hydrophobicity data for proteins pre-heated to 85°C as measured using the fluorescent probe method (Figure 4.1B) where hydrophobicity increased from 275.8 at pH 3 to 1527.3 at pH 5 followed by a decrease to 194.9 at pH 7.0. This observed increase at pH 5.0/85°C pre-treatment is attributed to the reduced electrostatic repulsion due to the relative neutral net charge (zeta potential of zero) of the proteins close to its isoelectric point (~pH 3.9 (Figure 4.2)). Slight pH dependence of hydrophobicity at the 25°C and 55°C may reflect minor changes to the native protein structure associated protein dynamics in solution (Kim *et al.*, 2002a). Alizadeh-Pasdar and Li-Chan (2000) reported similar trends for changes in surface hydrophobicity in unheated  $\beta$ -LG solutions due to changes in pH using the ANS fluorescent probe but when these  $\beta$ -LG solutions were heat treated, there was not a significant increase in hydrophobicity reported at pH 5.0. The corresponding difference at pH 5.0 could be attributed to differences in solvent makeup, while Alizadeh-Pasdar and Li-Chan (2000) used a citrate buffer, the solutions measured in Figure 4.1 were solubilized in pH adjusted water. Qi and co-workers (1997) reported the denaturation temperature of  $\beta$ -LG to be approximately 70°C as measured by circular dichroism and infrared spectroscopy, which was associated with the rapid decrease in helical structure beginning at 65°C and 70°C. Tcholakova and co-workers (2006a) reported  $\beta$ -LG structure unravelled during 85°C heat pre-treatment conditions, exposing buried hydrophobic groups to the surface. The effect was more pronounced at pH 5.0, where in combination with reduced net charge (near isoelectric point of protein) led to significantly higher hydrophobicity.

**Table 4.1** A summary of the two-way ANOVA tested for the main factors pH and temperature and their interaction on the physicochemical and emulsifying properties of  $\beta$ -lactoglobulin.

Property	pH	Temp.	pH x Temp
<b>a) Physicochemical property</b>			
Max. fluorescence intensity	p<0.001	p<0.001	p<0.001
Hydrophobicity (by ANS)	p<0.001	p<0.001	p<0.001
Zeta potential	p<0.001	NS	NS
Hydrodynamic radius	p<0.001	p<0.001	p<0.001
Interfacial tension	p<0.001	NS	NS
<b>b) Emulsifying properties</b>			
Emulsification activity index	p<0.001	p<0.001	p<0.001
Emulsification stability index	p<0.001	p<0.001	p<0.001

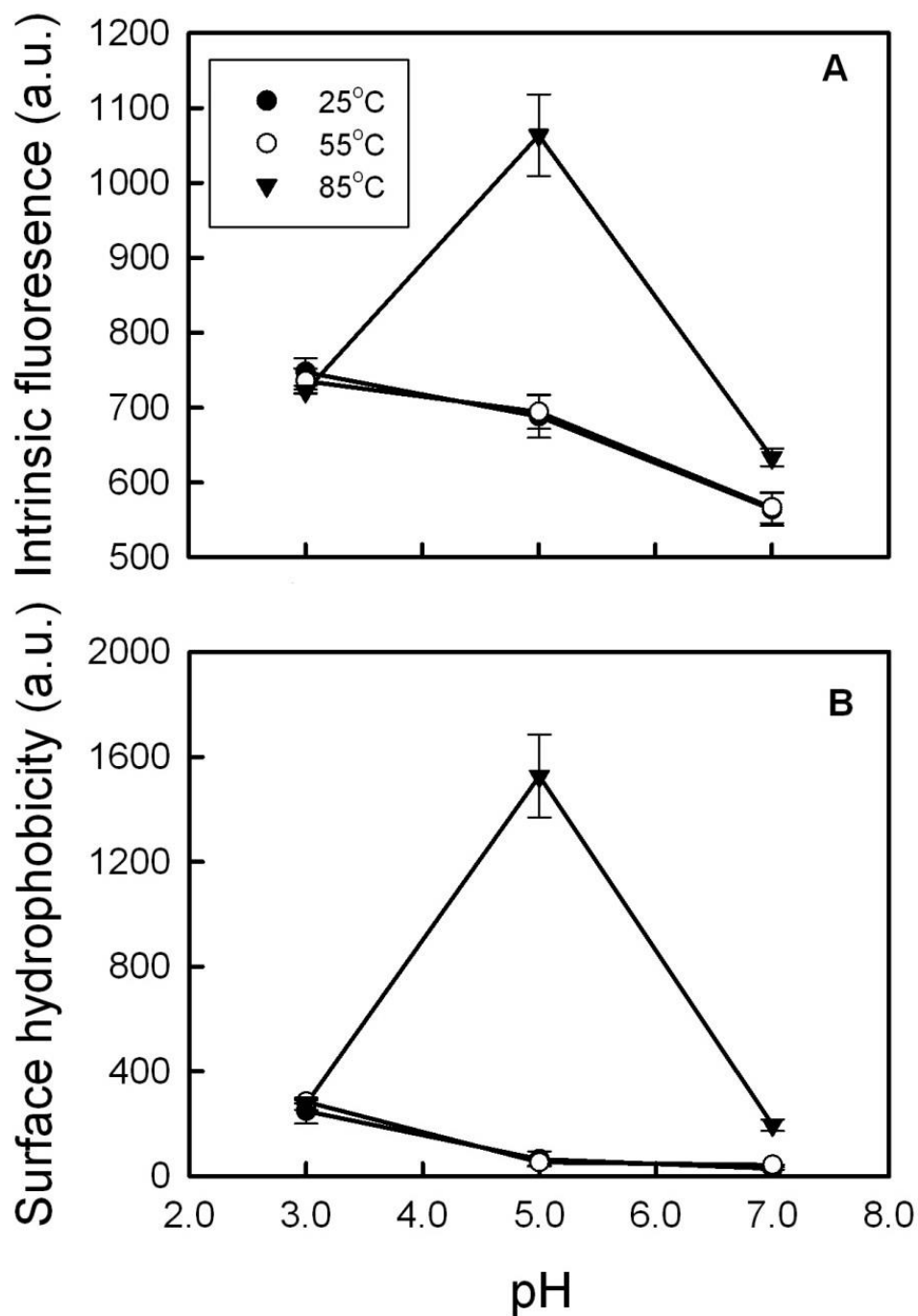


**Figure 4.1** Intrinsic fluorescence (arbitrary units (a.u.) (A) and surface hydrophobicity (a.u.) as measured using an ANS fluorescent probe (B) for  $\beta$ -lactoglobulin solutions as a function of pH and pre-treatment temperature conditions. Data represent the mean  $\pm$  one standard deviation ( $n=3$ ).

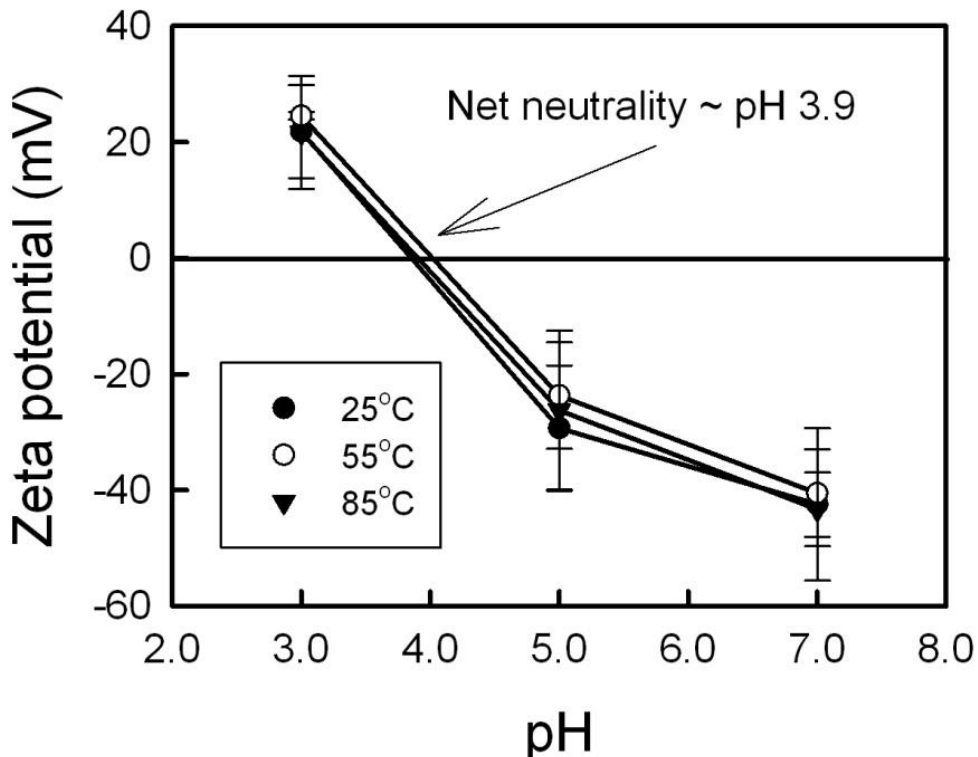


**Figure 4.2** Zeta potential (mV) for  $\beta$ -lactoglobulin solutions as a function of pH and pre-treatment temperature conditions. Data represent the mean  $\pm$  one standard deviation ( $n=3$ ).

The surface charge was also investigated for  $\beta$ -LG solutions as a function of pH and temperature pre-treatment conditions, and is given in Figure 4.2. An analysis of variance of  $\zeta$ -potential data found that only pH was significant ( $p<0.001$ ), whereas temperature ( $p>0.05$ ) and their interaction term (pH x temperature) ( $p>0.05$ ) was not (Table 4.1). In general, an increase in pH led to a decrease in  $\zeta$ -potential from  $\sim+22.9$  mV at pH 3.0,  $\sim-26.4$  mV at pH 5.0 and then  $\sim-42.1$  mV at pH 7.0 (Figure 4.2). The average isoelectric point (i.e.,  $\zeta$ -potential = 0 mV) was estimated to be at pH  $\sim 3.9$  (Figure 4.2). This value is counter intuitive to previously reported isoelectric values for  $\beta$ -LG to be pH  $\sim 5.1$  (Swaisgood, 2008; de Wit & van Kessel, 1996; Shin *et al.*, 2007). The difference is attributed to the way which these proteins were extracted, their conformation and association with neighboring  $\beta$ -LG proteins. The isoelectric point indicates that the net surface charge is zero where individual amino acid residues still carry charges at the protein surface. The varying charges on the surface of the protein may allow for proteins to associate electrostatically where these associations collectively may carry a charge. In a study by Basheva

and co-workers (2006)  $\beta$ -LG at an oil-water interface at its isoelectric point (pH 5.1) yielded a surface charge due to their orientation at the droplet surface. Therefore, the effect of pH and temperature pre-treatments on the size of  $\beta$ -LG aggregates was assessed.

#### 4.4.1.2 $\beta$ -Lg aggregation

The size (avg. hydrodynamic radius) of  $\beta$ -LG aggregates in solution was determined by light scattering as a function of pH and heat pre-treatment conditions (Figure 4.3). An analysis of variance of size data found that for both the main effects, pH ( $p<0.001$ ) and temperature ( $p<0.001$ ) and their associated interaction ( $p<0.001$ ) were significant (Table 4.1). Hydrodynamic

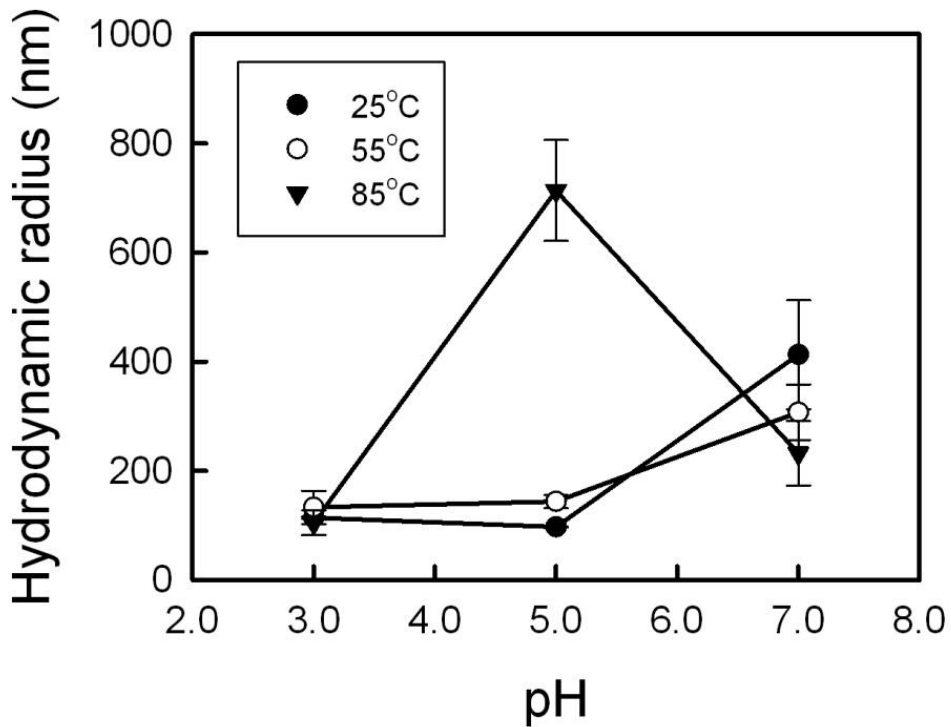


**Figure 4.3** Hydrodynamic radius (nm) for  $\beta$ -lactoglobulin solutions as a function of pH and pre-treatment temperature conditions. Data represent the mean  $\pm$  one standard deviation ( $n=3$ ).

radius data (Figure 4.3) for  $\beta$ -LG aggregates followed a similar pH and temperature trend as the hydrophobicity data (Figure 4.1A,B). At pH 3.0, any temperature dependence of hydrodynamic radius data was minimal (113.9 nm at 25°C, 133.1 nm at 55°C and 104.8 nm at 85°C). In contrast, at pH 7.0 a slight temperature dependence became apparent, where heat pre-treatments of 25, 55

and 85°C lead to hydrodynamic radii of 412.8 nm, 307.2 nm and 232.3 nm, respectively (Figure 4.3). The temperature dependence of  $\beta$ -LG aggregation behavior at pH 7.0 may be due to the heat-induced intermolecular  $\beta$ -sheet formation (Ngarize *et al.*, 2004) and increased hydrophobic interactions at higher temperatures.

In contrast, at pH 5.0 and pre-treated to 85°C,  $\beta$ -LG aggregates were found to be significantly larger (713.7 nm), then those pre-treated to 25°C (97.1 nm) and 55°C (143.6 nm) (Figure 4.3). Furthermore,  $\beta$ -LG solutions at pH 5.0 with 85°C heat treatment became turbid, whereas all other solutions remained clear. The turbidity is indicative of larger aggregate size as observed where 713.7 nm (hydrodynamic radii) aggregates were found. The larger aggregates under these conditions is thought to be associated with the increased hydrophobicity caused by protein unravelling in combination with a relatively neutral net charge (near its isoelectric point) to give more opportunities for the  $\beta$ -LG to aggregate *via* hydrophobic interactions. A Pearson correlation analysis indicated that protein hydrophobicity (*i.e.*, intrinsic fluorescence intensity ( $r = 0.507$ ,  $p < 0.01$ ) and surface hydrophobicity ( $r = 0.729$ ,  $p < 0.001$ )) and surface charge ( $r = -0.412$ ,  $p < 0.05$ ) were positively and negatively correlated with aggregate size, respectively.

Heating alters the structure of  $\beta$ -LG, such that at room temperature (*i.e.* 25°C) and below the denaturation temperature (*i.e.* 55°C) the protein is flexible and capable of refolding to its native state (Bhattacharjee *et al.*, 2005). Therefore their aggregative nature is thought to be dependent on the surface charge and hydrophobicity of  $\beta$ -LG at such temperatures. When  $\beta$ -LG is heated to denaturation temperatures (*i.e.* 85°C) the structures formed is dependent on the pH of the system (Jung *et al.*, 2008). It was previously reported that at pH 2.0, 5.8 and 7.0, the heat treatment of  $\beta$ -LG at temperatures  $\geq 85^\circ\text{C}$  will cause it to form rod-like, spherical or worm-like structures respectively (Jung *et al.*, 2008).

Protein aggregation due to heat treatment is a well-studied phenomenon, often affected by concentration, ionic strength pH and temperature (Hillier *et al.*, 1979; Hillier & Lyster, 1979; Dannenberg & Kessler, 1988; Luf, 1988; Parris *et al.*, 1993; Oldfield *et al.*, 1998; Schokker *et al.*, 2000b; Hoffmann *et al.*, 1997; Bauer *et al.*, 1998). Globular proteins tend to associate via non-covalent interactions (ionic, hydrophobic and van der Waals) which leads to the formation of large aggregates (Verheul *et al.*, 1998; Manderson *et al.*, 1998; Galani & Apeten, 1999; Hoffmann & van Mil, 1999; Schokker *et al.*, 1999; Zúñiga *et al.*, 2010). Furthermore, in the case of milk proteins, heat pre-treatments also causes the thiol and disulfide groups to be exposed to enable

thiol/disulfide exchange reactions to take place, and the formation of larger aggregate structures (Hoffmann *et al.*, 1997; Verheul *et al.*, 1998; Zúñiga *et al.*, 2010; Iametti *et al.*, 1996; Mounsey & O’Kennedy, 2007; Ryan *et al.*, 2012; Fessas *et al.*, 2001).

#### 4.4.1.3 Interfacial properties

The interfacial tension between the  $\beta$ -LG solutions as a function of pH and temperature pre-treatment conditions and canola oil at a water-oil interface is given in Figure 4.4. The presence of  $\beta$ -LG was found to reduce the interfacial tension between water and oil (~28 mN/m – without  $\beta$ -LG) to ~18 mN/m, indicating that  $\beta$ -LG is capable of adhering to the water-oil interface. An analysis of variance of interfacial tension data revealed that only pH was significant ( $p<0.001$ ), whereas temperature ( $p>0.05$ ) and their interaction ( $pH \times$  temperature) ( $p>0.05$ ) were not (Table 4.1). Although significant differences were found between pHs, differences in interfacial tension were minor. For instance, interfacial tension was ~17.8 mN/m at pH 3.0, ~18.6 mN/m at pH 5.0 and ~18.1 mN/m at pH 7.0 (Figure 4.4). Despite large differences seen in terms of hydrophobicity and size data under different pH and temperature pre-treatment conditions, this did appear to impact greatly on how well  $\beta$ -LG aligns to the interface. This suggests that despite physicochemical differences, proteins remain flexible and capable of reorienting themselves, and therefore  $\beta$ -LG may not have formed non-covalent bonds (*i.e.*, hydrogen and hydrophobic bonds) with neighboring proteins found to increase stability at an interface during the aging process (Tocholakova *et al.* 2006b).

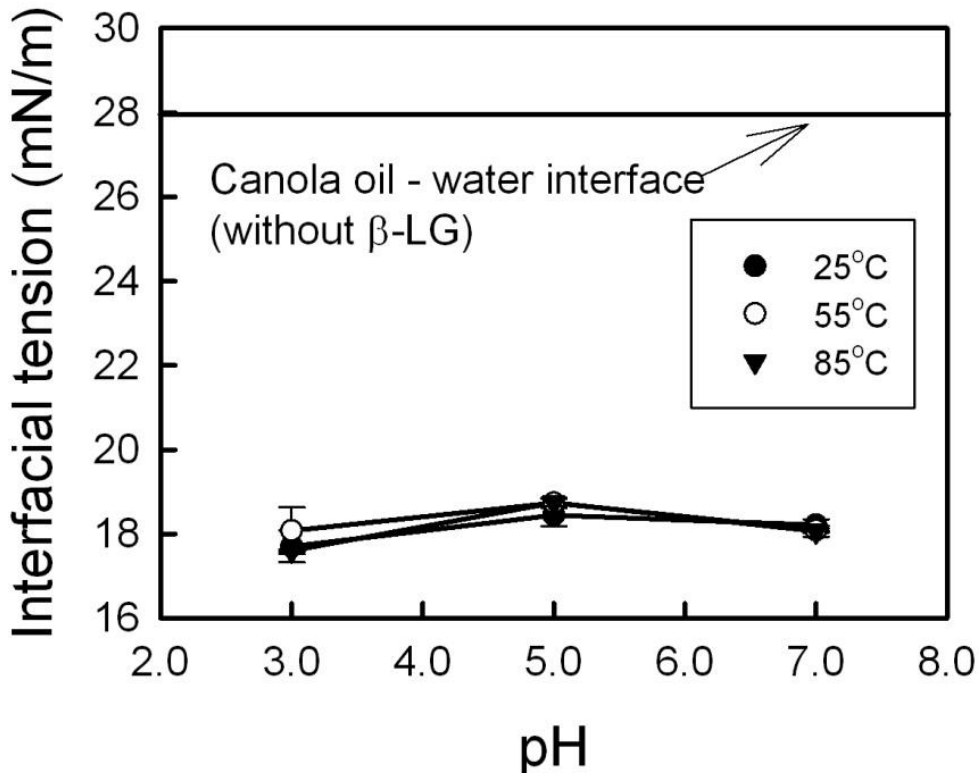


**Figure 4.4** The interfacial tension (mN/m) for  $\beta$ -lactoglobulin solutions as a function of pH and pre-treatment temperature conditions. Data represent the mean  $\pm$  one standard deviation ( $n=3$ ).

#### 4.4.2 Emulsifying properties

##### 4.4.2.1 Emulsion formation

Protein coverage on an oil droplet was measured by its emulsifying activity index (EAI) as a function of pH and temperature pre-treatment conditions (Figure 4.5A). An analysis of variance of EAI data found the main effects of pH ( $p<0.001$ ) and temperature ( $p<0.001$ ), along with their associated interaction ( $p<0.001$ ) were significant (Table 4.1). Regardless of the temperature pre-treatment conditions (25, 55 and 85°C) conditions, EAI values for  $\beta$ -LG solutions pre-heated were similar for pHs 3.0 and 5.0, declining from  $\sim 20.0 \text{ m}^2/\text{g}$  to  $\sim 14.3 \text{ m}^2/\text{g}$ , respectively. However at pH 7.0 significant differences in the EAI values arose depending on the temperature pre-treatment conditions. For instance, EAI values for pre-treatment temperatures of 25°C, 55°C and 85°C, EAI values were  $\sim 40.3 \text{ m}^2/\text{g}$ ,  $37.3 \text{ m}^2/\text{g}$ , and  $\sim 19.5 \text{ m}^2/\text{g}$ , respectively (Figure 4.5A).

Coating of emulsion droplets with  $\beta$ -LG seems to involve a complex relationship between hydrophobicity, surface charge and the level of protein aggregation in solution. Better surface coating is presumed to occur at pH 7.0 since surface charge ( $\sim -42$  mV) is much greater than the other pHs (pH/zeta potential = 3.0/ $\sim +22.7$  and 5.0/ $\sim -26.4$  mV), allowing  $\beta$ -LG to have increased mobility within the solution to the interface. However, this effect also seems to be related to hydrophobicity, where solutions displaying higher hydrophobicity (*e.g.*, 85°C) led to lowered EAI values. Pearson correlation coefficients for intrinsic fluorescence ( $r = -0.593$ ,  $p < 0.01$ ) and surface hydrophobicity ( $r = -0.366$ ,  $p < 0.10$ ) indicated a negative association between EAI and hydrophobicity. In contrast at pH 5.0,  $\beta$ -LG showed higher hydrophobicity than at pH 7.0 and lower net charge ( $\sim -26.4$  mV), leading to reduced ability for the protein to migrate to the interface and lower interfacial tension. At pH 3.0, surface charge was again reduced ( $\sim +22.7$  mV) and hydrophobicity raised relative to pHs 5.0 and 7.0 (with the exception of those heated to 85°C) influencing its ability to migrate and integrate into the interface. Aggregate size was not believed to influence EAI, with the exception of  $\beta$ -LG at pH 5.0 and heated to 85°C. When the surface hydrophobicity is increased, a protein may either increase its likelihood of forming an aggregate or adhere to an interface. Other factors which dictate whether which of the two options it assumes is dependent on the surface charge of the protein at the various pHs. Under highly surface charged conditions (*i.e.*, at pH 7.0/ $\sim -42$  mV versus the lower net charge at pH 3.0/ $\sim +22.7$  mV and pH 5.0/ $\sim -26.4$  mV), the electrostatic repulsive forces reduce the likelihood of aggregation and therefore a greater EAI is observed. Work done by Moro and co-workers (2001) indicate that an increase in heat treatment of whey protein concentrates will increase the surface hydrophobicity and EAI. This was not observed in this study which may be attributed to the solvent used on how these proteins unfold which are dependent on the pH of the system and ionic strength.

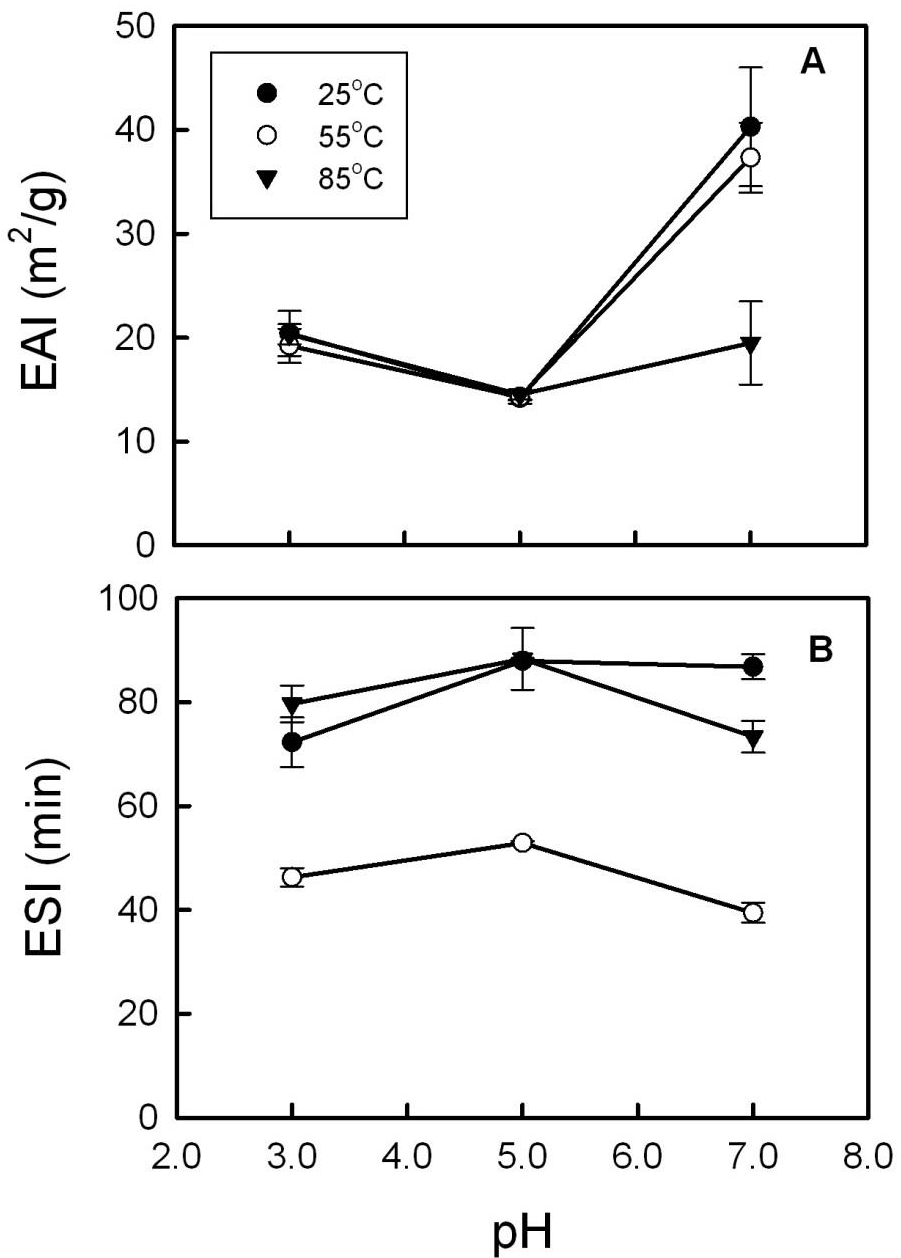


**Figure 4.5** The emulsion activity (EAI,  $\text{m}^2/\text{g}$ ) (A) and stability (ESI, min) indices for  $\beta$ -lactoglobulin solutions as a function of pH and pre-treatment temperature conditions. Data represent the mean  $\pm$  one standard deviation ( $n=3$ ).

#### 4.4.2.2 Emulsion stability

Emulsion stability indices for  $\beta$ -LG solutions as a function of pH and temperature pre-treatment conditions is given in Figure 4.5B. An analysis of variance of ESI data found the main effects of pH ( $p<0.001$ ) and temperature ( $p<0.001$ ), along with their associated interaction ( $p<0.001$ ) were significant (Table 4.1). Overall,  $\beta$ -LG solutions pre-treated to 55°C (~46.2 min) showed reduced ability to stabilize the oil-in-water emulsions than those pre-treated to 25°C (~82.3 min) or 85°C (~80.5 min) (Figure 4.5B). However, the trends at each pre-treatment temperature as a function of pH differed. For instance at pH 3.0, emulsion stability increased from those  $\beta$ -LG solutions pre-treated to 55°C (~46.3 min), followed by 25°C (~72.3 min) and then 85°C (~79.7 min) (Figure 4.5B). At pH 5.0, ESI increased from  $\beta$ -LG solutions pre-treated to 55°C (~52.9 min), followed by 25°C (~87.9 min) and 85°C (~88.3 min), which were similar (Figure 4.5B). And finally, at pH 7.0, ESI increased from those  $\beta$ -LG solutions pre-treated to 55°C (~39.4 min), followed by 85°C (~73.3 min) and then 25°C (~86.8 min) (Figure 4.5B).

Emulsion stability typically arises from electrostatic repulsive forces arising from the protein-viscoelastic film surrounding the oil droplets (Kim *et al.*, 2004), steric interference cause by protruding hydrophilic protein chains in solution (as loops or tails), or by increases in continuous phase viscosity as a result of unabsorbed proteins to the interface (Dickinson, 2001). In the present study, Pearson correlation coefficients for intrinsic fluorescence ( $r = -0.325$ ,  $p<0.10$ ) and surface hydrophobicity ( $r = -0.350$ ,  $p<0.10$ ) indicated a positive association between ESI and hydrophobicity. Overall, hydrophobicity was higher for  $\beta$ -LG solutions pre-treated to 85°C than those pre-treated to 25 and 55°C. At 85°C, it was presumed viscoelastic films were more elastic due to greater protein-protein associations, preventing droplet membranes from rupturing, leading to higher ESI than at 55°C.

The reduced ESI values observed at 55°C may be attributed to the interactions formed by partially unfolding  $\beta$ -LG at temperatures below denaturation. Eissa (2013) demonstrated that the aggregates formed by whey proteins below their denaturation temperature ( $\leq 60^\circ\text{C}$ ) are primarily held together by disulphide bonds. It is presumed that the partial unravelling of  $\beta$ -LG heated to 55°C encouraged the formation of disulphide bonds and other non-covalent bonds to form aggregates. The formation of these aggregates limited their ability to interact at the interface leading to reduced emulsion stability. At 85°C, the unfolded  $\beta$ -LG led to greater adherence to the interface due to greater flexibility followed by the formation of inter-protein bonds at the interface

which would increase the elasticity of the interfacial film leading to greater emulsion stability. Similar results were reported by Wang and co-workers (2012) where soy proteins exhibited greater emulsion stability when heat treated to 120°C compared to the partially unfolded state with 90°C and the native state. This is due to the increased molecular flexibility when proteins unfold at higher temperatures and the associated increase in molecular flexibility and enhanced inter-protein bond formation (Wang *et al.*, 2012).

#### **4.5 Conclusions**

This research investigated structure-function mechanisms associated with changes in  $\beta$ -LG physicochemical and emulsifying properties in response to changes in pH and temperature pre-treatment conditions. Aggregates of  $\beta$ -LG due to pH and heat treatments were found to be positively correlated with hydrophobicity while negatively correlated to surface charge. At pH 5.0 and 85°C pre-treatment, the largest aggregates were found which was attributed to the near neutral net surface charge and increased hydrophobicity. The surface charge and interfacial tension exhibited by  $\beta$ -LG was found to be only dependent on pH of the solution not temperature pre-treatments. EAI appeared to be higher in  $\beta$ -LG solutions that displayed high surface charge combined with moderate hydrophobicity. In contrast, ESI appears to be higher under conditions where  $\beta$ -LG solutions remained in a native (25°C) or fully denatured state (85°C) versus one in where partially unravelling may be occurring (55°C). With 55°C heat pre-treatment, the partially unravelled  $\beta$ -LG may form inter-protein bonds which lead to aggregate formation which reduces its flexibility and adherence towards a droplet interface. Under high temperature pre-treatments (*i.e.* 85°C), the fully unravelled  $\beta$ -LG may form inter-protein bonds with more flexibility and capacity to adhere to the interface. A full mechanistic understanding of the emulsifying properties of  $\beta$ -LG is clouded by the complexity of the system and inter-relationships between the physicochemical properties and changes to protein structure/conformational in response to pH and temperature pre-treatment conditions.

#### **4.6 Connection to the next study**

In this and the previous study, the effect of pH and temperature pre-treatments on the physicochemical and emulsifying properties of whey protein isolates and  $\beta$ -lactoglobulin were investigated. The following study focuses on the influence of temperature pre-treatments, pH and

the presence of calcium on the physicochemical and emulsifying properties of alpha-lactalbumin (ALA). Calcium is known to bind to ALA to alter its conformation, which is hypothesized to lead to different physicochemical and emulsifying properties than ALA without calcium. Solution pH was selected at 5.00 and 7.00 where the protein assumes a neutral and negative net charge, respectively. Both pHs also showed greater effects on the physicochemical and emulsifying properties for WPI and  $\beta$ -LG than at pH 3.00. As a result, only pHs 5.00 and 7.00 were investigated in this study. Temperature pre-treatments of 25, 65 and 95°C were selected for this study based on a literature survey to correspond to where ALA is believed to be its native conformation, partially denatured and fully denatured, respectively.

## **5. THE EFFECT OF PH AND TEMPERATURE PRE-TREATMENTS ON THE STRUCTURE, SURFACE CHARACTERISTICS AND EMULSIFYING PROPERTIES OF ALPHA-LACTALBUMIN<sup>4</sup>**

### **5.1 Abstract**

The effect of pH (5.0 or 7.0) and temperature (25.0, 65.0 and 95.0°C) on the physicochemical and emulsifying properties of type-1 (with calcium, ALA-1) and type-3 (without calcium, ALA-3) alpha-lactalbumin (ALA) were examined. By increasing the temperature of pre-treatment, changes in ALA conformation allowed for greater surface hydrophobicity and caused changes in its surface charge. pH also influenced surface charge for ALA where enhanced repulsion at pH 7.00 was observed resulting in reduced aggregation despite having greater hydrophobicity. Findings indicate that changes to protein conformation using various pH and temperature pre-treatments influenced their surface chemistry, aggregation and ability to align at the oil-water interface. Overall, emulsions were found to be more stable at pH 7.0 than 5.0 due to the presence of electrostatic repulsive forces between droplets. Under the conditions examined in this study, ALA-3 pre-treated at 65°C and at pH 7.00 resulted in the best emulsifying properties.

### **5.2 Introduction**

Alpha-lactalbumin (ALA) is the second major protein found in bovine whey next to beta-lactoglobulin. Its biological function in milk is to aid with lactose biosynthesis however, it's also highly nutritious and functional as a food ingredient (Berliner *et al.*, 1991; Heine *et al.*, 1991; Korhonen & Pihlanto, 2007; Bonnaillie & Tornasula, 2012). The functionality of ALA has been studied in terms of its foaming, gelling and emulsifying properties (Matsudomi *et al.*, 1993; Hunt & Dalglish, 1994a; Ibanoglu & Ibanoglu, 1999; Zhai *et al.*, 2012). The latter represents the primary focus of this study. Emulsions are formed when two immiscible liquids are mechanically

---

<sup>4</sup> Submitted as: Lam, R. & Nickerson, M.T. (2014). The effect of pH and temperature pre-treatments on the structure, surface characteristics and emulsifying properties of alpha-lactalbumin. *Food Chemistry*.

agitated whereby one becomes dispersed as droplets within the other. Proteins, which are amphiphilic in nature, serve to help stabilize the emulsion by decreasing the surface tension between the two phases. ALA also has been reported to change its secondary and tertiary structure upon adhering to the oil-water interface to enhance emulsion stability (Zhai *et al.*, 2012). Hunt and Dalgleish (1994a) reported that at pH < 7.0, ALA preferentially adsorbs to the oil-water interface over  $\beta$ -lactoglobulin ( $\beta$ -LG).

ALA is a globular protein that has a molecular mass of 14-16 kDa and an isoelectric point of 4.2. Structurally it is comprised of two domains: a  $\alpha$ -domain made of 4  $\alpha$ -helices and a  $\beta$ -domain made of  $\beta$ -sheets and looped regions (Bramaud *et al.*, 1995; Wu *et al.*, 1996; Wang & Lucey, 2003). In general, the presence of bound calcium leads to a less flexible protein with enhanced thermal stability (Relkin *et al.*, 1993; Rajaraman *et al.*, 1998; Hendrix *et al.*, 2000). For instance, ALA's denaturation temperature was reduced from  $\sim$ 64°C to  $\sim$ 35°C once calcium was removed (Relkin *et al.*, 1993). Hendrix and co-workers (2000) reported that increasing the CaCl<sub>2</sub> content from 0.0 to 2.0 mM CaCl<sub>2</sub> caused an increase in the enthalpy of unfolding from 271 to 318 kJ mol<sup>-1</sup>. Solvent conditions, such as pH and temperature have also been found to alter the conformation of ALA (Cornec *et al.*, 2001). For instance at extreme pH (*e.g.*, 2.0), ALA has been found to change in conformation to a more open structure (Cornec *et al.*, 2001). Fang & Dalgleish (1998) reported that when ALA is exposed to temperatures  $>$ 90°C, irreversible denaturation occurs, whereas at temperatures  $<$ 90°C, refolding of the protein conformation can occur.

The overall goal of this study is to investigate the effect of pH and temperature pre-treatments on the emulsifying properties of type-1 (with calcium) and type-3 (without calcium) ALA. Understanding the emulsifying properties of ALA may help scientists and industry design novel functional foods (*i.e.* infant formulas) using ALA as an encapsulating agent for the delivery of bioactives and or other nutraceuticals.

### **5.3 Materials and methods**

#### **5.3.1 Materials**

Type-1 (with calcium) and type-3 (without calcium) ALA were purchased form Sigma-Aldrich (Oakville, ON, Canada) and used without further purification. Henceforth, the two types of ALA will be referred to as ALA-1 and ALA-3. A certificate of analysis was provided by Sigma-Aldrich indicating the calcium content for ALA-1 (Product #: L5385, Lot #: 110M7003V) and

ALA-3 (Product #: L6010, Lot #: 110M7029V) to be 2 and 0.3 moles  $\text{Ca}^{2+}$  per mole of ALA, respectively. Protein content for ALA-1 and ALA-3 were determined to be 87.28% and 83.23% respectively ( $\% \text{N} \times 6.38$ ) as measured using a micro-Kjeldahl digester (Micro Digestor, Labconco, Kansas City, MO, USA) and distillation unit (RapidStill I, Labconco, Kansas City, MO, USA) according to AOAC Official Method 920.87 (AOAC, 2003). Canola oil used in this study was purchased from a local supermarket. All other chemicals used in this study were of reagent grade and purchased through Sigma-Aldrich (Oakville, ON, Canada). The water used in this research was filtered using a Millipore Milli-Q<sup>TM</sup> water purification system (Millipore Corp., Milford, MA, USA).

### **5.3.2 Sample preparation**

ALA stock solutions (0.1%, w/w corrected for protein content) were prepared by dispersing the ALA-1 and ALA-3 powder in water adjusted to pH 5.0 or 7.0 using either 0.5 M HCl or 0.5 M NaOH, followed by mechanically stirring (500 rpm) at room temperature (21-23°C) for 60 min. Protein solutions were then poured into screw capped 15 mL centrifuge tubes to prevent moisture losses, and held in a water bath for 30 min at 25°C, 65°C and 95°C. Tubes were left out to cool down to room temperature prior to analysis.

### **5.3.3 Circular dichroism**

Circular dichroism (CD) was performed on 0.02% (w/w) ALA-1 and ALA-3 solutions using a PiStar-180 spectrometer (Applied Photophysics, Surrey, UK) equipped with a 75W Mercury Xenon Lamp. CD was performed on samples contained in quartz curvettes with a 0.5 mm path length. A CD spectrum was taken from 190 to 240 nm at intervals of 0.5 nm where the slit width was set at 6.0 nm. A spectrum for the mean residue molar ellipticity (deg cm<sup>2</sup> dmol<sup>-1</sup>) was plotted as a function of wavelength for all samples. A comparison in raw spectra data was made to show relative changes to the secondary structure among sample treatments. Flattening of the CD spectra indicates loss in structure.

### **5.3.4 Surface hydrophobicity**

The surface hydrophobicity for each protein solution was determined by intrinsic fluorescence as a function of emission wavelength. A FluoroMax-4 spectrofluorometer (Horiba

Jobin Yvon Inc., Edison, N.J., USA) was used to determine the intrinsic fluorescence for 0.05% (w/w) protein solutions at a constant excitation wavelength of 275 nm as a function of emission wavelength between 285 to 450 nm using a 1 nm slit width. All intensity data was arbitrarily divided 10,000 prior to statistical analysis and graphing. This technique measures the fluorescence of the aromatic amino acids tyrosine, tryptophan and phenylalanine. The maximum fluorescence intensity (in arbitrary units) was determined for each spectra captured.

### 5.3.5 Surface charge

The electrophoretic mobility ( $U_E$ ) was determined using the Zetasizer Nano-ZS90 (Malvern Instruments, Westborough, MA) for all protein samples (0.05%, w/w). The zeta-potential ( $\zeta$ ; units: mV) was determined from the electrophoretic mobility ( $U_E$ ) using Henry's equation (eq. 5.1):

$$U_E = \frac{2\epsilon\zeta f(\kappa\alpha)}{3\eta} \quad (\text{eq. 5.1})$$

where  $\epsilon$  is the permittivity (units: F (Farad)/m),  $f(\kappa\alpha)$  is the function related to the ratio of particle radius ( $\alpha$ ; units: nm) and Debye length ( $\kappa$ ; units: nm<sup>-1</sup>), and  $\eta$  is the dispersion viscosity (units: mPa·s) (McClements, 2005). The Smoluchowski approximation  $f(\kappa\alpha)$  was set as 1.5, as is accustom for folded capillary cells and, with particles larger than 0.2 μm dispersed in moderate electrolyte concentration (>1 mM). The Smoluchowski approximation assumes that a) concentration of particles (proteins) is sufficiently high such that such thickness of the electric double layer (Debye length) is small relative to the particle size ( $\kappa\alpha \gg 1$ ); and b)  $\zeta$  is linearly related to  $U_E$ . All measurements are reported as the mean ± one standard deviation (n = 3).

### 5.3.6 Hydrodynamic radius

The hydrodynamic radius for ALA aggregates formed under the different pH and temperature pre-treatment conditions were measured using the Zetasizer Nano-ZS90 (Malvern Instruments, Westborough, MA, USA). Approximately, 1 mL of each protein solution (0.05%, w/w) was placed in a plastic curvette (1 cm path length) within the Zetasizer's sample holder. The scattering intensity was measured at a 90° angle at 633 nm using a 4 mW He/Ne laser at room temperature (21-23°C). The hydrodynamic radius was estimated based on the Stokes-Einstein equation (Eq. 5.2 and 5.3):

$$D = \frac{k_B T}{6\pi\eta r} \quad (\text{eq. 5.2})$$

which may be re-written as:

$$r = \frac{k_B T}{6\pi\eta D} \quad (\text{eq. 5.3})$$

Where,  $k_B$  is the Boltzmann constant ( $1.38062 \times 10^{-23} \text{ J K}^{-1}$ ),  $D$  is the self-diffusion constant ( $\text{m}^2 \text{ s}^{-1}$ ),  $T$  is the absolute temperature (K),  $\eta$  is viscosity of the medium ( $\text{Kg m}^{-1} \text{ s}^{-1}$ ) and  $r$  is the radius of the diffusing particle (m) (Hoffman *et al.*, 1998).

### 5.3.7 Interfacial tension

The interfacial tension for each protein solution (0.1%, w/w) was measured using a Lauda TD 2 Tensiometer (Lauda-Königshofen, Germany) equipped with a Du Nüoy ring (20 mm diameter). Within a 40 mm diameter glass sample cup, a 20 mL protein solution was added, followed by the immersion of the Du Nüoy ring and then the addition of upper canola oil layer (20 mL). The ring was then pulled upwards to stretch the interface to measure the maximum force without breaking into the oil phase. Samples were measured at 3 min intervals until three consecutive measurements obtained a standard deviation of less than 0.1 mN/m. Interfacial tension was calculated from the maximum force ( $F_{\max}$ ; units: milli-Newton; instrument measures mg x gravity) using the following equation (eq. 5.4):

$$\gamma = \frac{F_{\max}}{4\pi R\beta} \quad (\text{eq. 5.4})$$

where,  $\gamma$  is the interfacial tension (mN/m),  $R$  is the radius of the ring (20 mm),  $\beta$  is a correction factor that depends on the dimensions of the ring and the density of the liquid involved (McClements, 2005).

### 5.3.8 Emulsification stability and activity indices

Emulsions were prepared by mixing 5 g of the 0.1% (w/w) ALA solution with 2 g of canola oil within a 50 mL plastic centrifuge tube, followed by homogenization at 7,200 rpm for 5 min using an Omni Macro Homogenizer (Omni International Inc., Marietta, GA) equipped with a 20 mm saw tooth generating probe. Emulsion stability (ESI) and activity (EAI) indices were determined according to Pearce and Kinsella (1978). The EAI provides an estimate of the relative surface coverage of a protein on an oil droplet within a dilute emulsion, whereas the ESI gives an

estimate of its relative stability after a pre-determined time. Immediately after emulsion formation, a 50 µL aliquot is transferred into 7.5 mL of pH-adjusted water containing 0.1% sodium dodecyl sulphate (SDS), vortexed for 10 s, and then absorbance read at 500 nm using a ultraviolet-visible spectrophotometer (Genesys 20, Thermo Scientific, Madison, WI) and plastic cuvettes (1 cm path length). A second aliquot of the emulsion was then taken after 10 min, following the same procedure. The EAI and ESI were determined using eq. 5.5 and 5.6, respectively:

$$EAI(m^2/g) = \frac{2 \cdot 2.303 \cdot A_0 \cdot N}{c \cdot \varphi \cdot 10000} \quad (\text{eq. 5.5})$$

$$ESI(\text{min}) = \frac{A_0}{\Delta A} \cdot t \quad (\text{eq. 5.6})$$

where  $A_0$  is the absorbance of the diluted emulsion immediately after homogenization,  $N$  is the dilution factor ( $150\times$ ),  $c$  is the weight of protein per volume (g/mL),  $\varphi$  is the oil volume fraction of the emulsion,  $\Delta A$  is the change in absorbance between 0 and 10 min ( $A_0 - A_{10}$ ) and  $t$  is the time interval, 10 min.

### 5.3.9 Statistics

All experiments were performed in triplicate and reported as the mean ± one standard deviation. A three-way analysis of variance (ANOVA) was performed to test for significance in the main effects of type (ALA-1 and ALA-3), pH (5.0, 7.0) and heat pre-treatment conditions (25, 65, 95°C), along with their associated interactions on the physicochemical and emulsifying properties of ALA. Statistical analyses were performed with Systat (SPSS Inc., Ver. 10, 2000, Chicago, IL).

## 5.4 Results and discussion

### 5.4.1 Protein conformation

Circular dichroism was used to measure relative changes in ALA's secondary structure in response to pH and temperature pre-treatments for both ALA-1 and ALA-3 (Figure 5.1). Overall, mean molar ellipticity data for ALA-1 was more stable against temperature pre-treatments than ALA-3 presumed due to the presence of calcium. At pH 5.00, there was very little change in molar ellipticity as a function of temperature (Figure 5.1A). However at pH 7.00, ALA-1 underwent increased ordering in the secondary structure as temperatures increased from 25°C to

65°C as evident by a decreased mean ellipticity curve (Figure 5.1B). As temperatures increased to 95°C, a loss in secondary structure was then observed as evident by a rise in the mean ellipticity curve (higher than both the 25 and 65°C). It is hypothesized that at 65°C, the protein experiences increased conformational entropy allowing for the polypeptide chains to undergo greater ordering. However at 95°C, protein denaturation is thought to occur as the result of the breakage of hydrogen bonds at higher temperatures leading to a loss in structure. Similarly, it has been previously reported that temperatures above 90°C, ALA becomes irreversibly denatured (Fang & Dalgleish, 1998).

Conformational re-ordering have been previously reported in soy proteins (Miriani *et al.*, 2011), rice proteins (Ellepola & Ma, 2006) and ALA (Griko, 1999). Ellepola and Ma (2006) reported that rice proteins underwent partial denaturation depending on the time proteins were subjected to thermal treatment. They reported that by increasing the thermal pre-treatment on rice proteins, an increase in the denaturation temperature was observed which was complemented by a decrease in its denaturation enthalpy (Ellepola & Ma, 2006). Similarly, Griko (1999) reported a similar increase in denaturation temperature in ALA samples pre-treated at various temperatures. Furthermore, Griko (1999) stated that these changes in denaturation temperature were largely dependent on solvent conditions. Using various spectroscopic techniques, Miriani and co-workers (2011) reported tertiary structural re-orientation of soy proteins due to various temperatures of thermal treatment.

Biologically, calcium is known to bind to ALA to aid in the biosynthesis of lactose (Berliner *et al.*, 1991). The effect of calcium ions on the thermal properties of ALA has been well studied (Relkin *et al.*, 1993; Wehbi *et al.*, 2005; Atri *et al.*, 2010). It has been reported that the presence of calcium does not greatly affect the structure of ALA as it relates to the retention of the shape of the ellipticity curve as seen in Figure 5.1 A-B, and as reported by others (Pfeil & Sadowski, 1985; Kuwajima *et al.*, 1986). Cor nec and co-workers (2001) reported a similar ellipticity curve for native ALA at pH 7.5 in a 20 mM phosphate buffer at 25°C. Calcium has been found to enhance the thermal stability of ALA when its concentration increased in solution (Relkin *et al.*, 1993; Hendrix *et al.*, 2000). Hendrix and co-workers (2000) reported that the enthalpy associated with denaturation increased with calcium concentration which depended on the degree of saturation of calcium ions on ALA.

In the case of ALA-3, the mean molecular ellipticity curves appeared to be similar at both pH 5.00 and 7.00. ALA-3 increased structuring by a decreased in mean ellipticity as temperatures were raised from 25 to 65°C, which was followed by an increase in mean ellipticity as temperatures reached 95°C indicating a loss of structure (Figure 5.1 C, D). The larger extent

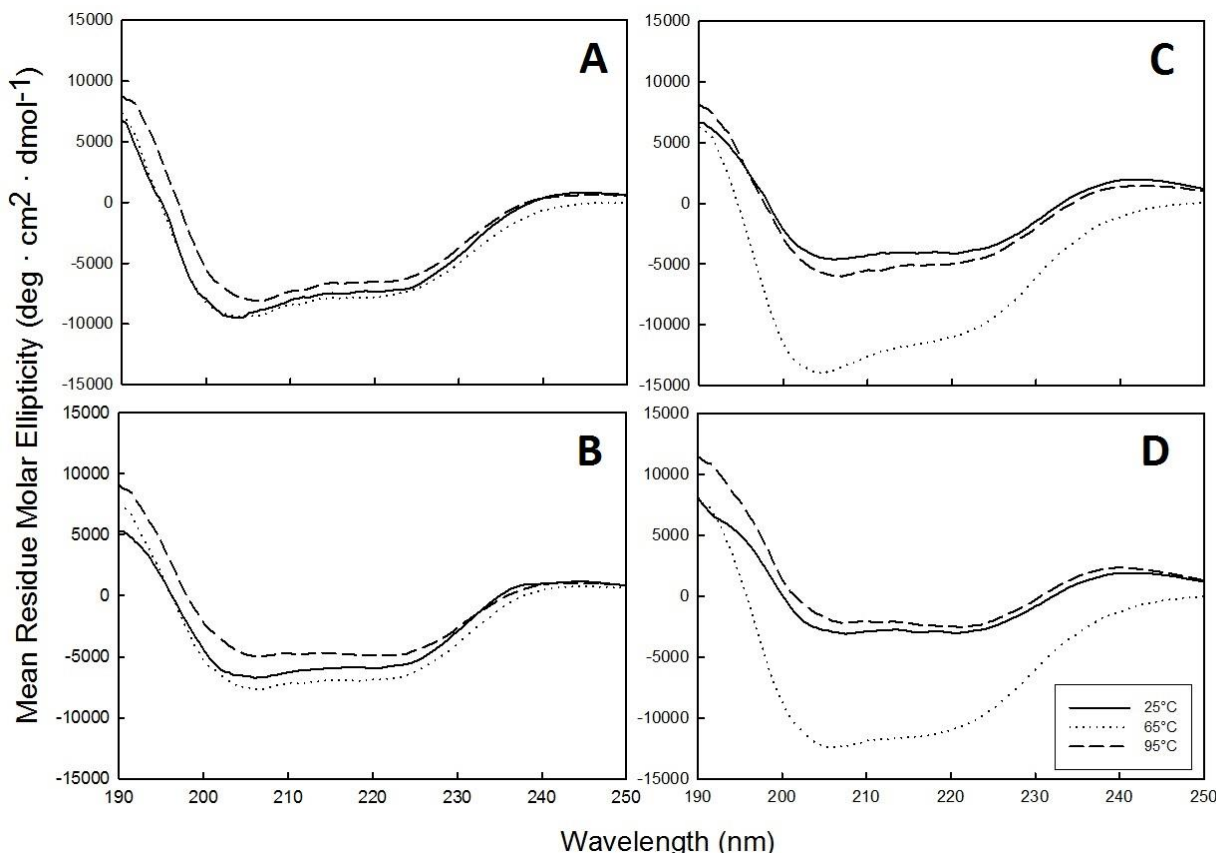


**Figure 5.1** Mean residue molar ellipticity data for ALA-1 (A-B) and ALA-3 (C-D) at pH 5.00 (A, C) and 7.00 (B, D) as a function of wavelength and temperature pre-treatments. Curves represent the means of 4 spectra.

of conformational changes in ALA-3 compared to ALA-1 is attributed to ALA-3 structure under these solvent and thermal conditions. It is speculated that the absence of calcium ions in ALA-3 can undergo greater changes to its structure in response to temperature pre-treatments, and possibly leading to a partially unravelled state depending on the solvent conditions. A partially unravelled state could also show increased surface hydrophobicity (Arai & Kuwajima, 1996), form aggregates (Rajaraman *et al.*, 1998) and have pronounced hydrogen bonding (Arai & Kuwajima, 1996) relative to the native state. The pronounced hydrogen bonding might explain for the enhanced

ordering seen with ALA-3 treated at 65°C. As ALA returns to room temperature, it re-folds from its unravelled state (Kuwajima, 1996; Permyakov & Berliner, 2000) sometimes into a non-native state (Rajaraman *et al.*, 1998; Hong & Creamer, 2002). From Figure 5.1, ALA-3 at 65°C suggests that its structure is not in its native conformation.

#### 5.4.2 Surface characteristics

The surface charge of ALA-1 and ALA-3 as a function of temperature pre-treatments and solution pH was determined by measuring the protein's zeta potential (Figure 5.2). A 3-way ANOVA determined that the main factors of protein-type ( $p<0.001$ ) and pH ( $p<0.001$ ) as well as the interactions pH  $\times$  temperature ( $p<0.001$ ), pH  $\times$  protein-type ( $p<0.05$ ) and temperature  $\times$  type ( $p<0.05$ ) were statistically significant. At pH 5.00, both ALA-1 and ALA-3 carried a low

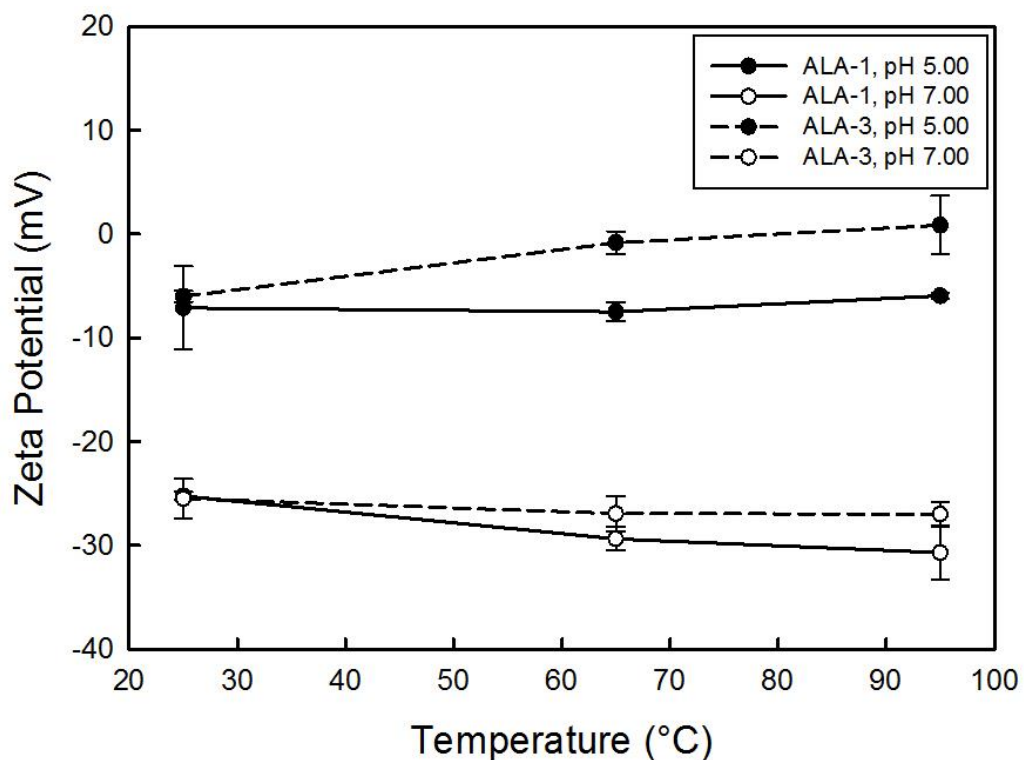


**Figure 5.2** Zeta potential of ALA-1 and ALA-3 proteins as a function of pH and temperature pre-treatments. Data represent the mean  $\pm$  one standard deviation ( $n = 3$ ). net charge regardless of the temperature. In the case of ALA-1, the zeta potential remained constant regardless of the temperature pre-treatment at  $\sim -6.83$  mV, whereas for ALA-3 the zeta potential rose slightly from  $\sim -5.99$  mV at 25°C to  $\sim +0.87$  mV at 95°C (Figure 5.2). The low net surface

charge at pH 5.00 is believed to be associated with the proximity to ALA's isoelectric point (pI 4.2 (Bramaud *et al.*, 1995; Wu *et al.*, 1996; Wang & Lucey, 2003)). At pH 7.00, ALA-3 remained constant regardless of the temperature at ~ -26.4 mV, whereas ALA-1 was much more temperature dependent. For instance, at 25°C the zeta potential was ~ -25.2 mV, then declined significantly to ~ -29.4 mV at 65°C where it remained relatively constant to 95°C (~ -30.7 mV) (Figure 5.2). Zeta potential values were highly negative at pH 7.00 since it is away from its pI value (pH 4.2). The factors which affected the surface charge were dominated by the pH effects on these proteins. Overall, it was observed that in the absence of calcium, changes in the conformation of ALA-1 caused the surface charge to be more negative than ALA-3 when these proteins were treated at higher temperatures.

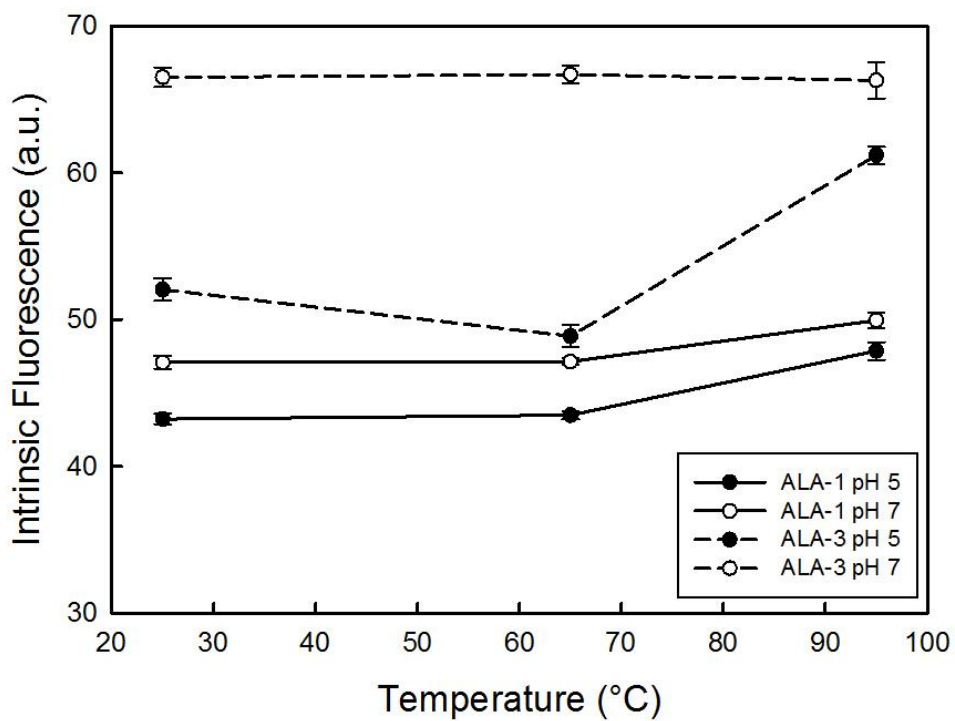


**Figure 5.3** Maximum fluorescent intensity of ALA-1 and ALA-3 proteins as a function of pH and temperature pre-treatments. Data represent the mean  $\pm$  one standard deviation ( $n = 3$ ).

The surface hydrophobicity of ALA-1 and ALA-3 were determined by measuring the fluorescence intensity of exposed hydrophobic amino acid residues tryptophan, phenylalanine and tyrosine in the solvent. The maximum fluorescent intensity was used for comparative purposes as

a function of protein-type, temperature and pH (Figure 5.3). A 3-way ANOVA indicated that the three main factors (protein-type, pH and temperature) and all its subsequent interactions were significantly different ( $p<0.001$ ). Overall, fluorescent intensity was greater for ALA-3 than ALA-1, and at pH 7.00 than pH 5.00 (Figure 5.3) indicating that at pH 7.00 proteins has a more open structure with exposed hydrophobic moieties than at a pH closer to its pI value. And that ALA-3 was structurally more open than ALA-1 presumed due to the lack of calcium.

ALA-3 at pH 7.00 was found to show the greatest fluorescent intensity (~66.5 a.u.) and was found to be temperature independent (Figure 5.3). These findings complement zeta potential data which also was found to be temperature independent (Figure 5.2). ALA-3 at pH 5.00, displayed the next highest hydrophobicity, however was more temperature dependent (Figure 5.3). For instance at 25°C maximum intensity was found at ~52.1 a.u., which then decreased to ~48.9 a.u. with a 65°C temperature pre-treatment, before increasing to ~61.2 a.u. at 95°C which suggests a change in the tertiary structure of the protein (Figure 5.3).

In the case of ALA-1, the temperature effect was similar where maximum fluorescent intensity was constant when temperatures were at 25°C and 65°C occurring at ~43.4 a.u. and ~47.1 for solvent pH of 5.00 and 7.00, respectively (Figure 5.3). Fluorescent intensity then increased to ~47.9 a.u. and ~50.0 a.u. at solvent pH of 5.00 and 7.00, respectively as temperatures were raised to 95°C (Figure 5.3). The rise in fluorescence reflects a change in tertiary structure conformation due to thermal denaturation where an increased amount of hydrophobic moieties become exposed attributed to the denaturation of ALA-1 at temperatures above 90°C (Fang & Dalgleish, 1998).

The presence of calcium was previously been reported to not affect the secondary structure of ALA (Pfeil & Sadowski, 1985; Kuwajima *et al.*, 1986). Therefore, in the present study it is hypothesized that observed changes in hydrophobicity may be attributed to the effect of calcium on the tertiary structure of ALA. In the absence of calcium, ALA-3 obtained an open conformation which allowed for greater exposure of the hydrophobic moieties normally shielded away in the presence of calcium (*i.e.* in ALA-1). This explains for the greater surface hydrophobicity in ALA-3 at all temperatures and pH conditions compared to ALA-1.

#### **5.4.3 Protein aggregation**

The hydrodynamic radius for ALA aggregates as a function of protein-type, pH and temperature pre-treatments were investigated by dynamic light scattering. A 3-way ANOVA determined that for all these main factors and subsequent interactions were found to be statistically

significant ( $p < 0.001$ ). ALA-3 at pH 5.00 showed the greatest size and temperature dependence relative to the other samples indicating an increased amount of protein-protein interactions which was attributed to very weak net charge over the complete temperature range (~ -5.99 mV at 25°C to ~ 0.874 mV at 95°C) (Figure 5.2) and relatively high hydrophobicity relative to the ALA-1 samples (at pH 5.00 and pH 7.00) (Figure 5.3). The lack of calcium to stabilize the ALA structure and the lack of surface charge is thought to lead to a more open structure than the other samples, which promotes protein-protein aggregation. The hydrodynamic radius was found to increase from ~503.3 nm at pH 25°C to ~1064 nm at 65°C where it remained constant at ~948.7 nm at 95°C (Figure 5.4). Similar behaviour was seen for ALA-3 at pH 7.00, and for ALA-1 at both pH 5.00 and 7.00, except the overall magnitude of the

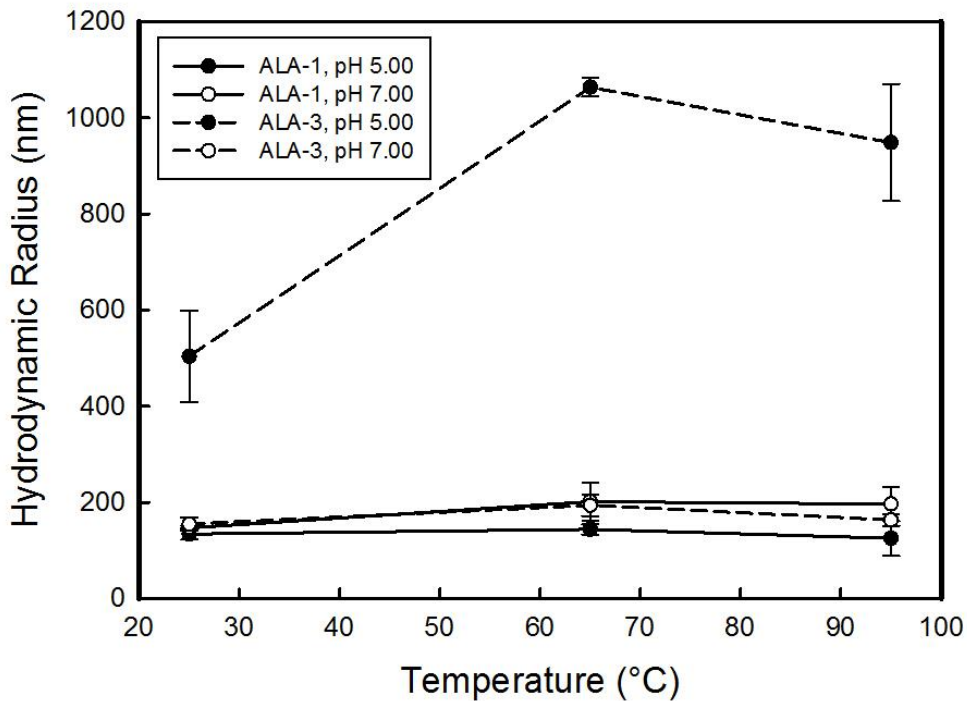


**Figure 5.4** Mean hydrodynamic radius (nm) of ALA-1 and ALA-3 proteins as a function of pH and temperature pre-treatments. Data represent the mean  $\pm$  one standard deviation ( $n = 3$ ).

hydrodynamic radius was ~200 nm or less. In all 3 samples, the radius increased slightly from 25°C to 65°C where it then remained constant even at 95°C (Figure 5.4).

Various authors have studied the denaturation and aggregation behavior of ALA (Bertrand-Harb *et al.*, 2002; Chaplin & Lyster, 1986; McGuffey *et al.*, 2005). The ability for ALA to form

aggregates depends on the protein concentration, heating profile and solvent properties (Bertrand-Harb *et al.*, 2002; Chaplin & Lyster, 1986; McGuffey *et al.*, 2005). ALA was found to denature when exposed to heat and refolded upon cooling (Kuwajima, 1996; Permyakov & Berliner, 2000). The degree of refolding depends on the aforementioned variables where one group reported that at temperatures above 90°C, irreversible denaturation was observed (Chaplin & Lyster, 1986; McGuffey *et al.*, 2005). The heating of ALA at 95°C was reported to induce the exposure of thiol groups which caused ALA to aggregate (McGuffey *et al.*, 2005). With these thiol groups exposed due to the breaking of the disulfide bonds, hydrophobic interactions caused large aggregates to form (McGuffey *et al.*, 2005). This explains for the large aggregates observed in Figure 4. The larger aggregates observed at 65 and 95°C compared to those at 25°C may be attributed to the exposure of thiol groups leading to protein-protein interactions and aggregate formation. The size of these aggregates are limited and speculated to be affected by the strong electrostatic repulsion experienced by ALA at pH 7.00. Similarly, Tcholakova and co-workers (2006b) have reported that electrostatic repulsive forces help keep whey proteins from aggregating whereby the smaller aggregates provide enhanced stability in solution. Calcium in ALA-1 may also restrict the ability for ALA to form aggregates thereby limiting the size of these aggregates also. There have also been reports where the presence of calcium was found to stabilize the disulfide bond in ALA which enhances its thermal stability (Chang & Li, 2001; Livney *et al.*, 2003). When proteins were exposed to near neutral conditions and in ALA samples depleted of calcium (i.e. ALA-3 at pH 5.00), the open structure, thermal denaturation and reduced electrostatic repulsion are all factors which promote the formation of large aggregates.

#### 5.4.4 Interfacial properties

The interfacial tension between canola oil and a 0.1% w/w ALA-1 and ALA-3 solution in response to temperature pre-treatments and solvent pH were measured using a Du Noüy ring method (Figure 5.5). Findings were analysed using a three-way ANOVA to find all main factors and the 2-way interaction between temperature and protein-type to be significant ( $p<0.001$ ). ALA-1 and ALA-3 were found to greatly reduce the interfacial tension of the water-canola oil interface from ~28 mN/m to ~14 mN/m. A Pearson correlation determined that the interfacial properties of ALA were significantly related to the surface charge of these proteins ( $r = 0.62$   $p<0.001$ ). In all cases, interfacial tension was lower at pH 5.00 than at pH 7.00 due to its proximity to its isoelectric

point where it carried less of a net charge allowing for better adsorption at the interface and protein-protein interactions to form a viscoelastic film. ALA-3 proteins were found to be temperature independent whereas ALA-1 experienced slight improvement in their ability to lower interfacial tension when exposed to higher temperatures (Figure 5.5). However this trend was only minor.

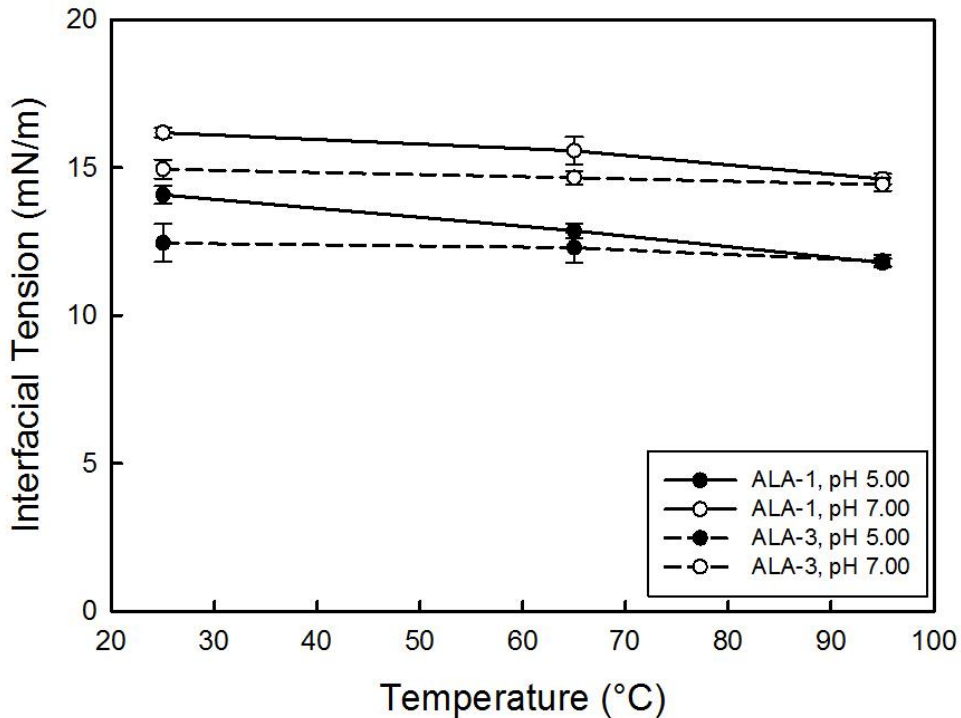


**Figure 5.5** Mean interfacial tension (mN/m) of ALA-1 and ALA-3 proteins as a function of pH and temperature pre-treatments. Data represent the mean  $\pm$  one standard deviation ( $n = 3$ ).

#### 5.4.5 Emulsifying properties

The emulsion activity index (EAI) (Figure 5.6A) and emulsion stability index (ESI) (Figure 5.6B) in response to pH and temperature pre-treatments was obtained using a turbidimetric technique developed by Pearce and Kinsella (1978) for dilute protein-stabilized emulsions. A 3-way ANOVA determined that for EAI, the main factors of pH and protein-type, and the two way interactions of: pH  $\times$  temperature and pH  $\times$  protein-type were significant ( $p < 0.001$ ). EAI measures how well a protein can coat an oil droplet surface (Pearce & Kinsella,

1978). Overall, it was found that ALA proteins at pH 7.00 (regardless of the type) coated the droplets better than those at pH 5.00; however ALA-3 experienced a much larger magnitude difference. For instance, ALA-3 increased from  $\sim$ 71.82 m<sup>2</sup>/g at pH 5.00 to  $\sim$ 209.2 m<sup>2</sup>/g at pH 7.00 (difference of  $\sim$ 137.4 m<sup>2</sup>/g), whereas ALA-1 increased from  $\sim$ 59.22 m<sup>2</sup>/g at pH 5.00 to  $\sim$ 113.9 m<sup>2</sup>/g at pH 7.00 (difference of  $\sim$ 54.68 m<sup>2</sup>/g) (Figure 5.6A). ALA-3 is thought to be more flexible and open than ALA-1 due to the absence of stabilizing calcium ions possibly allowing it to reorient at the oil-water interface with greater ease. Furthermore, less protein aggregation was evident (reduced hydrodynamic radius) at pH 7.00 than pH 5.00 due to charge repulsion possibly leading proteins being more spread out along the interface. The interaction of pH  $\times$  temperature in EAI values revealed a decrease in the magnitude difference between pH values as temperatures increased, most likely associated with increased hydrophobicity as the proteins start to unravel at higher temperatures. For instance, EAI values increased at 25°C from 65.06 m<sup>2</sup>/g at pH 5.00 to  $\sim$ 163.2 m<sup>2</sup>/g at pH 7.00 (difference of  $\sim$ 101.2 m<sup>2</sup>/g); at 65°C from 63.03 m<sup>2</sup>/g at pH 5.00 to  $\sim$ 164.7 m<sup>2</sup>/g at pH 7.00 (difference of  $\sim$ 101.7 m<sup>2</sup>/g); and at 95°C from 71.46 m<sup>2</sup>/g at pH 5.00 to  $\sim$ 156.8 m<sup>2</sup>/g at pH 7.00 (difference of  $\sim$ 85.32 m<sup>2</sup>/g) (Figure 5.6A).

The way which proteins coat an oil droplet surface are driven by its physical properties. Pearson correlation coefficients determined the relative significance between EAI and the physical properties of ALA: hydrodynamic radius ( $r = -0.34$ ,  $p < 0.05$ ), surface hydrophobicity ( $r = 0.83$ ,  $p < 0.001$ ), surface charge ( $r = -0.73$ ,  $p < 0.001$ ) and interfacial tension ( $r = 0.57$ ,  $p < 0.001$ ). With respect to hydrodynamic radius of these ALA aggregates, this relatively weak correlation is attributed to changes in tertiary conformation at the interface. Their ability to reorient and adhere to the interface may depend on the relative amounts of disulfide bonds

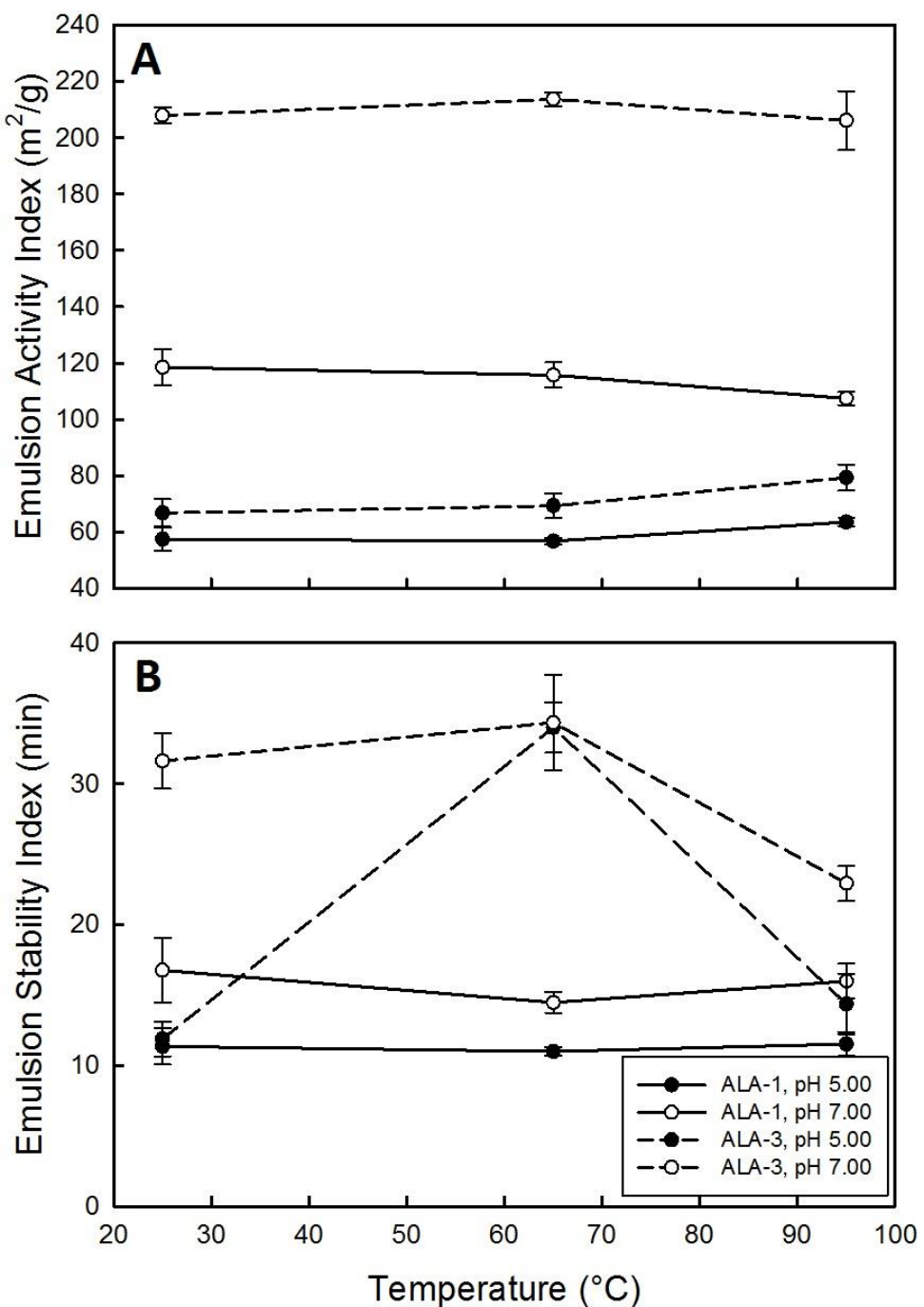


**Figure 5.6** Mean emulsification activity ( $\text{m}^2/\text{g}$ ) (A) and stability (min) (B) indices for ALA-1 and ALA-3 proteins as a function of pH and temperature pre-treatments. Data represent the mean  $\pm$  one standard deviation ( $n = 3$ ).

among ALA proteins. Those with many inter-protein disulfide bonds may be less capable of reorienting itself at the interface which prohibits an increase in EAI. Yet for the other physical properties (*i.e.* surface hydrophobicity, surface charge and interfacial tension), the strong significant correlation between them demonstrates the importance of controlling these parameters to enhance droplet coverage. For interfacial tension and surface charge, greater droplet coverage a higher interfacial tension, and a greater surface charge were found at pH 7.00. This suggests that better droplet coverage is not dependent on a neutrally charged protein probably due to electrostatic repulsive charges which may help ALA obtain a more open structure. Electrostatic repulsion may help proteins to spread out across a droplet surface which enhances its droplet coverage. Furthermore, electrostatic repulsive forces which keep proteins from aggregation may be more important in aiding in droplet coverage as opposed to a better adsorption to the droplet surface with a lower interfacial tension. Electrostatic repulsive forces may aid in an evenly coated droplet surface due to their limited ability to cause proteins to form aggregates. With respect to surface hydrophobicity, the strong correlation between these two properties is attributed to the ability for adherence to the interface where higher surface hydrophobicity promotes adsorption.

The ESI values for ALA-1 and ALA-3 in response to pH and temperature are given in Figure 5.6B, and analyzed using a 3-way ANOVA to find all main factors and subsequent interactions to be significant ( $p<0.001$ ). ESI values for ALA-3 proteins were highly pH and temperature dependent. At pH 7.00, ESI values increased slightly from ~31.62 min at 25°C to ~34.34 min at 65°C, and then declined substantially to ~22.92 min at 95°C. Whereas at pH 5.00, ESI values greatly increased from ~11.88 min at 25°C to ~33.99 min at 65°C, and then declined substantially to ~14.36 min at 95°C (Figure 5.6B). The peak in ESI values at 65°C was thought to be associated with partial unravelling of the ALA-3 structure and possibly a more open structure. With the exception of 65°C in which ESI values were similar, ESI was higher at pH 7.00 than pH 5.00 at both 25°C and 95°C (Figure 5.6B). At low temperatures (*i.e.* 25°C) the native of ALA may shield many of the charged groups that were successively revealed by unfolding at 65°C resulting in increased emulsion stability. At 95°C, the denaturation of ALA results in proteins that is more likely to form aggregates when cooled back to room temperature.

In the case of ALA-1, ESI values were relatively independent of temperature however were found to be higher at pH 7.00 (~15.74 min) than at pH 5.00 (~11.29 min) (Figure 5.6B). The lack of temperature dependence may be associated with a more stable tertiary structure due to the

presence of calcium ions, which restricts unraveling. Furthermore, the higher net charge at pH 7.00 would create increased electrostatic charge repulsion between the films surrounding oil droplets leading to the formation of more stable emulsions, than at pH 5.00 where films would have significantly reduced net charges since the proteins are near their pI values.

Though Pearson correlations revealed that EAI was correlated with the physical properties of ALA, ESI was found to be correlated to two properties investigated in this study: EAI ( $r = 0.66$ ,  $p < 0.001$ ) and surface hydrophobicity ( $r = 0.62$ ,  $p < 0.001$ ). There are several surprising factors with this result as it was hypothesized that electrostatic repulsive forces given by the surface charge of the proteins would have had an effect on the stability of these emulsions. Furthermore, since surface hydrophobicity and the droplet coverage were found to be significant, it was predicted that the interfacial tension would also play a role in stabilizing an emulsion. Therefore this suggests that the stability of the emulsion had more to do with the ability for these proteins to adhere to the interface as opposed to electrostatically keep droplets from flocculating.

Overall, the electrostatic repulsive forces due to the highly electronegative charge associated with ALA at pH 7.00 enhanced the emulsion stability of ALA. Electrostatic repulsion aided in keeping droplets from flocculating however was less effective for neutrally charged ALA at pH 5.00. Furthermore, increased stability found with ALA-3 compared to ALA-1 is attributed to the more open and flexible conformation of ALA-3 which gave greater ease for the reorientation at the interface. Yet this does not fully explain for the enhanced stability observed with ALA-3 when treated at 65°C. It was found that there were similar trends observed in ESI (Figure 5.6B) when compared to the relative amounts of secondary structure as measured by circular dichroism (Figure 5.1). The secondary structure and emulsion stability of ALA-1 was found to be relatively independent of the temperature pre-treatments. In ALA-3, the secondary structure and emulsion stability was found to be dependent on temperature pre-treatments such that an increase in structure and stability was observed when increasing temperature pre-treatments from 25 to 65°C followed by a decrease in structure and stability when increasing temperatures from 65 to 95°C. There appears to be a relationship between these two properties which may be explained by how secondary structure may affect the process by which a protein stabilizes a droplet surface. When there are less secondary structures present, it is hypothesized that there are a greater amounts of random loops and coils are present to cause proteins to become more entangled. Proteins may require a greater amount of conformational change as a more entangled protein to optimize its

ability to stretch out and adhere to the interface. As proteins adhere to an interface, an entangled protein may be limited in its ability to change in conformation which may yield a sub-optimal conformation at the interface which reduces its emulsion stability. The greater amount of secondary structure reduces the amount of conformational change a protein may undergo which such that less unfolding is needed to adhere to the interface.

## 5.5 Conclusions

The effect of pH and temperature pre-treatments on the ALA proteins impacted both their physicochemical and emulsifying properties to varying degrees. Changes in temperature altered the structure of the proteins which then affected its physicochemical properties by increasing their hydrophobicity especially under fully denatured temperatures (*i.e.* 95°C); and caused changes in the surface charge (*i.e.* from 25 to 65°C). Both of which influenced their aggregation behavior, especially ALA-3 at pH 5.00. The pH of the system also influenced the surface charge on both ALA-1 and ALA-3 where enhance electrostatic repulsion at pH 7.00 was observed, resulting in reduced aggregation despite having a greater amount of its hydrophobic moieties at the surface. Findings indicate that changes to protein conformation using various pH and temperature pre-treatments influences their surface chemistry, aggregation and ability to align at the oil-water interface. Conformational stability in the presence of calcium ions (*i.e.*, ALA-1) also played an important role in ALA performance, where it was found the both ALA-1 and ALA-3 differed considerably. ALA-1 was more resistant to conformational changes in response to pH and temperature pre-treatments than ALA-3. Overall, the absence of calcium ALA-3 was able to reduce interfacial tension more than ALA-1 where calcium stabilized the protein structure and restricted its ability to align and re-orient as well at the interface. As a result, higher droplet surface coverage (EAI) was obtained for ALA-3 than ALA-1. The increased ability of ALA-3 to adhere to the interface also allowed for greater emulsion stability. Overall, emulsions were more stable for ALA-1 and ALA-3 when at pH 7.00 than pH 5.00 due to the presence of electrostatic repulsive forces between protein coated droplets. Furthermore, a temperature pre-treatment of 65°C on ALA-3 resulted in an increase in its secondary structure resulting the greatest emulsion stability presumed due to the partially denaturation and refolding at this temperature. The greater amount of secondary structure allows for a less entangled protein which may enhance its ability to unfold to enhance emulsion stability. This demonstrates that it is possible to tailor the properties of the

protein by adjusting the main factors (*i.e.* pH, temperature and protein-type) to obtain desired functionality. Under the conditions examined in this study, ALA-3 pre-treated at 65°C and at pH 7.00 resulted in the best emulsifying properties.

## **5.6 Connection to the next study**

One way to enhance emulsion stability is to cause complexation between whey proteins with other biopolymers which were investigated in the next study. Whey protein isolates (WPI) have been reported to form electrostatic complexes with carrageenan (CG) when acidified from neutral conditions due to the presence of electrostatic attractive forces under dilute biopolymer conditions (0.25% w/w) (Stone & Nickerson, 2012). Carrageenan is an anionic polysaccharide extracted from red seaweed known for its gelling and thickening properties in foods. Its structure is well characterized, and differs by type by the number of sulfate groups per disaccharide repeating unit (van der Velde *et al.*, 2002). For instance,  $\kappa$ -,  $\iota$ - and  $\lambda$ -CG are known to contain 1, 2, and 3 sulfate groups respectively per disaccharide repeating unit (Campo *et al.*, 2009). In the next study, the rheological properties of WPI-CG mixtures was examined during the formation of electrostatic coupled biopolymer and emulsion gels, as a function of CG-type. Within this study, biopolymer blending ratios were selected based on optimal mixing ratios identified by Stone and Nickerson (2012). The authors reported this ratio to occur at 12:1 for WPI- $\kappa$ -CG and WPI- $\lambda$ -CG mixtures, and 20:1 for the WPI- $\iota$ -CG system (Stone & Nickerson, 2012). Maximum complexation of all mixtures was found to occur near pH 4.50. In this study, the formation of protein-polysaccharide electrostatic coupled gels and their use as an emulsifier were investigated.

## **6. THE RHEOLOGICAL PROPERTIES OF WHEY PROTEIN-CARRAGEENAN MIXTURES DURING THE FORMATION OF ELECTROSTATIC COUPLED BIOPOLYMER AND EMULSION GELS<sup>5</sup>**

### **6.1 Abstract**

The rheological properties of whey protein isolate (WPI) and WPI with carrageenan (CG) (kappa-, iota- and lambda-types) mixtures during a slow acidification process was investigated in a non-emulsified and emulsified system. For all systems, electrostatically coupled networks were formed leading to the formation of a biopolymer or emulsion-based gel network. However, network strength differed depending on the CG-type. In the case of biopolymer gels, the storage modulus within the plateau zone for WPI-kappa-CG and WPI-iota-CG mixtures were ~93 and ~73 Pa, respectively, whereas the WPI-lambda-CG network was weaker (~8 Pa). The gel point corresponded to the pH where complex coacervation occurred. WPI-CG mixtures were also able to lower interfacial tension from 28 to 18-22 mN/m before gelation. Emulsion gels followed a similar trend as the biopolymer networks, except they were stronger (WPI-kappa-CG, WPI-iota-CG and WPI-lambda-CG systems had storage moduli of ~435, ~320 Pa and ~103 Pa, respectively). The presence of CG decreased the average droplet size of these emulsions from ~38 to ~32  $\mu\text{m}$ , regardless of the CG type. Protein stabilized emulsion gels were presumed to form, where upon complexation with CG, flocculation between droplets was promoted until an electrostatic-stabilized gel network was formed within the continuous phase. The WPI control did not gel for both non-emulsified and emulsified systems.

---

<sup>5</sup> Accepted as: Lam, R. & Nickerson, M.T. (2014). The rheological properties of whey protein-carrageenan mixtures during the formation of electrostatic coupled biopolymer and emulsion gels. *Food Research International*.

## 6.2 Introduction

Proteins and polysaccharides are common ingredients in many food systems because of their gelling, thickening and/or emulsifying properties. However, they often require tailoring of their physiochemical properties to control precipitation and aggregation which influences their rheological or emulsion forming/stabilizing properties. In combination, proteins and polysaccharides have been reported to form electrostatic complexes *via* attractive forces under suitable pH and solvent conditions where biopolymers have opposing net charges (Turgeon *et al.*, 2007). The coacervation process (also known as associative phase separation) has been well studied and reviewed in the literature (de Kruif *et al.*, 2004; Turgeon *et al.*, 2007; Dickinson, 2008). The process involves separation of electrostatically attracted proteins and polysaccharides into a biopolymer-rich lower phase, and the formation of an upper solvent-rich phase within an aqueous mixture (Weinbreck *et al.*, 2003). During a pH-induced coacervation, proteins and polysaccharides initially interact near the protein's isoelectric point below which it assumes a net positive charge. The point of initial interactions as event by a slight change in optical density is known as  $\text{pH}_c$ , signifying the formation of 'soluble complexes' (de Kruif *et al.*, 2004). As pH decreases further, macroscopic phase separation occurs and a large rise in optical density initiates at a pH, noted as  $\text{pH}_{\phi 1}$  signifying the formation of 'insoluble complexes' (de Kruif *et al.*, 2004). The terms: 'soluble' and 'insoluble', are used to describe the level of biopolymer interactions rather than specific functionality testing (de Kruif *et al.*, 2004). Biopolymer interactions reach a maximum at  $\text{pH}_{\text{opt}}$  associated with a maximum optical density and where the overall charge of the biopolymers is close to zero (de Kruif *et al.*, 2004). And then complexes undergo dissolution as pH approaches the  $\text{pK}_a$  of the reactive sites on the protein, denoted at  $\text{pH}_{\phi 2}$ . Depending on the strength of biopolymer interactions, coacervate or precipitate structures may form. The coacervate structure is able to entrap a lot of solvent which allows it to remain suspended and have high biopolymer mobility (de Kruif *et al.*, 2004), and typically occurs involving both a strong and weakly charged biopolymer, such as WPI and gum arabic, respectively (Weinbreck *et al.*, 2003). In contrast, precipitate-type structures tend to fall out of solution quickly, and have significantly less entrapped solvent and biopolymer mobility (de Kruif *et al.*, 2004), and typically involve two strongly charged biopolymers (*e.g.* WPI and carrageenan) (Weinbreck *et al.*, 2004b).

Although coacervation studies are not limiting in the literature, systems shown to form electrostatic coupled biopolymer and emulsion networks are few. For instance, Singh and co-

workers (2007) reported electrostatic coupled networks to form in mixtures of agar-gelatin, Yuan and co-workers (2014) with soy protein-chitosan and Schmidt and co-workers (2009) with lysozyme-pectin. In the present study the formation of electrostatic coupled biopolymer and emulsion gels using WPI and CG mixtures, as a function of CG-type were studied. Whey proteins ( $\alpha$ -lactalbumin and  $\beta$ -lactoglobulin) from bovine milk have been extensively studied for its emulsifying (Britteen & Giroux, 1991; Reiffers-Magnani *et al.*, 2000; Hu *et al.*, 2004) gelling (Tang *et al.*, 1994; Elofsson *et al.*, 1997; Gulzar *et al.*, 2012) and surface active properties (Patino *et al.*, 1999; Davis & Foegeding, 2007; Yang & Foegeding, 2011). CG, is a family of anionic polysaccharide extracted from red seaweed (*Rhodophyta* species), commonly used as a gelling or thickening agent by the food industry (Trius *et al.*, 1996; van der Velde *et al.*, 2002; Campo *et al.*, 2009). Their physicochemical properties have also been very well characterized (Piculell *et al.*, 1992; Thanh *et al.*, 2002; Souza *et al.*, 2011) and reviewed (Rinaudo, 2006; Campo *et al.*, 2009). CG are typically comprised of a disaccharide repeating unit comprised of D-galactose and 3,6-anhydro-D-galactose residues which are sulfated with 1, 2 or 3 groups per disaccharide repeating unit which corresponds to  $\kappa$ -,  $\iota$ - and  $\lambda$ -type CG, respectively (Weinbreck *et al.*, 2004; Campo *et al.*, 2009). In addition to these three types, three others have also been identified ( $\mu$ -,  $\nu$ - and  $\theta$ -type) by Knutsen and co-workers (1994) however these are more minor in comparison. The use of CG of varying types allows for the effect of linear charge density on biopolymer interactions and their ability to alter the rheological properties.

Complex coacervates have been previously reported to improve emulsion stability (Nakagawa *et al.*, 2004; Li & McClements, 2011; Koupantis *et al.*, 2014). In some cases, emulsions may take on a gel-like nature (Dickinson, 2012). In the food industry, these protein-based gels containing emulsions are typically found as yoghurts, cheeses, sauces and reformulated meat products (sausages, patés, *etc.*) (Dickinson, 2012). Typically, emulsions are characterized into two main categories: emulsion-filled protein gels and protein-stabilized emulsion gels (Dickinson, 2012). The primary difference between these two types of emulsion gels are their internal structure. In emulsion-filled protein gels, the continuous aqueous phase is gelled with oil droplets dispersed within this gelled biopolymer network (Dickinson, 2012). In protein-stabilized emulsion gels, structure is attributed to the inter-connected flocculated network of oil droplets stabilized by the interfacial biopolymer film (Dickinson, 2012). Stone and Nickerson (2012) investigated the formation of electrostatic complexes involving WPI and CG molecules as a

function of CG type under dilute conditions (0.25% w/w), and then their emulsion stabilizing effects at a 1.0% (w/w) total biopolymer concentration with a 1:1 biopolymer solution to oil ratio. The authors reported this ratio to occur at 12:1 for WPI- $\kappa$ -CG and WPI- $\lambda$ -CG mixtures, and 20:1 for the WPI- $\iota$ -CG system (Stone & Nickerson, 2012). Maximum complexation of all mixtures was found to occur near pH 4.50. Furthermore, the authors reported the WPI-CG mixtures regardless of the CG-type enhanced the emulsion stability over WPI alone, but did not explore the underlying mechanisms.

The overall goal of the present study is to examine the underlying mechanisms driving the formation of WPI-CG coupled biopolymer and emulsion gel networks, as a function of CG-type. This information is essential for controlling and optimizing their use in food or controlled delivery-type applications.

### 6.3 Materials and methods

#### 6.3.1 Materials

WPI used in this study was generously donated by Davisco Foods International, Inc. (Le Sueur, MN, USA). Chemical composition of the commercial WPI powder was determined according to AOAC (2003) methods; 925.10 (moisture), 923.03 (ash), 920.87 (crude protein), and 920.85 (lipid). Carbohydrate content was determined on the basis of present differential from 100%. The WPI powder comprised of 89.78% protein (%N  $\times$  6.38), 0.10% lipid, 4.92% moisture, 2.06% ash (including 0.08% Ca<sup>2+</sup>, 0.01% Mg<sup>2+</sup>, 0.02% K<sup>+</sup>, and 0.66% Na<sup>+</sup>), and 3.13% carbohydrate (wet basis). CG ( $\kappa$ -,  $\iota$ -, and  $\lambda$ -) and glucono- $\delta$ -lactone (GDL) were purchased from Sigma-Aldrich (Oakville, ON, Canada). For all three types of CG, the supplier provided compositional information on them where  $\kappa$ -CG was comprised of 66.50% carbohydrate, 10.65% moisture and 22.86% ash (including 2.4% Ca<sup>2+</sup>, 0.16% Mg<sup>2+</sup>, 5.4% K<sup>+</sup>, 0.49% Na<sup>+</sup>);  $\iota$ -CG contained 64.40% carbohydrate, 10.82% moisture and 24.97% ash (including 3.4% Ca<sup>2+</sup>, 0.18% Mg<sup>2+</sup>, 3.2% K<sup>+</sup>, 1.2% Na<sup>+</sup>); and  $\lambda$ -CG contained 63.79% carbohydrate, 12.26% moisture and 23.95% ash (including 3.0% Ca<sup>2+</sup>, 0.83% Mg<sup>2+</sup>, 2.4% K<sup>+</sup>, 1.3% Na<sup>+</sup>). For  $\kappa$ -,  $\iota$ -, and  $\lambda$ -CG, their molecular weights were ~ 154 kDa, ~250 kDa and ~250 kDa respectively. Canola oil used in this study was purchased from a local supermarket. All other chemicals used in this study were of reagent grade and purchased through Sigma-Aldrich (Oakville, ON, Canada). The water used in this research was filtered using a Millipore Milli-Q<sup>TM</sup> water purification system (Millipore Corp.,

Milford, MA, USA). The WPI protein and CG solutions were corrected for protein and carbohydrate content respectively and used without further purification.

### **6.3.2 Sample preparation**

Biopolymer solutions (1.0% w/w biopolymer) were prepared by dispersing WPI and CG ( $\kappa$ -,  $\iota$ -, and  $\lambda$ -type) in water by mechanical stirring (500 rpm) at room temperature (21-23°C) for 60 min. A homogenous WPI solution (1.0% w/w) was also prepared as a control. A mixing ratio for WPI with  $\kappa$ -,  $\iota$ - and  $\lambda$ -carrageenan solutions of 12:1, 20:1 and 12:1, respectively was chosen based on work by Stone and Nickerson (2012), and correspond to the optimal complexation ratio. After 60 min of mixing, 0.5% w/w GDL was added to the biopolymer solution and then stirred for 1 min just prior to analysis to start slowly acidifying the solution. Changes in pH was measured using a pH meter (Thermo Scientific, Madison, WI, USA) from pH ~7.00 to ~4.20 within all three mixtures and an individual WPI solution and plotted vs. time.

Oil-in-water emulsions were prepared by first preparing the biopolymer solution as described above, followed by the addition of oil immediately after the addition of GDL at an oil: water ratio of 1:1 to a total weight of 10 g. This biopolymer-oil mixture was then homogenized at 7,200 rpm for 5 min using an Omni Macro Homogenizer (Omni International Inc., Marietta, GA) equipped with a 20 mm saw tooth generating probe.

### **6.3.3 Turbidimetric pH-titration over time for WPI: carrageenan mixtures**

The optical density (OD) for WPI: carrageenan mixtures at a concentration of 1.0% (w/w) were assessed over time during the slow acidification by GDL using a UV-Vis spectrophotometer (Thermo Scientific, Madison, WI) at 600 nm. Plastic cuvettes with a 1 cm path length were used. Measurements were taken every 1 min for a total of 90 min. Three replicates were measured with each data point is presented as a mean  $\pm$  one standard deviation. A 1.0% (w/w) WPI solution was also measured as a control. The critical pH associated with the formation of insoluble complexes was also evident at a pH (denoted as  $pH_{\phi 1}$ ) corresponding where macroscopic phase separation occurs corresponding to large increases in OD. This critical pH value was determined by extending the tangent of the steepest part of the rise to the OD baseline. Each critical pH were determined for individual curves, and then reported as the mean  $\pm$  one standard deviation (n = 3).

### 6.3.4 Interfacial tension

The interfacial tension for each WPI: carrageenan mixture (1.0% w/w) and the WPI control was measured using a Lauda TD 2 Tensiometer (Lauda-Königshofen, Germany) equipped with a Du Nüoy ring (20 mm diameter). Within a 40 mm diameter glass sample cup, a 20 mL biopolymer solution was added then stirred for 1 min after the addition of 0.5% (w/w) GDL, followed by the immersion of the Du Noüy ring and then the addition of upper canola oil layer (20 mL). The ring was then pulled upwards to stretch the interface to measure the maximum force without breaking into the oil phase. Interfacial tension measurements (mN/m) were taken every 600 s where the mean of three replicates  $\pm$  one standard deviation is presented at each data point. Interfacial tension was calculated from the maximum force ( $F_{\max}$ ; units: milli-Newton; instrument measures mg x gravity) using the following equation (eq. 6.1):

$$\gamma = \frac{F_{\max}}{4\pi R\beta} \quad (\text{eq. 6.1})$$

where,  $\gamma$  is the interfacial tension (mN/m),  $R$  is the radius of the ring (20 mm),  $\beta$  is a correction factor that depends on the dimensions of the ring and the density of the liquid involved (McClements, 2005). All measurements are reported as the mean  $\pm$  one standard deviation ( $n = 3$ ).

### 6.3.5 Small deformation rheology

Small deformation rheology was used to measure changes to the biopolymer and emulsion solutions during acidification by GDL (*i.e.*, WPI: carrageenan; WPI control). Approximately 1.5 mL of the biopolymer or emulsion solution with GDL was placed onto a AR-G2 Rheometer (TA Instruments, New Castle, DE) equipped with a 40 mm diameter 2° acrylic cone. A time sweep was conducted to capture the gelation process for 90 min where measurements were made at 1 Hz every 10 s, where the maximum amplitude for strain was set at 1.0%. Following a time sweep, a frequency and strain sweeps were measured. Frequency sweeps were used to characterize the gel formed where the maximum strain was set to 1.0% with frequencies ranging from 0.05 Hz to 100 Hz while capturing 15 points per logarithmic decade. Strain sweeps were used to characterize the physical properties of the gel where strains of 0.01% to 500% with 15 data points per logarithmic decade captured at 5 Hz was also taken. All measurements were made within the linear viscoelastic regime and in triplicates.

### **6.3.6 Light microscopy**

A Nikon Eclipse E400 light microscope equipped with a Nikon DS-FiL color camera and a long working distance 10x lens and condenser (Nikon Instruments Inc., Melville, NY, USA) was used to capture brightfield micrographs. Images were captured of a drop of the prepared emulsion with a coverslip after a 90 min time period at 10 $\times$  magnification (pH = ~ 4.20). Images were captured at a resolution of 2560 by 1920 pixels and analyzed using ImageJ (National Institutes of Health, Bethesda, MD, USA) to determine the width of emulsion droplets. Fifty droplets were measured and averaged per slide and the average of three slides  $\pm$  one standard deviation was reported for each sample.

### **6.3.6 Statistics**

The critical pH associated with the formation of insoluble complexes was determined from the turbidity curves and analyzed for statistical significance. Experiments were collected in triplicate for all WPI-CG types and the control WPI solution. A one-way analysis of variance (ANOVA) with Tukey's post hoc analysis was conducted to test for significance among the various WPI-CG types and WPI alone. Statistical analysis was performed with Systat (SPSS Inc., Ver. 10, 2000, Chicago, IL).

## **6.4 Results and discussion**

### **6.4.1 Turbidimetric pH titrations**

Optical density (OD) for an individual WPI solution and mixture of WPI and  $\kappa$ -CG (B),  $\iota$ -CG (C) and  $\lambda$ -CG during a slow acidification process using GDL over time is given in Figure 1. In the case of the WPI control (Figure 6.1A), a rise in OD initiated at occurred at pH  $6.15 \pm 0.32$  (~7 min), then peaked an OD of 1.56 at pH  $5.58 \pm 0.18$  (~20 min), followed by a steady decline to an OD of 0.60 at pH  $4.33 \pm 0.02$  (90 min) where the pH became stable. The rise and decline in OD is believed to be associated with protein-protein aggregation near the protein's isoelectric point (pI = 4.6 (Parris & Baginski, 1991)) where it assume no net charge in solution

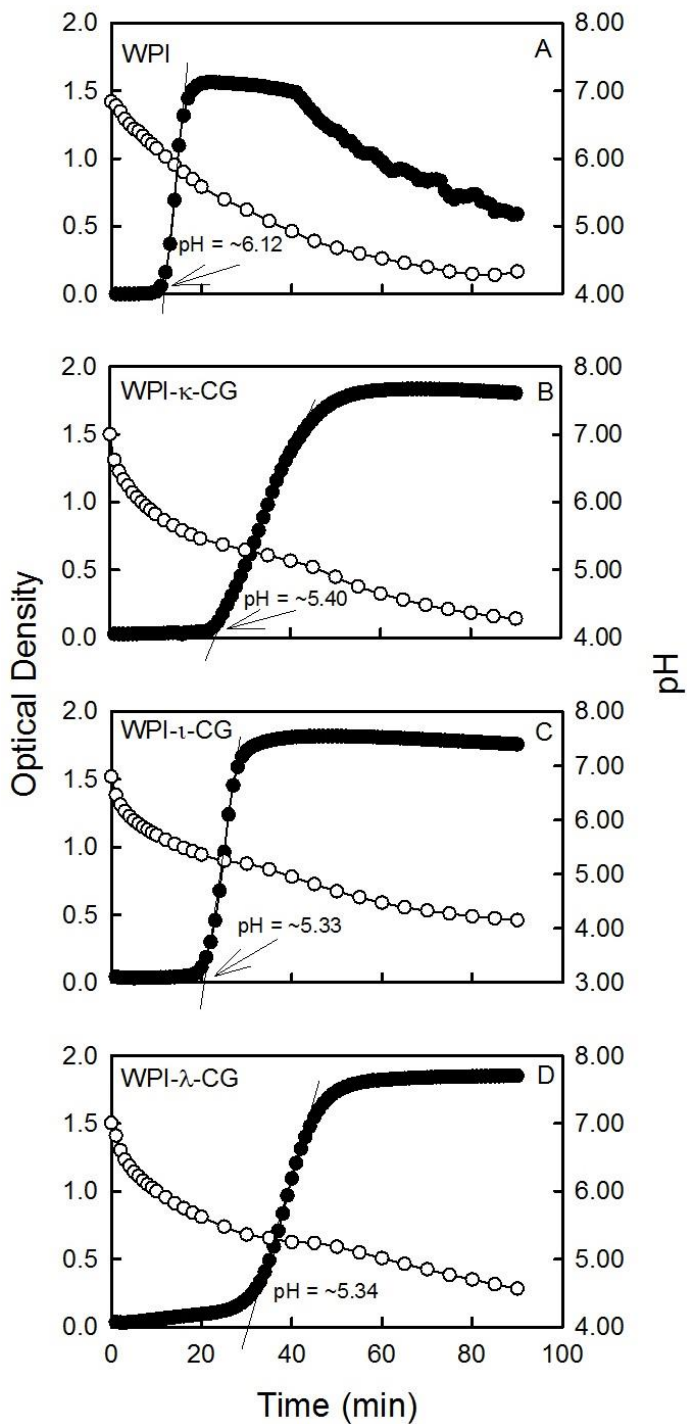


**Figure 6.1** Changes to the optical density for an individual WPI (A) solution and mixtures of WPI and  $\kappa$ -CG (B),  $\iota$ -CG (C) and  $\lambda$ -CG (D) solutions as a function of pH (open circles) and time (min). Curves represent the mean optical density for 3 separate samples. All solutions had a total biopolymer concentration of 1.0% (w/w) and were acidified using 0.5% (w/w) GDL.

The larger aggregates are more effective at scattering light, leading to the change in OD.

Net neutrality of a WPI solution at 25°C was found to occur at ~5.1 (data not shown), suggesting that interactions in the present study are initiating when both WPI and CG molecules are carrying a net negative charge. It is presumed at these pHs, the highly charged CG is electrostatically binding *via* attractive forces to positively charged patches on the protein's surface and charge fluctuations on the protein's surface near its pI (Weinbreck *et al.*, 2004; Stone & Nickerson, 2012). Others have reported a similar phenomenon in mixtures of proteins with highly charged polyelectrolytes, such as bovine serum albumin- acacia gum (Dubin *et al.*, 1994), whey proteins- gum arabic (Weinbreck *et al.*, 2003), and gelatin- agar (Boral & Bohidar, 2010).

The addition of CG, regardless of the type, resulted in a shift towards more acidic pHs in the pH associated with the start of the large rise in OD with pH (Figure 6.1, B-D) Within complex coacervation literature, this critical pH is known as  $pH_{\phi 1}$  and refers to where macroscopic phase separation occurs associated with the formation of insoluble complexes due to the electrostatic attraction of anionic carrageenan molecules and the whey proteins. The initial suppression of OD at higher pH is presumed to be the result of electrostatic repulsion between neighboring CG molecules which inhibited WPI-WPI aggregation. A shift in  $pH_{\phi 1}$  from pH 6.12 (WPI control) to 5.40, 5.33 and 5.34 was observed with the addition of  $\kappa$ -CG,  $\iota$ -CG and  $\lambda$ -CG, respectively (Figure 6.1). A one-way ANOVA with Tukey's post hoc analysis revealed a significant difference ( $p<0.001$ ) for WPI control compared to samples with CG while no significant difference between samples with CG. The shift in pH is believed to be associated with the linear charge density of the various types of CG in solution. For instance,  $\kappa$ -,  $\iota$ - and  $\lambda$ -type CG have 1, 2 and 3 sulphate reactive sites per disaccharide repeating unit on the polysaccharide backbone, respectively (Weinbreck *et al.*, 2004; Campo *et al.*, 2009), however the ordered conformation of the various types in solution differs. In the literature, the ordered conformation for  $\kappa$ - and  $\iota$ - types is thought to be a double helical structure (Rees *et al.*, 1970), aggregated single helices (Grasdalen & Smidsrød, 1981) or aggregated helical dimers (Rochas & Landry, 1987)), whereas in  $\lambda$ -type lacks an ordered conformation and behaves as a random coil due to the presence of a large number of sulphate groups that inhibits folding (Rochas *et al.*, 1980). Assuming in the present study that the ordered conformations exist for both  $\kappa$ - and  $\iota$ - types, then the larger shift would be explained by the higher linear charge density of the  $\iota$ - type CG chain. In contrast, the  $\lambda$ -type follows a different trend since it lacks an ordered conformation in solution. A similar linear charge/conformation dependence of

CG was proposed to Stone and Nickerson (2012) to described differences in magnitude for the maximum OD values; however the authors did not report the same trend with  $\text{pH}_{\phi 1}$  as in the present study. The differences were attributed to the method of acidification (GDL in the present study verses using HCl by Stone and Nickerson (2012)) and their rate of acidification which would have been greater in the present study.

#### 6.4.2 Rheology of WPI and WPI-carrageenan solutions

The dynamic storage (*i.e.*, elastic component) and loss (*i.e.*, viscous component) of an individual WPI solution and WPI-CG mixtures were investigated at a constant frequency as a function of time and pH during a GDL acidification (Figure 6.2). In the case of WPI, no gel networks were formed despite having a slightly higher storage modulus ( $G'$ ) than loss modulus ( $G''$ ) (Figure 6.2A). The higher elastic component is attributed to the formation of WPI-WPI aggregates which was further confirmed by frequency dependence of this solution under a frequency sweep.

However, as CG is added and pH is reduced, complexation with the WPI molecules leads to substantial changes to the viscoelastic spectrum. Based on the aforementioned OD data,  $\text{pH}_{\phi 1}$  for WPI- $\kappa$ -CG, WPI- $\iota$ -CG and WPI- $\lambda$ -CG mixtures occurred at 5.34, 5.33 and 5.40, respectively (Figure 6.1B-D). For these systems,  $G' < G''$  at  $\text{pHs} > \sim 5.33$  for WPI- $\kappa$ -CG and WPI- $\iota$ -CG; and  $\text{pHs} > \sim 5.53$  for WPI- $\lambda$ -CG mixtures indicating that the biopolymer mixtures were within the flow region of the viscoelastic spectrum behaving as a liquid (Figure 6.2B-D). The magnitude of  $G'$  of these WPI-CG mixtures was also lower than that of WPI over this time (and pH region) indicating the material was less structured most likely due to electrostatic repulsion between neighbouring CG molecules. However, at  $\text{pHs} < \sim 5.33$  for WPI- $\kappa$ -CG and WPI- $\iota$ -CG,  $G'$  became greater than  $G''$  (denoted as the gel point), after which a gel network was formed in the case of WPI- $\kappa$ -CG and WPI- $\iota$ -CG mixtures (Figure 6.2B,C). In this case, both viscoelastic moduli increased up to a plateau after  $\sim 40$  min (or  $\sim \text{pH } 5.00$ ). In contrast, greater time/pH dependence of the viscoelastic data, and reduced magnitude of  $G'$  was observed for the WPI- $\lambda$ -CG mixture relative to the WPI- $\kappa$ -CG and WPI- $\iota$ -CG mixtures suggesting that most likely a very weak gel

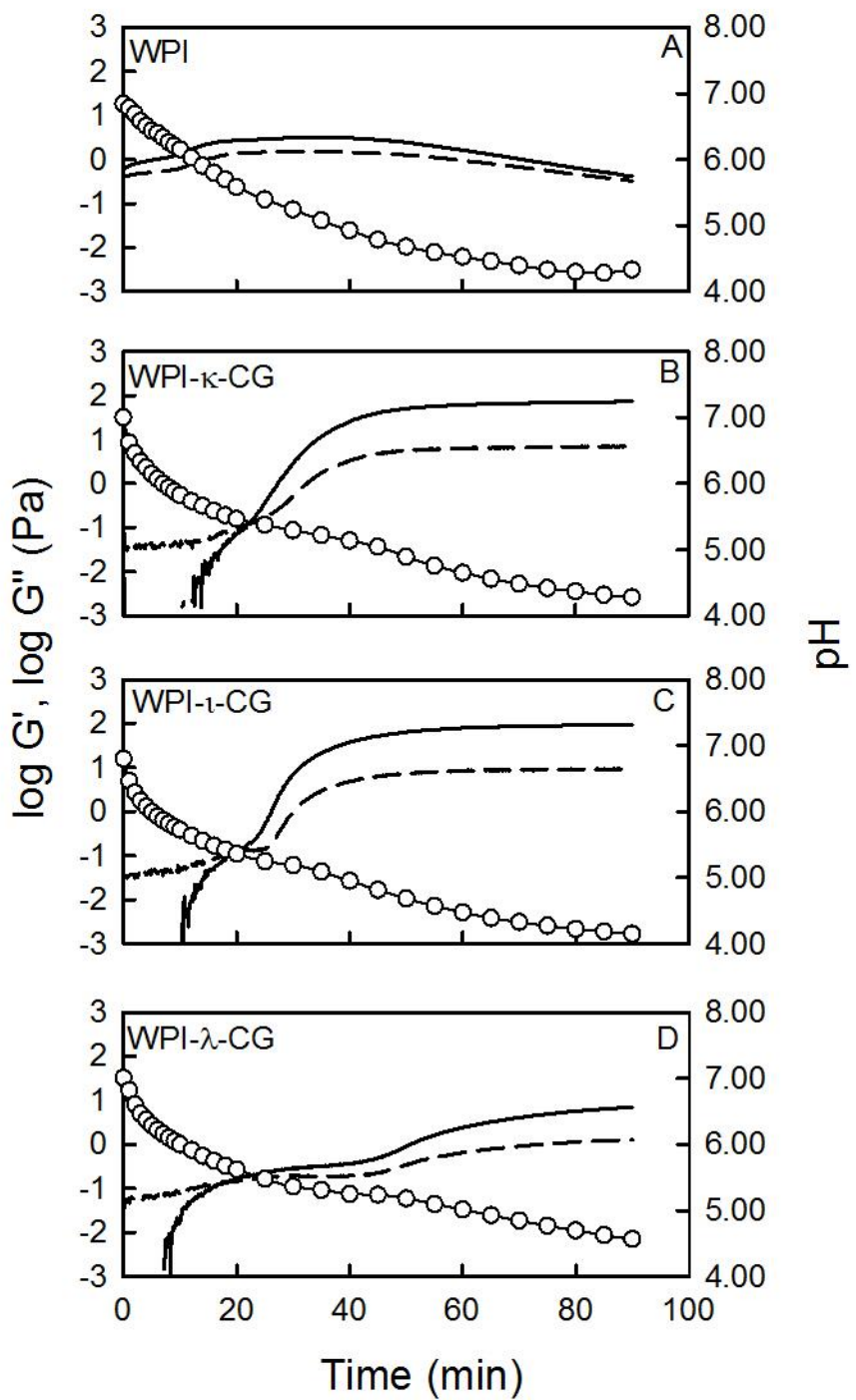


**Figure 6.2** Dynamic viscoelastic storage ( $G'$  (solid line)) and loss ( $G''$  (dashed line)) moduli for an individual WPI (A) solution and mixtures of WPI and  $\kappa$ -CG (B),  $\iota$ -CG (C) and  $\lambda$ -CG (D) as a function of pH (open circles) and time (min). Each curve is representative of 3 separate time sweep runs on separate samples. All solutions had a total biopolymer concentration of 1.0% (w/w) and were acidified using 0.5% (w/w) GDL.

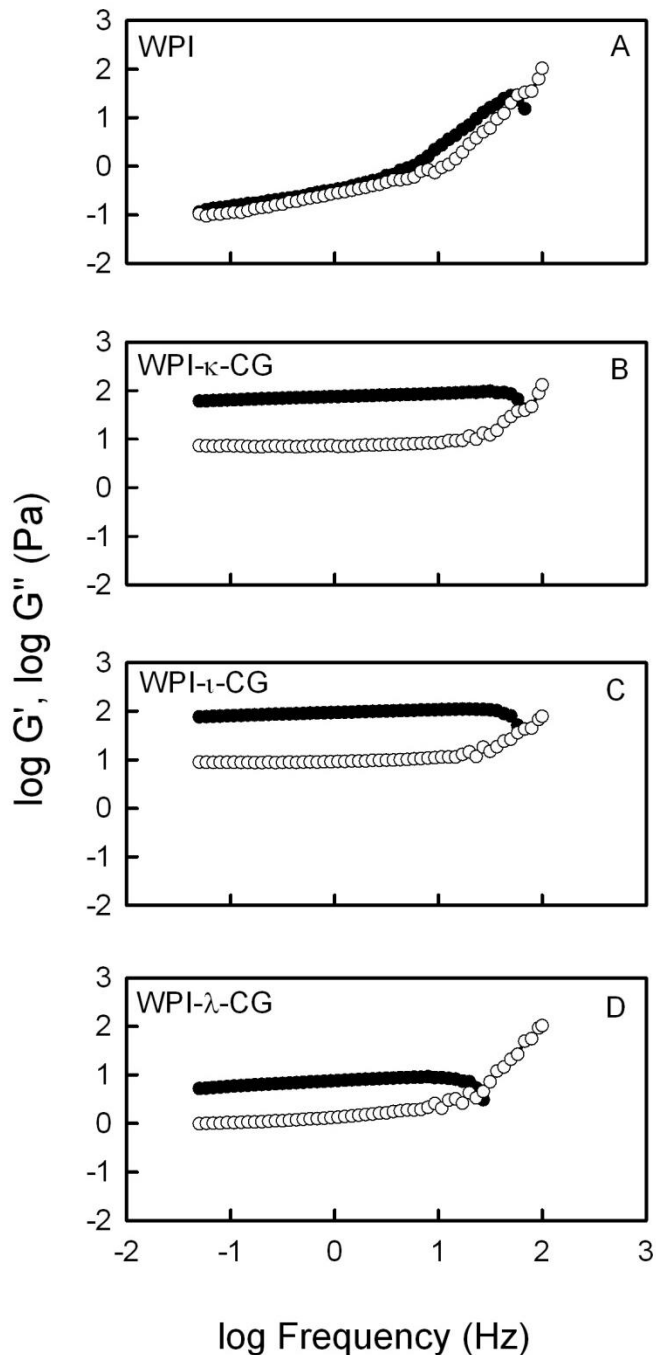


**Figure 6.3** Dynamic viscoelastic storage ( $G'$  (solid circles)) and loss ( $G''$  (open circles)) moduli for an individual WPI (A) solution and mixtures of WPI and  $\kappa$ -CG (B),  $\iota$ -CG (C) and  $\lambda$ -CG (D) as a function of frequency (Hz) (on double logarithmic axes) after 90 min of acidification with 0.5% (w/w) GDL and, after running the time sweep measurements.. All solutions had a total biopolymer concentration of 1.0% (w/w) and were at a pH of ~4.0-4.3 when measured.

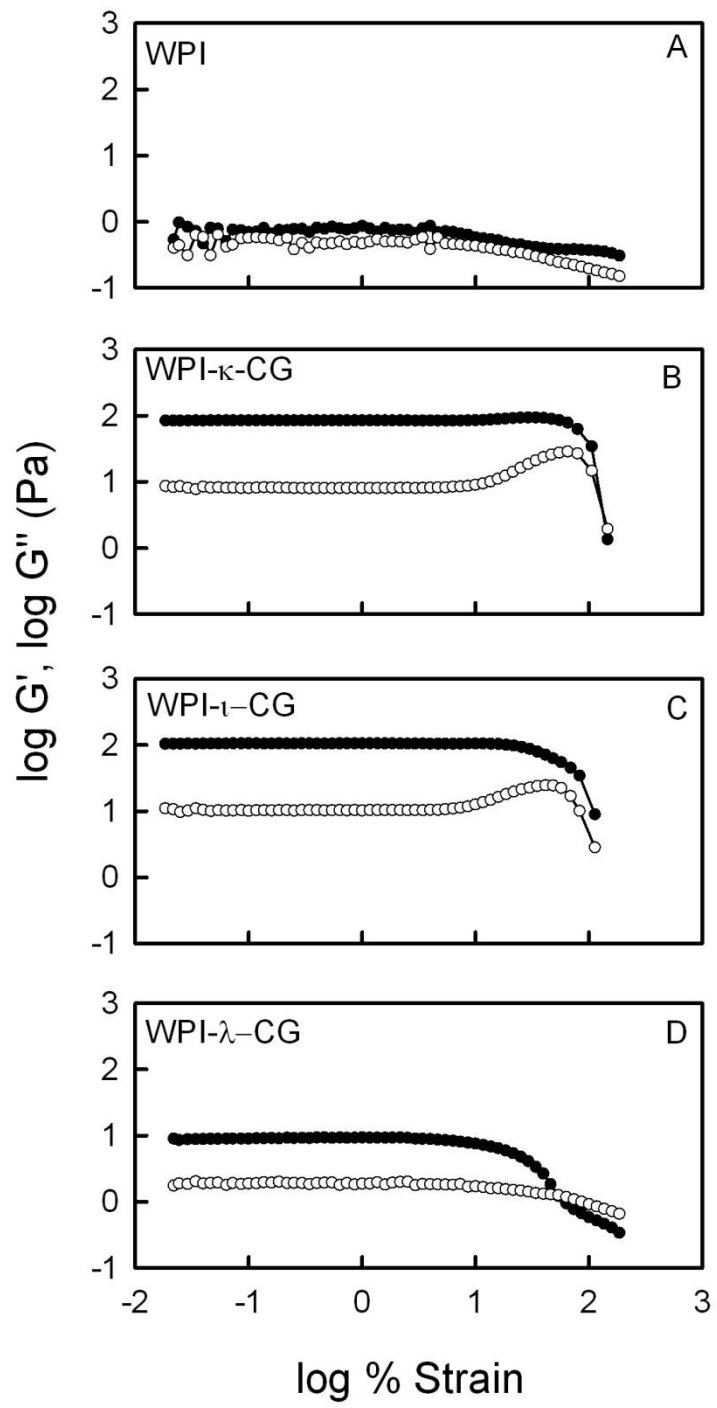


**Figure 6.4** Dynamic viscoelastic storage ( $G'$  (solid circles)) and loss ( $G''$  (open circles)) moduli for an individual WPI (A) solution and mixtures of WPI and  $\kappa$ -CG (B),  $\iota$ -CG (C) and  $\lambda$ -CG (D) as a function of shear strain (%) (on double logarithmic axes) after 90 min of acidification with 0.5% (w/w) GDL and, after running both the time and frequency sweep measurements. All solutions had a total biopolymer concentration of 1.0% (w/w) and were at a pH of ~4.0-4.3 when measured.

network (Figure 6.2D). The  $G'$  in the plateau region for WPI- $\kappa$ -CG and WPI- $\iota$ -CG mixtures was ~93 Pa and ~73 Pa, respectively, whereas the  $G'$  of the WPI- $\lambda$ -CG mixture after 90 min (pH ~4.4) was much weaker at ~8 Pa and never reached a plateau zone. The significantly reduced network strength in the WPI- $\lambda$ -CG mixture is most likely due to the large number of sulphate groups (3×) per repeating disaccharide units which makes  $\lambda$ -CG on its own a non-gelling polysaccharide. This would inhibit extensive ordering into network junction zones if sulphate groups were left free or unbound to the WPI. In contrast, both  $\kappa$ -CG and  $\iota$ -CG are known for the gelling abilities and rigid network structures.

Complexation between WPI and CG have been previously reported by Harrington and co-workers (2009) and Alizadeh-Pasdar and co-workers (2002). Changes in WPI structure due to complexes formed with CG have been previously reported by Alizadeh-Pasdar and co-workers (2002) and the thermally-induced gelation of WPI and CG individually and together have also been previously reported by Harrington and co-workers (2009). This current study departs from thermally-induced gelation and investigates the gelation of these biopolymers caused by the complexes formed between WPI and CG via a coacervation process.

Although Harrington and co-workers (2009) determined that CG and WPI are capable of co-gelling together, others have reported the formation of gelled networks using protein-polysaccharide interactions. Tavares and co-workers reported the formation of a gelled network between whey proteins and galactomannans (2005). They reported that network stiffness dependent on polysaccharide content (Tavares *et al.*, 2005). In this study, no networks formed in WPI in the absence of CG which suggests that CG and its ability to complex with WPI are essential for network formation. To better understand the type of network formed, frequency and strain sweeps were performed to characterize these gels.

After the 90 min acidification period (solution pH ~4.0-4.3), viscoelastic moduli were followed by both a frequency (Figure 6.3) and strain (Figure 6.4) sweeps. Individual WPI solutions were confirmed to be non-gel like, where both  $G'$  and  $G''$  were of similar in magnitude and highly frequency dependent, ranging from ~0.1 to ~30 Pa (Figure 6.3A). In contrast, WPI- $\kappa$ -CG, WPI- $\iota$ -CG and WPI- $\lambda$ -CG mixtures had both viscoelastic moduli to be relatively independent of frequency and with  $G' > G''$ , except at higher frequency where we saw an increase in  $G''$  and a corresponding decrease in  $G'$  (Figure 6.3B-D). This crossover point in the frequency sweeps where

$G''$  becomes larger than  $G'$  indicates that these are weak gels. From figure 6.3, the crossover point for WPI- $\lambda$ -CG and WPI- $\kappa$ -CG occurred at the lowest and highest frequency respectively indicating that the former was relatively the weakest and the latter being the stronger of the three WPI-CG gels. Similar results were found in the relative strength of collagen hydrogels characterized by frequency sweeps (Hu *et al.*, 2010).

A strain sweep for the WPI solution showed no structure which was expected as this was a solution comprised of WPI aggregates. In contrast, WPI- $\kappa$ -CG, WPI- $\iota$ -CG and WPI- $\lambda$ -CG mixtures showed a more distinct break in viscoelastic moduli with increasing strain, breaking at ~73.41%, ~74.52% and ~5.38% strain, respectively (Figure 6.4). The breakdown of the WPI- $\kappa$ -CG and WPI- $\iota$ -CG networks (as evident by  $G'$ ) were more abrupt with increasing strain than the WPI- $\lambda$ -CG system, suggesting that they formed stronger network structures. In the case of WPI- $\lambda$ -CG system, the more gradual break in  $G'$  reflects the increased polymer mobility within the network allowing for a greater ability to dissipate imposed strain.

#### 6.4.3 Interfacial properties of WPI and WPI-carrageenan complexes

Interfacial tension measurements for an aqueous system of an individual WPI solution and WPI-CG mixtures were investigated at a water-oil interface as a function of time and pH during a GDL titration (Figure 6.5). In general, proteins act to lower the tension at an interface by first migrating towards the interface and then re-align to position its hydrophobic moieties towards the oil phase and the hydrophilic moieties towards the aqueous phase; neighboring proteins at the interface then aggregate together to form a viscoelastic film (Tcholakova *et al.*, 2006b). Without the presence of any biopolymers, the water-canola oil interface in the present study had an interfacial tension of ~28 mN/m. The addition of WPI caused the interfacial tension to become reduced (~12 mN/m) as the whey proteins became integrated into the interface. For the WPI system, interfacial tension was observed relatively constant over time during the GDL acidification ranging between ~10 and ~12 mN/m (Figure 6.5A).

In the case of the WPI- $\kappa$ -CG and WPI- $\iota$ -CG systems, interfacial tension was found to be similar to the individual WPI solution during acidification under pH conditions where they were considered to be non-interacting, however abruptly increased at ~pH 5.60 near their  $pH_{\phi 1}$  (Figure 6.1B,C) and gel point (Figure 6.2B,C). The rapid rise in interfacial tension is thought to be associated with the complexation of WPI with the CG chains. The subsequent formation of a WPI-

$\kappa$ -CG and WPI- $\iota$ -CG gel network within the aqueous phase near its gel point is hypothesized to offset the equilibrium of proteins at the interface and within the aqueous phase causing previously integrated proteins to be drawn back into the aqueous phase. Interfacial tension was at the highest for WPI- $\kappa$ -CG and WPI- $\iota$ -CG at ~22 (pH 5.37) and ~18 mN/m (pH 5.24), respectively, and then started to decrease again over time/acidification as a new equilibrium tries to become established. Findings suggests that some of the electrostatic complexes may be moving back towards the oil-water interface over time and re-integrating into it. In contrast, the WPI- $\lambda$ -CG system behaved very similar to the individual WPI solution most likely since the attractive forces between WPI- $\lambda$ -CG were too weak to pull the WPI from its equilibrium at the interface to disrupt the interfacial tension. Interfacial tension data was measured only till ~45 min since for both the WPI- $\kappa$ -CG and WPI- $\iota$ -CG, further acidification resulted in increased elasticity of the formed electrostatic network, which reduced the flexibility of the oil-water interface causing the du Nüoy ring to slip through it. As a result, reliable measurements could not be made after 45 min.

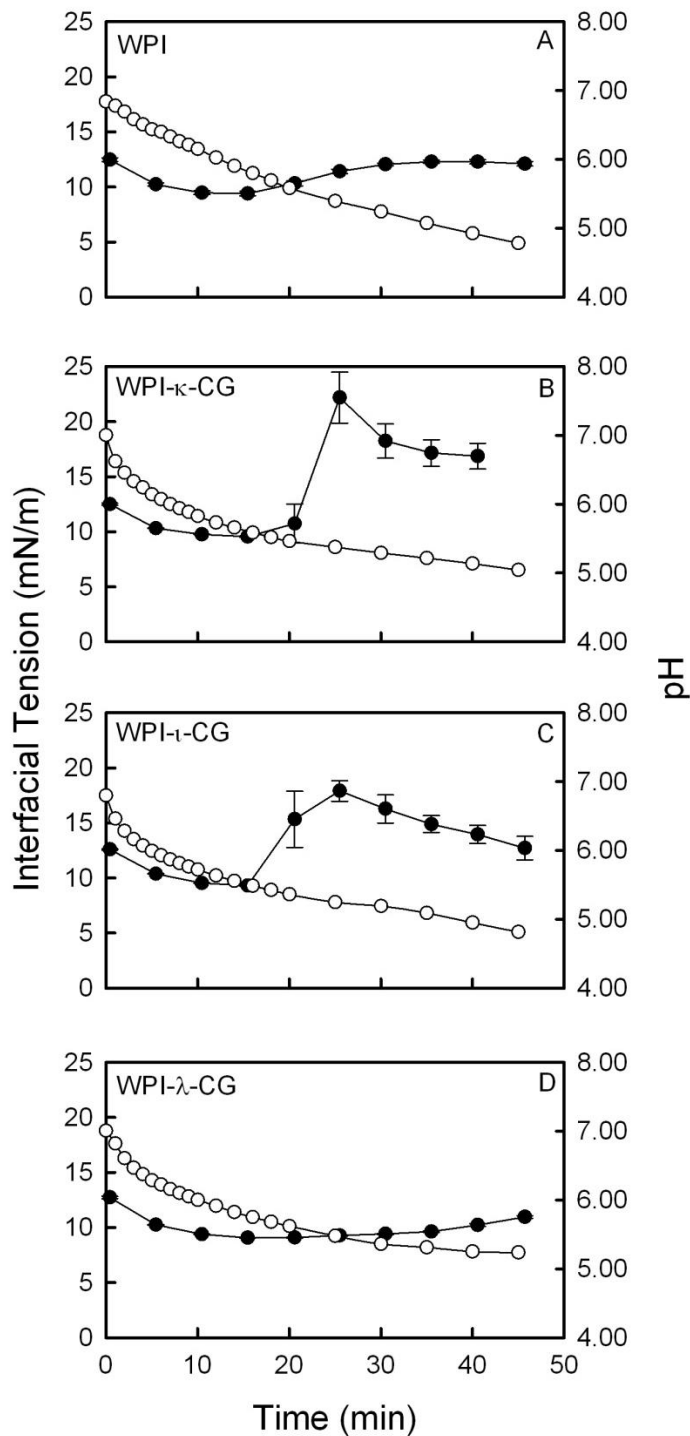


**Figure 6.5** Interfacial tension (nM/m) (solid circle) and pH (open circle) for an individual WPI (A) solution and mixtures of WPI and  $\kappa$ -CG (B),  $\iota$ -CG (C) and  $\lambda$ -CG (D) as a function of time (min). Interfacial data represent the mean values  $\pm$  one standard deviation. All solutions had a total biopolymer concentration of 1.0% (w/w) and were acidified using 0.5% (w/w) GDL.

#### **6.4.4 Rheology of WPI and WPI-carrageenan stabilized emulsions**

Based on the surface activity of WPI and WPI-CG systems and their ability to reduce interfacial tension, emulsions were prepared at a 1:1 oil: water ratio, and then followed by rheological measurements over time, frequency and strain in a similar capacity as for the biopolymer solutions without oil. Figure 6.6 shows changes to the viscoelastic moduli as a function of time/pH for all systems. The individual WPI stabilized emulsion formed a gel where the  $G'$  became greater than  $G''$  at a pH near 7.00 and then increased to a plateau upon over time/acidification as indicative of a gel network (Figure 6.6A). Formed networks were also showed greater elasticity than that of a non-emulsified system were  $G'$  values were ~12.9 Pa (Figure 6.6A) and ~0.2 Pa (Figures 6.2A), respectively after 90 min.

In the case of the WPI-CG mixtures, the gel point (*i.e.*, crossover point where  $G' > G''$ ) was found to occur at pHs ~6.0-6.5 (Figure 6.6B-D). Moduli both increased gradually until ~pH 5.5, in which an inflection point was seen, followed by an even steeper rise in  $G'$  and  $G''$ . This inflection point seemed to correspond to where complexation of WPI and CG molecules occurs. Moduli increase further until reaching a plateau. After 90 min,  $G'$  values were ~452.9, 305.8 and 103.5 Pa for WPI- $\kappa$ -CG, WPI- $\iota$ -CG and WPI- $\lambda$ -CG mixtures, respectively (Figure 6.6B-D). In all case viscoelastic moduli were slightly higher in the emulsion gels than the systems without oil.

In a recent study by Santipanichwong and Suphantharika (2009),  $\beta$ -glucans were used stabilize egg yolk emulsions. They reported that the addition of  $\beta$ -glucans enhanced the storage modulus of their emulsions and speculated the possibility for the  $\beta$ -glucans to enable a three dimensional network to form with the emulsified egg yolk emulsion (Santipanichwong & Suphantharika, 2009). Furthermore, differences in the modulus were found due to different  $\beta$ -glucans source whereby all emulsions formed with  $\beta$ -glucans were found to be weak-gels under frequency sweep analysis (Santipanichwong & Suphantharika, 2009).

Viscoelastic moduli as a function of frequency for all systems showed gel-like behaviour congruent with the time sweep experiments (Figure 6.7). All moduli were also higher in magnitude than seen for the individual biopolymer solutions (no oil) (Figure 6.3 and 6.7) indicating a stronger network is being formed. Based on the strain sweep data, structure breakdown was more gradual as strain was increased, whereas the WPI- $\kappa$ -CG (Figure 6.8B) showed a strong break at ~17.77% strain reflective of its stiff network. Both WPI- $\iota$ -CG and

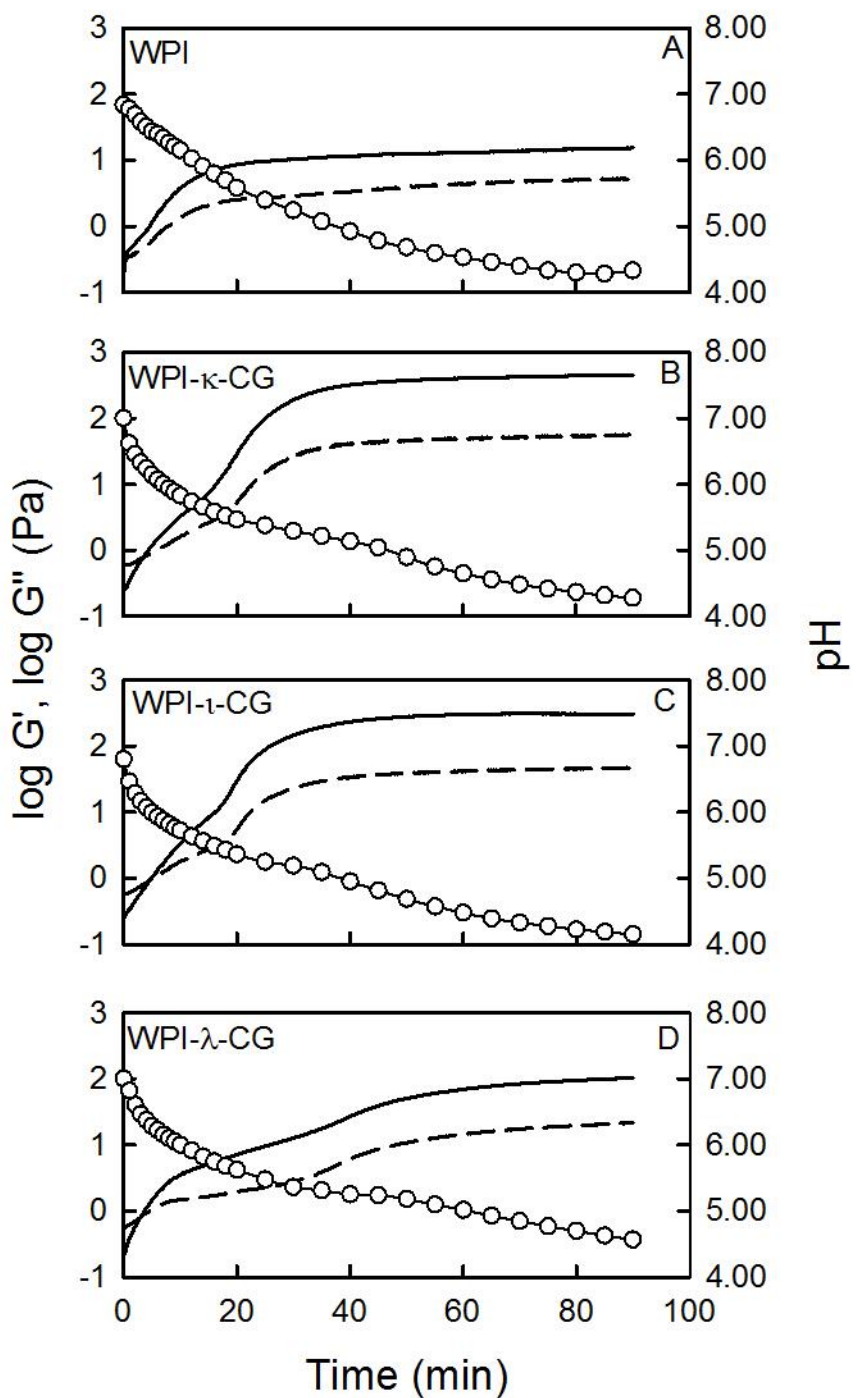


**Figure 6.6** Dynamic viscoelastic storage ( $G'$  (solid line)) and loss ( $G''$  (dashed line)) moduli for emulsions stabilized by an individual WPI (A) solution and mixtures of WPI and  $\kappa$ -CG (B),  $\iota$ -CG (C) and  $\lambda$ -CG (D) as a function of pH (open circles) and time (min). Each curve is representative of 3 separate time sweep runs on separate samples. All solutions had a total biopolymer concentration of 1.0% (w/w) and were acidified using 0.5% (w/w) GDL.

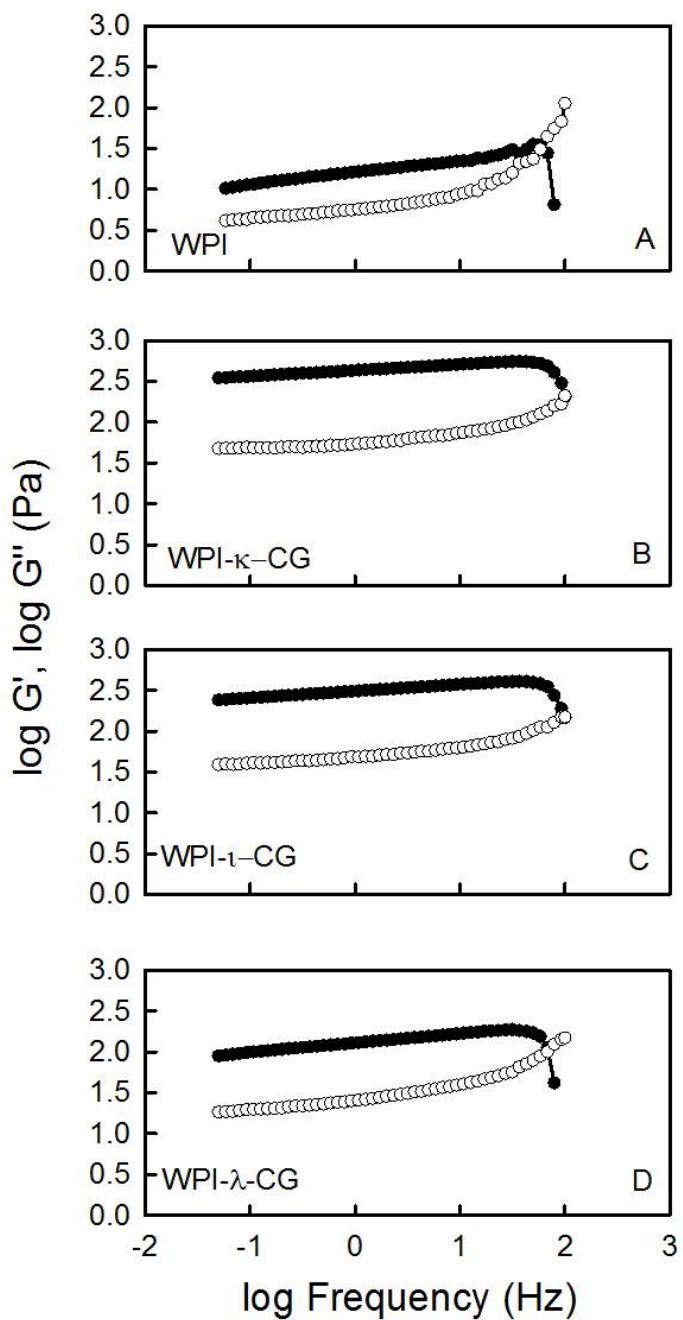


**Figure 6.7** Dynamic viscoelastic storage ( $G'$  (solid circles)) and loss ( $G''$  (open circles)) moduli for emulsions stabilized by an individual WPI (A) solution and mixtures of WPI and  $\kappa$ -CG (B),  $\iota$ -CG (C) and  $\lambda$ -CG (D) as a function of frequency (Hz) (on double logarithmic axes) after 90 min of acidification with 0.5% (w/w) GDL and, after running the time sweep measurements. All solutions had a total biopolymer concentration of 1.0% (w/w) and were at a pH of ~4.0-4.3 when measured.

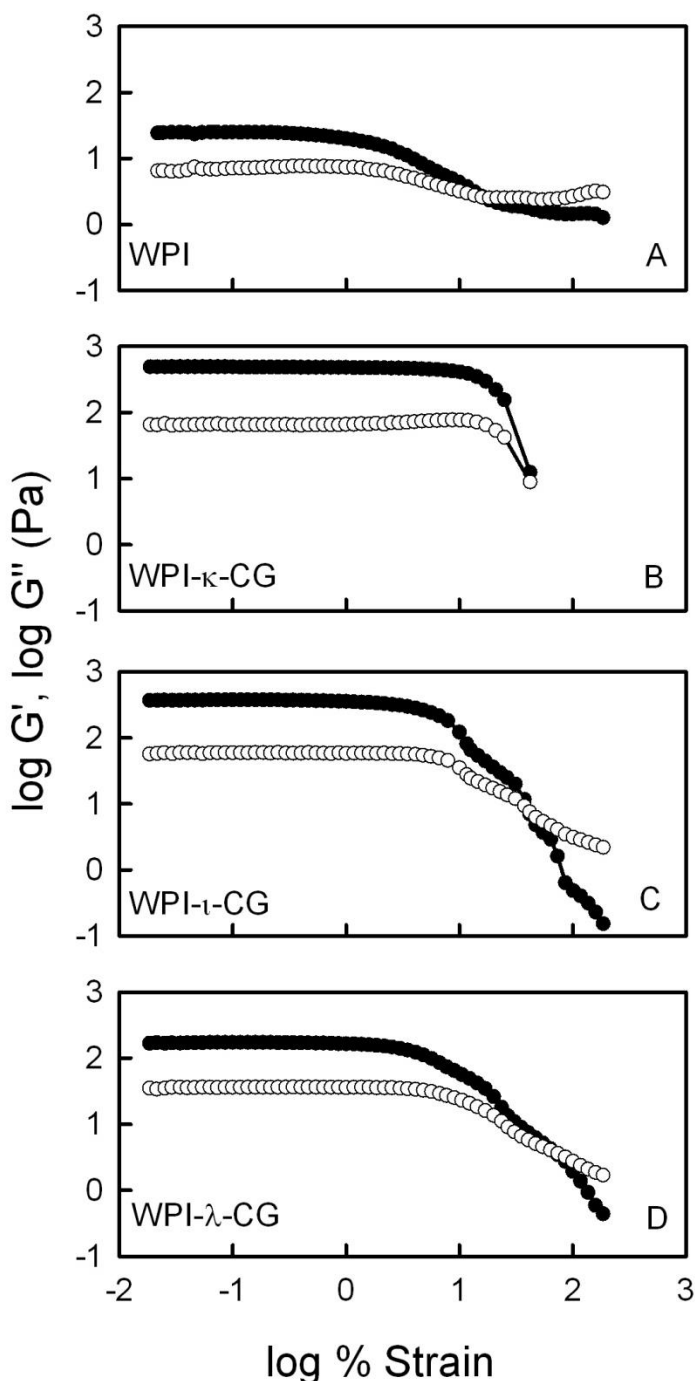


**Figure 6.8** Dynamic viscoelastic storage ( $G'$  (solid circles)) and loss ( $G''$  (open circles)) moduli for emulsions stabilized by an individual WPI (A) solution and mixtures of WPI and  $\kappa$ -CG (B),  $\iota$ -CG (C) and  $\lambda$ -CG (D) as a function of shear strain (%) (on double logarithmic axes) after 90 min of acidification with 0.5% (w/w) GDL and, after running both the time and frequency sweep measurements. All solutions had a total biopolymer concentration of 1.0% (w/w) and were at a pH of ~4.0-4.3 when measured.

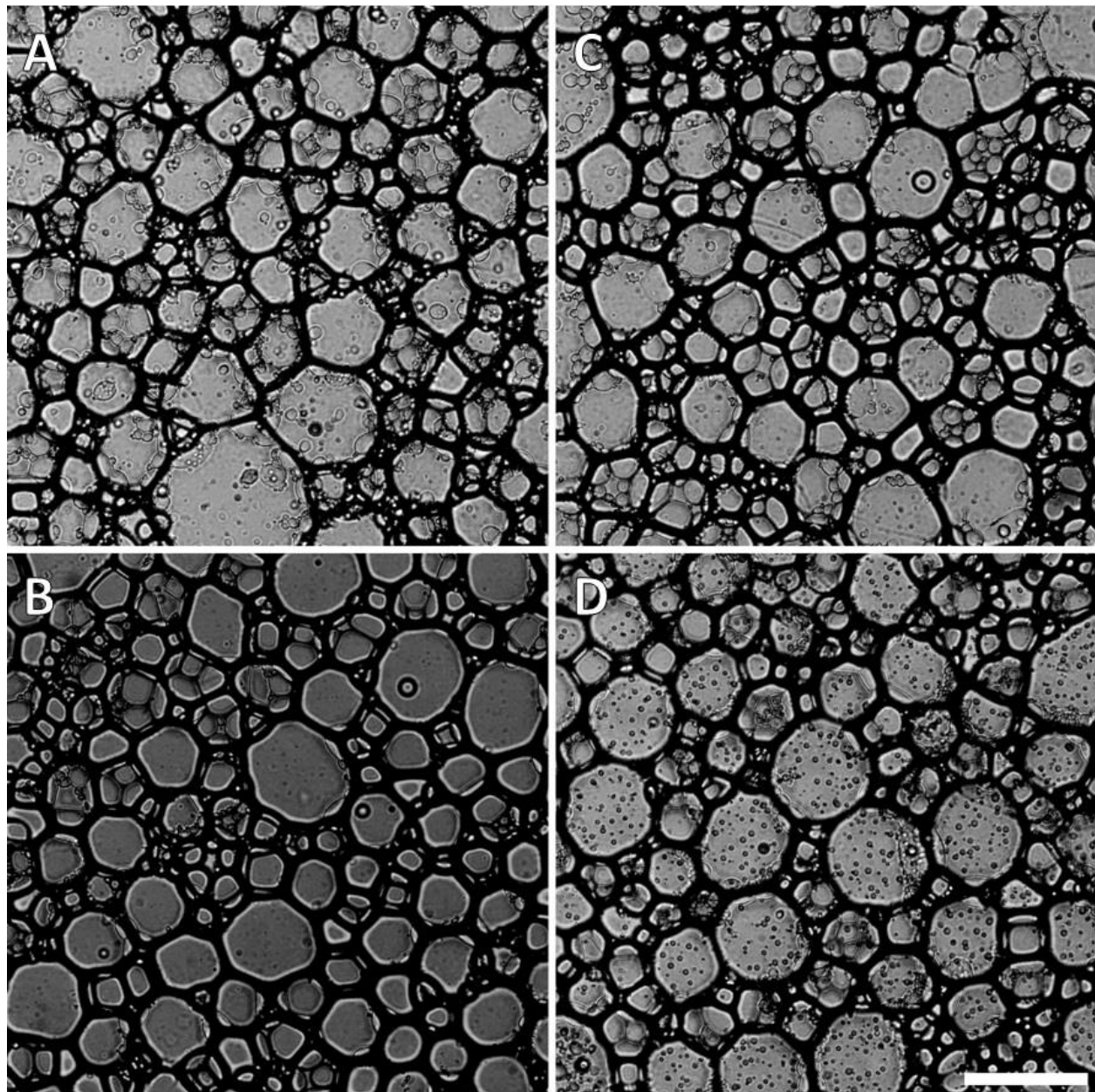


**Figure 6.9** Brightfield microscopy of emulsion gels stabilized with WPI- $\kappa$ -CG (A), WPI- $\tau$ -CG (B) and WPI- $\lambda$ -CG (C) mixtures, and an individual WPI solution (D). Scale bar = 100  $\mu\text{m}$ .

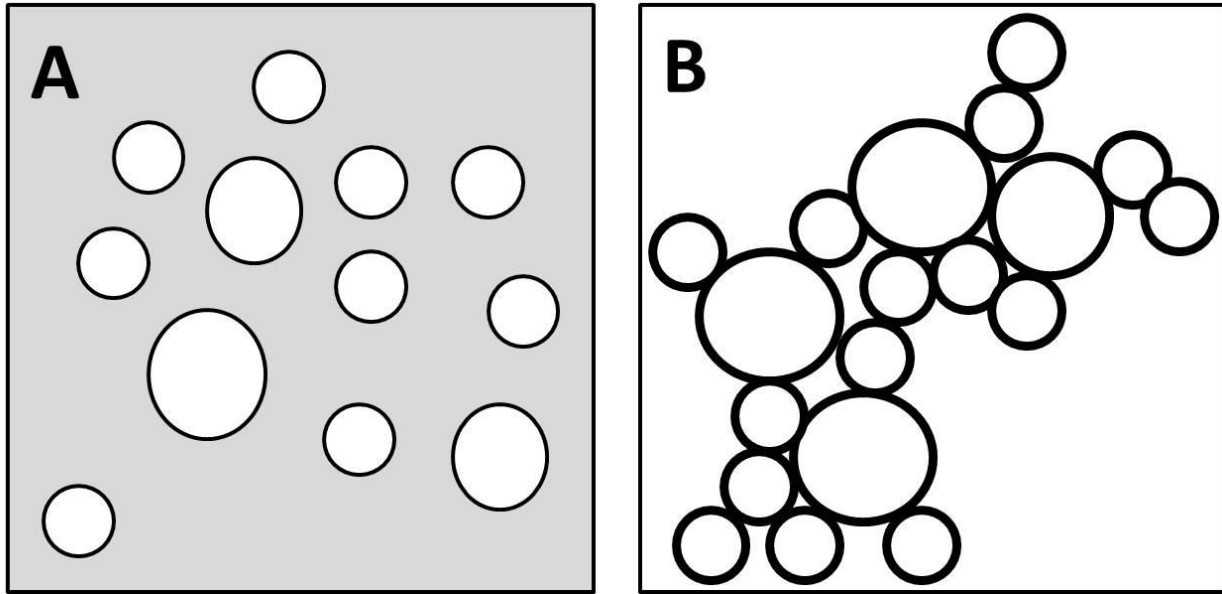


**Figure 6.10** Schematic of an emulsion-filled protein gel (A) and a protein stabilized-emulsion gel (B).

WPI- $\lambda$ -CG emulsion based systems also showed a strong break at  $\sim 9.33$  and  $\sim 2.60\%$  strain, respectively (Figure 6.8C,D). The smaller amount of strain needed to induce structure breakdown suggests a slightly weaker network being formed.

#### 6.4.5 Emulsion droplet sizes of WPI and WPI-CG emulsions

Emulsions were prepared, covered with a coverslip and left on a microscopy slide to acidify for 90 min before being imaged to observe the morphology of the gels at pH  $\sim 4.0$ -4.3. Images for WPI- $\kappa$ -CG, WPI- $\iota$ -CG and WPI- $\lambda$ -CG mixtures and for WPI alone are given in Figure 6.9A, B, C and D, respectively. Mean droplet diameters within the WPI stabilized emulsion was found to be  $37.88 \pm 0.46$   $\mu\text{m}$  based on averaging the diameter of 50 droplets per slide for three slides. In contrast, mean droplet sizes for WPI- $\kappa$ -CG, WPI- $\iota$ -CG and WPI- $\lambda$ -CG stabilized emulsions were  $32.95 \pm 0.31$   $\mu\text{m}$ ,  $31.30 \pm 0.23$   $\mu\text{m}$  and  $32.41 \pm 0.24$   $\mu\text{m}$ , respectively. The presence of CG decreased the average droplet size of these emulsions from  $\sim 38$  to  $\sim 32$   $\mu\text{m}$ . Due to the incompressibility of the droplets, larger droplets would exert a larger frictional force marked by a larger storage modulus under rheology. Since the strength of these emulsions, observed *via* their storage modulus ( $G'$ ), may be ranked as WPI- $\kappa$ -CG > WPI- $\iota$ -CG > WPI- $\lambda$ -CG > WPI control, droplet size seem to have little to no bearing on the strength of these gels. Therefore, it is the WPI-

CG interactions and the network they form which would explain for the elasticity of these gels. In a review by Dickinson (2012), protein-stabilized emulsion gels were separated into two types: 1) an emulsion-filled protein gel and 2) a protein-stabilized emulsion gel (Figure 6.10). In an emulsion-filled protein gel, oil droplets are embedded within a continuous gelled network (Figure 6.10A) (Dickinson, 2012). The presence of oil droplets within this network serves to weaken the overall gel structure whereby the magnitude of  $G'$  is smaller for the emulsion gel compared to the biopolymer gel (Dickinson, 2012). In a protein-stabilized emulsion gel, the proteins coat the oil droplets, followed by their gelation into a thick viscoelastic film on the droplet surface and flocculation, to eventually form a continuous gel network (Figure 6.10B) (Dickinson, 2012). Typically, emulsion gels exhibit a greater  $G'$  than biopolymer gels without oil. In the present study, emulsion gels are proposed to be formed. As the mixture is acidified from pH 7.00, proteins become reduced in charge to allow for greater interactions while at the interface. Upon reaching  $pH_{\phi_1}$ , complexation with the CG molecules *via* electrostatic attraction which strengthens the viscoelastic film formed at the interface. This is followed by flocculation between droplets until an electrostatic-stabilized gel network is formed within the continuous phase.

## 6.5 Conclusions

In the present work, all WPI-CG mixtures, regardless of the CG-type were able to form electrostatically coupled gel networks, however the network strength depended significantly on the CG-type present. Coupled networks were much stronger in the presence of  $\kappa$ -CG and  $\tau$ -CG, than  $\lambda$ -CG, since the latter experienced far greater electrostatic repulsion between chains than the other types. In the presence of oil, coacervation by CG with WPI at the interface affected the interfacial tension and enhanced emulsion stability. The effectiveness of CG influencing the rheology and emulsifying properties of WPI seems to be related to the linear charge density of the CG and possibly its conformation in solution. For instance, both  $\kappa$ -CG and  $\tau$ -CG formed stronger electrostatic coupled networks with WPI, whereas because of the high number of sulphate groups on  $\lambda$ -CG structure formation was hindered from the large repulsive forces between polysaccharide chains ultimately leading to weaker networks than the other CG types. The interactions between WPI and CG and their functionality continue to be of interest to researchers. As further information is reported on these WPI-CG systems, this will aid in manufacturers to known how to incorporate these mixtures in applications found in foods and cosmetics.

## **6.6 Connection to the next study**

In this study, mixtures involving whey proteins and carrageenan formed electrostatically coupled networks, when acidified with GDL, leading to either biopolymer or emulsion-based (in the presence of oil) gels. Only the optimal biopolymer mixing ratio (12:1 for WPI- $\kappa$ -CG and WPI- $\lambda$ -CG; 20:1 for the WPI- $\iota$ -CG system) was used as determined by Stone and Nickerson (2012). Regardless of the presence of oil, electrostatically coupled WPI-carrageenan networks were stronger in mixtures involving  $\kappa$ - or  $\iota$ -types, than when  $\lambda$ -type was used. In the next study, the effect of biopolymer mixing ratios on the formation of electrostatic biopolymer and emulsion-based networks were investigated, at ratios above, at and below the optimal ratios (*i.e.*, WPI- $\kappa$ -CG → 16:1, 12:1 and 8:1; WPI- $\iota$ -CG → 24:1, 20:1 and 16:1).

## **7. THE EFFECT OF BIOPOLYMER MIXING RATIO ON THE FORMATION OF ELECTROSTATICALLY COUPLED WHEY PROTEIN-(KAPPA- AND IOTA-TYPE) CARRAGEENAN NETWORKS IN THE PRESENCE AND ABSENCE OF OIL DROPLETS<sup>6</sup>**

### **7.1 Abstract**

The rheological properties of 1.0% (w/w) whey protein isolate (WPI) – kappa-/iota-carrageenan (CG) mixtures were investigated during a slow acidification process by glucono- $\delta$ -lactone from pH 7.0 to ~4.20 as a function of biopolymer mixing ratio and, in the presence and absence of oil droplets. In all cases, electrostatic coupled biopolymer and emulsion gel networks were formed at pHs corresponding to where attractive interactions between WPI-CG began. Formed WPI-CG complexes were found to be surface active, capable of lowering interfacial tension and forming viscoelastic interfacial films within emulsion based systems. Both biopolymer and emulsion based gels increased in strength and elasticity as the CG content increased, regardless of the type of CG present. However, WPI- $\iota$ -CG coupled networks were stronger than WPI- $\kappa$ -CG networks, presumed due to the higher number of sulfate groups attracting to the WPI molecules.

### **7.2 Introduction**

Whey protein and carrageenan (CG) are commonly used food ingredients in many applications (*e.g.*, baked goods, beverages, desserts, confectionary and meat products) due to their gelling, emulsifying or thickening abilities (Mulvihill, 1992). Whey proteins represent a mixture of proteins that are dominated by  $\alpha$ -lactalbumin and  $\beta$ -lactoglobulin. These proteins have been intensively studied over the years for their functional attributes such as gelation (Tang *et*

---

<sup>6</sup> Accepted as: Lam, R. & Nickerson, M.T. (2014). The effect of biopolymer mixing ratio on the formation of electrostatically coupled whey protein-(kappa- and iota-type) carrageenan networks in the presence and absence of oil droplets. *Journal of Agricultural and Food Chemistry*.

*al.*, 1994; Elofsson *et al.*, 1997; Gulzar *et al.*, 2012), and their capacity to stabilize emulsions (Reiffers-Magnani *et al.*, 2000; Tcholakova *et al.*, 2006b; Manoi & Rizvi, 2009).

In contrast, carrageenan polysaccharides are extracted from red seaweeds (*Rhodophyta* species) (van der Velde *et al.*, 2002), and consist of disaccharide repeating units comprised of D-galactose and 3,6-anhydro-D-galactose residues, with one, two or three sulphate groups associated each repeat unit for  $\kappa$ -,  $\iota$ - and  $\lambda$ -type carrageenan, respectively (Weinbreck *et al.*, 2004b). Although other minor types of CG have been identified by Knutsen and co-workers (1994), the present research will only focus on the  $\kappa$ - and  $\iota$ -types due to their abilities to form strong gels (Morris *et al.*, 1980; Rochas & Rinaudo, 1984; Souza *et al.*, 2011).

Mixtures of proteins and polysaccharides are known to undergo associative liquid/liquid phase separation (also known as complex coacervation) under conditions where biopolymers are oppositely charged and/or experiencing a significant amount of electrostatic attraction (de Kruif *et al.*, 2004). Whey protein-carrageenan mixtures have been explored previously with this respect by de Kruif and co-workers (2004), Weinbreck and co-workers (2004b) and, Stone and Nickerson (2012). During coacervation, pH is lowered until a negatively charged protein (*i.e.*, pH > pI), becomes neutral (*i.e.*, at pI) and then positively charged (*i.e.*, pH < pI), where it then can interact with a negatively charged polysaccharide. In the case of whey protein and CG, the initial interaction typically occurs at pH > pI where both biopolymers carry similar net charges due to the interaction between CG and positively charged ‘patches’ on a protein surface (Weinbreck *et al.*, 2004b). This initial interaction is denoted as pH<sub>c</sub> and is evident by a slight increase in the absorption or light scattering in the protein-polysaccharide solution (de Kruif *et al.*, 2004). As pH continues to decline, a sharp rise in the absorbance or light scattering of the biopolymer solution (designated as pH<sub>φ1</sub>) follows as the solution becomes turbid (de Kruif *et al.*, 2004). This sustained increase in absorbance and light scattering continues until a maximum is reached (designated as pH<sub>opt</sub>) (de Kruif *et al.*, 2004). Beyond this point, continual acidification causes the complex to dissociate and dissolve (de Kruif *et al.*, 2004). The area of complex coacervation has been well studied with a number of reviews in the area (Schmitt *et al.*, 1998; Doublier *et al.*, 2000; de Kruif *et al.*, 2004).

Recently, research has sought to use complexes as a means to stabilize emulsions (Nakagawa *et al.*, 2004; Katona *et al.*, 2010; Moschakis *et al.*, 2010; Li & McClements, 2011; Koupantis *et al.*, 2014). Emulsions are formed when two immiscible liquids are mechanically

agitated until one is dispersed as tiny droplets within the other. Since emulsions are thermodynamically unstable, the use of amphiphilic biopolymers (*e.g.*, proteins) can be used to inhibit emulsions from phase separation by reducing the surface tension between the droplets and the continuous solvent. Depending on the level of interactions, the biopolymers involved, and processing conditions, systems may become stable or unstable. For instance, in dilute systems, the addition of a polysaccharide to a protein-stabilized oil droplet could lead to either the formation of a viscoelastic bi-layer where the polysaccharide complexes to the interfacial film leading to increased emulsion stability (Salminen & Weiss, 2014), or it can cause instability *via* flocculation by the depletion interaction or bridging flocculation of neighbouring droplets (Blijdenstein *et al.*, 2004). In more concentrated systems, various mixed protein-polysaccharide systems may take on a gel-like structure (Dickinson, 2012). The nature of the gel may be considered as an ‘emulsion-filled protein gel’ whereby oil droplets are simply encased within a gelled protein or a protein-stabilized emulsion gel’ whereby the gel structure consists of an interconnected flocculated network of oil droplets stabilized by an interfacial coacervate film (Dickinson, 2012).

The inclusion of polysaccharides to protein-based emulsion systems have recently been research as a means to reduce the oxidation of the emulsified oil for bioactive delivery (Huang *et al.*, 2008) and for developing novel applications in controlled-release systems (Liu *et al.*, 2013). This body of work will continue to enhance our understanding of protein-polysaccharide interactions in emulsified systems (Zhu *et al.*, 2010). The overall goal of the present study is to examine the underlying mechanisms driving the formation of electrostatically coupled biopolymer and emulsion gel networks, as a function of CG-type ( $\kappa$ - and  $\iota$ -type) and mixing ratio between whey protein isolate (WPI) and the CG molecules. Stone and Nickerson investigated the formation of electrostatic complexes involving WPI and CG molecules as a function of CG type under dilute conditions (0.25% w/w), and reported the optimal mixing ratio to occur at 12:1 ratio for WPI- $\kappa$ -CG mixtures, and a 20:1 ratio for the WPI- $\iota$ -CG system (Stone & Nickerson, 2012). Information arising from this study will aid in controlling and optimizing their use in food or controlled delivery-type applications where gelation is important.

## **7.3 Materials and methods**

### **7.3.1 Materials**

Whey protein isolate used in this study was generously donated by Davisco Foods International, Inc. (Le Sueur, MN, USA). The chemical composition of the commercial WPI powder was determined according to AOAC (2003) methods; 925.10 (moisture), 923.03 (ash), 920.87 (crude protein), and 920.85 (lipid). Carbohydrate content was determined on the basis of present differential from 100%. The WPI powder comprised of 89.78% protein (%N × 6.38), 0.10% lipid, 4.92% moisture, 2.06% ash (including 0.08% Ca<sup>2+</sup>, 0.01% Mg<sup>2+</sup>, 0.02% K<sup>+</sup>, and 0.66% Na<sup>+</sup>), and 3.13% carbohydrate (wet basis). Carrageenan (CG) ( $\kappa$ -and  $\iota$ -) and glucono- $\delta$ -lactone (GDL) were purchased from Sigma-Aldrich (Oakville, ON, Canada). For the two types of CG, the supplier information indicated that  $\kappa$ -CG was comprised of 66.50% carbohydrate, 10.65% moisture and 22.86% ash (including 2.4% Ca<sup>2+</sup>, 0.16% Mg<sup>2+</sup>, 5.4% K<sup>+</sup>, 0.49% Na<sup>+</sup>) and  $\iota$ -CG contained 64.40% carbohydrate, 10.82% moisture and 24.97% ash (including 3.4% Ca<sup>2+</sup>, 0.18% Mg<sup>2+</sup>, 3.2% K<sup>+</sup>, 1.2% Na<sup>+</sup>). Canola oil used in this study was purchased from a local supermarket. All other chemicals used in this study were of reagent grade and purchased through Sigma-Aldrich (Oakville, ON, Canada). The water used in this research was filtered using a Millipore Milli-Q™ water purification system (Millipore Corp., Milford, MA, USA). WPI and CG were used without further purification and were corrected for protein and polysaccharide content respectively.

### **7.3.2 Sample preparation**

Biopolymer solutions (1.0% w/w biopolymer) were prepared by dispersing WPI and CG powders in water by mechanical stirring (500 rpm) at room temperature (21-23°C) for 60 min. Afterwards, 0.5% (w/w) of GDL was added to the biopolymer solution and stirred for 1 min prior to analysis to slowly acidify the solution. WPI and CG were mixed at ratios above and below the optimal ratio determined by Stone and Nickerson (2012). Mixing ratios of 8:1, 12:1 and 16:1 were tested for WPI:  $\kappa$ -CG, and ratios of 16:1, 20:1 and 24:1 were tested for WPI:  $\iota$ -CG. A total of 1.0% (w/w) biopolymer into the aqueous phase was used for all experiments. All WPI and CG powders weights used were corrected for both protein and carbohydrate concentration, respectively. Changes in pH upon GDL addition was monitored for each mixture using a Fisher Scientific Accumet pH meter equipped with an Ag/AgCl pH probe (Fisher Scientific, Ottawa, ON, Canada) over time.

*Emulsion preparation:* Initially biopolymer solutions were prepared as previously mentioned. Upon adding the GDL, and equal ratio (1:1) of the aqueous biopolymer solution and canola oil were mixed to a total weight of 10 g. The mixture was subsequently homogenized at 7,200 rpm for 5 min using an Omni Macro Homogenizer (Omni International Inc., Marietta, GA) equipped with a 20 mm saw tooth generating probe.

### 7.3.3 Interfacial tension

The interfacial tension for each WPI-CG mixture was measured using a Lauda TD 2 Tensiometer (Lauda-Königshofen, Germany) equipped with a Du Nüoy ring (20 mm diameter). Within a 40 mm diameter glass sample cup, a 20 g biopolymer solution was added then stirred for 1 min after the addition of 0.5% w/w GDL, followed by the immersion of the Du Nüoy ring and then the addition of upper canola oil layer (20 g). The ring was then pulled upwards to stretch the interface to measure the maximum force without breaking into the oil phase. Interfacial tension was measured over time (50 min) every 600 s, where the mean of three replicates  $\pm$  one standard deviation was reported. Interfacial tension was calculated from the maximum force ( $F_{\max}$ ; units: milli-Newtons; instrument measures mg x gravity) using the following equation (eq. 7.1):

$$\gamma = \frac{F_{\max}}{4\pi R\beta} \quad (\text{eq. 7.1})$$

where,  $\gamma$  is the interfacial tension (mN/m),  $R$  is the radius of the ring (20 mm),  $\beta$  is a correction factor that depends on the dimensions of the ring and the density of the liquid involved (McClements, 2005). All measurements are reported as the mean  $\pm$  one standard deviation ( $n = 3$ ).

### 7.3.4 Oscillatory shear deformation of the bulk solution

Oscillatory shear deformation of the bulk biopolymer and emulsion solutions during a GDL acidification was monitored over time using an AR-G2 Rheometer (TA Instruments, New Castle, DE) equipped with a 40 mm diameter 2° acrylic cone. A time sweep was performed over a 90 min period to monitor changes to the dynamic storage ( $G'$ ) and loss ( $G''$ ) moduli. Measurements were made within the linear viscoelastic region at a frequency of 1 Hz every 10 s where the maximum amplitude for strain set at 1.0%. Following the time sweep, a frequency and strain sweep was performed on the same material to better characterize the formed gel network. During frequency sweeps, frequencies were increased continuously from 0.05 Hz to 100 Hz with 15 points per

logarithmic decade being captured, with maximum strain set at 1%. In contrast, strain sweeps were conducted by increasing the applied strain continuously from 0.01% to 500% with 15 data points per logarithmic decade captured at a frequency of 5 Hz. Each sample was prepared in triplicate.

### **7.3.5 Oscillatory shear deformation at the oil-water interface**

Interfacial oscillatory shear deformation was applied to the oil-water interface using an AR-G2 Rheometer (TA Instruments, New Castle, DE) equipped with their interfacial bi-cone fixture. Interfacial oscillatory shear was performed in time sweep mode for 90 min at a frequency of 1 Hz and maximum stain set at 1.0%. Biopolymer solutions with GDL comprised of the denser phase beneath the bicone while canola oil comprised of the less dense phase above the bicone. All measurements were made within the linear viscoelastic regime. Each sample was prepared in triplicate.

## **7.4 Results and discussion**

### **7.4.1 Formation of electrostatic coupled biopolymer networks**

The rheological properties of WPI-CG mixtures as a function of CG-type and mixing ratio during a slow acidification from pH 7.00 to ~4.20 using GDL is given in Figure 7.1. In all cases, gel-like properties ( $G' > G''$ ) were evident once the solution pH was reduced to induce complexation between the WPI and CG molecules. In the absence of CG, WPI solutions did not exhibit gel-like properties (data not shown). In the case of the WPI- $\kappa$ -CG mixture, the cross over point (denoted as the gel point; Winter & Chambon, 1986) of  $G'$  with  $G''$  was found to correspond to pH 5.37, 5.33 and 5.29 for the 16:1, 12:1 and 8:1 WPI- $\kappa$ -CG mixing ratios, respectively (Figure 7.1A-C). The pI of WPI has been reported to be at pH 4.6 (Parris & Baginski, 1991), suggesting that complexation is occurring where both biopolymers are carrying a negative net charge and most likely involve CG interactions with positively charged patches on the protein's surface (Weinbreck *et al.*, 2004b). At pH above the gel point, biopolymers were

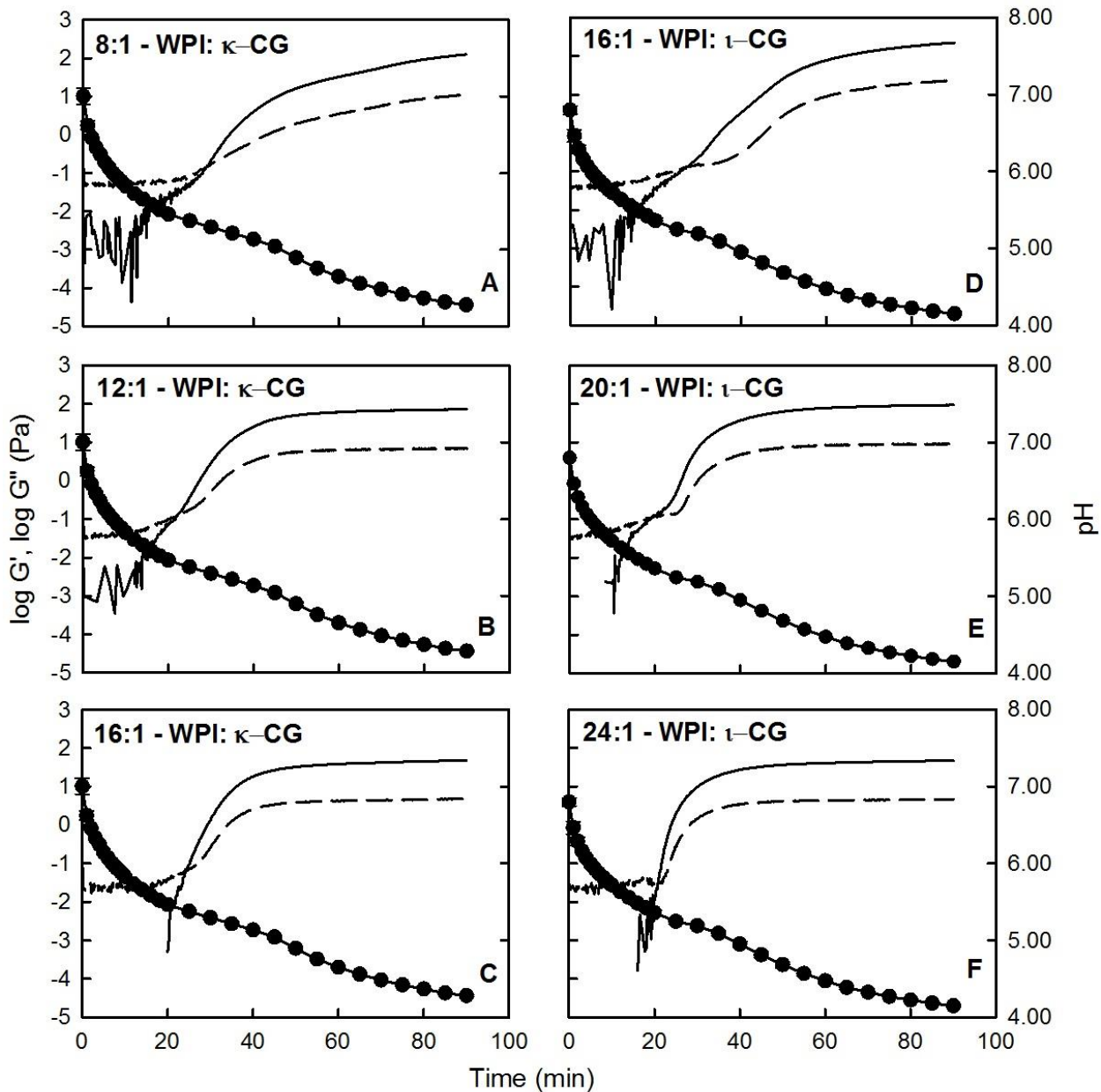


**Figure 7.1** Dynamic viscoelastic storage ( $G'$  (solid line)) and loss ( $G''$  (dashed line)) moduli for mixtures of WPI- $\kappa$ -CG (A-C) and WPI- $\iota$ -CG (D-F) at various mixing ratios as a function of pH (closed circles) and time (min). Each curve is the mean  $\pm$  1 standard deviation of 3 separate time sweep runs on separate samples. All solutions had a total biopolymer concentration of 1.0% (w/w) and were acidified using 0.5% (w/w) GDL.

**Table 7.1** The dynamic storage ( $G'$ ) and loss ( $G''$ ) moduli for electrostatic coupled networks involving WPI-CG mixtures as a function of mixing ratio and in the absence and presence of oil after a 90 min time sweep. All biopolymer solutions were at 1.0%, and were acidified with 0.5% (w/w) GDL to pH 4.28 and 4.15 for the WPI- $\kappa$ -CG and WPI- $\iota$ -CG mixtures, respectively. Data represent the mean value  $\pm$  once standard deviation.

Mixing ratio	<u>Biopolymer gel</u>		<u>Emulsion gel</u>	
	$G'$ (Pa)	$G''$ (Pa)	$G'$ (Pa)	$G''$ (Pa)
<b>WPI-<math>\kappa</math>-carrageenan</b>				
8:1	108.0 $\pm$ 15.6	10.0 $\pm$ 0.9	522.9 $\pm$ 49.8	67.5 $\pm$ 0.7
12:1	73.1 $\pm$ 2.2	6.9 $\pm$ 0.7	435.3 $\pm$ 16.2	54.5 $\pm$ 0.8
16:1	45.4 $\pm$ 6.8	4.5 $\pm$ 0.6	257.3 $\pm$ 28.5	36.2 $\pm$ 5.3
<b>WPI-<math>\iota</math>-carrageenan</b>				
16:1	256.8 $\pm$ 29.8	26.6 $\pm$ 2.9	658.5 $\pm$ 60.0	91.4 $\pm$ 9.3
20:1	93.1 $\pm$ 1.6	9.1 $\pm$ 0.2	320.4 $\pm$ 17.4	45.9 $\pm$ 3.3
24:1	52.9 $\pm$ 12.5	5.1 $\pm$ 1.0	70.8 $\pm$ 16.6	15.8 $\pm$ 1.2

assumed to be co-soluble and non-interacting, leading to fluid-like flow behaviour ( $G' < G''$ ). Afterwards,  $G'$  increased substantially indicating a rise in network strength. In the case of the 8:1 mixing ratio,  $G'$  approached a plateau regime whereas for the 12:1 and 16:1 ratio a plateau was reached (Figure 7.1 A-C). The magnitude of  $G'$  was found to increase as the CG concentration increased within the ratio, where  $G'$  was found to be 45.4, 73.1 and 108.0 Pa for 16:1, 12:1 and 8:1 WPI- $\kappa$ -CG mixing ratios, respectively (Table 7.1). It was hypothesized that the lower pH at the gel point for the 8:1 mixing ratio reflects a greater viscosity imparted by the higher CG content. Similarly, Perez and co-workers (2009) reported that an increase in polysaccharide content led to slower mobility of whey protein-polysaccharide complexes. Therefore it was hypothesized that the reduced mobility of WPI-CG complexes led to a slower gelation time due to the high viscosity imparted by the high CG content of the system. In the case of the WPI- $\iota$ -CG mixture, the gel point was found to correspond to pH 5.34, 5.34 and 5.20 for the 24:1, 20:1 and 16:1 mixing ratios, respectively (Figure 7.1 D-E). A similar increase in the maximum  $G'$  with increasing CG content, where the magnitude was found at 52.9, 93.1 and 256.9 Pa for mixing ratios from 24:1, 20:1 and 16:1, respectively (Table 7.1) suggesting it was following a similar mechanism of network formation.

An increase in the G' or the stiffness of the network have been previously been reported by Tavares and co-workers (2005) where the stiffness of whey protein - galactomannan networks were found with an increase in the polysaccharide content. In the absence of CG, acidified WPI solutions do not form a network (data not shown). Therefore it is assumed that the formation of WPI-CG networks are attributed to the formation of WPI-CG electrostatic complexes due to GDL acidification which act as junction zones within the gel. Complex formation has been previously reported on by others (de Kruif *et al.*, 2004; Weinbreck *et al.*, 2004b; Stone & Nickerson, 2012) and is a well known phenomenon and therefore is beyond the scope of this report. In part, coacervation requires the phase-separation of the networks where it is presumed that as proteins approach their pI, the precipitation of the proteins and their coacervation with polysaccharides enhance the strength of these networks. In a study of the effects of  $\beta$ -glucans complexed onto egg yolk stabilized oil-in-water emulsions, Santipanichwong and Suphantharika (2009) reported that insoluble  $\beta$ -glucans compared to soluble  $\beta$ -glucans exhibited a greater degree of structuring on its own. To gain greater insights to the nature of these networks and to uncover their structural mechanism, they were physically characterized using frequency and strain sweeps.

Oscillatory frequency sweeps for both WPI- $\kappa$ -CG and WPI- $\iota$ -CG systems after the 90 min time sweep indicated that all materials exhibited gel-like features, regardless of the mixing ratio. Within this regime, both moduli were slightly frequency dependent, and the magnitude of G' was greater than G'' (Figure 7.2A, C). Without acidification, frequency sweeps of these WPI-CG biopolymer solutions were strongly frequency dependent suggesting a non-interacting mixed biopolymer solution (data not shown). The slight dependence of these GDL acidified WPI-CG mixtures indicate a weak gel structure. Similarly, whey protein – galactomannan networks were also found to be slightly frequency dependent (Tavares *et al.*, 2005).

Critical strains are helpful in characterizing the breakup of these gels under strain. In a previous study on pure CG gels, Azevedo and co-workers (2014) reported that in low ionic content CG mixtures, the critical strain was dependent on the CG content. Similar to present, the critical strain decreases with increasing CG content (Azevedo *et al.*, 2014). CG content allowed for greater elasticity within these networks such that critical strains increased with CG content. Critical strain at break for WPI- $\kappa$ -CG was found at ~58.83%, ~73.41%, and ~116.4% for mixing ratios of 16:1, 12:1, and 8:1, respectively, whereas for the WPI- $\iota$ -CG, critical strain at the break occurred at ~46.67%, ~74.52%, and ~98.25% for mixing ratios of 24:1, 20:1, and 16:1 respectively (Figure

7.2 B,D). For both systems, the most elastic networks were formed at the highest CG content (*i.e.* lowest WPI: CG ratios). Networks were also more brittle (*i.e.* lower

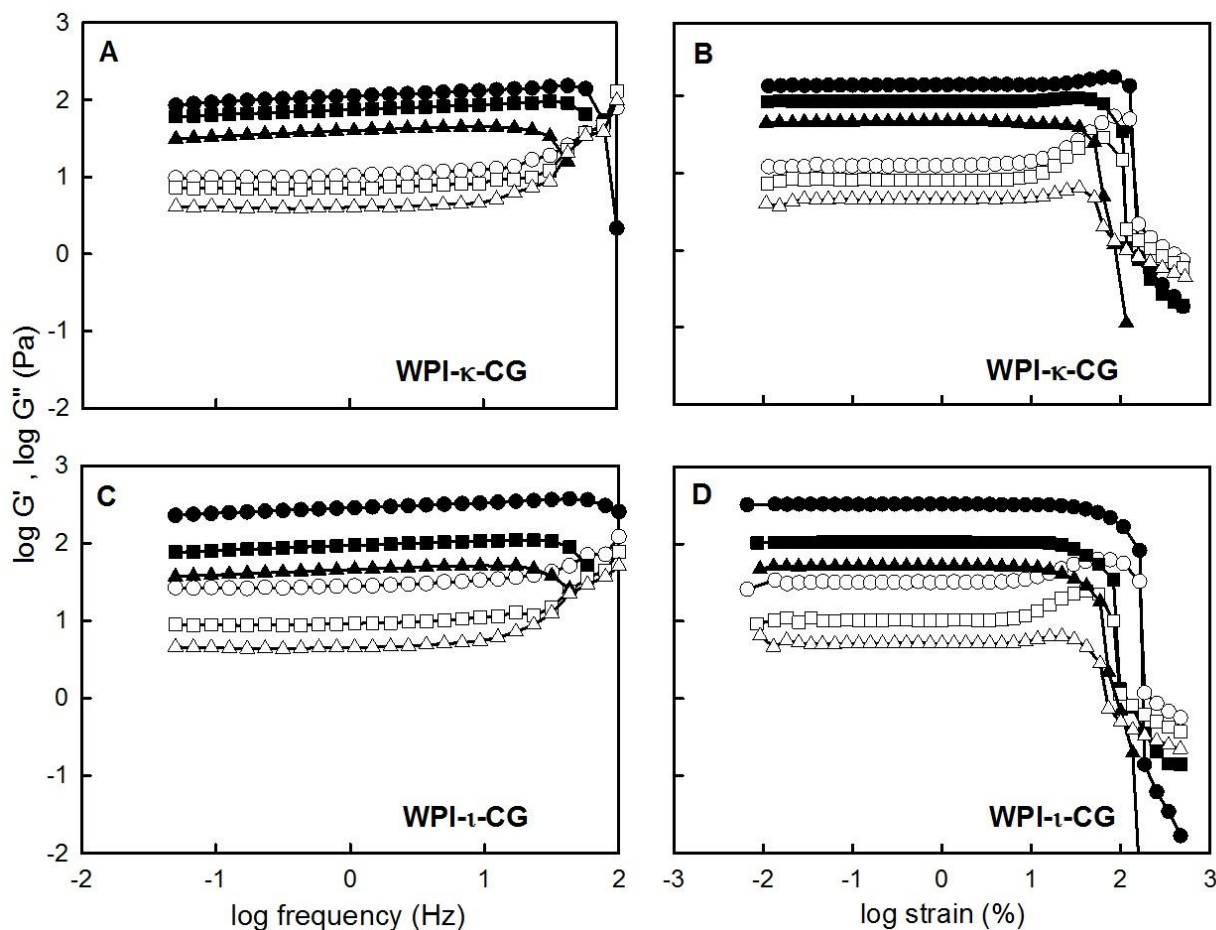


**Figure 7.2** Dynamic viscoelastic storage ( $G'$  (closed symbol)) and loss ( $G''$  (open symbol)) moduli for mixtures of WPI- $\kappa$ -CG (A-B) and WPI- $\tau$ -CG (C-D) at various mixing ratios as a function of frequency (A and C) and strain (B and D). WPI- $\kappa$ -CG (A-B) mixtures were mixed at ratios of 8:1 (circle symbol), 12:1 (square symbol) and 16:1 (triangle symbol) while WPI- $\tau$ -CG (C-D) were mixed at 16:1 (circle symbol), 20:1 (square symbol) and 24:1 (triangle symbol). Each curve is representative of 3 separate sweep runs on separate samples. All solutions had a total biopolymer concentration of 1.0% (w/w) and were measured at a pH of 4.28 and 4.15 for WPI- $\kappa$ -CG and WPI- $\tau$ -CG mixtures respectively.

critical strain) when  $\kappa$ -CG was present relative to  $\tau$ -CG, possibly due to its lower linear charge density which reduces the number of potential bonds while allowing it to have greater conformational entropy (*e.g.*, flexibility) possibly more flexible cross-links between WPI

molecules within the electrostatic coupled network. In contrast,  $\iota$ -CG would have a higher number of sulphate groups present leading to a stiffer polysaccharide molecule in-between the WPI molecules which builds a stronger network.

The breakdown behavior in the strain sweep reveals the nature of these networks (Figure 7.2B, D) where the strain independent behavior observed initially is a result of the elasticity exhibited by the network under low strains. At higher strains, the loss modulus increases slightly before decreasing along with the storage modulus. This strain behavior has been previously characterized as weak strain overshoot behavior by Hyun and co-workers (2002). In weak strain overshoot behavior, though frequency sweeps demonstrate gel-like behavior, their anionic polysaccharide (*e.g.* xanthan gum in a study by Hyun *et al.* (2002) and CG in this study) was explained to possess large conformational entropy due to electrostatic repulsion within its structure (Hyun *et al.*, 2002). This allows for alignment and association between biopolymers allowing for a network to form (Hyun *et al.*, 2002). Hyun and co-workers (2011) later reported that weak strain overshoot behavior which results in a local  $G''$  maximum is the result of junctions both breaking and forming new ones within the network under high strains. Others have suggested that this localized  $G''$  maximum is due to structural rearrangements due to the shear imposed onto the network (Parthasarathy & Klingenber, 1999). Weak strain overshoot behavior was observed for all biopolymer networks formed with WPI- $\iota$ -CG mixtures and for WPI- $\kappa$ -CG mixtures at a ratio of 16:1. In the case of WPI- $\kappa$ -CG mixtures at ratios of 8:1 and 12:1, strong overshoot behavior was observed (Hyun *et al.* 2002) which is caused by the strong interactions formed by the interacting biopolymers. Under strong overshoot behavior, a local maximum for both  $G'$  and  $G''$  is observed before both rapidly decrease at higher strains. The decrease in both moduli is attributed to the breakdown of the network by shearing. This strain overshoot phenomena is not unique to these WPI-CG systems but have also been previously reported in other associative biopolymer solutions (Tirtaatmadja *et al.*, 1997; Tam *et al.*, 1999). WPI-CG networks within the present study are formed as a result of GDL acidification causing coacervation. The conformational entropy associated with CG allows for junction zones to be formed with either other CGs or WPIs present in solution (*i.e.*, WPI-WPI, CG-CG and WPI-CG

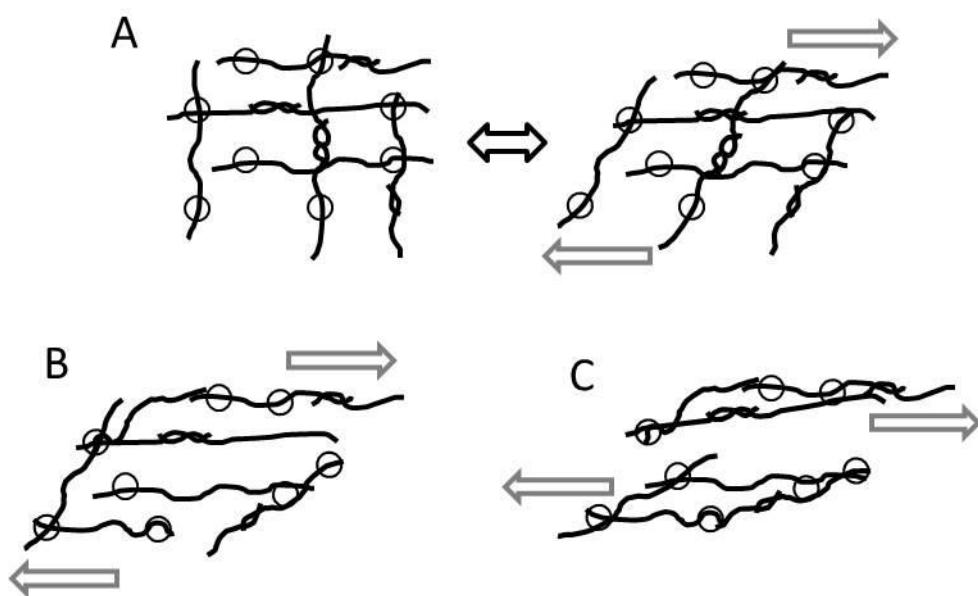
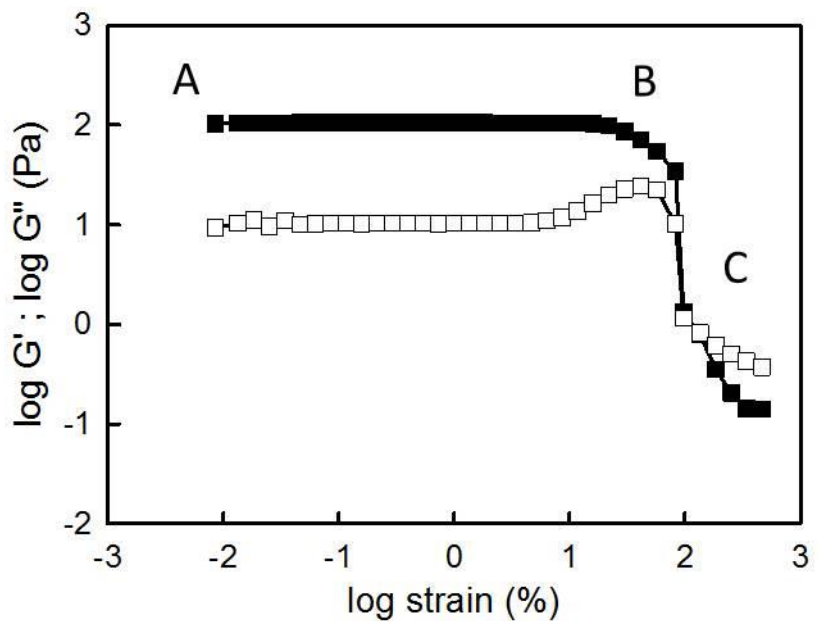


**Figure 7.3** A schematic of a sample WPI-t-CG biopolymer gel at the ratio of 20:1 in response to strain (graph:  $G'$  (closed symbols) and  $G''$  (open symbols)) where the gelled network comprised of WPI (open circle) complexed with CG (lines) are elastic at low strains (A), re-arrange in their molecular bonding at higher strains (B) which leads to the breakdown of the network (C). The grey arrows indicate the direction of the applied shear.

interactions). These interactions, formed due to acidification over time, allows for a continuous network to be formed as captured by time sweeps under oscillatory stress measurements. Though a continuous network is formed, it is by no means uniform. Figure 7.3 provides a visual representation of the breakdown of networks under strain which are linked together *via* CG chains with other CG or WPI biopolymers. These networks are elastic under low-strain amplitudes (Figure 7.3A) while undergo stress overshoot behavior at higher strains (Figure 7.3B) which eventually leads to their breakdown (Figure 7.3C).

#### 7.4.2 Interfacial properties of WPI-CG complexes at the oil-water interface

Due to the amphiphilicity of WPI, the surface activity of WPI-CG mixtures during acidification was measured at the canola oil-water interface. In the absence of biopolymers, the interfacial tension between canola-oil and water was found to be ~28 mN/m where the addition of WPI-alone lowered the interfacial tension to ~12 mN/m where interfacial tension remain relatively constant between ~10 to ~12 mN/m for the duration for GDL acidification. Interfacial tension and interfacial rheology for WPI-CG mixtures as a function of mixing ratio during a slow acidification with GDL are given in Figures 7.4 and 7.5, respectively. Interfacial tension for all systems was found to decrease until reaching a pH where WPI and CG formed electrostatic complexes (Figure 7.4 and 7.5). This decline in tension is presumed to be caused by a highly surface active WPI molecule, which is presumed to be integrating alone into the interface rather than the CG molecule over this pH range (7.00 to 5.46 and 5.36 for WPI- $\kappa$ -CG and WPI- $\iota$ -CG mixtures, respectively). At ~20 min (pH = 5.46 and 5.36 for WPI- $\kappa$ -CG and WPI- $\iota$ -CG mixtures, respectively), a dramatic increase in tension was seen believed to be associated with the electrostatic interactions between WPI-CG. The rise in tension suggests that possibly, WPI adhering to the interface is being pulled away by electrostatic attractive forces with CG molecules in solution, reducing its ability to lower the interfacial tension. Upon electrostatically interacting with CG molecules, WPI-CG complexes can re-adhere to the interface to form a stable film, to lower the interfacial tension once again. The decrease in interfacial tension can only be measured until ~45 min/pH ~5.00 after which the Du Nuoy ring punctures through the interface due to the formation of an electrostatic coupled gel network within the continuous phase which would restrict the mobility of the interfacial film (Figure 7.4). However it is

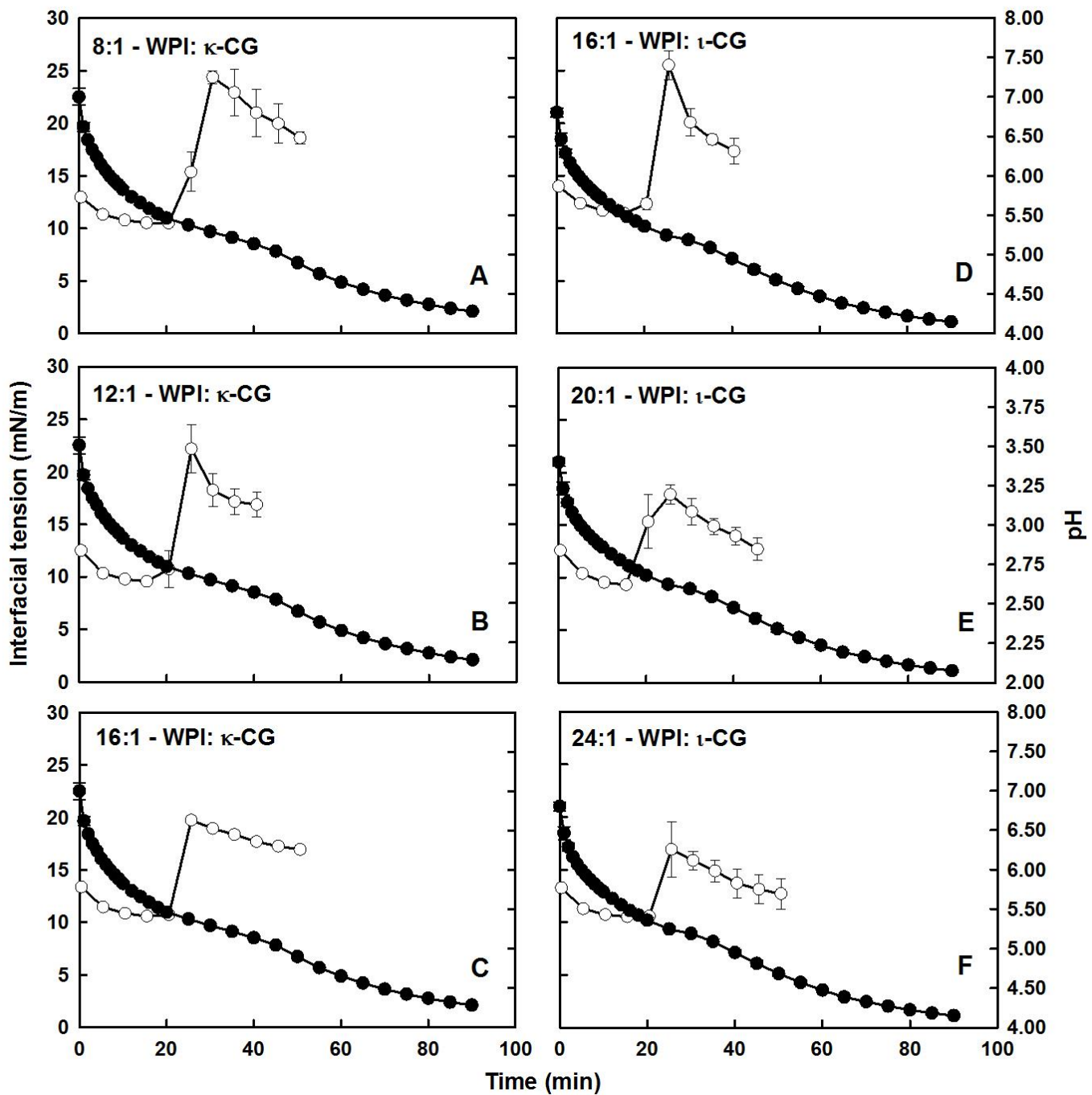


**Figure 7.4** Interfacial properties of WPI:CG mixtures at the canola oil: water interface measured by interfacial tension (open circles) for mixtures of WPI- $\kappa$ -CG (A-C) and WPI- $\iota$ -CG (D-F) at various mixing ratios as a function of pH (closed circles) and time (min). All solutions had a total biopolymer concentration of 1.0% (w/w) and were acidified using 0.5% (w/w) GDL.

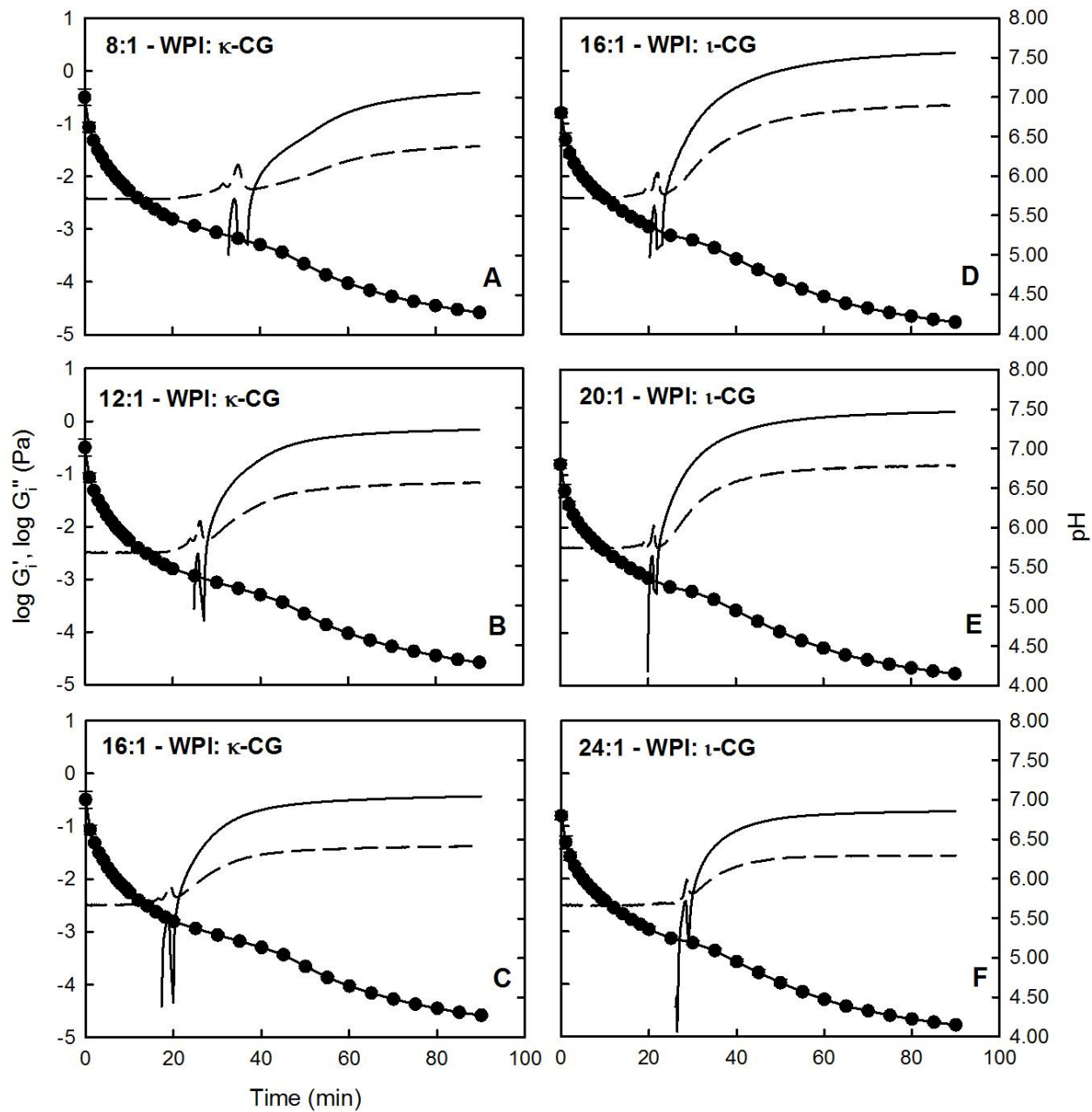


**Figure 7.5** Interfacial rheological properties of WPI:CG mixtures at the canola oil: water interface measured by interfacial storage moduli (solid line) and interfacial loss moduli (dashed line) for mixtures of WPI- $\kappa$ -CG (A-C) and WPI- $\tau$ -CG (D-F) at various mixing ratios as a function of pH (closed circles) and time (min). All solutions had a total biopolymer concentration of 1.0% (w/w) and were acidified using 0.5% (w/w) GDL.

presumed that, free WPI and WPI-CG complexes not involved within the network may still adhere to the interface to form a viscoelastic interfacial film.

The interfacial  $G_i'$  and  $G_i''$  values (Figure 7.5) within the pH range (7.00-5.41) where the two biopolymers were non-interacting (electrostatically) remained relatively constant. Since the interfacial tension decreased during this interval (Figure 7.4), it is possible that only WPI molecules were adhering to the oil-water interface. Near the time/pH corresponding to rise in interfacial tension, small fluctuations or peaks in the  $G_i'$  and  $G_i''$  data were evident for all materials (Figure 7.5). These small peaks were found to be dependent upon the mixing ratio suggesting they might be related to biopolymer interactions and complex formation. In the case of WPI- $\kappa$ -CG mixtures, a small peak was observed in both the  $G_i'$  and  $G_i''$  near pH ~5.22, ~5.33 and ~5.42 for the mixing ratios of 8:1, 12:1 and 16:1, respectively (Figure 5 A-C). Similarly, for WPI- $\iota$ -CG mixtures, a small peak was observed in both the  $G_i'$  and  $G_i''$  within the pH range of ~5.37, ~5.33 and ~5.27 for the mixing ratios of 16:1, 20:1 and 24:1 respectively (Figure 7.5 D-E). As pH is reduced further, a rise in the  $G_i'$  values (*i.e.*, so that they become greater than  $G_i''$ ) occurs, until a plateau is reached corresponding to the formation of a viscoelastic interfacial film (Figure 7.3). For the WPI- $\kappa$ -CG mixtures at pH ~4.2, the magnitude of  $G_i'$  values were found to be 366.5 mPa, 729.6 mPa and 424.2 mPa for the mixing ratios of 16:1, 12:1 and 8:1, respectively (Figure 7.5 A-C). Whereas for the WPI- $\iota$ -CG mixtures at pH ~4.2, the magnitude of  $G_i'$  values were found to be 173.6 mPa, 1358 mPa and 2149 mPa for the mixing ratios of 24:1, 20:1 and 16:1, respectively (Figure 7.5 D-E). Differences in the interfacial rheological properties of these two WPI-CG mixtures are attributed to the nature of their coacervation and their sensitivity towards changes in mixing ratio. While WPI- $\kappa$ -CG mixtures were reported by Stone and Nickerson (2012) to be sensitive towards changes in mixing ratio such that a peak optical density was reached when a 12:1 ratio was used, in contrast, WPI- $\iota$ -CG mixtures were not found to be as sensitive to changes in mixing ratio whereas at the ratio of 20:1 the optical density approached its plateau region. This would account for the viscoelastic maxima at the interface observed for 12:1 WPI- $\kappa$ -CG mixtures and the increasing moduli values observed as a function of CG content in WPI- $\iota$ -CG mixtures.

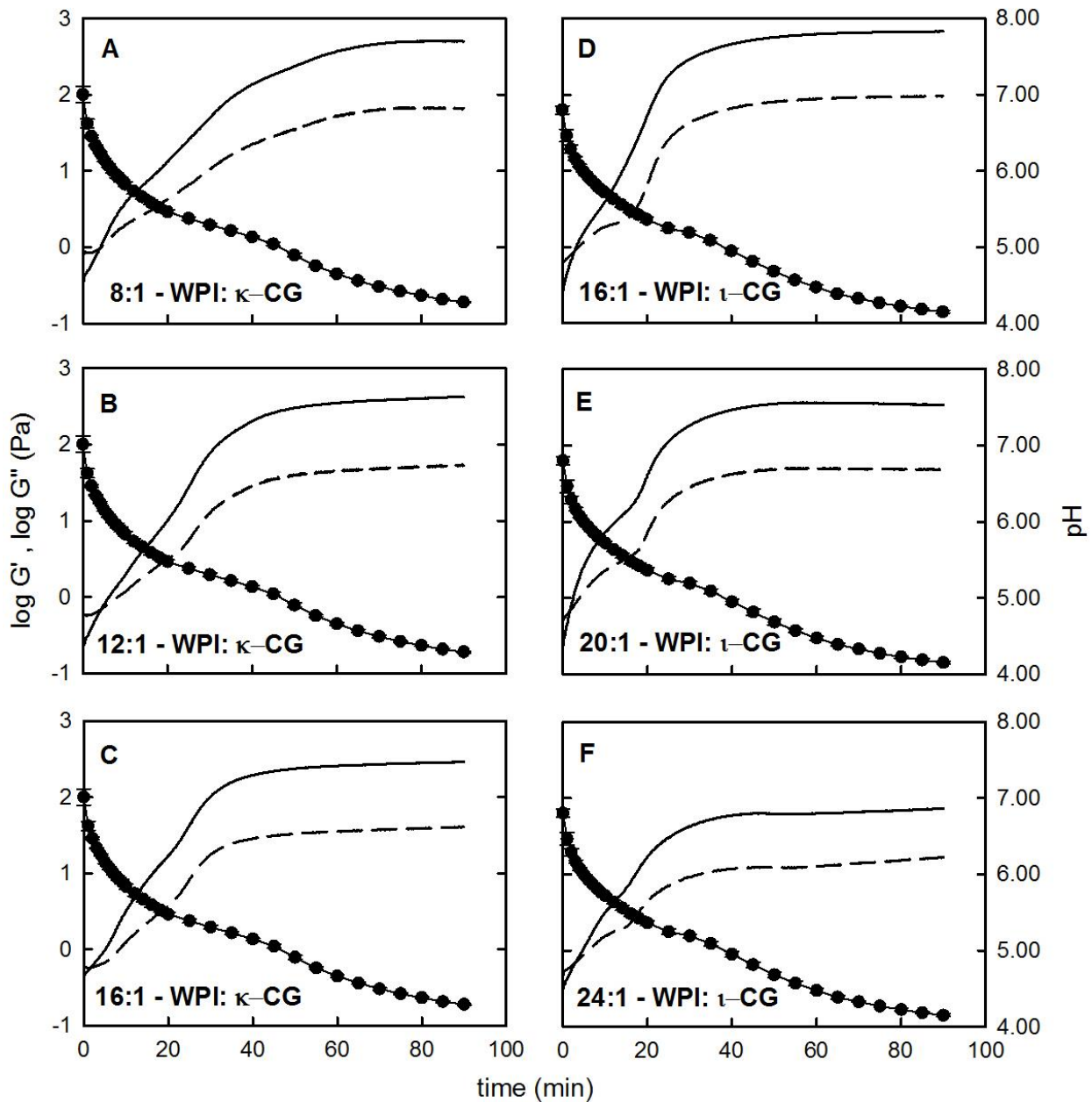


**Figure 7.6** Dynamic viscoelastic storage ( $G'$  (solid line)) and loss ( $G''$  (dashed line)) moduli for 1:1 water: canola oil emulsions stabilized with WPI- $\kappa$ -CG (A-C) and WPI- $\tau$ -CG (D-F) at various mixing ratios as a function of time (min) and pH (closed circles). Each curve is a representative of 3 separate time sweep runs on separate samples. All solutions had a total biopolymer concentration of 1.0% (w/w) and were acidified using 0.5% (w/w) GDL.

### **7.4.3 Formation of electrostatic coupled biopolymer emulsion gels**

The rheological properties of WPI-CG mixtures as a function of CG-type and mixing ratio during a slow acidification from pH 7.00 to ~4.20 using GDL, after being homogenized with canola oil to make an O/W emulsion is given in Figure 7.6. For all materials, electrostatic coupled networks were formed as evident by a constant plateau region where  $G'$  was greater than  $G''$  (Figure 7.6). For both biopolymer mixtures, the magnitude of  $G'$  at pH ~4.2 was found to increase as the mixing ratio decreased corresponding to an increasing CG content indicating an increase in network strength (Figure 7.6). For instance  $G'$  was found to be 257.3 Pa, 435.3 Pa and 522.9 Pa for the 16:1, 12:1 and 8:1 mixing ratios, respectively for the WPI- $\kappa$ -CG mixture (Table 7.1). Similarly,  $G'$  was found to be 70.8 Pa, 320.4 Pa and 658.5 Pa for the 24:1, 20:1 and 16:1 mixing ratios, respectively for the WPI- $\iota$ -CG mixture (Table 7.1). CGs are known for their gelling ability and capacity to form coacervates with WPI where here, CGs are speculated to form bonds among themselves and with WPI. It is presumed that three intermolecular interactions are present in this system: CG-CG, WPI-CG coacervate, and CG-CG. Therefore an increase in CG content leads to better coverage of CG polymers throughout the solvent leading to a greater number of junction zones and a stronger network. Therefore, the primary difference between mixtures containing  $\kappa$ -CG and  $\iota$ -CG is that the latter contains a greater number of sulfated groups allowing for a greater number of bonds lending to its comparatively stronger networks.

After the 90 min time sweep, the frequency and strain dependence of the viscoelastic moduli were measured to characterize these networks (Figure 7.7). For both the WPI- $\kappa$ -CG and WPI- $\iota$ -CG mixtures, moduli was relatively frequency independent with  $G' > G''$  (Figure 7.7 A,B). The slight frequency dependence seen suggests that these networks may be considered as weak gels (Figure 7.7 A,B). In the absence of acidification by GDL, these emulsions were found to be largely frequency dependent (data not shown). This suggests that the coacervation of WPI with CG led to the formation of a continuous gel-like network. Therefore the strain response of these networks was captured to understand the nature of these networks in order to propose how these emulsion networks are structured.

Critical strain at the break was found to be ~26.22%, ~17.77% and ~8.83% for WPI- $\kappa$ -CG with mixing ratios of 8:1, 12:1 and 16:1, respectively, and ~27.35%, ~9.33% and ~2.41% for WPI- $\iota$ -CG with mixing ratios of 16:1, 20:1 and 24:1, respectively (Figure 7.7 C,D). Findings from this

study indicate that as the CG content is higher (*i.e.*, lower mixing ratios) within the sample, a more brittle network is formed. Compared to their biopolymer counterparts, these emulsion networks are much more brittle in nature. These emulsion networks were found to be

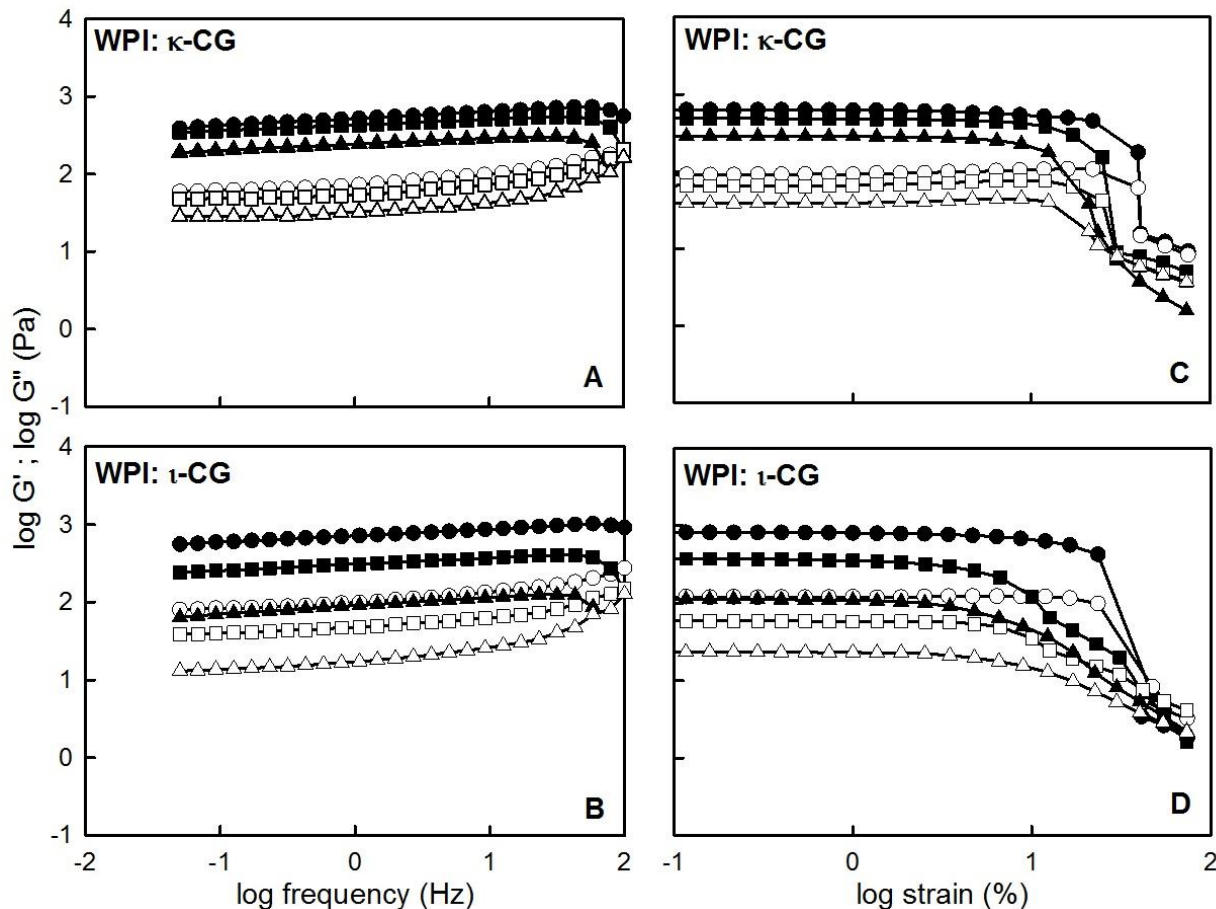


**Figure 7.7** Dynamic viscoelastic storage ( $G'$  (closed symbol)) and loss ( $G''$  (open symbol)) moduli for 1:1 water: canola oil emulsions stabilized with WPI- $\kappa$ -CG (A and C) and WPI- $\iota$ -CG (B and D) at various mixing ratios as a function of frequency (A-B) and strain (C-D). WPI- $\kappa$ -CG (A and C) mixtures were mixed at ratios of 8:1 (circle symbol), 12:1 (square symbol) and 16:1 (triangle symbol) while WPI- $\iota$ -CG (B and D) were mixed at 16:1 (circle symbol), 20:1 (square symbol) and 24:1 (triangle symbol). Each curve is representative of 3 separate sweep runs on separate samples. All solutions had a total biopolymer concentration of 1.0% (w/w) and were measured at a pH of 4.28 and 4.15 for WPI- $\kappa$ -CG and WPI- $\iota$ -CG mixtures respectively.

elastic under low strain stresses and broke down when exposed to higher strains. These networks exhibited strain thinning behavior (Hyun *et al.*, 2011) where structures within the network reorient in the direction of the applied strain. At higher strains, these networks begin to break in the direction of the applied strain and the viscous drag of the system decreases (Hyun *et al.*, 2011). Beyond this point, increasing strains further breaks down the network.

Emulsion-based gels also were found to have higher network strength than the corresponding material in the biopolymer only gels (Figures 7.1 and 7.6; Table 7.1). It is presumed that the greater stiffness of the network is attributed to the incompressibility of droplets and inter-droplet interactions occurring within the continuous phase. The critical strains were found to increase with increasing CG-content similar to the biopolymer only networks, however the strain needed for the emulsion based gels to induce breakage was much less than the biopolymer gel counterparts suggesting that they were more brittle in nature. These networks are more brittle in nature in part due to the presence of WPI-CG coacervates at the water-oil interface. Interfacial properties for WPI-CG coacervates reveal their ability to form a viscoelastic film at the water-oil interface. At interface, the rheological properties are sensitive to mixing ratio due to the limited space at the surface for bond formation whereas in a continuous network, network strength is enhanced depending on the availability and opportunity to form bonds which create junction zones that gives the network strength.

In a study by Santipanichwong and Suphantharika (2009),  $\beta$ -glucans were found to enhance the stability of egg yolk emulsions. They were speculated to enhance emulsion stability by either increasing the viscosity of the continuous phase or creation of a 3-dimensional network of flocculated droplets (Santipanichwong & Suphantharika, 2009). Similar to results reported here, frequency sweeps revealed that Santipanichwong and Suphantharika (2009) formed weak gels as well and that the addition of  $\beta$ -glucans to egg yolk emulsions had improved their creaming stability. Furthermore, an addition of the polysaccharides to the emulsions had increased the storage modulus (*i.e.* stiffness) of the networks formed (Santipanichwong & Suphantharika, 2009). Kontogiorgos and co-workers (2004) who also studied the influence of  $\beta$ -glucans on egg-yolk stabilized emulsions reported that the mechanism for stability depended on the molecular weight of the polysaccharide. Polysaccharides containing lower molecular weights

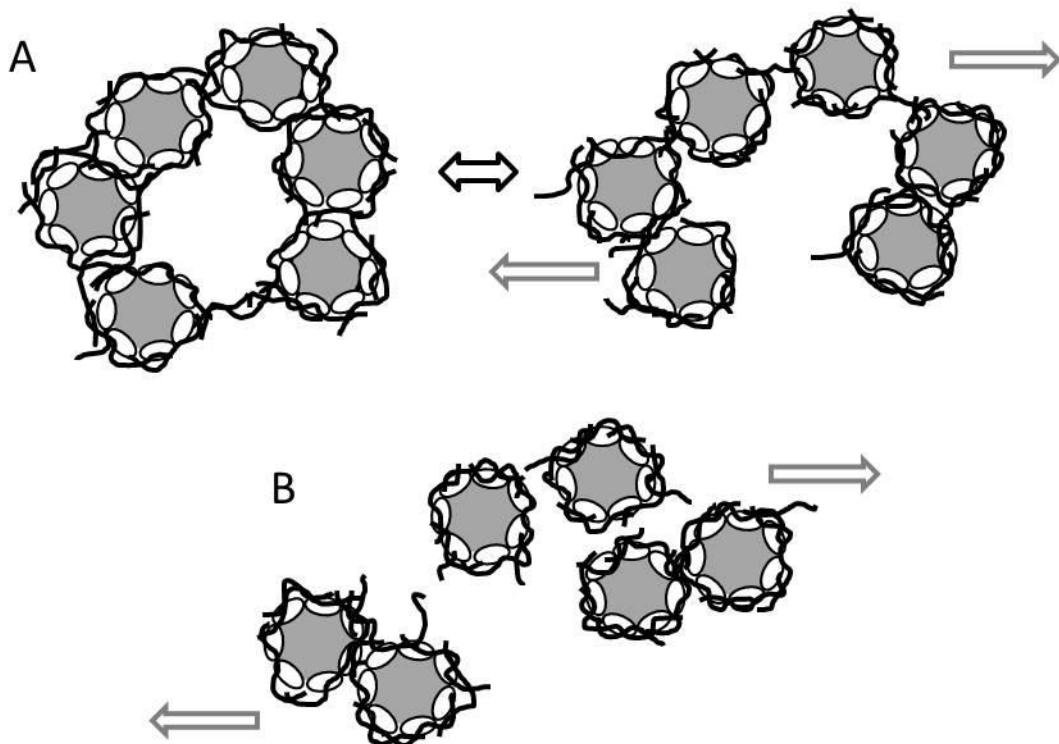
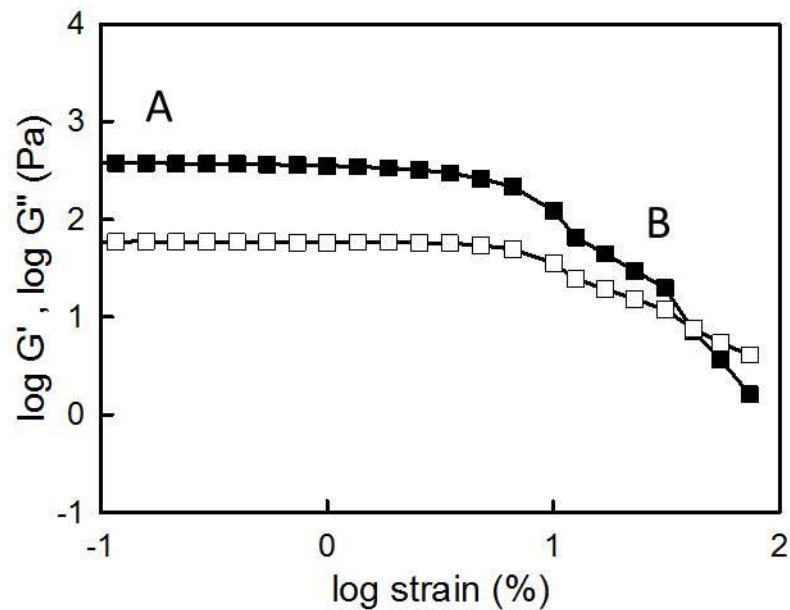


**Figure 7.8** A schematic of a sample WPI-t-CG emulsion gel at the biopolymer ratio of 20:1 and an aqueous: oil ratio of 1:1 in response to strain (graph:  $G'$  (closed symbols) and  $G''$  (open symbols)) where the gelled network comprised of WPI (open oval) complexed with CG (lines) stabilizing oil droplets (grey circles) are elastic at low strains (A) and their breakdown at higher strains (B). The grey arrows indicate the direction of the applied shear.

tended to form a network in the continuous phase while higher molecular weight polysaccharides increased the viscosity of the continuous phase (Kontogiorgos *et al.*, 2004). Therefore, enhanced emulsion stability in systems containing multiple biopolymers is reliant on the interactions between the biopolymers involved.

It is speculated that as WPI adheres to the water-oil interface, GDL acidification leads to a coacervate to form at the interface whereby the CG on the outside could bind and cause flocculation with other WPI or CG molecules bound to other droplets. This allows for a continuous network of droplets to form which becomes the primary means for structuring these emulsion networks. Their brittleness may be attributed to the limited surface interactions between flocculated droplets. This reduces the number of available bonds between the biopolymers which are needed to stabilize the network. A schematic of these emulsion systems are presented in Figure 7.8 which represents the breakdown of these emulsion networks under strain. It is speculated that any biopolymers not bound to the water-oil interface becomes available for interacting in the continuous phase which provides additional strength to the network.

## 7.5 Conclusions

In conclusion, WPI-CG mixtures were found to complex to form an electrostatic coupled continuous network during a slow acidification process using GDL. Networks formed with WPI- $\iota$ -CG complexes were found to be stronger than those with WPI- $\kappa$ -CG. Though a similar mechanism is proposed for network formation, the difference is attributed to the number of sulfated bonds whereby  $\iota$ -CG may form a greater number of bonds compared to  $\kappa$ -CG. Frequency sweeps determined that the networks formed were relatively frequency independent and gel-like. An increase in the CG content led to increased stiffness of these gels. Strain sweeps revealed that gels became increasingly elastic with rising CG levels within the mixing ratio. WPI-CG complexes were found to be surface active and capable of forming viscoelastic films at the water-oil interface. Furthermore, as WPI-CG formed electrostatic complexes, they had a profound impact on the interface which was observed both by interfacial tension and interfacial rheology. Due to the surface active properties of the WPI-CG complexes, they were used to stabilize the formed emulsions during gelation. Emulsion gels made with WPI-CG complexes were stiffer compared to their biopolymer counterparts but were comparatively much more brittle. The comparative

difference in brittleness is attributed to the differences in the structure of these two networks. It is speculated that the large conformational entropy associated with CGs enabled their capacity to form a 3-dimensionsal network as a biopolymer solution. Overall, the surface activity of WPI and their coacervation with CGs enabled a WPI-stabilized, flocculated emulsion inter-linked by CGs to form.

## **8. GENERAL DISCUSSION**

The overall goal of this thesis was to enhance the stability of whey protein based emulsions through physicochemical modification (*e.g.*, temperature and pH) and controlled protein-polysaccharide interactions. To achieve this goal, two approaches were taken: 1) by investigating the effect of pH and temperature pre-treatments on the physicochemical and emulsifying properties of whey protein isolate (WPI) and its main proteins,  $\beta$ -lactoglobulin ( $\beta$ -LG) and  $\alpha$ -lactalbumin (ALA); and 2) by investigating the effect of complexation of WPI with carrageenan (CG), *via* electrostatic attractive forces. In the first approach, the structure of WPI and its main components were modified by pH in combination with temperature pre-treatments and their physicochemical and emulsifying properties were examined. This determined whether the emulsifying properties of WPI were dominated by either one of its main proteins. The study of their physicochemical properties helped give insight to their changes in relation to changes to the emulsifying properties of proteins. In the second approach, the complexation of CG to WPI was used to enhance the viscoelastic film at the interface to improve emulsion stability. Complexes formed *via* electrostatic attraction between positively charged WPI and negatively charged CG. WPI-CG complexes formed a viscoelastic film around oil droplet surfaces which provided enhanced emulsion stability.

### **8.1 Comparisons of the physicochemical and emulsifying properties of WPI, $\beta$ -LG and ALA**

For WPI,  $\beta$ -LG and ALA, changes in pH greatly affected their physicochemical and emulsifying properties. Overall, emulsion stability was found to be greatest at pH 7.0 which was away from the isoelectric point of these proteins. Emulsion stability is enhanced by the electrostatic repulsive force which acts to keep protein-coated droplets from flocculating. With respect to temperature pre-treatments, samples left at room temperature (*i.e.* 25°C) at pH 7.0 were more stable than those subjected to other pH and temperature pre-treatment combinations.

Although heat pre-treatments did have an effect on the structure of these proteins, changes in their structure due to heating did not translate into greater emulsion stability. Among the three proteins, WPI and  $\beta$ -LG exhibited similar physicochemical and emulsifying properties. Similarities were attributed to the high  $\beta$ -LG content found in the WPI [~75% of total whey proteins was  $\beta$ -LG (Weinbreck *et al.*, 2004b)]. The effect of pH and temperature pre-treatments influenced the physicochemical properties of the proteins differently. For instance, surface charge and interfacial tension of the proteins were primarily affected by pH only, whereas surface hydrophobicity and aggregate size were influenced by both pH and temperature. With respect to their emulsifying properties, pH dependent trends were observed for all three proteins, whereas no correlating trends were observed for the effect of pH and temperature pre-treatments on emulsion stability.

## **8.2 Comparison of pH-dependent physicochemical properties such as the surface charge and interfacial tension of WPI, $\beta$ -LG and ALA**

Physicochemical properties such as surface charge and interfacial tension were predominantly influenced by changes in pH. Temperature pre-treatments were thought to cause unfolding of these proteins to expose hidden amino acid residues which would cause changes in their surface charge and possibly lower their interfacial tension by allowing better adherence of these proteins to the interface. Unfortunately, changes in structure due to temperature pre-treatments did not cause changes in the surface charge and interfacial tension of these proteins. For all three proteins, surface charge decreased as a function of pH. Furthermore, WPI and  $\beta$ -LG passed through their respective isoelectric point at different pHs. The isoelectric point of WPI (pH = ~5.2) was found to be much higher than that of  $\beta$ -LG (pH = ~3.9). Differences in isoelectric point were attributed to the presence of other proteins (*e.g.* ALA) in WPI which was not found with  $\beta$ -LG samples. With respect to ALA, an ANOVA determined that, like WPI and  $\beta$ -LG, surface charge changed significantly with pH but not temperature pre-treatments. As the pH increases away from the isoelectric point of ALA [ $pI = 4.2$  (Bramaud *et al.*, 1995; Wu *et al.*, 1996; Wang & Lucey, 2003)] the surface charge of ALA becomes more negative. Unfortunately, the data collected for ALA cannot be directly compared to that collected for WPI and  $\beta$ -LG primarily due to differences in the temperatures selected for pre-treatment which were chosen to reflect a different denaturation temperature (as reported in literature) for ALA than the other two proteins. Changes to the surface charge of a protein may affect its ability to adhere to the water-oil interface.

The onset of larger interfacial tensions may be caused by the inability of proteins to adhere to the interface, due to their conformation and or electrostatic repulsive forces.

Interfacial tension changed as a function of pH, in that WPI first decreased in interfacial tension from pH 3.0 to 5.0 and then increased when pH was raised from pH 5.0 to 7.0. In contrast,  $\beta$ -LG increased in interfacial tension when pH changed from 3.0 to 5.0 and decreased when the pH was raised from 5.0 to 7.0. These different trends in interfacial tension as a function of pH are thought to be attributable to the presence of proteins other than  $\beta$ -LG in WPI [*i.e.* ALA, serum albumins, protease peptones and immunoglobulins (Walstra & Jennes, 1984)]. Proteins other than  $\beta$ -LG may better adhere to the interface at pH 5.0, displacing  $\beta$ -LG at the interface. Competitive adsorption between proteins has been reported previously with respect to the preferential adsorption of proteins (Zhang *et al.*, 2004), in that one protein may displace another at the interface (Damodaran & Rammovsky, 2003) and that proteins may require binary or ternary electrostatic complexes with other proteins to facilitate their adsorption to the interface (Damodaran *et al.*, 1998).

Unlike WPI and  $\beta$ -LG, ALA interfacial tension was found to change significantly as a function of both pH and temperature pre-treatments. Although changes in interfacial tension were observed between different temperature pre-treatments, the greatest change was due to changes in pH (*i.e.*  $\sim 12.39$  to  $\sim 15.07$  mN/m for ALA from pH 5.0 to 7.0). Changes to the interfacial properties of ALA were also found to depend on whether or not these proteins were depleted of calcium. In its absence, the interfacial properties of ALA-3 changed little when exposed to higher temperatures, yet for ALA-1, a steady decrease in interfacial tension was observed when proteins were exposed to higher pre-treatment temperatures. At 95°C, the interfacial tension for ALA-1 and ALA-3 converged for their respective pHs (Figure 5.5). This convergence in their interfacial properties at 95°C suggests that as ALA-1 unravels due to increasingly higher pre-treatment temperatures, their ability to adsorb to the interface is enhanced which leads to a decrease in interfacial tension. For ALA-3, the absence of calcium allows ALA to obtain an open conformation such that temperature pre-treatments do not significantly alter its conformation and ability to adhere to the interface. At 95°C, ALA-1 is unravelled and is presumed to obtain protein conformations similar to ALA-3 which would explain their convergence. This data suggest that the presence of calcium effectively dictates both ALA structure and interfacial functionality. Changes in structural conformation have been reported previously to affect protein alignment at

interfaces. A study on ovalbumin reported changes in conformation when adsorbed onto the interface which restricts their mobility and ability to interact with neighboring protein molecules (Kudryashova *et al.*, 2003). Furthermore, protein aggregation was also reported previously to restrict reorientation of proteins at the interface in bovine serum albumins located at the air-water interface (Wang *et al.*, 2003).

### **8.3 Comparison of pH and temperature dependent changes to the surface hydrophobicity and aggregate size of WPI, $\beta$ -LG and ALA**

For WPI,  $\beta$ -LG and ALA, surface hydrophobicity and aggregate size changed significantly as a function of pH and temperature pre-treatments. WPI and  $\beta$ -LG both decreased in surface hydrophobicity when treated at 25 and 55°C as a function of increasing pH, whereas proteins treated at 85°C increased in surface hydrophobicity from pH 3.0 to 5.0 and decreased when the pH increased from 5.0 to 7.0. This trend observed for WPI was attributed to the surface hydrophobicity of  $\beta$ -LG, since there was relatively little change in the surface hydrophobicity of ALA observed with increasing thermal treatments. Furthermore, ALA increased in surface hydrophobicity when the pH was raised from 5.0 to 7.0, which was opposite to trends observed for  $\beta$ -LG and WPI. It is possible that this increase in ALA surface hydrophobicity reduced the decrease observed in WPI when the pH was raised from 5.0 to 7.0. The similar trends observed between WPI and  $\beta$ -LG are thought to be attributable to the high content of  $\beta$ -LG in the WPI and the smaller changes in surface hydrophobicity observed in ALA.

The size of the aggregates formed depended on the type of protein, whether the pH was near or far from the isoelectric point, and its pre-treatment temperature. WPI and its main protein components did not change significantly as a function of temperature at pHs away from their isoelectric points (*i.e.* pH 3.0 for WPI and  $\beta$ -LG; and pH 7.0 for WPI,  $\beta$ -LG and ALA). This effect is attributed to the high electrostatic repulsive forces which reduced aggregation. For instance, although surface hydrophobicity was found to be the greatest for all temperature pre-treatments for ALA-3 at pH 7.0, this did not translate into the formation of large aggregates due to their electrostatic repulsive forces. Instead, at near neutral surface charge conditions (*i.e.* pH 5.0),  $\beta$ -LG and ALA were found to increase in aggregate size as a function of temperature pre-treatment, whereas WPI decreased in its aggregate size as a function of temperature pre-treatment. At near neutrally charged conditions, there was a reduction in electrostatic repulsive forces which

enhanced their ability to aggregate. Therefore, it was predicted that protein aggregates would increase in size as a function of temperature pre-treatment at near neutrally charged conditions. Although this proved to be true for  $\beta$ -LG, this was not the case for ALA and WPI. For the purpose of this discussion, it is assumed that the ALA found in WPI would be similar to the calcium-present ALA-1, as the manufacturer of the WPI indicated the presence of calcium in its composition. ALA-1 changed very little in its surface hydrophobicity and aggregate size as a function of temperature pre-treatment. This result was not anticipated, which might suggest that aggregate formation in ALA-1 is limited by the number of locations on a protein surface where aggregation may occur. An alternate explanation relies on the re-folding capability of ALA proteins upon denaturation, and therefore there would appear to have little to no differences between temperature pre-treatments for aggregate formation in ALA-1. Although  $\beta$ -LG increased its aggregate size as a function of temperature pre-treatments at pH 5.0, the complex formed between  $\beta$ -LG and ALA-1 may have prohibited large aggregates to form leading to a reduction in aggregate size as a function of temperature pre-treatment as observed for WPI at pH 5.0.

#### **8.4 The effect of protein conformation on the functionality of WPI, $\beta$ -LG and ALA**

Thus far, it was predicted that changes in structure would greatly affect the physicochemical and emulsifying properties of WPI,  $\beta$ -LG and ALA. It was thought that pH and temperature pre-treatments would modify the proteins allowing for better adherence to the oil-droplet surface which would enhance emulsion stability. Therefore, changes in the secondary structure of WPI and ALA were observed by circular dichroism (CD). Relative changes to structure were determined using CD, where a flattening of the mean residue molar ellipticity suggested a loss in overall structure. CD measures the secondary structures found in proteins such as random coils,  $\alpha$ -helices and  $\beta$ -sheets. Although CD may be used to quantify the types of secondary structure present in proteins, this was not possible with WPI due to the multiple proteins it is comprised of. Overall, the mean residue molar ellipticity was greater in WPI samples compared to ALA suggesting it had more ordered structure. WPI also was found to be much more sensitive to changes in structure due to pH and the application of thermal treatments, which was attributed to the various proteins found in WPI. WPI structure was found to change minimally at pH 3.0 and most at pH 5.0 for all temperature pre-treatments. Conversely, changes to ALA structure were found to be dependent on the presence of calcium. In calcium-depleted ALA-3, its

structure was similar at temperature pre-treatments of 25 and 95°C and different when pre-treated at 65°C. Unfortunately, no obvious similarities in the trends observed under CD could be used to explain specific physicochemical properties which suggest that changes in structure may only be part of the explanation for stability in whey-based emulsions.

## **8.5 Comparison of changes in the emulsifying properties of WPI, $\beta$ -LG and ALA**

The emulsifying properties of WPI,  $\beta$ -LG and ALA were characterized based on how well they coated oil droplets [*i.e.* emulsion activity index (EAI)] and an emulsion stability index (ESI). Similarities in the EAIs of WPI and  $\beta$ -LG were attributed to the predominance of  $\beta$ -LG in WPI, as both decreased and then increased in EAI when the pH changed from 3.0 to 5.0 and 5.0 to 7.0, respectively. ALA increased in EAI similarly to WPI and  $\beta$ -LG when the pH was raised from 5.0 to 7.0, and changed slightly in EAI as a function of temperature pre-treatment. This increase in EAI contradicts the need for proteins to be neutrally charged (*i.e.* pH 5.0) in order to be more effective at coating an oil droplet surface. Instead, at higher surface charges, electrostatic repulsive forces across the surface of a protein might aid in maintaining an open structure, allowing for the protein to cover a greater surface area on an oil droplet. This is supported by the increase in EAI observed when the pH was raised from 5.0 to 7.0.

Although no trends were observed in the ESIs of WPI,  $\beta$ -LG and ALA, maximal emulsion stability occurred when proteins were left at room temperature (*i.e.* 25°C) and at pH 7.0 for all proteins investigated. Specifically,  $\beta$ -LG at pH 7.0 at 25°C experienced the greatest emulsion stability of the three proteins. Although it was predicted that better adsorption onto oil droplet surfaces would enhance emulsion stability, this was not observed in the present results. Demetriades and co-workers (1997) reported while studying the effects of pH on emulsion stability that stability decreased near the isoelectric point of whey proteins and increased at pHs away from it. They observed that instability occurred when droplets flocculated due to creaming (Demetriades *et al.*, 1997). Stability may be attributed to electrostatic repulsion from proteins adsorbed to the interface or steric repulsion of multi-layered (*i.e.* physically separated droplets) and mono-layered (*i.e.* repulsive forces induced by the close proximity of two proteins) adsorption (Tcholakova *et al.*, 2006b). Due to the low concentration of protein used in the present results (*i.e.* 0.1% w/w), it was presumed that stability may be attributed to electrostatically repulsive forces. This implies that

should these emulsions require a pH near the isoelectric point of whey, stability could only be achieved at higher protein concentrations.

## **8.6 The effect of carrageenan addition on WPI-stabilized emulsions**

The addition of carrageenan (CG) enhanced the stability of WPI-based emulsions. WPI-CG emulsions were found to be much more stable compared to emulsions made with WPI alone. WPI-based emulsions rapidly destabilized (*i.e.* within an hour) whereas WPI-CG emulsions were much more stable (*i.e.* greater than a day) under the biopolymer, solvent and emulsification conditions used in this study. The enhanced stability of these emulsions was attributed to the WPI-CG complexes that formed by the slow acidification of these biopolymer mixtures using glucono- $\delta$ -lactone (GDL). Emulsions made with WPI-CG mixtures were found to hold more oil compared to WPI-based emulsions (50% w/w and 28% w/w, respectively) which was presumed to be the effect of increasing the concentration of biopolymers in the aqueous phase (0.1% w/w to 1.0% w/w in WPI-emulsions and WPI-CG emulsions, respectively). When  $\kappa$ - and  $\iota$ -CGs were used, WPI-CG emulsions became self-standing gels. Even without oil, these WPI-CG mixtures were found to form self-standing gels. Therefore, the rheological properties of these WPI-CG mixtures were investigated to characterize the physical properties and formation of these networks.

## **8.7 The effect of carrageenan-type and mixing ratio on the rheological properties of WPI-CG coupled networks and emulsion gels**

The electrostatic attraction of CG to WPI was originally thought to increase the viscosity of the aqueous layer and enhance the viscoelastic properties of the interfacial layer at the oil-water interface. Yet WPI-CG interactions were found to lead to stronger gel networks when  $\kappa$ - and  $\iota$ -CG were present, whereas a weak fluid gel was formed when  $\lambda$ -CG was used. This was attributed to the known gel-forming properties of  $\kappa$ - and  $\iota$ -CG which have been widely studied (Ridout *et al.*, 1996; Maingonnat *et al.*, 2008; Azizi & Farahnaky, 2013). WPI- $\lambda$ -CG mixtures yielded a weak-gel structure when studied under rheology. In the absence of CG, no gel network was formed even though whey proteins are known to form gels at higher protein concentrations when thermally treated and under acidified conditions (van Vliet *et al.*, 2004; Foegeding, 2006). This indicates that the concentration of WPI was well below the requirement for gelation, and any subsequent structure detected was attributed to the formation of complexes with CG. The formation of WPI-

CG complexes *via* a coacervation process was previously investigated by Stone and Nickerson (2012) who reported on the optimal ratio for complexation. The formation of WPI- $\kappa$ -CG gels was reported previously on by Harrington and co-workers (2009), where gelation occurred at pH 7.0 at a protein concentration of 10.0% (w/w) and where gelation was induced by supplying calcium ions. In this study, gels were formed at much lower concentrations than those reported by Harrington and co-workers (2009) *via* a coacervation process. When CG content deviated from its optimal ratio, gels with higher CG content were found to be stiffer. Furthermore, the nature of these gels appeared to depend on the gelling properties of CG such that self-standing gels formed with CG-types known to form gels. Increases in gel stiffness as a function of CG content were also observed when gelled emulsions were formed. This led to the investigation of the effect of WPI-CG coacervation at the water-oil interface. Surprisingly, the strength of the viscoelastic film did not increase as a function of CG content, but the strongest viscoelastic films were found at the optimal mixing ratio. This different trend observed warrants future studies into the nature of WPI-CG interactions at the water-oil interface.

## 8.8 Summary

In summary, whey proteins can act as effective emulsifiers to stabilize oil-in-water emulsions properties that can be enhanced depending on the solvent or pre-treatment conditions experienced by the proteins. Whey proteins offer tremendous potential for the food, pharmaceutical/supplement and dairy industries because of their functional and nutritional value. Besides emulsification, whey proteins can be used as thickeners, gelling or foaming agents, and have enhanced solubility over a range of pHs. Whey proteins are highly nutritive, contain all essential amino acids and have been linked to several health benefits (Walzem *et al.*, 2002). Whey proteins are well known for their ability to promote muscle growth and tissue repair (Paul, 2009), help reduce milk protein intolerances when in a hydrolysate form (Exl, 2001), and have been investigated for their role in boosting the immune system (Barth & Behnke, 1997). As a result, whey protein ingredients are often used in infant formulas, nutritional supplements or meal replacement products. Whey proteins are now being used for higher valued applications such as edible films (Banerjee & Chen, 1995) and encapsulation/controlled delivery (Livney *et al.*, 2003). Dairy producers and associated agri-food processing sectors stand to benefit from increased market diversification of whey protein-based products, as product demand increases.

## **8.9 Future directions**

Emulsions play a significant role in many food and non-food applications. Over the last decade there has been growing interest in the use of proteins as emulsifiers in nano-emulsion applications where droplet sizes are <100 nm diameter (Shakeel *et al.*, 2012). Understanding the relationship between WPI structure, solvent conditions and its ability to form nano-scale droplets will be an essential component in its development and for ensuring long term stability. Changes in protein conformation and relative flexibility may dictate how proteins adhere to a small droplet size. It is predicted that proteins with greater flexibility and less structure, especially at the tertiary level, will allow for better adherence to oil droplets in the nanoscale region. The effectiveness of electrostatic repulsive forces to keep emulsions stable also may be investigated to determine the limits of stability whether by droplet size or volume in the continuous phase.

This current body of work also raises questions regarding the nature of coacervation, especially between WPI and CG. One main question which may be further investigated is the difference between soluble and insoluble complexes that form during acidification. Techniques such as nuclear magnetic resonance may reveal how solvent is bound to and within the complexes. As WPI-CG complexes are known to form gels, this affords opportunities to investigate them as dried-out gels (*i.e.* xerogels) so that changes in protein conformation and WPI-CG coacervation may be studied using techniques such as Fourier transform infrared-photoacoustic spectroscopy. The structure of these gels also may be visualized *via* SEM and TEM in order to determine structural differences depending on CG-type. Techniques such as confocal microscopy might provide a three-dimensional view of the network, potentially enabling differentiation of the various components of the system. Coacervate-based micro-beads could potentially be formed should the aqueous solution be dispersed as droplets in oil, providing opportunities to investigate their potential to encapsulate or be employed as bioactive or pharmaceutical delivery agents.

## 9. GENERAL CONCLUSION

The overall goal of this thesis was to enhance the emulsifying properties of whey proteins through solvent modification and controlled protein-polysaccharide interactions. Solvent modification was achieved by changes in pH and the application of temperature pre-treatments which results in changes to the physicochemical and emulsifying properties of whey protein isolate (WPI) and its main proteins:  $\beta$ -lactoglobulin ( $\beta$ -LG) and  $\alpha$ -lactalbumin (ALA). Protein-polysaccharide interactions were controlled by slow acidification where electrostatic complexes formed *via* a coacervation process.

The physicochemical and emulsifying properties of WPI and its two major proteins: ALA and  $\beta$ -LG, may be tailored by changing the pH and applying temperature pre-treatments. For instance, calcium depleted ALA-3 samples were found to possess an open conformation which increased their surface hydrophobicity, formed larger aggregates, improved their ability to lower interfacial tension, increased oil droplet surface coverage and enhanced emulsion stability. Heating of the proteins exposes their hydrophobic moieties which causes aggregation and better adherence to the interface. WPI and  $\beta$ -LG were found to be most hydrophobic at a pH of 5.0 with an 85°C pre-treatment. Under neutrally charged, thermally treated conditions, these proteins unfold revealing their hydrophobic moieties which lead to the formation of larger aggregates. Although neutrally charged proteins aid in interfacial adsorption, they did not promote better coverage onto the droplet surface due to their propensity for aggregation as indicated by their EAI. Emulsions formed at pHs away from the isoelectric point were found to be more stable (*i.e.* at pH 7.0). At pHs away from their isoelectric point, proteins formed smaller aggregates which allowed for better adsorption to the water-oil interface which was observed by their EAI. Emulsion stability was also found when proteins were away from their isoelectric point at pH 7.0. Unfortunately, thermal treatments reduced emulsion stability where the greatest stability for all proteins was obtained at pH 7.0 at room temperature (*i.e.* 25°C). Due to the low concentration of protein (0.1% w/w) and the conditions at which the most stable emulsions formed, emulsion stability was attributed to electrostatic repulsion.

When carrageenan (CG) was added to WPI mixtures, complexation occurred *via* electrostatic attraction upon acidifying the solvent. Turbidimetric techniques, tensiometry and interfacial rheology were used to profile their complexation, whereas small deformation rheology was found to effectively capture their gelling profile. For all WPI-CG mixtures, a gel network was formed. The complexation occurring in WPI-CG mixtures led to the formation of stiff gels with  $\kappa$ -CG and  $\iota$ -CG present, and a weak fluid gel in the presence of  $\lambda$ -CG. The ability to form stronger gels was related to the gelling potential of CG (*i.e.*  $\kappa$ -CG and  $\iota$ -CG are known to form polysaccharide gels, whereas  $\lambda$ -CG is used as a thickener because of its non-gelling properties). Furthermore, when the ratio of WPI-CG was altered, gel stiffness was found to increase with CG content. These WPI-CG mixtures were also found to be capable of forming gels when an oil phase was dispersed throughout the aqueous gel. This warranted an investigation of the interfacial properties of these gels. WPI-CG complexation was found to cause changes in the interfacial properties such as interfacial tension and interfacial rheology. Interfacial tension decreased for WPI- $\lambda$ -CG samples where only a weak fluid gel network was formed. When WPI- $\kappa$ -CG and WPI- $\iota$ -CG were investigated, large changes in the interfacial tension data was observed correlating to structure forming events in the coacervation process. Similar changes also were observed using interfacial rheology for WPI- $\kappa$ -CG and WPI- $\iota$ -CG mixtures. Furthermore, interfacial rheology indicated the development of viscoelasticity about the water-oil interface indicating the formation of a viscoelastic film.

## 10. REFERENCES

- Abduragimov, A. R., Gasymov, O. K., Ysifov, T. N., & Glasgow, B. J. (2000). Functional cavity dimensions of tear lipocalin. *Current Eye Research*, 21, 824-832.
- Agboola, S. O. & Dalgleish, D. G. (1996). Enzymatic hydrolysis of milk proteins used for emulsion formation. 1. Kinetics of protein breakdown and storage stability of emulsions. *Journal of Agricultural and Food Chemistry*, 44, 3631-3636.
- Agyare, K. K., Addo, K., & Xiong, Y. L. L. (2009). Emulsifying and foaming properties of transglutaminase-treated wheat gluten hydrolysate as influenced by pH, temperature and salt. *Food Hydrocolloids*, 23, 72-81.
- van Aken, G. A. (2003). Competitive adsorption of protein and surfactants in highly concentrated emulsions: effect on coalescence mechanisms. *Colloids and Surfaces A: Physicochemical and Engineering Aspects*, 213, 203-219.
- van Aken, G. A., Blijdenstein, T. B. J., & Hotrum, N. E. (2003). Colloidal destabilisation mechanisms in protein-stabilised emulsions. *Current Opinion in Colloid and Interface Science*, 8, 371-379.
- van Aken, G. A., Bomhof, E., Zoet, F. D., Verbeek, M., & Oosterveld, A. (2011). Differences in *in vitro* gastric behavior between homogenized milk and emulsions stabilised by Tween 80, whey protein, or whey protein and caseinate. *Food Hydrocolloids*, 25, 781-788.
- Alizadeh-Pasdar, N. & Li-Chan, E. C. Y. (2000). Comparison of protein surface hydrophobicity measured at various pH values using three different fluorescent probes. *Journal of Agricultural and Food Chemistry*, 48, 328-334.
- Alizadeh-Pasdar, N., Nakai, S., & Li-Chan, E. C. Y. (2002). Principal component similarity analysis of Raman spectra to study the effects of pH, heating, and kappa-carrageenan on whey protein structure. *Journal of Agricultural and Food Chemistry*, 50, 6042-6052.
- Altinga, A. C., Hamer, R. J., de Kruif, C. G., & Visschers, R. W. (2000). Formation of disulfide bonds in acid-induced gels of preheated whey protein isolate. *Journal of Agricultural and Food Chemistry*, 48, 5001-5007.
- Aluko, R. E. & McIntosh, T. (2001). Polypeptide profile and functional properties of defatted meals and protein isolates of canola seeds. *Journal of the Science of Food and Agriculture*, 81, 391-396.

- Aluko, R. E., Mofolassayo, O. A., & Watts, B. A. (2009). Emulsifying and foaming properties of commercial yellow pea (*Pisum sativum L.*) seed flours. *Journal of Agricultural and Food Chemistry*, 57, 9793-9800.
- AOAC. (2003). *Official method of analysis (17th ed.)*. Washington, DC: Association of Official Analytical Chemists.
- Arai, M. & Kuwajima, K. (1996). Rapid formation of a molten globule intermediate in refolding of  $\alpha$ -lactalbumin. *Folding & Design*, 1, 275-287.
- Atri, M. S., Saboury, A. A., Yousefi, R., Dalgalarondo, M., Chobert, J. M., Haertle, T., & Moosavi-Movahedi, A. A. (2010). Comparative study on heat stability of camel and bovine apo and holo alpha-lactalbumin. *Journal of Dairy Research*, 77, 43-49.
- Augustin, M. A. & Hemar, Y. (2009). Nano- and micro-structured assemblies for encapsulation of food ingredients. *Chemical Society Reviews*, 38, 902-912.
- Azevedo, G., Bernardo, G., & Hilliou, L. (2014). NaCl and KCl phase diagrams of kappa/ iota-hybrid carrageenans extracted from *Mastocarpus stellatus*. *Food Hydrocolloids*, 37, 116-123.
- Azizi, R. & Farahnaky, A. (2013). Ultrasound assisted cold gelation of kappa carrageenan dispersions. *Carbohydrate Polymers*, 95, 522-529.
- Baier, S. K. & McClements, D. J. (2005). Influence of cosolvent systems on the gelation mechanism of globular proteins: Thermodynamic, kinetic, and structural aspects of globular protein gelation. *Comprehensive Reviews in Food Science and Food Safety*, 4, 43-54.
- Banerjee, R. & Chen, H. (1995). Functional-properties of edible films using whey-protein concentrate. *Journal of Dairy Science*, 78, 1673-1683.
- Basheva, E. S., Gurkov, T. D., Christov, N. C., & Campbell, B. (2006). Interactions in oil/water/oil films stabilized by beta-lactoglobulin; role of the surface charge. *Colloids and Surfaces A – Physicochemical and Engineering Aspects*, 282, 99-108.
- Bauer, R., Hansen S. & Øgendal, L. (1998). Detection of intermediate oligomers, important for the formation of heat aggregates of  $\beta$ -lactoglobulin. *International Dairy Journal*, 8, 105-112.

- Bengoechea, C., Romero, A., Aguilar, J. M., Cordobés, F., & Guerrero, A. (2010). Temperature and pH as factors influencing droplet size distribution and linear viscoelasticity of O/W emulsions stabilised by soy and gluten proteins. *Food Hydrocolloids*, 24, 783-791.
- Berliner, L. J., Meinholtz, D. C., Hirai, Y., Musci, G., & Thompson, M. P. (1991). Functional implications resulting from disruption of the calcium-binding loop in bovine  $\alpha$ -lactalbumin. *Journal of Dairy Science*, 74, 2394-2402.
- Bernal, V. & Jelen, P. (1985). Thermal stability of whey proteins – A calorimetric study. *Journal of Dairy Science*, 68, 2847-2852.
- Bernard, H., Creminon, C., Yvon, M., & Wal, J. M. (1998). Specificity of the human IgE response to the different purified caseins in allergy to cow's milk proteins. *International Archives of Allergy and Immunology*, 155, 235-244.
- Bertrand-Harb, C., Baday, A., Dalgalarrodo, M., Chobert, J. M., & Haertle, T. (2002). Thermal modifications of structure and co-denaturation of  $\alpha$ -lactalbumin and  $\beta$ -lactoglobulin induce changes of solubility and susceptibility to proteases. *Nahrung Food*, 46, 283-289.
- Bhattacharjee, C., Saha, S., Biswas, A., Kundu, M., Ghosh, L., & Das, K. P. (2005). Structural changes of  $\beta$ -lactoglobulin during thermal unfolding and refolding – An FT-IR and circular dichroism study. *The Protein Journal*, 24, 27-35.
- Blijdenstein, T. B. J., van Winden, A. J. M., van Vliet, T., van der Linden, E., & van Aken, G. A. (2004). Serum separation and structure of depletion- and bridging- flocculated emulsions: a comparison. *Colloids and Surfaces A: Physicochemical and Engineering Aspects*, 245, 41-48.
- Bohin, M. C., Vincken, J.-P., van der Hijden, H. T. W. M., & Gruppen, H. (2012). Efficacy of food proteins as carriers for flavonoids. *Journal of Agricultural and Food Chemistry*, 60, 4136-4143.
- Bombara, N., Anon, M. C., & Pilosof, A. M. R. (1997). Functional properties of protease modified wheat flours. *Lebensmittel-Wissenschaft und-Technologie*, 30, 441-447.
- Bonnaillie, L. M. & Tornasula, P. M. (2012). Fractionation of whey protein isolate with supercritical carbon dioxide to produce enriched alpha-lactalbumin and beta-lactoglobulin food ingredients. *Journal of Agricultural and Food Chemistry*, 60, 5257-5266.

- Boral, S. & Bohidar, H. B. (2010). Effect of ionic strength on surface-selective patch binding-induced phase separation and coacervation in similarly charged gelatin-agar molecular systems. *Journal of Physical Chemistry B*, 37, 12027-12035.
- Bos, M. A. & van Vliet, T. (2001). Interfacial rheological properties of adsorbed protein layers and surfactants: a review. *Advances in Colloid and Interface Science*, 91, 437-471.
- Bouyer, E., Mekhloufi, G., Rosilio, V., Grossiord, J.-L., & Agnely, F. (2012). Proteins, polysaccharides, and their complexes used as stabilizers for emulsions: Alternatives to synthetic surfactants in the pharmaceutical field? *International Journal of Pharmaceutics*, 436, 359-378.
- Boye, J. I. & Alli, I. (2000). Thermal denaturation of mixtures of  $\alpha$ -lactalbumin and  $\beta$ -lactoglobulin: a differential scanning calorimetric study. *Food Research International*, 33, 673-682.
- Barth, C. A. & Behnke, U. (1997). Nutritional significance of whey and whey components. *Nahrung Food*, 41, 2-12.
- Bramaud, C., Aimar, P., & Daufin, G. (1995). Thermal isoelectric precipitation of alpha-lactalbumin from a whey-protein concentrate – influence of protein-calcium complexation. *Biotechnology and Bioengineering*, 47, 121-130.
- Britten, M. & Giroux, H. J. (1991). Emulsifying properties of whey-protein and casein composite blends. *Journal of Dairy Science*, 74, 3318-3325.
- Bryant, C. M. & McClements, D. J. (1999). Ultrasonic spectrometry study of the influence of temperature on whey protein aggregation. *Food Hydrocolloids*, 13, 439-444.
- Bueno, A. S., Pereira, C. M., Menegassi, B., Arêas, J. A. G., & Castro, I. A. (2009). Effect of extrusion on the emulsifying properties of soybean proteins and pectin mixtures modelled by response surface methodology. *Journal of Food Engineering*, 90, 504-510.
- Campbell, L., Raikos, V., & Euston, S. R. (2005). Heat stability and emulsifying ability of whole egg and egg yolk as related to heat treatment. *Food Hydrocolloids*, 19, 553-539.
- Campo, V. L., Kawano, D. F., de Silva, D. B., & Carvalho, I. (2009). Carrageenans: Biological properties, chemical modifications and structural analysis – A review. *Carbohydrate Polymers*, 77, 167-180.

- Can Karaca, A., Low, N., & Nickerson, M. (2011a). Emulsifying properties of chickpea, faba bean, lentil and pea proteins produced by isoelectric precipitation and salt extraction. *Food Research International*, 44, 2742-2750.
- Can Karaca, A., Low, N., & Nickerson, M. (2011b). Emulsifying properties of canola and flaxseed protein isolates produced by isoelectric precipitation and salt extraction. *Food Research International*, 44, 2991-2998.
- Capek, I. (2004). Degradation of kinetically-stable o/w emulsions. *Advances in Colloid and Interface Science*, 107, 125-155.
- Chaplin, L. C. & Lyster, R. L. J. (1986). Irreversible heat denaturation of bovine  $\alpha$ -lactalbumin. *Journal of Dairy Science*, 53, 249-258.
- Castelain, C. & Genot, C. (1996). Partition of adsorbed and non-adsorbed bovine serum albumin in dodecane-in-water emulsions calculated from front-face intrinsic fluorescence measurements. *Journal of Agricultural and Food Chemistry*, 44, 1635-1640.
- Chanamai, R. & McClements, D. J. (2006). Depletion flocculation of beverage emulsions by gum Arabic and modified starch. *Journal of Food Science*, 66, 457-463.
- Chang, J.-Y. & Li, L. (2001). The structure of denatured  $\alpha$ -lactalbumin elucidated by the technique of disulfide scrambling. *Journal of Biological Chemistry*, 276, 9705-9712.
- Charlambous, G. & Doxastakis, G. (1989). *Food Emulsifiers: Chemistry, Technology, Functional Properties and Applications*. Amsterdam: Elsevier.
- Chen, J. S. & Dickinson, E. (1993). Time-dependent competitive adsorption of milk-proteins and surfactants in oil-in-water emulsions. *Journal of the Science of Food and Agriculture*, 62, 283-289.
- Chen, L., Chen, J., Ren, J., & Zhao, M. (2011). Modifications of soy protein isolates using combined extrusion pre-treatment and controlled enzymatic hydrolysis for improved emulsifying properties. *Food Hydrocolloids*, 25, 887-897.
- Chobert, J.-M., Bertrand-Harb, C., & Nicolas, M.-G. (1988). Solubility and emulsifying properties of caseins and whey proteins modified enzymatically by trypsin. *Journal of Agricultural and Food Chemistry*, 36, 883-892.
- Chourpa, I., Ducel, V., Richard, J., Dubois, P., & Boury, F. (2006). Conformational modifications of  $\alpha$ -gliadin and globulin proteins upon complex coacervates formation with gum Arabic as studied by Raman microspectroscopy. *Biomacromolecules*, 7, 2616-2623.

- Conde, J. M. & Patino, J. M. R. (2007). The effect of enzymatic treatment of a sunflower protein isolate on the rate of adsorption at the air-water interface. *Journal of Food Engineering*, 78, 1001-1009.
- Cornec, M., Kim, D. A., & Narsimhan, G. (2001). Adsorption dynamics and interfacial properties of  $\alpha$ -lactalbumin in native and molten globule state conformation at air-water interface. *Food Hydrocolloids*, 15, 303-313.
- Dalgleish, D. G. (1993). The sizes and conformations of the proteins in adsorbed layers of individual caseins on lattices and in oil-in-water emulsions. *Colloids and Surfaces B: Biointerfaces*, 1, 1-8.
- Dalgleish, D. G. (2006). Food emulsions - their structures and structure-forming properties. *Food Hydrocolloids*, 20, 415-422.
- Damodaran, S. (1996). Amino Acids, Peptides and Proteins. In O. R. Fennema (Eds.). *Food Chemistry*, 3<sup>rd</sup> ed. (321-430). New York: Marcel Dekker.
- Damodaran, S. (2006). Protein stabilization of emulsions and foams. *Journal of Food Science*, 70, R54-R66.
- Damodaran, S., Anand, K., & Razumovsky, L. (1998). Competitive adsorption of egg white proteins at the air-water interface: Direct evidence for electrostatic complex formation between lysozyme and other egg proteins at the interface. *Journal of Agricultural and Food Chemistry*, 46, 872-876.
- Damodaran, S. & Rammovsky, L. (2003). Competitive adsorption and thermodynamic incompatibility of mixing of beta-casein and gum arabic at the air-water interface. *Food Hydrocolloids*, 17, 355-363.
- Dannenberg, F., & Kessler, H., G. (1988). Reaction kinetics of the denaturation of whey proteins in milk. *Journal of Food Science*, 53, 258-263.
- Date, A. A., Desai, N., Dixit, R., & Nagarsenker, M. (2010). Self-nanoemulsifying drug delivery systems: formulation insights, applications and advances. *Nanomedicine*, 5, 1595-1616.
- Davis, J. P. & Foegeding, E. A. (2007). Comparisons of the foaming and interfacial properties of whey protein isolate and egg white proteins. *Colloids and Surfaces B-Biointerfaces*, 54, 200-210.

- Demetriades, K., Coupland, J. N., & McClements, D. J. (1997). Physical properties of whey protein stabilized emulsions as related to pH and NaCl. *Journal of Food Science*, 62, 342-347.
- Derkach, S. R., Levachev, S. M., Kukushkina, A. N., Novoselova, N. V., Kharlov, A. E., & Matveenko, V. N. (2007). Viscoelasticity of concentrated emulsions stabilized by bovine serum albumin in the presence of a non-ionic surfactant. *Colloid Journal*, 69, 152-158.
- Dickinson, E. (1992). *Introduction to Food Colloids*. Oxford, UK: Oxford University Press.
- Dickinson, E. (2001). Milk protein interfacial layers and the relationship to emulsion stability and rheology. *Colloids and Surfaces B- Biointerfaces*, 20, 197-210.
- Dickinson, E. (2003). Hydrocolloids at interfaces and the influence on the properties of dispersed systems. *Food Hydrocolloids*, 17, 25-39.
- Dickinson, E. (2008). Interfacial structure and stability of food emulsions as affected by protein-polysaccharide interactions. *Soft Matter*, 4, 932-942.
- Dickinson, E. (2012). Emulsion gels: The structuring of soft solids with protein-stabilized oil droplets. *Food Hydrocolloids*, 28, 224-241.
- Dickinson, E. & Hong, S. T. (1994). Surface coverage of beta-lactoglobulin at the oil-water interface – influence of protein heat – treatment and various emulsifiers. *Journal of Agricultural and Food Chemistry*, 42, 1602-1606.
- Dickinson, E. & James, J. D. (1999). Influence of competitive adsorption on flocculation and rheology of high-pressure-treated milk protein-stabilized emulsions. *Journal of Agricultural and Food Chemistry*, 47, 25-30.
- Dickinson, E. & Matsumura, Y. (1991). Time-dependent polymerization of  $\beta$ -lactoglobulin through disulphide bonds at the oil-water interface in emulsions. *International Journal of biology and Macromolecules*, 13, 26.
- Dickinson, E. & Parkinson, E. L. (2004). Heat-induced aggregation of milk protein-stabilized emulsions: sensitivity to processing and composition. *International Dairy Journal*, 14, 63-645.
- Dickinson, E., Owusu, R. K. Tan, S., & Williams, A. (1993). Oil-soluble surfactants have little effect on competitive adsorption of alpha-lactalbumin and beta-lactoglobulin in emulsions. *Journal of Food Science*, 58, 295-298.

- Dickinson, E. & Pawlowsky, K. (1996). Effect of high-pressure treatment of protein on the rheology of flocculated emulsions containing protein and polysaccharide. *Journal of Agricultural and Food Chemistry*, 44, 2992-3000.
- Dickinson, E. & Semenova, M. G. (1992). Emulsifying behavior of protein in the presence of polysaccharide under conditions of thermodynamic incompatibility. *Journal of the Chemical Society, Faraday Transactions*, 88, 849-854.
- Dickinson, E. & Stainsby, G. (1982). *Colloids in Foods*. London, UK: Elsevier.
- Diftis, N. & Kiosseoglou, V. (2004). Competitive adsorption between a dry-heated soy protein-dextran mixture and surface-active materials in oil-in-water emulsions. *Food Hydrocolloids*, 18, 639-646.
- Dissanayake, M. & Vasiljevic, T. (2009). Functional properties of whey proteins affected by heat treatment and hydrodynamic high-pressure shearing. *Journal of Dairy Science*, 92, 1387-1397.
- Divsalar, A., Saboury, A. A., Mohammad, N., Zare, Z., Kefayati, M. E., & Seyedarabi, A. (2012). Characterization and side effect analysis of a newly designed nanoemulsion targeting human serum albumin for drug delivery. *Colloids and Surfaces B: Biointerfaces*, 98, 80-84.
- Djordjevic, D., Kim, H.-J., McClements, D. J., & Decker, E. A. (2004). Physical stability of whey protein-stabilized oil-in-water emulsions at pH 3: Potential ω-3 fatty acid delivery systems (part A). *Journal of Food Science*, 69, C351-C355.
- Doi, H., Tokuyama, T., Kuo, F.-H., Ibuki, F., & Kanamori, M. (1983). Heat-induced complex formation between κ-casein and α-lactalbumin. *Agricultural and Biological Chemistry*, 47, 2817-2824.
- Doublier, J. L., Garnier, C., Renard, D., & Sanchez, C. (2000). Protein-polysaccharide interactions. *Current Opinion in Colloid & Interface Science*, 5, 202-214.
- Drakos, A. & Kiosseoglou, V. (2006). Stability of acidic egg white protein emulsions containing xanthan gum. *Journal of Agricultural and Food Chemistry*, 54, 10164-10169.
- Dubin, P. L., Gao, J., & Mattison, K. (1994). Protein-purification by selective phase-separation with polyelectrolytes. *Separation and Purification Methods*, 23, 1-16.

- Dufour, E., Dalgalarondo, M., & Adam, L. (1998). Conformation of  $\beta$ -lactoglobulin at an oil/water interface as determined from proteolysis and spectroscopic methods. *Journal of Colloid and Interface Science*, 207, 264-272.
- Einhorn-Stoll, U., Weiss, M., & Kunzek, H. (2002). Influence of the emulsion components and preparation method on the laboratory-scale preparation of o/w emulsions containing different types of dispersed phases and/or emulsifiers. *Nahrung Food*, 46, 294-301.
- Eissa, A. S. (2013). Newtonian viscosity behavior of dilute solutions of polymerized whey proteins. Would viscosity measurements reveal more detailed molecular properties? *Food Hydrocolloids*, 30, 200-205.
- Ellepola, S. W. & Ma, C.-Y. (2005). Thermal properties of globulin from rice (*Oryza sativa*) seeds. *Food Research International*, 39, 257-264.
- Elofsson, C., Djmek, P., Paulsson, M., & Burling, H. (1997). Characterization of a cold-gelling whey protein concentrate. *International Dairy Journal*, 7, 601-608.
- El-Salam, M. H. A., El-Shibiny, S., & Salem, A. (2009). Factors affecting the functional properties of whey protein products: a review. *Food Reviews International*, 25, 251-270.
- Ercelebi, E. A. & İbanoğlu, E. (2007). Influence of hydrocolloids on phase separation and emulsion properties of whey protein isolate. *Journal of Food Engineering*, 80, 454-459.
- Exl, B. M. (2001). A review of recent developments in the use of moderately hydrolyzed whey formulae in infant nutrition. *Nutrition Research*, 21, 355-379.
- Fang, Y. & Dalgleish, D. G. (1993). Dimensions of the adsorbed layers in oil-in-water emulsions stabilized by caseins. *Journal of Colloid and Interface Science*, 156, 329-334.
- Fang, Y. & Dalgleish, D. G. (1997). Conformation of beta-lactoglobulin studied by FTIR: Effect of pH, temperature, and adsorption to the oil-water interface. *Journal of colloid and Interface Science*, 196, 292-298.
- Fang, Y. & Dalgleish, D. G. (1998). The conformation of alpha-lactalbumin as a function of pH, heat treatment and adsorption at hydrophobic surfaces studied by FTIR. *Food Hydrocolloids*, 12, 121-126.
- Fessas, D., Iametti, S., Schiraldi, A., & Bonomi, F. (2001). Thermal unfolding of monomeric and dimeric  $\beta$ -lactoglobulins. *European Journal of Biochemistry*, 268, 5439-5448.
- Foegeding, E. A. (2006). Food biophysics of protein gels: A challenge of nano and macroscopic proportions. *Food Biophysics*, 1, 41-50.

- Foegeding, E. A. & Davis, J. P. (2011). Food protein functionality: A comprehensive approach. *Food Hydrocolloids*, 25, 1853-1864.
- Friberg, S. E. & Larsson, K. (1997). *Food Emulsions*, 3<sup>rd</sup> ed. New York: Marcel Dekker.
- Galani, D. & Apenten, R. K. O., (1999). Heat-induced denaturation and aggregation of  $\beta$ -lactoglobulin: kinetics of formation of hydrophobic and disulphide-linked aggregates. *International Journal of Food Science and Technology*, 34, 467-476.
- Galazka, V. B., Dickinson, E., & Ledward, D. A. (2000). Emulsifying properties of ovalbumin in mixtures with sulphated polysaccharides: effects of pH, ionic strength, heat and high-pressure treatment. *Journal of the Science of Food and Agriculture*, 80, 1219-1229.
- Garti, N. (1997). Progress in Stabilization and Transport Phenomena of Double Emulsions in Food Applications. *Lebensmittel-Wissenschaft und-Technologie*, 30, 222-235.
- Gezimati, J., Creamer, L. K., & Singh, H. (1997). Heat-induced interactions and gelation of mixtures of  $\beta$ -lactoglobulin and  $\alpha$ -lactalbumin. *Journal of Agricultural and Food Chemistry*, 45, 1130-1136.
- Gharsallaoui, A., Yamauchi, K., Chambin, O., Cases, E., & Saurel, R. (2010). Effect of high methoxyl pectin on pea protein in aqueous solution and at oil-water interface. *Carbohydrate Polymers*, 80, 817-827.
- Goff, D. (2011). *Dairy Science and Technology Education Series*. Retrieved from <http://www.foodsci.uoguelph.ca/dairyedu/home.html>
- Goldstein, A. & Seetharaman, K. (2011). Effect of a novel monoglyceride stabilized oil in water emulsion shortening on cookie properties. *Food Research International*, 44, 1476-1481.
- Govindaraju, K. & Srinivas, H. (2006). Studies on the effects of enzymatic hydrolysis on functional and physic-chemical properties of arachin. *LWT – Food Science and Technology*, 39, 54-62.
- Grasdalen, H. & Smidsrød, O. (1981). Iodide-specific formation of kappa-carrageenan single helices – I-127 NMR spectroscopic evidence for selective site binding of iodide anions in the ordered conformation. *Macromolecules*, 14, 1842-1845.
- Griko, Y. V. (1999). Denaturation versus unfolding: energetic aspects of residual structure in denatured  $\alpha$ -lactalbumin. *Journal of Protein Chemistry*, 18, 361-369.

- Gulzar, M., Lechevalier, V., Bouhallab, S., & Croguennec, T. (2012). The physicochemical parameters during dry heating strongly influence the gelling properties of whey proteins. *Journal of Food Engineering*, 112, 296-303.
- Guzey, D. & McClements, D. J. (2006). Influence of environmental stresses on OAV emulsions stabilized by beta-lactoglobulin-pectin and beta-lactoglobulin-pectin-chitosan membranes produced by the electrostatic layer-by-layer-deposition technique. *Food Biophysics*, 1, 30-40.
- Guzey, D. & McClements, D. J. (2007). Impact of electrostatic interactions on formation and stability of emulsions containing oil droplets coated by  $\beta$ -lactoglobulin-pectin complexes. *Journal of Agricultural and Food Chemistry*, 55, 475-485.
- Haug, I. J., Skar, H. M., Vegarud, G. E., Langsrud, T., & Draget, K. I. (2009). Electrostatic effects on  $\beta$ -lactoglobulin transitions during heat denaturation as studied by differential scanning calorimetry. *Food Hydrocolloids*, 23, 2287-2293.
- Harnsilawat, T., Pongsawatmanit, R., & McClements, D. J. (2006). Stabilization of model beverage cloud emulsions using protein-polysaccharide electrostatic complexes formed at the oil-water interface. *Journal of Agricultural and Food Chemistry*, 54, 5540-5547.
- Harrington, J. C., Foegeding, E. A., Mulvihill, D. M., & Morris, E. R. (2009). Segregative interactions and competitive binding of Ca<sup>2+</sup> in gelling mixtures of whey protein isolate with Na<sup>+</sup> kappa-carrageenan. *Food Hydrocolloids*, 23, 468-489.
- Hayati, I. N., Man, Y. B. C., Tan, C. P., & Aini, I. N. (2009). Droplet characterization and stability of soybean oil/palm kernel olein O/W emulsions with the presence of selected polysaccharides. *Food Hydrocolloids*, 23, 233-243.
- Heine, W. E., Klein, P. D., & Reeds, P. J. (1991). The importance of alpha-lactalbumin in infant nutrition. *Journal of Nutrition*, 121, 277-283.
- Hendrix, T., Griko, Y. V., & Privalov, P. L. (2000). A calorimetric study of the influence of calcium on the stability of bovine  $\alpha$ -lactalbumin. *Biophysical Chemistry*, 84, 27-34.
- Hillier, R. M. & Lyster, R. L. J. (1979). Whey protein denaturation in heated milk and cheese whey. *Journal of Dairy Research*, 46, 95-102.
- Hillier, R. M., Lyster, R. L. J., & Cheeseman, G. C. (1979). Thermal denaturation of  $\alpha$ -lactalbumin and  $\beta$ -lactoglobulin in cheese whey: effect of total solids concentration and pH. *Journal of Dairy Research*, 46, 103-111.

- Hoffmann, M. A. M. & van Mil, P. J. J. M. (1999). Heat-induced aggregation of  $\beta$ -lactoglobulin as a function of pH. *Journal of Agricultural and Food Chemistry*, 47, 1895-1905.
- Hoffmann, M. A. M., Sala, G., Olieman, C., & de Kruif, K. G. (1997). Molecular mass distributions of heat-induced  $\beta$ -lactoglobulin aggregates. *Journal of Agriculture and Food Chemistry*, 45, 2949-2957.
- Hoffman, R. E., Shabtai, E., Rabinovitz, M., Iyer, V. S., Müllen, K., Rai, A. K., Bayard, E., & Scott, L. T. (1998). Self-diffusion measurements of polycyclic aromatic hydrocarbon alkali metal salts. *Journal of the Chemical Society-Perkin Transactions 2*, 7, 1659-1664.
- Hong, Y. H., & Creamer, L. K. (2002). Changed protein structures of bovine  $\beta$ -lactoglobulin b and  $\alpha$ -lactalbumin as a consequence of heat treatment. *International Dairy Journal*, 12, 345-359.
- Hu, M., McClements, J., & Decker, E. A. (2003). Lipid oxidation in corn oil-in-water emulsions stabilized by casein, whey protein isolate, and soy protein isolate. *Journal of Agricultural and Food Chemistry*, 51, 1696-1700.
- Hu, M., McClements, D. J., & Decker, E. A. (2004). Impact of chelators on the oxidative stability of whey protein isolate-stabilized oil-in-water emulsions containing omega-3 fatty acids. *Food Chemistry*, 88, 57-62.
- Hu, Y., Wang, H., Wang, J., Wang, S., Wang, L., Yang, Y., Zhang, Y., Kong, D., & Yang, Z. (2010). Supramolecular hydrogels inspired by collagen for tissue engineering. *Organic & Biomolecular Chemistry*, 8, 3267-3271.
- Huang, P. H., Lu, H. T., Wang, Y. T., & Wu, M. C. (2011). Antioxidant activity and emulsion-stabilizing effect of pectic enzyme treated pectin in soy protein isolate-stabilized oil/water emulsion. *Journal of Agricultural and Food Chemistry*, 59, 9623-9628.
- Hunt, J. A. & Dalgleish, D. G. (1994a). Effect of pH on the stability and surface-composition of emulsions made with whey-protein isolate. *Journal of Agricultural and Food Chemistry*, 42, 2131-2135.
- Hunt, J. A. and Dalgleish, D. G. (1994b). Adsorption behavior of whey-protein isolate and caseinate in soya oil-in-water emulsions. *Food Hydrocolloids*, 8, 175-187.
- Hunt, J. A. & Dalgleish, D. G. (1995). Heat-stability of oil-in-water emulsions containing milk-proteins – effect of ionic-strength and pH. *Journal of Food Science*, 60, 1120-1123.

- Hussain, R., Gaiani, C., Jeandel, C., Ghanbaja, J., & Scher, J. (2012). Combined effect of heat treatment and ionic strength on the functionality of whey proteins. *Journal of Dairy Science*, 95, 6260-6273.
- Hyun, K., Kim, S. H., Ahn, K., H., & Lee, S. J. (2002). Large amplitude oscillatory shear as a way to classify the complex fluids. *Journal of Non-Newtonian Fluid Mechanics*, 107, 51-65.
- Hyun, K., Wilhelm, M., Klein, C. O., Cho, K. S., Nam, J. G., Ahn, K. H., Lee, S. J., Ewoldt, R. H., & McKinley, G. H. (2011). A review of nonlinear oscillatory shear tests: Analysis and application of large amplitude oscillatory shear (LAOS). *Progress in Polymer Science*, 36, 1697-1753.
- Iametti, S., de Gregori, B., Vecchio, G., & Bonomi, F. (1996). Modifications occur at different structural levels during the heat denaturation of  $\beta$ -lactoglobulin. *European Journal of Biochemistry*, 237, 106-112.
- Ibanoglu, E. & Ibanoglu, S. (1999). Foaming behavior of EDTA-treated alpha-lactalbumin. *Food Chemistry*, 66, 477-481.
- Ipsen, R., Otte, J., Sharma, R., Nielsen, A., & Hansen, L. G. (2001). Effect of limited hydrolysis on the interfacial rheology and foaming properties of  $\beta$ -lactoglobulin A. *Colloids and Surfaces B: Biointerfaces*, 21, 173-178.
- Jafari, S. M., Beheshti, P., & Assadpoor, E. (2012). Rheological behavior and stability of D-limonene emulsions made by a novel hydrocolloid (Angum gum) compared with Arabic gum. *Journal of Food Engineering*, 109, 1-8.
- Jenkins, P. & Snowden, M. (1996). Depletion flocculation in colloidal dispersions. *Advances in Colloid and Interface Science*, 68, 57-75.
- Joshi, M., Adhikari, B., Aldred, P., Panizzo, J. F., Kasapis, S., & Barrow, C. J. (2012). Interfacial and emulsifying properties of lentil protein isolate. *Food Chemistry*, 134, 1343-1353.
- Jourdain, L., Leser, M. E., Schmitt, C., Michel, M., & Dickinson, E. (2008). Stability of emulsions containing sodium caseinate and dextran sulfate: Relationship to complexation in solution. *Food Hydrocolloids*, 22, 647-659.
- Jönsson, B., Lindman, B., Holmberg, K., & Kronberg, B. (1998). *Surfactants and Polymers in Aqueous Solution*. Chichester, UK: John Wiley & Sons.
- Ju, Z. Y., Hettiarachchy, N., & Kilara, A. (1999). Thermal properties of whey protein aggregates. *Journal of Dairy Science*, 82, 1882-1889.

- Jung, S., Murphy, P. A., & Johnson, L. A. (2005). Physiochemical and functional properties of soy protein substrates modified by low levels of protease hydrolysis. *Journal of Food Science*, 70, C180-C187.
- Jung, J.-M., Savin, G., Pouzot, M., Schmitt, C., & Mezzenga, R. (2008). Structure of heat-induced  $\beta$ -lactoglobulin aggregates and their complexes with sodium-dodecyl sulfate. *Biomacromolecules*, 9, 2477-2486.
- Kato, A. & Nakai, S. (1980). Hydrophobicity determined by a fluorescence probe method and its correlation with surface properties of proteins. *Biochimica et Biophysica Acta*, 624, 13-20.
- Katona, J. M., Sovilj, V. J., & Petrovic, L. B. (2010). Microencapsulation of oil by polymer mixture-ionic surfactant interaction induced coacervation. *Carbohydrate Polymers*, 79, 563-570.
- Kazmierski, M. & Corredig, M. (2003). Characterization of soluble aggregates from whey protein isolate. *Food Hydrocolloids*, 17, 685-692.
- Keerati-u-rai, M. & Corredig, M. (2009). Heat-induced changes in oil-in-water emulsions stabilized with soy protein isolate. *Food Hydrocolloids*, 23, 2141-2148.
- Khalloufi, S., Corredig, M., & Alexander, M. (2009). Interactions between flaxseed gums and WPI-stabilized emulsion droplets assessed *in situ* using diffusing wave spectroscopy. *Colloids and Surfaces B: Biointerfaces*, 68, 145-153.
- Kilara, A. (2008). Whey and Whey Products. In R. C. Chandan, A. Kilara, N. P. Shah (Eds.). *Dairy Processing & Quality Assurance* (pp. 337-356). Ames, Iowa: Blackwell Publishing.
- Kim, H. J., Decker, E. A., & McClements, D. J. (2002a). Impact of protein surface denaturation on droplet flocculation in hexadecane oil-in-water emulsions stabilized by beta-lactoglobulin. *Journal of Agricultural and Food Chemistry*, 50, 7131-7137.
- Kim, H. J., Decker, E. A., & McClements, D. J. (2002b). Role of post-adsorption conformation changes of beta-lactoglobulin on its ability to stabilize oil droplets against flocculation during heating at neutral pH. *Langmuir*, 18, 7577-7583.
- Kim, H. J., Decker, E. A., & McClements, D. J. (2004). Comparison of droplet flocculation in hexadecane oil-in-water emulsions stabilized by beta-lactoglobulin at pH 3 and 7. *Langmuir*, 20, 5753-5758.

- Kim, H. J., Decker, E. A., & McClements, D. J. (2005). Influence of protein concentration and order of addition on the thermal stability of beta-lactoglobulin stabilized n-hexadecane oil-in-water emulsions at neutral pH. *Langmuir*, 21, 134-139.
- Kim, H. J., Choi, S. J., Shin, W.-S., & Moon, T. W. (2003). Emulsifying properties of bovine serum albumin-galactomannan conjugates. *Journal of Agricultural and Food Chemistry*, 51, 1049-1056.
- Kimura, A., Fukuda, T. Zhang, M., Motoyama, S., Maruyama, N., & Utsumi, S. (2008). Comparison of physicochemical properties of 7S and 11S globulins from pea, fava bean, cowpea, and French bean with those of soybean-French bean 7S globulin exhibits excellent properties. *Journal of Agricultural and Food Chemistry*, 56, 10273-10279.
- Klemaszewski, J. L. & Kinsella, J. E. (1991). Sulfitolysis of whey proteins: Effects of emulsion properties. *Journal of Agricultural and Food Chemistry*, 39, 1033-1036.
- Klinkesorn, U., Sophanodora, P., Chinachoti, P., Decker, E. A., & McClements, D. J. (2005). Encapsulation of emulsified tuna oil in two-layered interfacial membranes prepared using electrostatic layer-by-layer deposition. *Food Hydrocolloids*, 19, 1044-1053.
- Knudsen, J. C., Øgendal, L. H., & Skibsted, L. H. (2008). Droplet surface properties and rheology of concentrated oil in water emulsions stabilized by heat-modified  $\beta$ -Lactoglobulin B. *Langmuir*, 24, 2603-2610.
- Knutsen, S. H., Myladobodski, D. E., Larsen, B., & Usov, A. I. (1994). A modified system of nomenclature for red algal galactans. *Botanica Marina*, 37, 163-169.
- Kontogiorgos, V., Biliaderis, C. G., Kiosseoglou, V., & Doxastakis, G. (2004). Stability and rheology of egg-yolk-stabilized concentrated emulsions containing cereal  $\beta$ -glucans of varying molecular size. *Food Hydrocolloids*, 18, 987-998.
- Korhonen, H. & Pihlanto, A. (2007). Technological options for the production of health-promoting proteins and peptides derived from milk and colostrum. *Current Pharmaceutical Design*, 13, 829-843.
- Koupantsis, T., Pavlidou, E., & Paraskevopoulou, A. (2014). Flavor encapsulation in milk proteins – CMC coacervate-type complexes. *Food Hydrocolloids*, 37, 134-142.
- Krebs, M. R. H., Devlin, G. L., & Donald, A. M. (2007). Protein particulates: Another generic form of protein aggregation? *Biophysical Journal*, 92, 1336-1342.

- de Kruif, C. G., Weinbreck, F., & de Vries, R. (2004). Complex coacervation of proteins and anionic polysaccharides. *Current Opinion in Colloid & Interface Science*, 9, 340-349.
- Kudryashova, E. V., Meinders, M. B. J., Visser, A. J. W. G., van Hoek, A., & de Jongh, H. H. J. (2003). Structure and dynamics of egg white ovalbumin adsorbed at the air/water interface. *European Biophysics Journal with Biophysics Letters*, 32, 553-562.
- Kulmyrzaev, A., Chanamai, R., & McClements, D. J. (2000). Influence of pH and CaCl<sub>2</sub> on the stability of dilute whey protein stabilized emulsions. *Food Research International*, 33, 15-20.
- Kuwajima, K. (1996). The molten globule state of  $\alpha$ -lactalbumin. *FASEB Journal*, 10, 102-109.
- Kuwajima, K., Harushima, Y., & Sugai, S. (1986). Influence of Ca-2+ binding on the structure and stability of bovine alpha-lactalbumin studied by circular-dichroism and nuclear-magnetic-resonance spectra. *International Journal of Peptide and Protein Research*, 27, 18-27.
- Laleye, L. C., Jobe, B., & Wasesa, A. A. H. (2008). Comparative study on heat stability and functionality of camel and bovine milk whey proteins. *Journal of Dairy Science*, 91, 4527-4534.
- Laligant, A., Dumay, E., Valencia, C. C., Cuq, L. L., & Cheftel, J. C. (1991). Surface hydrophobicity and aggregation of  $\beta$ -lactoglobulin heated under neutral pH. *Journal of Agricultural and Food Chemistry*, 39, 2147-2155.
- Lamsal, B. P., Jung, S., & Johnson, L. A. (2007). Rheological properties of soy protein hydrolysates obtained from limited enzymatic hydrolysis. *LWT – Food Science and Technology*, 40, 1215-1223.
- Lee, S. H., Subirade, M., & Paquin, P. (2008). Effects of ultra-high pressure homogenization on the emulsifying properties of whey protein isolates under various pH. *Food Science and Biotechnology*, 17, 324-329.
- Li, J.-L., Cheng, Y.-Q., Wang, P., Zhao, W.-T., Yin, L.-J., & Saito, M. (2012). A novel improvement in whey protein isolate emulsion stability: Generation of an enzymatic cross-linked beet pectin layer using horseradish peroxidase. *Food Hydrocolloids*, 26, 448-455.
- Li, Y. & McClements, D. J. (2011). Controlling lipid digestion by encapsulation of protein-stabilized lipid droplets within alginate-chitosan complex coacervates. *Food Hydrocolloids*, 25, 1025-1033.

- Linfield, W. M. (1976). *Anionic Surfactants: Parts I and II*. New York: Marcel Dekker.
- Liu, F., Jiang, Y. F., Du, B. J., Chai, Z., Jiao, T., Zhang, C. Y., Ren, F. Z., & Leng, X. J. (2013). Design and characterization of controlled-release edible packaging films prepared with synergistic whey-protein polysaccharide complexes. *Journal of Agricultural and Food Chemistry*, 61, 5824-5833.
- Liu, S., Elmer, C., Low, N. H., & Nickerson, M. T. (2010). Effect of pH on the functional behaviour of pea protein isolate-gum Arabic complexes. *Food Research International*, 43, 489-495.
- Liu, S., Low, N. H., & Nickerson, M. T. (2009). Effect of pH, salt, and biopolymer ratio on the formation of pea protein isolate-gum Arabic complexes. *Journal of Agricultural and Food Chemistry*, 57, 1521-1526.
- Livney, Y. D., Verespej, E., & Dalgleish, D. G. (2003). Steric effects governing disulfide bond interchange during thermal aggregation in solutions of  $\beta$ -lactoglobulin b and  $\alpha$ -lactalbumin. *Journal of Agricultural and Food Chemistry*, 51, 8098-8106.
- Luf, W. (1988). Zur Kinetik der Thermodenaturierung von  $\alpha$ -lactalbumin und  $\beta$ -lactoglobulin A und B in Magermilch Temperaturbereich zwischen 70°C und 95°C. Anwendung der Hochleistungs-Flüssigkeits-Chromatographie (HPLC). [On kinetics of thermal denaturation of  $\alpha$ -lactalbumin and  $\beta$ -lactoglobulin A and B in skim milk between 70°C and 95°C by means of high performance liquid chromatography (HPLC)]. *Österreichische Milchwirtschaft*, 43, (21, Beilage 2), 7-12.
- Mackie, A. R., Ridout, M. J., Moates, G., Husband, F. A., & Wilde, P. J. (2007). Effect of the interfacial layer composition on the properties of emulsion creams. *Journal of Agricultural and Food Chemistry*, 55, 5611-5619.
- Magdassi, S. (1996). *Surface Activity of Proteins: Chemical and Physicochemical Modifications*. New York: Marcel Dekker.
- Maingonnat, J. F., Doublier, J. L., Lefebvre, J., & Delaplace, G. (2008). Power consumption of a double ribbon impeller with Newtonian and shear thinning fluids and during the gelation of a iota-carrageenan solution. *Journal of Food Engineering*, 87, 82-90.
- Maldonado-Valderrama, J., Wilde, P. J., Mulholland, F., & Morris, V. J. (2012). Protein unfolding at fluid interfaces and its effect on proteolysis in the stomach. *Soft Matter*, 8, 4402-4414.
- Malmsten, M. (2003). *Biopolymers at Interfaces*, 2<sup>nd</sup> ed. New York: Marcel Dekker.

- Manderson, G. A., Hardman, M. J., & Creamer, L. K. (1998). Effect of heat treatment on the conformation and aggregation of  $\beta$ -lactoglobulin A, B and C. *Journal of Agricultural and Food Chemistry*, 46, 5052-5061.
- Manoi, K. & Rizvi, S. S. H. (2009). Emulsification mechanisms and characterizations of cold, gel-like emulsions produced from texturized whey protein concentrate. *Food Hydrocolloids*, 23, 1837-1847.
- Mao, X. Y., Tong, P. S., Gualco, S., & Vink, S. (2012). Effect of NaCl addition during diafiltration on the solubility, hydrophobicity, and disulfide bonds of 80% milk protein concentrate powder. *Journal of Dairy Science*, 95, 3481-3488.
- Matsudomi, N., Oshita, T., Kobayashi, K. & Kinsella, J. E. (1993). Alpha-lactalbumin enhances the gelation properties of bovine serum-albumin. *Journal of Agricultural and Food Chemistry*, 41, 1053-1057.
- Matsumura, Y., Mitsui, S., Dickinson, E., & Mori, T. (1994). Competitive adsorption of alpha-lactalbumin in the molten globule state. *Food Hydrocolloids*, 8, 555-566.
- McClements, D. J. (2005). *Food emulsions: principles, practice and techniques*, 2<sup>nd</sup> ed. Boca Raton, FL USA: CRC Press Taylor & Francis Group.
- McClements, D. J. (2012). Advances in fabrication of emulsions with enhanced functionality using structural design principles. *Current Opinion in Colloid & Interface Science*, 17, 235-245.
- McClements, D. J., Decker, E. A., & Weiss, J. (2007). Emulsion-based delivery systems for lipophilic bioactive components. *Journal of Food Science*, 72, R109-R124.
- McClements, D. J. Monahan, F.J., & Kinsella, J. E. (1993). Disulfide bond formation affects the stability of whey protein stabilized emulsions. *Journal of Food Science*, 58, 1036.
- McGuffey, M. K., Epting, K. L., Kelly, R. M., & Foegeding, E. A. (2005). Denaturation and aggregation of three  $\alpha$ -lactalbumin preparations at neutral pH. *Journal of Agricultural and Food Chemistry*, 53, 3182-3190.
- Mine, Y., Noutomi, T., & Haga, N. (1991). Emulsifying and structural properties of ovalbumin. *Journal of Agricultural and Food Chemistry*, 39, 443-446.
- Miriani, M., Keerati-u-rai, M., Corredig, M., Iametti, S., & Bonomi, F. (2011). Denaturation of soy proteins in solution and at the oil-water interface: a fluorescence study. *Food Hydrocolloids*, 25, 620-626.

- Mishchuk, N. A., Sanfeld, A., & Steinchen, A. (2004). Interparticle interactions in concentrate water-oil emulsions. *Advances in Colloid and Interface Science*, 112, 129-157.
- Moro, A., Gatti, C., & Delorenzi, N. (2001). Hydrophobicity of whey protein concentrates measured by fluorescence quenching and its relation with surface functional properties. *Journal of Agricultural and Food Chemistry*, 49, 4784-4789.
- Moschakis, T., Murray, B. S., & Biliaderis, C. G. (2010). Modifications in stability and structure of whey protein-coated o/w emulsions by interacting chitosan and gum arabic mixed dispersions. *Food Hydrocolloids*, 24, 8-17.
- Mounsey, J. S. & O'Kennedy, B. T. (2007). Conditions limiting the influence of thiol-disulphide interchange reactions on the heat-induced aggregation kinetics of  $\beta$ -lactoglobulin. *International Dairy Journal*, 17, 1034-1042.
- Moure, A., Sineiro, J., Domínguez, H., & Parajó, J. C. (2006). Functionality of oilseed protein products: A review. *Food Research International*, 39, 945-963.
- Morris, E. R., Rees, D. A., & Robinson, G. (1980). Cation-specific aggregation of carrageenan helices – domain model of polymer gel structure. *Journal of Molecular Biology*, 138, 349-362.
- Mulvihill, D. M. (1992). Production, functional properties and utilization of milk protein products, In P. F. Fox (Eds.). *Advanced Dairy Chemistry. 1. Proteins* (369-404). London: Elsevier Applied Science.
- Mulvihill, D. M. & Murphy, P. C. (1991). Surface active and emulsifying properties of caseins/caseinates as influenced by state of aggregation. *International Dairy Journal*, 1, 13-37.
- Mun, S., Cho, Y., Decker, E. A., & McClements, D. J. (2008). Utilization of polysaccharide coatings to improve freeze-thaw and freeze-dry stability of protein-coated lipid droplets. *Journal of Food Engineering*, 86, 508-518.
- Muschiolik, G. (2007). Multiple emulsions for food use. *Current Opinion in Colloid & Interface Science*, 12, 213-220.
- Myers, D. (1988). *Surfactant Science Technology*. Weinheim, Germany: VCH Publishers.
- Nakagawa, K., Iwamoto, S., Nakajima, M., Shono, A., & Satoh, K. (2004). Microchannel emulsification using gelatin and surfactant-free coacervate microencapsulation. *Journal of Colloid and Interface Science*, 278, 198-205.

- Ngarize, S., Herman, H., Adams, A., & Howell, N. (2004). Comparison of changes in the secondary structure of unheated, heated, and high-pressure-treated  $\beta$ -lactoglobulin and ovalbumin proteins using Fourier transform Raman spectroscopy and self-deconvolution. *Journal of Agricultural and Food Chemistry*, 52, 6470-6477.
- Najbar, L. V., Considine, R. F., & Drummond, C. J. (2003). Heat-induced aggregation of a globular egg-white protein in aqueous solution: investigation by atomic force microscope imaging and surface force mapping modalities. *Langmuir*, 19, 2880-2887.
- Nakamura, S., Kato, A., & Kobayashi, K. (1992). Enhanced antioxidative effect of ovalbumin due to covalent binding of polysaccharides. *Journal of Agricultural and Food Chemistry*, 40, 2033-2037.
- Neirynck, N., van der Meeren, P., Gorbe, S. B., Dierckx, S., & Dewettinck, K. (2004). Improved emulsion stabilizing properties of whey protein isolate by conjugation with pectins. *Food Hydrocolloids*, 18, 949-957.
- Norde, W. (2003). *Colloids and Interfaces in Life Sciences*. New York, NY USA: Marcel Dekker.
- O'Regan, J. & Mulvihill, D. M. (2010). Sodium caseinate-maltodextrin conjugate stabilized double emulsions: Encapsulation and stability. *Food Research International*, 43, 224-231.
- Oldfield, D. J., Singh, H., Taylor, M. W., & Pearce, K. N. (1998). Kinetics of denaturation and aggregation of whey proteins in skim milk heated in an ultra-high temperature (UHT) pilot plant. *International Dairy Journal*, 8, 311-318.
- Olijve, J., Mori, F., & Toda, Y. (2001). Influence of the molecular-weight distribution of gelatin on emulsion stability. *Journal of Colloid and Interface Science*, 243, 476-482.
- Owusu, R. K. (1992). The effect of calcium on bovine  $\alpha$ -lactalbumin conformational transitions by ultraviolet difference and fluorescence. *Food Chemistry*, 43, 41-45.
- Padala, S. R., Williams, P. A., & Philips, G. O. (2009). Adsorption of gum Arabic, egg white protein, and their mixtures at the oil-water interface in limonene oil-in-water emulsions. *Journal of Agricultural and Food Chemistry*, 57, 4964-4973.
- Pal, R. (2011). Rheology of simple and multiple emulsions. *Current Opinion in Colloid & Interface Science*, 16, 41-60.
- Palacios, L. E. & Wang, T. (2005). Egg-yolk lipid fractionation and lecithin characterization. *Journal of the American Oil Chemist Society*, 82, 571-578.

- Palazolo, G. G., Sorgentini, D. A., & Wagner, J. R. (2005). Coalescence and flocculation in o/w emulsions of native and denatured whey soy proteins in comparison with soy protein isolates. *Food Hydrocolloids*, *19*, 595-604.
- Papalamprou, E. M., Doxastakis, G. I., & Kiosseoglou, V. (2010). Chickpea protein isolates obtained by wet extraction as emulsifying agents. *Journal of the Science of Food Agriculture*, *90*, 304-313.
- Parthasarathy, M. & Klingenberg, D. J. (1999). Large amplitude oscillatory shear of ER suspensions. *Journal of Non-Newtonian Fluid Mechanics*, *81*, 83-104.
- Parris, N., Anema, S. G., Singh, H., & Creamer, L. K. (1993). Aggregation of whey proteins in heated sweet whey. *Journal of Agricultural and Food Chemistry*, *41*, 460-464.
- Parris, N. & Baginski, M. A. (1991). A rapid method for the determination of whey-protein denaturation. *Journal of Dairy Science*, *74*, 58-64.
- Patino, J. M. R., Nino, M. R. R., & Sanchez, C. C. (1999). Dynamic interfacial rheology as a tool for the characterization of whey protein isolates gelation at the oil-water interface. *Journal of Agricultural and Food Chemistry*, *47*, 3640-3648.
- Paul, G. L. (2009). The rational for consuming protein blends in sports nutrition. *Journal of the American College of Nutrition*, *28*, 464S-472S.
- Perez, A. A., Carrara, C. R., Sánchez, C. C., Santiago, L. G., & Patino, J. M. R. (2009). Interfacial dynamic properties of whey protein concentrate/polysaccharide mixtures at neutral pH. *Food Hydrocolloids*, *23*, 1253-1262.
- Permyakov, E. A., & Berliner, L. J. (2000).  $\alpha$ -lactalbumin: structure and function. *FEBS Letters*, *473*, 269-274.
- Perrechil, F. A. & Cunha, R. L. (2012). Development of multiple emulsions based on the repulsive interaction between sodium caseinate and LBG. *Food Hydrocolloids*, *26*, 126-134.
- Pfeil, W., & Sadowski, M. L. (1985). A scanning calorimetric study of bovine and human apo—alpha-lactalbumin. *Studia Biophysica*, *109*, 163-170.
- Piculell, L., Nilsson, S., & Muhrbeck, P. (1992). Effects of small amounts of kappa-carrageenan on the rheology of aqueous iota-carrageenan. *Carbohydrate Polymers*, *18*, 199-208.
- Pongsawatmanit, R., Harnsilawat, T., & McClements, D. J. (2006). Influence of alginate, pH and ultrasound treatment on palm oil-in-water emulsions stabilized by beta-lactoglobulin. *Colloids and Surfaces A- Physicochemical and Engineering Aspects*, *287*, 59-67.

- Popineau, Y., Pineau, F., Evon, P., & Bérot, S. (1999). Influence of pH and salt concentration on the emulsifying properties of native wheat gliadins and of their chymotryptic hydrolysates. *Food Nahrung*, 43, 361-367.
- Puppo, M. C., Beaumal, V., Speroni, F., de Lamballerie, M., Añón, M. C., & Anton, M. (2011).  $\beta$ -conglycinin and glycinin soybean protein emulsions treated by combined temperature-high-pressure treatment. *Food Hydrocolloids*, 25, 389-397.
- Qi, X. L., Holt, C., McNulty, D., Clarke, D. T., Brownlow, S., & Jones, G. R. (1997). Effect of temperature on the secondary structure of beta-lactoglobulin at pH 6.7, as determined by CD and IR spectroscopy: A test of the molten globule hypothesis. *Biochemical Journal*, 324, 341-346.
- Radha, C. & Prakash, V. (2009). Structural and functional properties of heat-processed soybean flour: Effect of proteolytic modification. *Food Science and Technology International*, 15, 453-463.
- Rajaraman, K., Raman, B., Ramakrishna, T., & Mohan Rao, C. (1998). The chaperone-like  $\alpha$ -crystallin forms a complex only with the aggregation-prone molten globule state of  $\alpha$ -lactalbumin. *Biochemical and Biophysical Research Communications*, 249, 917-921.
- Ramkumar, C., Singh, H., Munro, P. A., & Singh, A. M. (2000). Influence of calcium, magnesium, or potassium ions on the formation and stability of emulsions prepared using highly hydrolyzed whey proteins. *Journal of Agricultural and Food Chemistry*, 48, 1598-1604.
- Rampon, V., Brossard, C., Mouhous-Riou, N., Bousseau, B., Llamas, G., & Genot, C. (2004). The nature of the apolar phase influences the structure of the protein emulsifier in oil-in-water emulsions stabilized by bovine serum albumin: A front-surface fluorescence study. *Advances in Colloid and Interface Science*, 108-109, 87-94.
- Rees, D. A., Scott, W. E., & Williamson, F. B. (1970). Correlation of optical activity with polysaccharide conformation. *Nature*, 227, 390-392.
- Reiffers-Magnani, C. K., Cuq, J. L., & Watzke, H. J. (2000). Depletion flocculation and thermodynamic incompatibility in whey protein stabilised O/W emulsions. *Food Hydrocolloids*, 14, 521-530.
- Relkin, P., Launay, B., & Eynard, L. (1993). Effect of sodium and calcium addition on thermal denaturation of apo-alpha-lactalbumin: a differential scanning calorimetry study. *Journal of Dairy Science*, 76, 36-47.

- Richmond, J. M. (1990). *Cationic surfactants: Organic Chemistry*. New York: Marcel Dekker.
- Ridout, M. J., Garza, S., Brownsey, G. J., & Morris, V. J. (1996). Mixed iota-kappa carrageenan gels. *International Journal of Biological Macromolecules*, 18, 5-8.
- Robins, M. M. (2000). Emulsions – creaming phenomena. *Current Opinion in Colloid & Interface Science*, 5, 265-272.
- Robins, M. M., Watson, A. D., & Wilde, P. J. (2002). Emulsions- creaming and rheology. *Current Opinion in Colloid & Interface Science*, 7, 419-425.
- Rochas, C. & Landry, S. (1987). Molecular organization of kappa carrageenan in aqueous solution. *Carbohydrate Polymers*, 7, 435-447.
- Rochas, C. & Rinaudo, M. (1984). Mechanism of gel formation in kappa-carrageenan. *Biopolymers*, 23, 735-745.
- Rochas, C., Rinaudo, M., & Vincendon, M. (1980). Structural and conformational investigation of carrageenans. *Biopolymers*, 19, 2165-2175.
- Romero, A., Beaumal, V., David-Braind, E., Cordobés, F., Guerrero, A., & Anton, M. (2011a). Interfacial and oil/water emulsions characterization of potato protein isolates. *Journal of Agricultural and Food Chemistry*, 59, 9466-9474.
- Romero, A., Beaumal, V., David-Briand, E., Cordobes, F., Anton, M., & Guerrero, A. (2011b). Interfacial and emulsifying behavior of crayfish protein isolate. *LWT- Food Science and Technology*, 44, 1603-1610.
- Roudsari, M., Nakamura, A., Smith, A., & Corredig, M. (2006). Stabilizing behavior of soy soluble polysaccharide or high methoxyl pectin in soy protein isolate emulsions at low pH. *Journal of Agricultural and Food Chemistry*, 54, 1434-1441.
- Ryan, K. N., Vardhanabhuti, B., Jaramillo, D. P., van Zanten, J. H., & Coupland, J. N. (2012). Stability and mechanism of whey protein soluble aggregates thermally treated with salts. *Food Hydrocolloids*, 27, 411-420.
- Sajjadi, S., Zerfa, M. & Brooks, B. W. (2002). Dynamic behavior of drops in oil/water/oil dispersions. *Chemical Engineering Science*, 57, 663-675.
- Salminen, H. & Weiss, J. (2014). Electrostatic adsorption and stability of whey protein-pectin complexes on emulsion interfaces. *Food Hydrocolloids*, 35, 410-419.

- Santipanichwong, R. & Suphantharika, M. (2009). Influence of different  $\beta$ -glucans on the physical and rheological properties of egg yolk stabilized oil-in-water emulsions. *Food Hydrocolloids*, 23, 1279-1287.
- Schmitt, C., Sanchez, C., Desobry-Banon, S., & Hardy, J. (1998). Structure and technofunctional properties of protein-polysaccharide complexes: a review. *Critical Reviews in Food Science and Nutrition*, 38, 689-753.
- Schmidt, I., Cousin, F., Huchon, C., Boue, F., & Axelos, M. A. V. (2009). Spatial structure and composition of polysaccharide-protein complexes from small angle neutron scattering. *Biomacromolecules*, 10, 1346-1357.
- Schnack, U. & Klostermeyer, H. (1980). Thermal decomposition of  $\alpha$ -lactalbumin. 1. Destruction of cysteine residues. *Milchwissenschaft*, 35, 206-208.
- Schokker, E. P., Singh, H., & Creamer, L. K. (2000a). Heat-induced aggregation of  $\beta$ -lactoglobulin A and B with  $\alpha$ -lactalbumin. *International Dairy Journal*, 10, 843-853.
- Schokker, E. P., Singh, H., Pinder, D. N., & Creamer, L. K. (2000b). Heat-induced aggregation of beta-lactoglobulin AB at pH 2.5 as influenced by ionic strength and protein concentration. *International Dairy Journal*, 10, 233-240.
- Schokker, E. P., Singh, H., Pinder, D. N., Norris, G. E., & Creamer, L. K. (1999). Characterization of intermediates formed during heat-induced aggregation of  $\beta$ -lactoglobulin AB at neutral pH. *International Dairy Journal*, 9, 791-800.
- Schmitt, C., Sanchez, C., Desobry-Banon, S., & Hardy, J. (1998). Structure and technofunctional properties of protein-polysaccharide complexes: a review. *Critical Reviews in Food Science and Nutrition*, 38, 689-753.
- Schultz, S., Wagner, G., Urban, K., & Ulrich, J. (2004). High-pressure homogenization as a process for emulsion formation. *Chemical Engineering & Technology*, 27, 361-368.
- Shakeel, F., Shafiq, S., Haq, N., Alanazi, F. K., & Alsarra, A. (2012). Nanoemulsions as potential vehicles for transdermal and dermal delivery of hydrophobic compounds: an overview. *Expert Opinion on Drug Delivery*, 9, 953-974.
- Sharma, S., Kumar, P., Betzel, C., & Singh, T. P. (2001). Structure and function of proteins involved in milk allergies. *Journal of chromatography B*, 756, 183-187.
- Sharma, R. & Singh, H. (1998). Adsorption behavior of commercial milk protein and milk powder products in low-fat emulsions. *Milchwissenschaft*, 53, 373-377.

- Shin, Y.-S., Drolet, B., Mayer, R., Dolence, K., & Basile, F. (2007). Desorption electrospray ionization-mass-spectrometry of proteins. *Analytical Chemistry*, 79, 3514-3518.
- Singh, S. S., Aswal, V. K., & Bohidar, H. B. (2007). Structural studies of agar-gelatin complex coacervates by small angle neutron scattering, rheology and differential scanning calorimetry. *International Journal of Biological Macromolecules*, 41, 301-307.
- Sliwinski, E. L., Roubos, P. J., Zoet, F. D., van Boekel, M. A. J. S., & Wouters, J. T. M. (2003). Effects of heat on physicochemical properties of whey protein-stabilised emulsions. *Colloids and Surfaces B: Biointerfaces*, 31, 231-242.
- Souza, H. K. S., Hilliou, L., Bastos, M., & Goncalves, M. P. (2011). Effect of molecular weight and chemical structure on thermal and rheological properties of gelling kappa/iota-hybrid carrageenan solutions. *Carbohydrate Polymers*, 85, 429-438.
- Spuergin, P., Walter, M., Schiltz, E., Deichmann, K., Forster, J., & Mueller, H. (1997). Allergenicity of alpha-caseins from cow, sheep and goat. *Allergy*, 52, 293-298.
- Stone, A. K. & Nickerson, M. T. (2012). Formation and functionality of whey protein isolate-(kappa-, iota-, and lambda-type) carrageenan electrostatic complexes. *Food Hydrocolloids*, 27, 271-277.
- Su, J., Flanagan, J., Hemar, Y., & Singh, H. (2006). Synergistic effects of polyglycerol ester of pollyricinoleic acid and sodium caseinate on the stabilisation of water-oil-water emulsions. *Food Hydrocolloids*, 20, 261-268.
- Surh, J., Decker, E. A., & McClements, J. (2006). Properties and stability of oil-in-water emulsions stabilized by fish gelatin. *Food Hydrocolloids*, 20, 596-606.
- Swaisgood, H. E. (2008). Characteristics of Milk. In S. Damodaran, K. Parkin, & O. R. Fennema (Eds.), *Fennema's Food Chemistry*, 4<sup>th</sup> Ed. (pp. 885-921). Boca Raton, FL USA: CRC Press Taylor & Francis Group.
- Syrbe, A., Bauer, W. J., & Kostermeyer, N. (1998). Polymer science concepts in dairy systems – An overview of milk protein and food hydrocolloid interaction. *International Dairy Journal*, 8, 179-193.
- Taherian, A. R., Britten, M., Sabik, H., & Fustier, P. (2011). Ability of whey protein isolate and/or fish gelatin to inhibit physical separation and lipid oxidation in fish oil-in-water beverage emulsion. *Food Hydrocolloids*, 25, 868-878.

- Tam, K. C., Guo, L., Jenkins, R. D., & Bassett, D. R. (1999). Viscoelastic properties of hydrophobically modified alkali-soluble emulsions in salt solutions. *Polymer*, 40, 6369-6379.
- Tang, Q. N., McCarthy, O. J., & Munro, P. A. (1994). Gelling characteristics of egg-white, whey-protein concentrates, whey-protein isolate, and beta-lactoglobulin. *Journal of Agricultural and Food Chemistry*, 42, 2126-2130.
- Tavares, C., Monteiro, S. R., Moreno, N., & Lopes da Silva, J. A. (2005). Does the branching degree of galactomannans influence their effect on whey protein gelation? *Colloids and Surfaces A: Physicochemical Engineering Aspects*, 270-271, 213-219.
- Taylor, P. (1998). Ostwald ripening in emulsions. *Advances in Colloid and Interface Science*, 75, 107-163.
- Tcholakova, S., Denkov, N. D., Sidzhakova, D., & Campbell, B. (2006a). Effect of thermal treatment, ionic strength, and pH on the short-term and long-term coalescence stability of  $\beta$ -lactoglobulin emulsions. *Langmuir*, 22, 6042-6052.
- Tcholakova, S., Denkov, N. D., Ivanov, I. B., & Campbell, B. (2006b). Coalescence stability of emulsions containing globular milk proteins. *Advances in Colloid and Interface Science*, 123-126, 259-293.
- Thanh, T. T. T., Yuguchi, Y., Mimura, M., Yasunaga, H., Takano, R., Urakawa, H., & Kajiwara, K. (2002). Molecular characteristics and gelling properties of the carrageenan family, 1-Preparation of novel carrageenans and their dilute solution properties. *Macromolecular Chemistry and Physics*, 203, 15-23.
- Tippetts, M. & Martini, S. (2012). Influence of iota-carrageenan, pectin, and gelatin on the physicochemical properties and stability of milk protein-stabilized emulsions. *Journal of Food Science*, 77, C253-C260.
- Tirtaatmadja, V., Tam, K. C., & Jenkins, R. D. (1997). Superposition of oscillations on steady shear flow as a technique for investigating the structure of associative polymers. *Macromolecules*, 30, 1426-1433.
- Tossavainen, O., Rantamaki, P., Outinen, M., Tupasela, T., & Koskela, P. (1998). Functional properties of the whey protein fractions produced in pilot scale processes. *Milchwissenschaft*, 53, 453-458.

- Tran, T. & Rousseau, D. (2013). Stabilization of acidic soy protein-based dispersions and emulsions by soy soluble polysaccharides. *Food Hydrocolloids*, 30, 382-392.
- Trius, A., Sebranek, J. G., & Lanier, T. (1996). Carrageenans and their use in meat products. *Critical Reviews in Food Science and Nutrition*, 36, 69-85.
- Tsumura, K. (2009). Improvement of the physicochemical properties of soybean proteins by enzymatic hydrolysis. *Food Science and Technology Research*, 15, 381-388.
- Tual, A., Bourles, E., Barey, P., Houdoux, A., Desprairies, M., & Courthaudon, J.-L. (2006). Effect of surfactant sucrose ester on physical properties of dairy whipped emulsions in relation to those of O/W interfacial layers. *Journal of Colloid and Interface Science*, 295, 495-503.
- Turgeon, S. L., Beaulier, M., Schmitt, C., Sanchez, C. (2003). Protein-polysaccharide interactions: phase-ordering kinetics, thermodynamics and structural aspects. *Current Opinion in Colloid Interface Science*, 8, 401-414.
- Turgeon, S. L., Schmitt, C., & Sanchez, C. (2007). Protein-polysaccharide complexes and coacervates. *Current Opinion in Colloid & Interface Science*, 12, 166-178.
- Uruakpa, F. O. & Arntfield, S. D. (2005). Emulsifying characteristics of commercial canola protein-hydrocolloid systems. *Food Research International*, 38, 659-672.
- Vega, C., Dalgleish, D. G., & Goff, H. D. (2005). Effect of kappa-carrageenan addition to dairy emulsions containing sodium caseinate and locust bean gum. *Food Hydrocolloids*, 19, 187-195.
- van de Velde, F., Knutsen, S. H., Usov, A. L., Rollema, H. S., & Cerezo, A. S. (2002). <sup>1</sup>H and <sup>13</sup>C high resolution NMR spectroscopy of carrageenans: Application in research in industry. *Trends in Food Science & Technology*, 13, 73-92.
- van de Velde, F., Peppelman, H. A., Rollema, H. S., & Tromp, R. H. (2001). On the structure of kappa/iota-hybrid carrageenans. *Carbohydrate Research*, 331, 271-283.
- Verheul, M., Roefs, S. P. F. M., & de Kruif, K. G. (1998). Kinetics of heat-induced aggregation of  $\beta$ -lactoglobulin. *Journal of Agricultural and Food Chemistry*, 46, 896-903.
- van Vliet, T., Lakemond, C. M. M., & Visschers, R. W. (2004). Rheology and structure of milk protein gels. *Current Opinion in Colloids & Interface Science*, 9, 298-304.
- Voutsinas, L. P., Cheung, E., & Nakai, S. (1983). Relationships of hydrophobicity to emulsifying properties of heat denatured proteins. *Journal of Food Science*, 48, 26-32.
- Walstra, P. (2003). *Physical chemistry of Foods*. New York: Marcel Dekker, Inc.

- Walstra, P. & Jenness, R. (1984). *Dairy Chemistry and Physics*. New York, NY: John Wiley and Sons.
- Walzem, R. L., Dillard, C. J., & German, J. B. (2002). Whey components: Millennia of evolution create functionalities for mammalian nutrition: What we know and what we may be overlooking. *Critical Reviews in Food Science and Nutrition*, 42, 353-375.
- Wang, J., Buck, S. M., & Chen, Z. (2003). The effect of surface coverage on conformation changes of bovine serum albumin molecules at the air-solution interface detected by sum frequency generation vibrational spectroscopy. *Analyst*, 128, 773-778.
- Wang, B., Li, D., Wang, L.-J., Adhikari, B., & Shi, J. (2010). Ability of flaxseed and soybean protein concentrates to stabilize oil-in-water emulsions. *Journal of Food Engineering*, 100, 417-426.
- Wang, T. & Lucey, J. A. (2003). Use of multi-angle laser light scattering and size-exclusion chromatography to characterize the molecular weight and types of aggregates present in commercial whey protein products. *Journal of Dairy Science*, 86, 3090-3101.
- Wang, J. M., Xia, N., Yang, X.-Q., Yin, S.-W., Qi, J.-R., He, X.-T., Yuan, D.-B., & Wang, L.-J. (2012). Adsorption and dilatational rheology of heat-treated soy protein at the oil-water interface: relationship to structural properties. *Journal of Agricultural and Food Chemistry*, 60, 3302-3310.
- Wang, Q. W., Allen, J. C., & Swaisgood, H. E. (1997). Binding of vitamin D and cholesterol to beta-lactoglobulin. *Journal of Dairy Science*, 80, 1054-1059.
- Wang, C. R. & Zayas, J. F. (1992). Comparative-study of corn germ and soy proteins utilization in comminuted meat-products. *Journal of Food Quality*, 15, 153-167.
- Wang, J., Zhao, M., Yang, X., & Jiang, Y. (2006). Improvement on functional properties of wheat gluten by enzymatic hydrolysis and ultrafiltration. *Journal of Cereal Science*, 44, 93-100.
- Weinbreck, F., de Vries, R., Schrooyen, P., & de Kruif, C. G. (2003). Complex coacervation of whey protein and gum Arabic. *Biomacromolecules*, 4, 293-303.
- Weinbreck, F., Minor, M., & de Kruif, C. G. (2004a). Microencapsulation of oils using whey protein/gum Arabic coacervates. *Journal of Microencapsulation*, 21, 667-679.
- Weinbreck, F., Nieuwenhuijse, H., Robijn, G. W., & de Kruif, C. G. (2004b). Complexation of whey proteins with carrageenan. *Journal of Agricultural and Food Chemistry*, 52, 3550-3555.

- Wehbi, Z., Perez, M. D., Sanchez, L., Pocovi, C., Barbana, C., & Calvo, M. (2005). Effect of heat treatment on denaturation of bovine alpha-lactalbumin: determination of kinetic and thermodynamic parameters. *Journal of Agricultural and Food Chemistry*, 53, 9730-9736.
- Wiacek, A. E. & Chibowski, E. (2005). Comparison of the properties of vegetable oil/water and n-tetradecane/water emulsions stabilized by alpha-lactalbumin or beta-casein. *Adsorption Science & Technology*, 23, 777-789.
- Winter, H. H. & Chambon, F. (1986). Analysis of linear viscoelasticity of a crosslinking polymer at the gel point. *Journal of Rheology*, 30, 367-392.
- de Wit, J. N. & van Kessel, T. (1996). Effects of ionic strength on the solubility of whey protein products. A colloid chemical approach. *Food Hydrocolloids*, 10, 143-149.
- Wong, B. T., Zhai, J. L., Hoffmann, S. V., Aguilar, M. I., Augustin, M., Wooster, T. J., & Day, L. (2012). Conformational changes to deamidated wheat gliadins and beta-casein upon adsorption to oil-water emulsion interfaces. *Food Hydrocolloids*, 27, 91-101.
- Wu, L. C., Shulman, B. A., Peng, Z. Y., & Kim, P. S. (1996). Disulfide determinants of calcium-induced packing in  $\alpha$ -lactalbumin. *Biochemistry*, 35, 859-863.
- Wu, M., Xiong, Y. L., & Chen, J. (2011). Role of disulphide linkages between protein-coated lipid droplets and the protein matrix in the rheological properties of porcine myofibrillar protein-peanut oil emulsion composite gels. *Meat Science*, 88, 384-390.
- Yang, X. & Foegeding, E. A. (2011). The stability and physical properties of egg white and whey protein foams explained based on microstructure and interfacial properties. *Food Hydrocolloids*, 25, 1687-1701.
- Ye, A. Q. & Singh, H. (2006). Adsorption behavior of lactoferrin in oil-in-water emulsions as influenced by interactions with beta-lactoglobulin. *Journal of Colloid and Interface Science*, 295, 249-254.
- Yin, B. R., Deng, W., Xu, K. K., Huang, L. W., & Yao, P. (2012). Stable nano-sized emulsions produced from soy protein and soy polysaccharide complexes. *Journal of Colloid and Interface Science*, 380, 51-59.
- Yuan, Y., Wang, Z. L., Yang, X. Q., & Yin, S. W. (2014). Associative interactions between chitosan and soy protein fractions: Effects of pH, mixing ratio, heat treatment and ionic strength. *Food Research International*, 55, 207-214.

- Zhai, J. L., Hoffmann, S. V., Day, L., Lee, T. H., Augustin, M. A., Aguilar, M. I., & Wooster, T. J. (2012). Conformational changes of alpha-lactalbumin adsorbed at oil-water interfaces: interplay between protein structure and emulsion stability. *Langmuir*, 28, 2357-2367.
- Zhang, Z., Dalgleish, D. G., & Goff, H. D. (2004). Effect of pH and ionic strength on competitive protein adsorption to air/water interfaces in aqueous foams made with mixed milk proteins. *Colloids and Surfaces B- Biointerfaces*, 34, 113-121.
- Zhu, D., Damodaran, S., & Lucey, J. A. (2010). Physicochemical and emulsifying properties of whey protein isolate (WPI)-dextran conjugates produced in aqueous solution. *Journal of Agricultural and Food Chemistry*, 58, 2988-2994.
- Zúñiga, R. N., Tolkach, A., Kulozik, U., & Aguilera, J. M. (2010). Kinetics of formation and physicochemical characterization of thermally-induced  $\beta$ -lactoglobulin aggregates. *Journal of Food Science*, 75, E261-E268.